TATIANE DULCINEIA SILVA

MORPHOPHYSIOLOGY AND 20-HYDROXYECDYSONE PRODUCTION IN *Pfaffia glomerata* (SPRENG.) PEDERSEN IN RESPONSE TO CO_2-ENRICHMENT AND DROUGHT STRESS

Thesis submitted to the Plant Physiology Graduate Program of the Universidade Federal de Viçosa in partial fulfillment of the requirements for the degree of *Doctor Scientiae*.

Advisor: Wagner Campos Otoni

Co-advisors: Adriano Nunes-Nesi
Diego Silva Batista
José Eduardo Serrão

VIÇOSA - MINAS GERAIS
2022

Ficha catalográfica elaborada pela Biblioteca Central da Universidade Federal de Viçosa - Campus Viçosa

T
S586m
2022

Silva, Tatiane Dulcineia, 1991-
Morphophysiology and 20-hydroxyecdysone production in *Pfaffia glomerata* (Spreng.) Pedersen in response to CO2-enrichment and drought stress / Tatiane Dulcineia Silva. – Viçosa, MG, 2022.
1 tese eletrônica (166 f.): il. (algumas color.).

Texto em inglês.
Orientador: Wagner Campos Otoni.
Tese (doutorado) - Universidade Federal de Viçosa, Departamento de Biologia Vegetal, 2022.
Inclui bibliografia.
DOI: https://doi.org/10.47328/ufvbbt.2022.461
Modo de acesso: World Wide Web.

1. *Pfaffia glomerata*. 2. Ecdiesteróides. 3. 20-hydroxyecdysone. 4. Estresse hídrico. 5. *Pfaffia glomerata* - Metabolismo. I. . II. Universidade Federal de Viçosa. Departamento de Biologia Vegetal. Programa de Pós-Graduação em Fisiologia Vegetal. III. Título.

CDD 22. ed. 583.53

Bibliotecário(a) responsável: Bruna Silva CRB-6/2552

TATIANE DULCINEIA SILVA

MORPHOPHYSIOLOGY AND 20-HYDROXYECDYSONE PRODUCTION IN *Pfaffia glomerata* (SPRENG.) PEDERSEN IN RESPONSE TO CO_2-ENRICHMENT AND DROUGHT STRESS

Thesis submitted to the Plant Physiology Graduate Program of the Universidade Federal de Viçosa in partial fulfillment of the requirements for the degree of *Doctor Scientiae*

APPROVED: July 25, 2022.

Assent:

Tatiane Dulcineia Silva
Author

Wagner Campos Otoni
Advisor

ACKNOWLEDGEMENTS

Primeiramente gostaria de agradecer aos meus pais, Terezinha e João. Sem o apoio de vocês, eu jamais conseguiria conquistar tudo o que conquistei até aqui. Pelo incentivo imensurável na minha educação (mesmo nunca tendo a oportunidade de estar em uma sala de aula universitária). Por terem me passado os maiores valores da vida: amor, respeito e humildade. Sem vocês, eu seria tão pouco, obrigado por tudo!

Aos meus irmãos Cláudia, Gilberto e Eliane e minha sobrinha Cecília, por todos os ensinamentos, carinho, cuidado, boas conversas e pelos valiosos concelhos.

Ao meu marido e melhor amigo, Thiago durante todos esses anos você foi meu maior incentivador e companheiro (juntamente como os nossos filhos pet: Léo, Yuri e Amora) que esteve ao meu lado em todos os momentos. Agradeço a Deus por ter colocado um homem tão maravilhoso na minha vida! Te amo cada dia mais.

Ao meu querido orientador, Prof. Wagner Otoni por ser mais que um orientador, mas o meu pai científico, amigo e mestre. Obrigada pelos valiosos ensinamentos e confiança depositada em mim durante toda minha trajetória acadêmica. O senhor é minha maior referência de profissional e pessoa. Wagner, serei eternamente grata a você por tudo!

Ao meu coorientador e amigo, Prof. Diego Batista por estar ao meu lado durante esses últimos 9 anos. Pela paciência e dedicação em transmitir todos os seus conhecimentos! Obrigada pelo incentivo e por me ensinar tanto!

Ao meu coorientador Prof. Adriano Nunes-Nesi pelas valiosas sugestões metodológicas, discussões dos resultados e demais contribuições desta tese.

Aos meus queridos amigos e irmãos "fáfieiros", Evandro, Kristhiano e Sérgio sem vocês esse trabalho não teria sido viável! A disponibilidade de vocês em ajudar são admiráveis. Muito obrigada por me ensinarem tanto e pela valiosa amizade! Eu tenho muito orgulho do nosso grupo!

A todos os meus amigos do Laboratório de Cultura de Tecidos Vegetal (LCT). Obrigada pela acolhida, pelos ensinamentos e principalmente pelos grandes momentos de descontração, sem os quais não deixaria essa jornada tão prazerosa! Agradeço em especial à Jessenia, Quezia, José Victor, Andréa e Daniele, por toda ajuda disponibilizada na avaliação dos experimentos e execução das análises.

Ao Laboratório de Biologia Celular e Tecidual e Laboratório de Biotecnologia da UENF, nas pessoas de Profa. Claudete Santa-Catarina, Prof. Vanildo Silveira, Dr. Vitor Pinto, Dr. Renan Carrari e Dr. Tadeu Oliveira, pela disponibilidade nas análises de proteômica e pelas contribuições ao trabalho.

À Unidade de Crescimento de Plantas, ao Laboratório de Anatomia Vegetal e ao Núcleo de Microscopia e Microanálise da UFV, pela infraestrutura oferecida. Agradeço em especial à Dra. Mariana Machado e Dra. Auxiliadora Martin, por todo suporte e ajuda nas análises metabólicas, e ao Gilmar Valente, pelo inestimado auxílio com as imagens de ultraestrutura.

Ao Laboratório de Biodiversidade (DBB/UFV), nas pessoas de Prof. João Paulo Leite e Letícia Faria pela disponibilidade nas análises de 20E.

Ao Laboratório de Ecologia e Evolução de Plantas (DBV/UFV), em especial à Larissa Muller, pela medição e análise dos dados hiperespectrais.

Ao Laboratório de Metabolismo Vegetal e Metabolômica (Heinrich-Heine-Universität Düsseldorf, Alemanha), em nome do Prof. Andreas Weber e Dr. Philipp Westhoff pela disponibilidade nas análises metabólicas.

Ao Prof. José Serrão, pela coorientação, e à Dra. Jamile Cossolin, pelos ensinamentos e processamento do material para microscopia eletrônica de transmissão.

Ao Prof. Samuel Martins e ao Dr. Moab Andrade, por toda contribuição e auxílio nas medições do potencial hídrico.

Aos professores do Departamento de Biologia Vegetal, pelas disciplinas oferecidas, que contribuíram de forma valiosa para o meu aprendizado e aos meus colegas da pós-graduação, por todo companheirismo e pela boa convivência.

À Universidade Federal de Viçosa (UFV), principalmente ao Programa de Pós-Graduação em Fisiologia Vegetal, pelo apoio e por fornecer todas as condições necessárias durante o desenvolvimento da minha pesquisa. Sou também grata à Coordenação de Aperfeiçoamento de Pessoal de Nível Superior – Brasil (CAPES) – Código de Financiamento 001 pela bolsa de estudo concedida e à Fundação de Amparo à Pesquisa do Estado de Minas Gerais [FAPEMIG; APQ-00772-19 e RED-00053-16 - Rede Mineira em Fisiologia de Plantas sob Condições de (Rede Mineira Estresse em Plantas)] e ao Conselho Nacional de Desenvolvimento Científico e Tecnológico (CNPq; Processo 313901/2018-0), pelo suporte financeiro.

Agradeço a todos que direta ou indiretamente contribuíram para a realização deste trabalho, sem vocês eu não teria conseguido. Muito obrigada!

ABSTRACT

SILVA, Tatiane Dulcineia, D.Sc., Universidade Federal de Viçosa, July, 2022. **Morphophysiology and 20-hydroxyecdysone production in *Pfaffia glomerata* (Spreng.) Pedersen in response to CO_2-enrichment and drought stress**. Advisor: Wagner Campos Otoni. Co-Advisors: Adriano Nunes-Nesi, Diego Silva Batista and José Eduardo Serrão.

Anthropogenic activities have been catalyzing climate changes, owing to increased atmospheric carbon dioxide concentration ([CO_2]). In respect to CO_2, its general effects on the regulation of plant growth, development and metabolism are widely explored, especially in agricultural crops. However, the changes in medicinal species under elevated [CO_2] are still poorly understood. *Pfaffia glomerata* (Spreng.) Pedersen, a plant species native to Brazil and popularly known as Brazilian ginseng, stands out by the production of 20-hydroxyecdysone (20E), a phytoecdysteroid molecule with proven therapeutic and nutraceutical activities in mammals. Previous findings from our research group revealed that in vitro CO_2-enrichment led to physiological changes *in P. glomerata.* We hypothesize that CO_2-enrichment affects the production of primary and secondary metabolites, such as 20E, in *P. glomerata*. Therefore, the objective here was to evaluate the effect of the CO_2-enriched atmosphere on morphophysiological, biochemical, structural, molecular aspects, as well as in water deficit tolerance responses. For this, two independent experiments were conducted in open top chambers (OTCs). For both experiments, clonally micropropagation-derived plantlets from the in vitro germplasm bank were used. In experiment I, we assessed the influence of two CO_2 concentrations: ambient (a[CO_2], ± 400 µmol mol^{-1} CO_2) and elevated (e[CO_2] ± 800 µmol mol^{-1} CO_2). After approximately 21 days of cultivation in OTC, our data showed that e[CO_2] increased photosynthesis (A_N), and water use efficiency (WUE), biomass accumulation, photosynthetic pigments, carbohydrate content, expression of genes of the lignin biosynthetic pathway, and induced changes in the proteomic profile. On the other hand, e[CO_2] promoted reduction in total protein, amino acids and 20E contents. In experiment II, the physiological and biochemical responses of plants exposed to combined e[CO_2] and under water deficit were analyzed. During the first 14 days of cultivation, all plants were regularly irrigated to maintain soil water at field capacity. Then, the plants were subjected for 21 days to the following treatments: (**I**) a[CO_2] and well-watered (a[CO_2]WW); (**II**) e[CO_2] and well-watered (e[CO_2]WW); (**III**) a[CO_2] and drought stressed (a[CO_2]D); and (**IV**) e[CO_2] and

drought stressed (e[CO_2]D). Our data demonstrate that e[CO_2] mitigates drought impacts by reducing stomatal conductance (g_S), improving WUE, and promoting less negative water potentials. Although the reduction in gs decreased water loss by evapotranspiration, it negatively affected A_N, and consequently plant growth. Hyperspectral analysis corroborates these findings and is a great non-destructive tool to analyse the effects of drought on plants. We found that *P. glomerata* exhibits different drought response mechanisms depending on [CO_2]. Plants exposed to a[CO_2]D increased root/shoot ratio, stem rustification, non-enzymatic antioxidant system by increased anthocyanin content and proteins of ascorbate and glutathione metabolism. Conversely, plants under e[CO_2]D invested strongly in osmoregulatory metabolites (e.g. soluble sugars and amino acids). We found that e[CO_2] associated to drought promoted changes in the proteomic profile, dramatically affecting the accumulation of stress response proteins. On the other hand, we show that drought positively affected the activity of antioxidant enzymes (CAT and SOD) and 20E content in both [CO_2] in *P. glomerata* plants. However, only in plants exposed to e[CO_2]D was there an increase in 20E production, overcoming the biomass limitation caused by this stress. Here, we report for the first time, the up-regulation of cytochrome P450 CYP72A219-like protein in plants grown in the combination e[CO_2]D. Therefore, we hypothesize a relationship of this protein with 20E biosynthesis and hypothesize possible ROS signaling (indirectly by increased CAT and SOD) under abiotic stress condition. These data provide relevant information in elucidating the pathway of 20E biosynthesis, as well as enabling biotechnological strategies to increase the production of this metabolite in *P. glomerata* plants.

Keywords: Brazilian ginseng. 20-hydroxyecdysone. Phytoecdysteroids. Water stress. CO_2 enrichment. Secondary metabolism.

RESUMO

SILVA, Tatiane Dulcineia, D.Sc., Universidade Federal de Viçosa, julho de 2022. **Morfofisiologia e produção de 20-hidroxiecdisona em *Pfaffia glomerata* (Spreng.) Pedersen em resposta à atmosfera enriquecida com CO_2 e estresse hídrico**. Orientador: Wagner Campos Otoni. Coorientadores: Adriano Nunes-Nesi, Diego Silva Batista e José Eduardo Serrão.

Atividades antrópicas têm vindo a provocar alterações climáticas, tais como o aumento da concentração atmosférica de dióxido de carbono ([CO_2]). Em relação ao CO_2, os seus efeitos gerais na regulação do crescimento, desenvolvimento e metabolismo das plantas são amplamente explorados, especialmente nas culturas agrícolas. No entanto, essas alterações nas espécies medicinais sob [CO_2] elevado ainda são mal compreendidas. Entre as espécies de interesse fitoterápico, destaca-se a *Pfaffia glomerata* (Spreng.) Pedersen, planta nativa do Brasil e popularmente conhecida como ginseng-brasileiro. As suas propriedades medicinais devem-se principalmente à produção do metabólito secundário 20-hidroxiecdisona (20E), um fitoecdisteroide com comprovadas atividades terapêutica e nutracêutica em mamíferos. Estudos do nosso grupo de pesquisa têm revelado que o enriquecimento da [CO_2] in vitro leva à alterações fisiológicas em *P. glomerata*. Levantamos a hipótese de que o enriquecimento da [CO_2] afeta a produção de metabólitos primários e secundários, como o 20E, na espécie-alvo. Portanto, avaliamos o efeito da elevada [CO_2] (e[CO_2]) nos aspectos morfofisiológicos, bioquímicos, estruturais e moleculares, bem como nas respostas de tolerância ao estresse hídrico. Para tal, foram realizados dois experimentos independentes em câmaras de topo aberto (CTA). Para ambos os experimentos, foram utilizadas plântulas derivadas da micropropagação clonal a partir do banco de germoplasma in vitro. No experimento I, foi analisado a influência de duas concentrações de CO_2: ambiente (a[CO_2]) ± 400 µmol mol^{-1}) e elevada (e[CO_2]) ± 800 µmol mol^{-1}). Após aproximadamente 21 dias de cultivo em OTC, os nossos dados mostraram que a e[CO_2] afetou positivamente a fotossíntese (A_N) e uso eficiente da água (WUE), o acúmulo de biomassa, os pigmentos fotossintéticos, o conteúdo de carboidratos, genes da rota de biossíntese de lignina, além de promover alterações no perfil proteômico. Por outro lado, a e[CO_2] promoveu redução no teor de proteínas totais, de alguns aminoácidos e do conteúdo de 20E. No experimento II, foram analisadas as respostas fisiológicas e bioquímicas de plantas expostas a e[CO_2] e sob estresse hídrico. Durante os 14 dias iniciais do experimento, todas as plantas foram regularmente irrigadas para manter o

conteúdo de água do solo próximo da capacidade do campo. Posteriormente, as plantas foram submetidas por 20 dias aos seguintes tratamentos: (**I**) a[CO_2] e sob irrigação regular (a[CO_2]I); (**II**) e[CO_2] e sob irrigação regular (e[CO_2]I); (**III**) a[CO_2] e sob estresse hídrico (a[CO_2]S); e (**IV**) e[CO_2] e sob estresse hídrico (e[CO_2]S);. Os nossos dados demonstraram que a e[CO_2] alivia os impactos da seca através da redução da condutância estomática (g_S), melhorando o WUE e promovendo potenciais hídricos menos negativos. Embora a redução da g_S tenha favorecido a economia de água, ela afetou negativamente a A_N, e consequentemente o crescimento das plantas. A análise hiperespectral corrobora com estes achados, sendo uma ótima ferramenta não destrutiva para analisar os efeitos da seca nas plantas. Descobrimos que *P. glomerata* apresenta diferentes mecanismos de resposta à seca dependendo da [CO_2]. Plantas expostas a a[CO_2]S investiram no aumento da razão raiz/parte aérea, na rustificação do caule, no sistema antioxidante não enzimático, pelo aumento no teor de antocianina e proteínas do metabolismo do ascorbato e glutationa. Enquanto que as plantas sob e[CO_2]S investiram em metabólitos osmorreguladores (e.g. açúcares solúveis e aminoácidos). Verificamos que a e[CO_2] promoveu alterações no perfil proteômico, afetando drasticamente o acúmulo de proteínas de resposta ao estresse. Por outro lado, mostramos que a seca promoveu aumento na atividade de enzimas antioxidantes (CAT e SOD) e o conteúdo 20E em ambas as [CO_2] em plantas de *P. glomerata*. Porém, somente nas plantas expostas a e[CO_2]S houve aumento da produção de 20E, superando a limitação de biomassa causada por esse estresse. Aqui, relatamos pela primeira vez, a regulação positiva da proteína cytochrome P450 CYP72A219-like em plantas cultivadas na combinação e[CO_2] e seca. Portanto, acreditamos em uma relação dessa proteína com a biossíntese de 20E e supomos uma possível sinalização de ROS (indiretamente pelo aumento de CAT e SOD) na produção de 20E em condição de estresse abiótico. Por fim, nossos dados fornecem informações importantes na elucidação da rota de biossíntese de 20E, além de possibilitar estratégias biotecnológicas para aumentar a produção desse metabólito em plantas de *P. glomerata*.

Palavras-chave: Ginseng-brasileiro. 20-hidroxiecdisona. Fitoecdisteroides. Estresse hídrico. enriquecimento de CO_2. Metabolismo secundário.

CONTENTS

GENERAL INTRODUCTION

Medicinal plants and secondary metabolites

The use of medicinal plants is of the most ancient ways of disease prevention and treatment, and in many communities it is still the main therapeutic resource (Almeida et al. 2017; Roy et al. 2018). The International Union for Conservation of Nature (IUCN) estimates that approximately 80,000 species of angiosperms have medicinal properties (Jeyasri et al. 2020). Despite the importance of plants with pharmacological potential, many of their bioactive compounds are not yet validated (Russell and Duthie 2011; Singh et al. 2019).

Secondary metabolites are bioactive molecules derived from primary metabolism (Jacoby et al. 2021; Kliebenstein and Osbourn 2012). Although not considered essential for plant development, secondary metabolites play a key role in plant adaptation to environmental changes and in defense against pathogens (Aguirre-Becerra et al. 2021; Thakur et al. 2019). Besides the ecological aspects, many of these molecules have great economic relevance, being used in the industry of pharmaceuticals, perfumes, dyes, and insecticides (Maganha et al. 2010; Mastinu et al. 2021).

Secondary metabolites are generally grouped according to their chemical structure, and can be classified into three major groups: nitrogen compounds (such as alkaloids, glycosinolates, and cyanogenic glycosides), phenolic compounds (such as phenolic acid, tannins, lignins, and flavonoids) and terpenes or isoprenoids (such as carotenoids, volatile compounds, and sterols) (Kabera et al. 2014; Li et al. 2020; Othman et al. 2019; Zhang et al. 2020). Ecdysone is a type of steroid, denominated zooecdysteroid in arthropods; it is a developmental regulatory hormone in this group. Their analogues in plants are called phytoecdysteroids, being a secondary metabolites present in higher concentrations in plants (up to 3% of dry mass) than in invertebrates (Dinan 2001; Dinan and Lafont 2006; Nakagawa and Henrich 2009).

20-hydroxyecdysone (20E)

20E is the main ecdysteroid found in insects, and the one with the highest biological activity. Together with the juvenile hormone, 20E promotes the metamorphosis process in insects, leading to ecdysis (Guo et al. 2021; Jindra et al. 2013; Lin and Smagghe 2019; Riddiford et al. 2003). About four hundred ecdysteroid analogues have been identified from

plant sources, with 20E the majority compound (Dinan et al. 2020). The biological functions of 20E in plants have not been fully elucidated. The main hypothesis is that 20E is a protective compound against unadapted phytophagous insects (Bakrim et al. 2008; Festucci-Buselli et al. 2008; Lafont, 1997), deregulating their endocrine system, and, as a consequence, impairing larval development and ecdysis process (Dinan et al. 2020; Rharrabe et al. 2010). Therefore, phytoecdysteroids can be an excellent substitute for synthetic insecticides (Chaubey 2018).

20E is associated with several beneficial effects on mammals, including humans (Dinan et al. 2021). In a clinical trial with ovariectomized rats fed a high-fat, high-fructose diet, 20E was found to attenuate cardiometabolic symptoms (Buniam et al. 2020). Furthermore, 20E can reduce stress, anxiety and depression, while maintaining the antioxidant defenses of the cortex (Franco et al. 2021), and does not promote any cytotoxic or mutagenic activity (Almeida et al. 2017). A recent work proposes the use of BIO101, an immediate release oral pharmaceutical formulation of 20E (with 97% purity extracted from *Cyanotis* sp. plants), for patients with COVID-19. BIO101 acts by activating the MasR receptor promoting the balance of the renin-angiotensin system, improving the health of patients with pneumonia due to COVID-19 (Dioh et al. 2021; Latil et al. 2021).

Physiological and molecular mechanisms that regulate 20E biosynthesis in plants are not well understood, in contrast to insects (Tsukagoshi et al. 2016). However, in both groups it is already known that genes related to cytochrome P450 are required as an adaptor enzyme for oxidative modification of different compounds, e.g., ecdysteroids (Park et al. 2020; Rewitz and Gilbert 2008; Zhou and Pichersky 2020). Recent studies have validated the participation of the cytochrome P450 gene family in the biosynthetic route of ecdysteroids in plants. Furthermore, the biosynthesis of ecdysteroids in wheat plants can be limited by the action of fenarimol, an inhibitor of the cytochrome P450 monooxygenases (Janeczko et al. 2021).

Transcriptome data from *Cyanotis arachnoidea* (Lei et al. 2018), *Ajuga lobata* (Wang and Chi 2018) and *Pfaffia glomerata* (Batista et al. 2019a) provide a valuable resource for understanding 20E biosynthesis. The *Spook* and *Phantom* genes - *Halloween* class genes - are described as regulators of 20E biosynthesis in insects, and were identified also in *P. glomerata* (Batista et al. 2019a). The expression level of these two genes can be regulated by changes in abiotic conditions (Batista et al. 2019a; Felipe et al. 2019a; Fortini et al. 2020). Thus, further studies need to be conducted for the understanding on physiological and molecular levels of 20E biosynthesis in *P. glomerata* plants.

Pfaffia glomerata

P. glomerata (Amaranthaceae) is popularly known as Brazilian ginseng , due to the morphological similarity of its roots with those of Korean-ginseng (*Panax ginseng* C.A. Meyer.) (Neves et al. 2016). *P. glomerata* is an herbaceous species native to South America, widely distributed in Brazil, being a typical plant of riparian vegetation and river floodplains (Marchioretto et al. 2010). The species is extensively used in traditional medicine, and it carries several verified as medicinal properties medicinal properties, such as stimulant, analgesic, anabolic, anti-inflammatory, immunostimulant, sedative, hypocholesterolemic (Dias et al. 2019; Franco et al. 2021; Moura et al. 2011; Neto et al. 2005; Neves et al. 2016). These medicinal effects are mainly due to the compounds 20E, pterosterone, polypodin B and ginsenosides. 20E is the major compound in *P. glomerata* and are obtained from its roots, mainly through extraction (Dinan et al. 2021; Kamada et al. 2009; Neves et al. 2016).

P. glomerata presents great plasticity and adaptability to changes in abiotic conditions. The species is responsive to light conditions, and its morphophysiology and 20E production could be modified by irradiance levels (Silva et al. 2020b), spectral quality (Felipe et al. 2019a; Silva et al. 2020a) and photoperiod conditions (Fortini et al. 2020). The species also exhibits tolerance to cadmium, mercury, lead, arsenic and zinc levels, and possibly these responses are related to changes observed in enzymatic (such as oxidative stress enzymes) and non-enzymatic (e.g, anthocyanins and 20E) mechanisms (Bernardy et al. 2020; Calgaroto et al. 2010; Gomes et al. 2012; Gupta et al. 2013; Pereira et al. 2018; Skrebsky et al. 2008). Salt stress also affects the growth and development of *P. glomerata*, and plants exposure to moderate levels of salinity increased 20E concentration (Felipe et al. 2019b; Fortini et al. 2022). However, the impacts that abiotic changes may have on the 20E biosynthesis pathway are still poorly understood.

Furthermore, the increase in gas exchange and CO_2 enrichment in *P. glomerata* plants grown in vitro have shown promising results. A pioneer work demonstrated that this species has agreat potential for in vitro propagation under photoautotrophy (Iarema et al. 2012). Plants of *P glomerata* grown on sucrose-free medium and with membranes that allow greater gas exchange (natural ventilation), showed significant increases in photosynthetic rate, biomass, and 20E (Iarema et al. 2012; Saldanha et al. 2012). Another pioneering study revealed that the CO_2-enriched atmosphere (750 µmol mol^{-1} CO_2) in vitro contributed to higher plant growth and lower relative leaf water loss in *P. glomerata*, but this CO_2 input did not lead to the highest accumulation of 20E (Saldanha et al. 2013).

Subsequently, it was demonstrated that an enriched atmosphere (forced air ventilation) at 1000 µmol mol^{-1} of CO_2, associated with cultivation on a porous substrate (Florialite®), increased growth and 20E levels in the leaves of *P. glomerata* (Ferreira et al. 2019; Saldanha et al. 2014). Furthermore, ultrastructural changes at the chloroplast level were observed in *P. glomerata* in response to elevated CO_2 levels, such as changes in the thylakoid membranes, the number of stacks, and the shape of plastids (Saldanha et al. 2014). Further studies would allow a better understanding of the ultrastructural changes of plastids, in *P. glomerata* plants grown under CO_2-enriched atmosphere.

CO_2-enrichment also regulates the profile of several metabolites in *P. glomerata* plants. Under these conditions, plants increase production of 20E, in the levels of amino acids, sugars, intermediates of the tricarboxylic acid cycle, compounds related to osmotic adjustment, and of metabolites related to the shikimate biosynthesis pathway (Ferreira et al. 2019; Tzin and Galili 2010). The shikimate pathway in plants is the source of several secondary metabolites, such as the phenylpropanoids, precursors mainly of flavonoids, phenolic acids and monolignols (e.g. lignin and suberin) (Deng and Lu 2017; Vogt 2010). These secondary compounds play key roles in plant development, such as pollinator attraction, herbivores and pathogens defense, antioxidant protection, cell wall injury maintenance, and other plant responses to biotic and abiotic stimuli (Deng and Lu 2017; Sharma et al. 2019).

Immunohistochemical analysis of the cell wall of *P. glomerata* showed increased deposition of pectic polymers (homogalacturonan), hemicellulose (heteroxylan) and proteoglycan (arabinogalactan) when exposed to high concentrations of CO_2 (Louback et al. 2021). The authors associated higher pectin detection (JIM7 antibody) with increased growth and biomass accumulation; already the deposition of hemicellulose (antibody LM10) and proteoglycan (antibody JIM13) as a marker of secondary cell wall development (Louback et al. 2021). This study opens possibilities for upcoming CO_2-enrichment work to address not only novel antibodies to cell wall epitopes, but key genes related to the biosynthesis pathway of these structural compounds.

Increased atmospheric concentration of carbon dioxide (CO_2)

The global warming will surpass 1.5°C in the following decades, leading to irreversible loss of the most fragile ecosystems, and crisis after crisis for the most vulnerable

people and societies (IPCC, 2022). Furthermore, currently the CO_2 concentration in the atmosphere is over 400 μmol mol^{-1}, and will possibly reach more than 800 ppm by the end of this century (IPCC, 2022; Hirsch et al. 2017) mainly due to intense anthropogenic activities. Therefore, several studies have sought to understand the physiological and metabolic mechanisms involved in the response to elevated CO_2, especially in agricultural cultivars such as rice (Madan et al. 2012), maize (Durand et al. 2018), coffee (Avila et al. 2020), and tomato (Brito et al. 2020). However, little is known about the effects of CO_2-enrichment on medicinal plants and the impact on the biosynthesis of secondary metabolites (Ahmed et al. 2019; Das et al. 2016).

CO_2 concentration can affect the secondary metabolism of plants, and as a consequence, the defense responses against herbivory (Sun et al. 2013). In *Catharanthus roseus*, elevated CO_2 concentrations led to an enhanced production of alkaloids (Singh et al. 2015). Indian tea (*Camellia sinensis*) plants grown under high CO_2 increased expression of genes related to phenylpropanoid biosynthesis and decreased the genes related to caffeine biosynthesis, as well as increased salicylic acid concentrations (Li et al. 2019). The impacts of elevated CO_2 concentrations on primary metabolism can affect the secondary metabolism of plants, and as a consequence, in the production of defense compounds (Sun et al. 2016).

The increase in atmospheric CO_2 concentration is not a climate condition isolated from global warming. Extreme adversities such as drought, heat, frost or the combination of these stresses are associated with the impact of elevated CO_2, which variously affects the production of primary and secondary metabolites in plants (Ahmed et al. 2019; Birami et al. 2020). To understand the physiological and metabolic responses of plants to climate change it is recommended to use CO_2-enrichment in open air (FACE) or open top chambers (OTCs).

In light of the facts described above and due to the inexistence so far of CO_2-enrichment studies in an *ex vitro* environment in *P. glomerata*, and its potential use as a tool for studies of phytoecdysteroid metabolism, it is necessary to investigate how biotic and abiotic factors regulate the 20E biosynthesis pathway. We aimed to evaluate the effect of CO_2-enriched atmosphere on morphophysiological responses and 20E production to drought stress in plants of *P. glomerata*. Thus, the following questions are raised: (i) Can CO_2-enrichment increase the production of 20E? (ii) Does elevated CO_2 promote higher photosynthetic performance and production of primary metabolites? (iii) Can morphoanatomy and the composition of the cell wall, as well genes involved in its biosynthesis, be influenced by the CO_2-enriched atmosphere? (iv) Does high CO_2 and drought stress alter the profile of

proteins and metabolites? (v) Can CO_2-enrichment associated with drought stress lead to changes in morphophysiology and increase the 20E content? (vi) Can CO_2-enrichment mitigate the effects of drought stress?

REFERENCES

Aguirre-Becerra, H., Vazquez-Hernandez, M. C., Saenz de la O, D., Alvarado-Mariana, A., Guevara-Gonzalez, R. G., Garcia-Trejo, J. F., Feregrino-Perez, A. A. (2021). Role of stress and defense in plant secondary metabolites production. *Bioactive Natural Products for Pharmaceutical Applications, 140,* 151–195. https://doi.org/10.1007/978-3-030-54027-2_5

Ahmed, S., Griffin, T. S., Kraner, D., Schaffner, M. K., Sharma, D., Hazel, M., Leitch, A. R., Orians, C. M., Han, W., Stepp, J. R., Robbat, A., Matyas, C., Long, C., Xue, D., Houser, R. F., Cash, S. B. (2019). Environmental factors variably impact tea secondary metabolites in the context of climate change. *Frontiers in Plant Science*, *10*, 939. https://doi.org/10.3389/fpls.2019.00939

Almeida, I. V., Düsman, E., Mattge, G. I., Toledo, F., Reusing, A. F., Vicentini, V. E. P. (2017). In vivo antimutagenic activity of the medicinal plants *Pfaffia glomerata* (Brazilian ginseng) and *Ginkgo biloba*. *Genetics and Molecular Research*, *16*(3), 16039785. https://doi.org/10.4238/gmr16039785

Avila, R. T., Cardoso, A. A., de Almeida, W. L., Costa, L. C., Machado, K. L. G., Barbosa, M. L., de Souza, R. P. B., Oliveira, L. A., Batista, D. S., Martins, S. C. V., Ramalho, J. D. C., DaMatta, F. M. (2020). Coffee plants respond to drought and elevated [CO_2] through changes in stomatal function, plant hydraulic conductance, and aquaporin expression. *Environmental and Experimental Botany*, *177*, 104148. https://doi.org/10.1016/j.envexpbot.2020.104148

Bakrim, A., Maria, A., Sayah, F., Lafont, R., Takvorian, N. (2008). Ecdysteroids in spinach (*Spinacia oleracea* L.): Biosynthesis, transport and regulation of levels. *Plant Physiology and Biochemistry*, *46*(10), 844–854. https://doi.org/10.1016/j.plaphy.2008.06.002

Batista, D. S., Koehler, A. D., Romanel, E., de Souza, V. C., Silva, T. D., Almeida, M. C., Maciel, T. E. F., Ferreira, P. R. B., Felipe, S. H. S., Saldanha, C. W., Maldaner, J., Dias, L. L. C., Festucci-Buselli, R. A., Otoni, W. C. (2019). *De novo* assembly and transcriptome of *Pfaffia glomerata* uncovers the role of photoautotrophy and the P450 family genes in 20-hydroxyecdysone production. *Protoplasma*, *256*(3), 601–614. https://doi.org/10.1007/s00709-018-1322-1

Bernardy, K., Farias, J. G., Pereira, A. S., Dorneles, A. O. S., Bernardy, D., Tabaldi, L. A., Neves, V. M., Dressler, V. L., Nicoloso, F. T. (2020). Plants' genetic variation approach

applied to zinc contamination: secondary metabolites and enzymes of the antioxidant system in *Pfaffia glomerata* accessions. *Chemosphere*, *253*, 126692. https://doi.org/10.1016/j.chemosphere.2020.126692

Birami, B., Thomas, N., Gattmann, M., Preisler, Y., Gast, A., Arneth, A., Ruehr, N. K. (2020). Hot drought reduces the effects of elevated CO_2 on tree water- use efficiency and carbon metabolism. *New Phytologist*, *226*, 1607–1621. https://doi.org/10.1111/nph.16471

Brito, F. A. L., Pimenta, T. M., Henschel, J. M., Martins, S. C. V., Zsögön, A., Ribeiro, D. M. (2020). Elevated CO_2 improves assimilation rate and growth of tomato plants under progressively higher soil salinity by decreasing abscisic acid and ethylene levels. *Environmental and Experimental Botany*, *176*, 104050. https://doi.org/10.1016/j.envexpbot.2020.104050

Buniam, J., Chukijrungroat, N., Rattanavichit, Y., Surapongchai, J., Weerachayaphorn, J., Bupha-Intr, T., Saengsirisuwan, V. (2020). 20-hydroxyecdysone ameliorates metabolic and cardiovascular dysfunction in high-fathigh-fructose-fed ovariectomized rats. *BMC Complementary Medicine and Therapies*, *20*(1), 1–12. https://doi.org/10.1186/s12906-020-02936-1

Calgaroto, N. S., Castro, G. Y., Cargnelutti, D., Pereira, L. B., Gonçalves, J. F., Rossato, L. V., Antes, F. G., Dressler, V. L., Flores, E. M. M., Schetinger, M. R. C., Nicoloso, F. T. (2010). Antioxidant system activation by mercury in *Pfaffia glomerata* plantlets. *BioMetals*, *23*(2), 295–305. https://doi.org/10.1007/s10534-009-9287-3

Chaubey, M. K. (2018). Role of phytoecdysteroids in insect pest management: a review. *Journal of Agronomy*, *17*, 1–10.

Das, M., Jain, V., Malhotra, S. K. (2016). Impact of climate change on Medicinal and aromatic plants: Review. *Indian Journal of Agricultural Sciences*, *86*(11), 1375–1382.

Deng, Y., Lu, S. (2017). Biosynthesis and regulation of phenylpropanoids in plants. *Critical Reviews in Plant Sciences*, *36*(4), 257–290. https://doi.org/10.1080/07352689.2017.1402852

Dias, F. C. R., Martins, A. L. P., Melo, F. C. S. A., Cupertino, M. C., Gomes, M. L. M., Oliveira, J. M., Damasceno, E. M., Silva, J., Otoni, W. C., da Matta, S. L. P. (2019). Hydroalcoholic extract of *Pfaffia glomerata* alters the organization of the seminiferous tubules by modulating the oxidative state and the microstructural reorganization of the mice testes. *Journal of Ethnopharmacology*, *233*, 179–189.

https://doi.org/10.1016/j.jep.2018.12.047

Dinan, L. (2001). Phytoecdysteroids: biological aspects. *Phytochemistry*, *57*, 325–339. https://doi.org/10.1016/S0031-9422(01)00078-4

Dinan, L., Balducci, C., Guibout, L., Foucault, A. S., Bakrim, A., Kumpun, S., Girault, J. P., Tourette, C., Dioh, W., Dilda, P. J., Veillet, S., Lafont, R. (2021). Ecdysteroid metabolism in mammals: The fate of ingested 20-hydroxyecdysone in mice and rats. *Journal of Steroid Biochemistry and Molecular Biology*, *212*, 105896. https://doi.org/10.1016/j.jsbmb.2021.105896

Dinan, L., Lafont, R. (2006). Effects and applications of arthropod steroid hormones (ecdysteroids) in mammals. *Journal of Endocrinology*, *191*(1), 1-8. https://doi.org/10.1677/joe.1.06900

Dinan, L., Mamadalieva, N. Z., Lafont, R. (2020). Dietary Phytoecdysteroids. *Handbook of Dietary Phytochemicals,* pp. 1–54. Springer Singapore. https://doi.org/10.1007/978-981-13-1745-3_35-1

Dioh, W., Chabane, M., Tourette, C., Azbekyan, A., Hajjar, L. A., Lins, M., Nair, G. B. (2021). Testing the efficacy and safety of BIO101, for the prevention of respiratory deterioration, in patients with COVID-19 pneumonia (COVA study): a structured summary of a study protocol for a randomised controlled trial. *Trials*, *22*, 1–5. https://doi.org/10.1186/s13063-020-04998-5

Durand, J. L., Delusca, K., Boote, K., Lizaso, J., Manderscheid, R., Weigel, H. J., Ruane, A. C., Rosenzweig, C., Jones, J., Ahuja, L., Anapalli, S., Basso, B., Baron, C., Bertuzzi, P., Biernath, C., Deryng, D., Ewert, F., Gaiser, T., Gayler, S., Zhao, Z. (2018). How accurately do maize crop models simulate the interactions of atmospheric CO_2 concentration levels with limited water supply on water use and yield? *European Journal of Agronomy*, *100*, 67–75. https://doi.org/10.1016/j.eja.2017.01.002

Felipe, S. H. S., Batista, D. S., Chagas, K., Correia, L. N. F., Silva, T. D., Fortini, E. A., Silva, P. O., Otoni, W. C. (2019a). Accessions of Brazilian ginseng (*Pfaffia glomerata*) with contrasting anthocyanin content behave differently in growth, antioxidative defense, and 20-hydroxyecdysone levels under UV-B radiation. *Protoplasma*, *256*(6), 1557–1571. https://doi.org/10.1007/s00709-019-01400-3

Felipe, S. H. S., Batista, D. S., Vital, C. E., Chagas, K., Silva, P. O., Silva, T. D., Fortini, E. A., Correia, L. N. F., Avila, R. T., Maldaner, J., Festucci-Buselli, R. A., DaMatta, F. M., Otoni, W. C. (2019b). Salinity-induced modifications on growth, physiology and 20-

hydroxyecdysone levels in Brazilian-ginseng [*Pfaffia glomerata* (Spreng.) Pedersen]. *Plant Physiology and Biochemistry*, *140*, 43–54. https://doi.org/10.1016/j.plaphy.2019.05.002

Ferreira, P. R. B., da Cruz, A. C. F., Batista, D. S., Nery, L. A., Andrade, I. G., Rocha, D. I., Felipe, S. H. S., Koehler, A. D., Nunes-Nesi, A., Otoni, W. C. (2019). CO_2 enrichment and supporting material impact the primary metabolism and 20-hydroxyecdysone levels in Brazilian ginseng grown under photoautotrophy. *Plant Cell, Tissue and Organ Culture*, *139*(1), 77–89. https://doi.org/10.1007/s11240-019-01664-w

Festucci-Buselli, R. A., Contim, L. A. S., Barbosa, L. C. A., Stuart, J., Otoni, W. C. (2008). Biosynthesis and potential functions of the ecdysteroid 20-hydroxyecdysone - A review. *Botany*, *86*(9), 978–987). https://doi.org/10.1139/B08-049

Fortini, E.A., Batista, D.S., Felipe, S.H.S., Silva, T.D., Correia, L.N.F., Farias, L.M., Faria, D.V., Pinto, V.B., Santa-Catarina, C, Silveira, V., Clelia De-la-Peña, C., Castillo-Castro, E., Otoni, W.C. (2022). Physiological, epigenetic, and proteomic responses in *Pfaffia glomerata* growth in vitro under salt stress and 5-azacytidine. *Protoplasma*. https://doi.org/10.1007/s00709-022-01789-4

Franco, R. R., de Almeida Takata, L., Chagas, K., Justino, A. B., Saraiva, A. L., Goulart, L. R., Melo Rodrigues Ávila, V., Otoni, W. C., Espindola, F. S., Silva, C. R. (2021). A 20-hydroxyecdysone-enriched fraction from *Pfaffia glomerata* (Spreng.) pedersen roots alleviates stress, anxiety, and depression in mice. *Journal of Ethnopharmacology*, *267*, 113599. https://doi.org/10.1016/j.jep.2020.113599

Gomes, M. O., Marques, T. C. L. L. S. M., Martins, G. A., Carneiro, M. M. L. C., Soares, A. M. (2012). Cd-tolerance markers of *Pfaffia glomerata* (Spreng.) Pedersen plants: anatomical and physiological features. *Brazilian Journal of Plant Physiology*, *24*(4), 293-304. https://doi.org/10.1590/S1677-04202012000400008

Guo, S., Tian, Z., Wu, Q. W., King-Jones, K., Liu, W., Zhu, F., Wang, X. P. (2021). Steroid hormone ecdysone deficiency stimulates preparation for photoperiodic reproductive diapause. *PLoS Genetics*, *17*(2), e1009352. https://doi.org/10.1371/JOURNAL.PGEN.1009352

Gupta, D. K., Huang, H. G., Nicoloso, F. T., Schetinger, M. R., Farias, J. G., Li, T. Q., Razafindrabe, B. H. N., Aryal, N., Inouhe, M. (2013). Effect of Hg, As and Pb on biomass production, photosynthetic rate, nutrients uptake and phytochelatin induction in *Pfaffia glomerata*. *Ecotoxicology*, *22*(9), 1403–1412. https://doi.org/10.1007/s10646-

013-1126-1

Hirsch, A. L., Wilhelm, M., Davin, E. L., Thiery, W., Seneviratne, S. I. (2017). Can climate-effective land management reduce regional warming? *Journal of Geophysical Research: Atmospheres*, *122*(4), 2269–2288. https://doi.org/10.1002/2016JD026125

Iarema, L., Cruz, A. C. F., Saldanha, C. W., Dias, L. L. C., Vieira, R. F., Oliveira, E. J., Otoni, W. C. (2012). Photoautotrophic propagation of Brazilian ginseng [*Pfaffia glomerata* (Spreng.) Pedersen]. *Plant Cell, Tissue and Organ Culture*, *110*(2), 227–238. https://doi.org/10.1007/s11240-012-0145-6

IPCC (2022). Global Warming of 1.5°C. An IPCC Special Report on the impacts of global warming of 1.5°C above pre-industrial levels and related global greenhouse gas emission pathways, in the context of strengthening the global response to the threat of climate change. Cambridge University Press. https://doi.org/10.1017/9781009157940

Jacoby, R. P., Koprivova, A., Kopriva, S. (2021). Pinpointing secondary metabolites that shape the composition and function of the plant microbiome. *Journal of Experimental Botany*, *72*(1), 57–69. https://doi.org/10.1093/jxb/eraa424

Janeczko, A., Oklestkova, J., Tarkowská, D., Drygaś, B. (2021). Naturally occurring ecdysteroids in *Triticum aestivum* l. And evaluation of fenarimol as a potential inhibitor of their biosynthesis in plants. *International Journal of Molecular Sciences*, *22*(6), 1–13. https://doi.org/10.3390/ijms22062855

Jeyasri, R., Muthuramalingam, P., Suba, V., Ramesh, M., Chen, J. T. (2020). *Bacopa monnieri* and their bioactive compounds inferred multi-target treatment strategy for neurological diseases: A cheminformatics and system pharmacology approach. *Biomolecules*, *10*(4), 536. https://doi.org/10.3390/biom10040536

Jindra, M., Palli, S. R., Riddiford, L. M. (2013). The juvenile hormone signaling pathway in insect development. *Annual Review of Entomology*, *58*, 181–204. https://doi.org/10.1146/annurev-ento-120811-153700

Kabera, J. N., Semana, E., Mussa, A. R., He, X. (2014). Plant secondary metabolites: biosynthesis, classification, function and pharmacological properties. *Journal of Pharmacy and Pharmacology*, *2*, 377–392.

Kamada, T., Picoli, E., Vieira, R., Barbosa, L., Cruz, C., Otoni, W.C. (2009). Variation of morphological and physiological characters in natural populations of *Pfaffia glomerata* (Spreng.) Pedersen and their correlation with β-ecdysone production. *Revista Brasileira de Plantas Medicinais*, *11*(3), 247–256. https://doi.org/10.1590/S1516-

05722009000300004

Kliebenstein, D. J., Osbourn, A. (2012). Making new molecules - evolution of pathways for novel metabolites in plants. *Current Opinion in Plant Biology*, *15*(4), 415–423. https://doi.org/10.1016/j.pbi.2012.05.005

Lafont, R. (1997). Ecdysteroids and related molecules in animals and plants. *Archives of Insect Biochemistry and Physiology*, *35*(1–2), 3–20. https://doi.org/10.1002/(SICI)1520-6327(1997)35:1/2<3::AID-ARCH2>3.0.CO;2-X

Latil, M., Camelo, S., Veillet, S., Lafont, R., Dilda, P. J. (2021). Developing new drugs that activate the protective arm of the renin–angiotensin system as a potential treatment for respiratory failure in COVID-19 patients. *Drug Discovery Today*, *26*(5), 1311–1318. https://doi.org/10.1016/j.drudis.2021.02.010

Lei, X. Y., Xia, J., Wang, J. W., Zheng, L. P. (2018). Comparative transcriptome analysis identifies genes putatively involved in 20-hydroxyecdysone biosynthesis in *Cyanotis arachnoidea*. *International Journal of Molecular Sciences*, *19*(7), 1885. https://doi.org/10.3390/ijms19071885

Li, L., Wang, M., Pokharel, S. S., Li, C., Parajulee, M. N., Chen, F., Fang, W. (2019). Effects of elevated CO_2 on foliar soluble nutrients and functional components of tea, and population dynamics of tea aphid, *Toxoptera aurantii*. *Plant Physiology and Biochemistry*, *145*, 84–94. https://doi.org/10.1016/j.plaphy.2019.10.023

Li, Y., Kong, D., Fu, Y., Sussman, M. R., Wu, H. (2020). The effect of developmental and environmental factors on secondary metabolites in medicinal plants. *Plant Physiology and Biochemistry*, *148*, 80–89. https://doi.org/10.1016/j.plaphy.2020.01.006

Lin, X., Smagghe, G. (2019). Roles of the insulin signaling pathway in insect development and organ growth. *Peptides*, *122*, 169923. https://doi.org/10.1016/j.peptides.2018.02.001

Louback, E., Batista, D. S., Pereira, T. A. R., Mamedes-Rodrigues, T. C., Silva, T. D., Felipe, S. H. S., Rocha, D. I., Steinmacher, D. A., Otoni, W. C. (2021). CO_2 enrichment leads to altered cell wall composition in plants of *Pfaffia glomerata* (Spreng.) Pedersen (Amaranthaceae). *Plant Cell, Tissue and Organ Culture*, *145*(3), 603–613. https://doi.org/10.1007/s11240-021-02031-4

Madan, P., Jagadish, S. V. K., Craufurd, P. Q., Fitzgerald, M., Lafarge, T., Wheeler, T. R. (2012). Effect of elevated CO_2 and high temperature on seed-set and grain quality of rice. *Journal of Experimental Botany*, *63*(10), 3843–3852. https://doi.org/10.1093/jxb/ers077

Maganha, E. G., Halmenschlager, R. da C., Rosa, R. M., Henriques, J. A. P., Ramos, A. L. L. de P., Saffi, J. (2010). Pharmacological evidences for the extracts and secondary metabolites from plants of the genus *Hibiscus*. *Food Chemistry*, *118*(1), 1–10. https://doi.org/10.1016/j.foodchem.2009.04.005

Marchioretto, M. S., Miotto, S. T. S., Siqueira, C. De. (2010). O gênero *Pfaffia* Mart. (Amaranthaceae) no Brasil Maria. *Hoehnea*, *37*(3), 461–511.

Mastinu, A., Bonini, S. A., Premoli, M., Maccarinelli, G., Sweeney, E. Mac, Zhang, L., Lucini, L., Memo, M. (2021). Protective effects of *Gynostemma pentaphyllum* (Var. ginpent) against lipopolysaccharide-induced inflammation and motor alteration in mice. *Molecules*, *26*(3). https://doi.org/10.3390/molecules26030570

Moura, C. L., Casemiro, L. A., Martins, C. H. G., Cunha, W. R., Silva, M. L. de A., Cury, A. H. V. (2011). Evaluation of the antimicrobial activity of the plant species *Pfaffia glomerata* against oral pathogens. *Investigação*, *11*, 24–28.

Nakagawa, Y., Henrich, V. C. (2009). Arthropod nuclear receptors and their role in molting. *The FEBS Journal*, *276*, 6128–6157. https://doi.org/10.1111/j.1742-4658.2009.07347.x

Neto, A. G., Costa, J. M. L. C., Belati, C. C., Vinh, A. H. C., Possebom, L. S., Bastos, J. K., Silva, M. L. A. (2005). Analgesic and anti-inflammatory activity of a crude root extract of *Pfaffia glomerata* (Spreng.) Pedersen. *Journal of Ethnopharmacology*, *96*, 87–91. https://doi.org/10.1016/j.jep.2004.08.035

Neves, C. S., Gomes, S. S. L., Santos, T. R., Almeida, M. M., Souza, Y. O., Garcia, R. M. G., Otoni, W. C., Chedier, L. M., Raposo, N. R. B., Viccini, L. F., Campos, J. M. S. (2016). "Brazilian ginseng" (*Pfaffia glomerata* Spreng. Pedersen, Amaranthaceae) methanolic extract: cytogenotoxicity in animal and plant assays. *South African Journal of Botany*, *106*, 174–180. https://doi.org/10.1016/j.sajb.2016.07.003

Othman, L., Sleiman, A., Abdel-Massih, R. M. (2019). Antimicrobial activity of polyphenols and alkaloids in middle eastern plants. *Frontiers in Microbiology, 10*(5), 911. https://doi.org/10.3389/fmicb.2019.00911

Park, H., Park, G., Jeon, W., Ahn, J., Yang, Y.-H., Choi, K.Y. (2020). Whole-cell biocatalysis using cytochrome P450 monooxygenases for biotransformation of sustainable bioresources (fatty acids, fatty alkanes, and aromatic amino acids). *Biotechnology Advances*, *40* (12), 107504. https://doi.org/10.1016/j.biotechadv.2020.107504

Pereira, A. S., Dorneles, A. O. S., Bernardy, K., Sasso, V. M., Bernardy, D., Possebom, G., Rossato, L. V., Dressler, V. L., Tabaldi, L. A. (2018). Selenium and silicon reduce

cadmium uptake and mitigate cadmium toxicity in *Pfaffia glomerata* (Spreng.) Pedersen plants by activation antioxidant enzyme system. *Environmental Science and Pollution Research*, *25*(19), 18548–18558. https://doi.org/10.1007/s11356-018-2005-3

Rewitz, K. F., Gilbert, L. I. (2008). *Daphnia* Halloween genes that encode cytochrome P450s mediating the synthesis of the arthropod molting hormone: Evolutionary implications. *BMC Evolutionary Biology*, *8*(1), 1–8. https://doi.org/10.1186/1471-2148-8-60

Rharrabe, K., 1Δ, S., Lafont, R. (2010). Dietary effects of four phytoecdysteroids on growth and development of the Indian meal moth, *Plodia interpunctella*. *Journal of Insect Science*, *10*(13), 13. https://academic.oup.com/jinsectscience/article/10/1/13/825747

Riddiford, L. M., Hiruma, K., Zhou, X., Nelson, C. A. (2003). Insights into the molecular basis of the hormonal control of molting and metamorphosis from *Manduca sexta* and *Drosophila melanogaster*. *Insect Biochemistry and Molecular Biology*, *33*(12), 1327–1338. https://doi.org/10.1016/j.ibmb.2003.06.001

Roy, A., Jauhari, N., Bharadvaja, N. (2018). Medicinal plants as a potential source of chemopreventive agents. *Anticancer Plants: Natural Products and Biotechnological Implements, 2*, 109–139. Springer Singapore. https://doi.org/10.1007/978-981-10-8064-7_6

Russell, W., Duthie, G. (2011). Session 3: Influences of food constituents on gut health: Plant secondary metabolites and gut health: The case for phenolic acids. *Proceedings of the Nutrition Society*, *70*(3), 389–396. https://doi.org/10.1017/S0029665111000152

Saldanha, C. W., Otoni, C. G., Azevedo, J. L. F., Dias, L. L. C., Rêgo, M. M., Otoni, W. C. (2012). A low-cost alternative membrane system that promotes growth in nodal cultures of Brazilian ginseng [*Pfaffia glomerata* (Spreng.) Pedersen]. *Plant Cell, Tissue and Organ Culture*, *110*(3), 413–422. https://doi.org/10.1007/s11240-012-0162-5

Saldanha, C. W., Otoni, C. G., Notini, M. M., Kuki, K. N., Cruz, A. C. F., Neto, A. R., Dias, L. L. C., Otoni, W. C. (2013). A CO_2-enriched atmosphere improves in vitro growth of Brazilian ginseng [*Pfaffia glomerata* (Spreng.) Pedersen]. *In Vitro Cellular & Developmental Biology - Plant*, *49*(4), 433–444. https://doi.org/10.1007/s11627-013-9529-5

Saldanha, C. W., Otoni, C. G., Rocha, D. I., Cavatte, P. C., Detmann, K. da S. C., Tanaka, F. A. O., Dias, L. L. C., DaMatta, F. M., Otoni, W. C. (2014). CO_2-enriched atmosphere and supporting material impact the growth, morphophysiology and ultrastructure of in vitro Brazilian-ginseng [*Pfaffia glomerata* (Spreng.) Pedersen] plantlets. *Plant Cell,*

Tissue and Organ Culture, *118*(1), 87–99. https://doi.org/10.1007/s11240-014-0464-x

Sharma, A., Shahzad, B., Rehman, A., Bhardwaj, R., Landi, M., Zheng, B. (2019). Response of phenylpropanoid pathway and the role of polyphenols in plants under abiotic stress. *Molecules*, *24*(13), 2452. https://doi.org/10.3390/molecules24132452

Silva, T. D., Batista, D. S., Castro, K. M., Fortini, E. A., Felipe, S. H. S., Fernandes, A. M., Sousa, R. M. J., Chagas, K., Silva, J. V. S., Correia, L. N. F., Torres-Silva, G., Farias, L. M., Otoni, W. C. (2020b). Irradiance-driven 20-hydroxyecdysone production and morphophysiological changes in *Pfaffia glomerata* plants grown in vitro. *Protoplasma, 258*(1), 151–167. https://doi.org/10.1007/s00709-020-01558-1

Silva, T. D., Batista, D. S., Fortini, E. A., Castro, K. M., Felipe, S. H. S., Fernandes, A. M., Sousa, R. M. J., Chagas, K., Silva, J. V. S., Correia, L. N. F., Farias, L. M., Leite, J. P. V., Rocha, D. I., Otoni, W. C. (2020a). Blue and red light affects morphogenesis and 20-hydroxyecdisone content of in vitro *Pfaffia glomerata* accessions. *Journal of Photochemistry and Photobiology B: Biology*, *203*, 111761. https://doi.org/10.1016/j.jphotobiol.2019.111761

Singh, A., Pandey, B., Kumari, S., Agrawal, M. (2015). Nitrogen availability modulates CO_2-induced responses of *Catharanthus roseus*: Biomass allocation, carbohydrates and alkaloids profile. *Journal of Applied Research on Medicinal and Aromatic Plants*, *2*(4), 160–167. https://doi.org/10.1016/j.jarmap.2015.07.002

Singh, S., Singh, D. B., Singh, S., Shukla, R., Ramteke, P. W., Misra, K. (2019). Exploring medicinal plant legacy for drug discovery in post-genomic era. *Proceedings of the National Academy of Sciences, India Section B: Biological Sciences*, *89*(4), 1141–1151. https://doi.org/10.1007/s40011-018-1013-x

Skrebsky, E. C., Tabaldi, L. A., Pereira, L. B., Rauber, R., Maldaner, J., Cargnelutti, D., Gonçalves, J. F., Castro, G. Y., Shetinger, M. R. C., Nicoloso, F. T. (2008). Effect of cadmium on growth, micronutrient concentration, and δ-aminolevulinic acid dehydratase and acid phosphatase activities in plants of *Pfaffia glomerata*. *Brazilian Journal of Plant Physiology*, *20*(4), 285–294. https://doi.org/10.1590/S1677-04202008000400004

Sun, Y., Guo, H., Ge, F. (2016). Plant – aphid interactions under elevated CO_2: Some cues from aphid feeding behavior. *Frontiers in Plant Science*, *7*, 1–10. https://doi.org/10.3389/fpls.2016.00502

Sun, Y., Guo, H., Zhu-Salzman, K., Ge, F. (2013). Elevated CO_2 increases the abundance of the peach aphid on *Arabidopsis* by reducing jasmonic acid defenses. *Plant Science*, *210*,

128–140. https://doi.org/10.1016/j.plantsci.2013.05.014

Thakur, M., Bhattacharya, S., Khosla, P. K., Puri, S. (2019). Improving production of plant secondary metabolites through biotic and abiotic elicitation. *Journal of Applied Research on Medicinal and Aromatic Plants*, 12, 1–12. https://doi.org/10.1016/j.jarmap.2018.11.004

Tsukagoshi, Y., Ohyama, K., Seki, H., Akashi, T., Muranaka, T., Suzuki, H., Fujimoto, Y. (2016). Functional characterization of CYP71D443, a cytochrome P450 catalyzing C-22 hydroxylation in the 20-hydroxyecdysone biosynthesis of *Ajuga hairy* roots. *Phytochemistry*, *127*, 23–28. https://doi.org/10.1016/j.phytochem.2016.03.010

Tzin, V., Galili, G. (2010). The biosynthetic pathways for shikimate and aromatic amino acids in *Arabidopsis thaliana*. *The Arabidopsis Book*, *8*, e0132. https://doi.org/10.1199/tab.0132

Vogt, T. (2010). Phenylpropanoid biosynthesis. *Molecular Plant*, *3*(1), 2–20. Oxford University Press. https://doi.org/10.1093/mp/ssp106

Wang, Y., Yang, Y., Chi, D. (2018). Transcriptome analysis of abscisic acid induced 20E regulation in suspension *Ajuga lobata* cells. *3 Biotech*, *8*(8), 320. https://doi.org/10.1007/s13205-018-1352-6

Zhang, Y., Deng, T., Sun, L., Landis, J. B., Moore, M. J., Wang, H., Wang, Y., Hao, X., Chen, J., Li, S., Xu, M., Puno, P. T., Raven, P. H., Sun, H. (2021). Phylogenetic patterns suggest frequent multiple origins of secondary metabolites across the seed-plant "tree of life." *National Science Review*, *8*(4), nwaa105. https://doi.org/10.1093/nsr/nwaa105

Zhou, F., Pichersky, E. (2020). More is better: the diversity of terpene metabolism in plants. *Current Opinion in Plant Biology*, *55*, 1–10. https://doi.org/10.1016/j.pbi.2020.01.005

CHAPTER 1

Effect of CO_2-enriched atmosphere on morphophysiological, biochemical and molecular in *Pfaffia glomerata*

Abstract

Carbon dioxide (CO_2) is an important regulator of plant growth and development, and its concentration in the atmosphere continues to increase progressively due to intense anthropogenic activities. In order to investigate the effects of elevated CO_2 on morphophysiological, biochemical, and molecular responses, *Pfaffia glomerata* were exposed to two CO_2 concentrations: a[CO_2] (± 400 µmol mol^{-1}) and e[CO_2] (± 800 µmol mol^{-1}), in open top chambers (OTC). Our data showed that at e[CO_2] the photosynthetic rate (A_N) increased significantly, while stomatal conductance (g_s) and transpiration rate (E) reduced, resulting in a significant increase in water use efficiency (WUE). The higher photosynthetic efficiency of plants under e[CO_2] favoring higher growth, biomass accumulation, and increase in photosynthetic pigments, and consequently higher accumulation of glucose and sucrose in the early evening. Proteomics analysis revealed 33 common differential accumulated proteins (DAPs), mainly related to carbohydrate and energy metabolism (e.g. Ribulose-1,5-bisphosphate carboxylase/oxygenase), reinforce the influence of e[CO_2] on increased carbohydrate production. In contrast, e[CO_2] promoted a reduction in total protein content and some amino acids (e.g. aspartate and glutamate). We also observed that the methionine and cysteine metabolism pathways were down-accumulated. Secondary metabolism was also affected by e[CO_2] by means of a positive regulation in three genes (*PgCAD*, *PgC4H*, and *PgCCR*) and in the biosynthesis of both phenylalanine and tyrosine, which regulate the phenylpropanoid pathway, a precursor of lignin. In addition, the anatomical characterization of the stem strengths the hypothesis that e[CO_2] favors lignin accumulation. However, stem and root 20-hydroxyecdysone (20E) levels were reduced in plants under e[CO_2], suggesting that 20E contents, as well as other primary and secondary metabolites can be altered by e[CO_2]. In conclusion, growing *P. glomerata* plants in e[CO_2] may represent a strategy toobtain plants with higher biomass, as well as to alter the content of plant defense compounds.. This work opens new perspectives to understand the effect of increasing [CO_2] in *P. glomerata*.

Keywords: Brazilian ginseng. Climatic changes. Medicinal plants. Photosynthesis. Proteomics.

INTRODUCTION

The increase in the atmospheric concentration of carbon dioxide (CO_2) by anthropogenic activities is a key factor in climate change. Since the industrial revolution to date, the CO_2 concentration has increased by more than 66% (www.esrl.noaa.gov/gmd/ccgg/trends/), with a projection of reaching more than 800 ppm by 2100 (IPCC, 2022). However, the increase in CO_2 concentration is not a climate condition isolated from global warming, extreme weather events such as storms, heat wave, frost, drought, and salinity are associated with the impact of elevated CO_2 concentration (e[CO_2]) (Soares et al., 2019).

The general effects of e[CO_2] on the regulation of plant growth, development and metabolism are widely explored, especially in agricultural crops (Chumley and Hewlings, 2020; DaMatta et al., 2018; Madan et al., 2012). Studies show that e[CO_2] can optimize net photosynthetic rate (A_N), reduce stomatal conductance (g_S), transpiration rate (E), and photorespiration (Drake et al., 1997; Dusenge et al., 2019; Gasparini et al., 2019) favoring greater plant growth and production (Avila et al., 2020b; Brito et al., 2020; Terrer et al., 2021). In addition, e[CO_2] can promote the accumulation of soluble sugars, such as glucose, fructose, and sucrose, and the accumulation of antioxidants, including phenolic compounds, ascorbates, alkaloids, and some antioxidant enzyme activities (Dong et al., 2018; Ehleringer and Bjorkman, 1977; Yi et al., 2018). However, e[CO_2] can reduce the levels of protein, nitrate, Mg, Fe, and Zn affecting the nutritional quality of plants, especially grains (Bisbis et al., 2018; Ebi et al., 2021). This dietary nutrient deficiency can occur through "carbohydrate dilution" in which there is an increase in assimilated carbon (C) relative to nitrogen (N) ratio concentration, decrease in transpiration rates that reduce nutrient mass flow, and a shift in nutrient allocation by biochemical processes (Houshmandfar et al., 2015; Matimati et al., 2014; Soares et al., 2019).

Although the physiological and biochemical responses of agricultural plants under e[CO_2] are well elucidated, these changes in medicinal plants are still poorly understood (Al Jaouni et al., 2018; Almuhayawi et al., 2021; Gairola et al., 2010). The e[CO_2] was responsible for altering the phytochemical content, especially phenolic compounds, and biological activities of several species such as *Panax ginseng*, *Labisia pumila*, *Gynostemma pentaphyllum*, *Isatis indigotica* (Ali et al., 2005; Chang et al., 2016; Jaafar et al., 2012; Li et al., 2017). In fenugreek (*Trigonella foenum-graecum* L.) e[CO_2] represented an efficient strategy to increase hypocholesterolemic, antioxidant and antibacterial activities (Hozzein et al., 2020).

In *Camellia Sinensis* (Indian tea) e[CO_2] increases the content of flavonoids, theanine and salicylic acid, but decreases the content of caffeine, which seems to have attenuated the defense responses of this plant (Ahammed et al., 2020). Studies on the possible effects of climate change on medicinal plants are particularly significant because of their value within folk medicine and as economically useful plants.

Medicinal plants are highly valuable for human livelihood and Brazil is well recognized among areas rich in unique medicinal plants of global importance. Among the species of herbal interest stands out *Pfaffia glomerata* (Amaranthaceae), popularly known as Brazilian ginseng (Neves et al., 2016), an herbaceous species native to South America and widely distributed in Brazil (Marchioretto et al., 2010). *P. glomerata* is a medically and economically important species with proven phytotherapeutic properties (Dias et al., 2019; Franco et al., 2021; Moura et al., 2011; Neto et al., 2005; Neves et al., 2016). Its medicinal properties are mainly due to 20-hydroxyecdysone (20E). 20E is the main hormone related to the ecdysis process in insects (zooecdysteroid), but acts as a secondary metabolite (phytoecdysteroid) in plants (Dinan, 2001; Dinan and Lafont, 2006b; Nakagawa and Henrich, 2009b). The pathway of 20E biosynthesis is not fully elucidated (Felipe et al., 2019a; Festucci-Buselli et al., 2008; Tsukagoshi et al., 2016); moreover, the role of 20E in plants is also not entirely clear. Due to the economic interest of 20E, it is necessary to understand how climate change impacts the production of this compound in order to clarify its biosynthesis pathway and function in plants.

Several studies have demonstrated that *P. glomerata* shows great plasticity and adaptability to changes in abiotic conditions, such as different light conditions (Felipe et al., 2019a; Fortini et al., 2020; Silva et al., 2020a, 2020b), heavy metals (Bernardy et al., 2020; Gomes et al., 2013; Gupta et al., 2013; Pereira et al., 2018), and salinity (Felipe et al., 2019b). In addition, previous studies have shown improvements in the quality of in vitro plants of *P. glomerata* grown in a CO_2-enriched atmosphere. The e[CO_2] contributed to higher biomass growth and accumulation, higher photosynthetic rate, lower relative leaf water loss, and modification of primary cell wall compounds in *P. glomerata* (Louback et al., 2021; Saldanha et al., 2013). Subsequently, it was demonstrated in this same species that e[CO_2] associated with cultivation on porous substrate (Florialite®), increased growth and 20E levels, caused ultrastructural changes in chloroplasts (Saldanha et al., 2014) and regulated the profile of several metabolites (Ferreira et al., 2019). However, so far CO_2-enrichment studies in *ex vitro* environment in *P. glomerata* are lacking. Therefore, here the objective was to evaluate the

effect of the CO_2-enriched atmosphere on morphophysiological, biochemical, structural and molecular aspects in *P. glomerata*.

MATERIALS AND METHODS

Plant material and experimental design

P. glomerata plants (Accession 22) came from a germplasm bank of the Plant Tissue Culture Laboratory (LCT-II, BIOAGRO, Universidade Federal de Viçosa). Voucher material was deposited at the Leopoldo Krieger Herbarium (UFJF, Juiz de Fora, MG, Brazil) under code number CESJ 63317. Access to the genetic material (permission number AA2A367) was granted by the Brazilian National System for the Management of Genetic Heritage and Associated Traditional Knowledge (SISGEN), in accordance with current Brazilian biodiversity legislation.

Nodal segments (≈ 1.5 cm) without leaves of *P. glomerata* were grown in vitro on MS medium (Murashige and Skoog, 1962), supplemented with vitamins, and myo-inositol (100 mg L^{-1}) (Sigma-Aldrich Co, St Louis, MO, USA), and solidified with 5.5 g L^{-1} agar (PhytoTechnology Laboratories®, KS, USA). The flasks were closed with rigid polypropylene lids with two 10 mm holes covered by two 0.45 μm-pore hydrophobic fluoropore polytetrafluoroethylene membranes (MilliSeal AVS-045 Air Vent, Tokyo, Japan), with the CO_2 exchange rate of 25 μL L^{-1} s^{-1} (Batista et al., 2017). The cultures were maintained at 25 ± 2 °C, under 60 μmol m^{-2} s^{-1} irradiance and 16 h light photoperiod for 30 days.

After the in vitro culture, plants were acclimatized for 7 days in 300 mL plastic cups (COPOBRAS, São Ludgero, SC, Brazil). Then, they were transplanted into plastic pots with 2 kg of commercial substrate Tropstrato HT® (Vida Verde, Mogi Mirim, Brazil) and the plants were grown in a greenhouse (average temperature 25/21 ± 2 °C, day/night; naturally fluctuating air humidity and photosynthetic photon flux density (PPFD)). The plants were transferred to open top chambers (OTC) (1.15 m diameter and 1.40 m high) and subjected to a CO_2-enriched atmosphere. CO_2 fumigation was accomplished from 06:00 to 18:00 h and was checked daily the [CO_2], temperature, and humidity using portable CO_2 sensors (model CO277, Akso Produtos Eletrônicos, São Leopoldo, Brazil). During the greenhouse cultivation (28 days in total, being 7 days of acclimation and 21 days of experiment), the plants were fertilized on days 1 and 15 with 5.5 g NPK - 15:09:12 (Osmocote® Plus, São Paulo, Brazil). Three independent experiments were conducted from October 2019 to February 2021 within the same OTC.

The experiment was designed in a completely randomized design, corresponding to two CO_2 concentration regimes: ambient [CO_2] (a[CO_2], ≈400 μmol mol^{-1}); and elevated

[CO_2] (e[CO_2], ≈800 μmol mol^{-1}). After 21 days of cultivation in OTC, growth and photosynthetic parameters were evaluated. Sections of leaves of different ages (expanding, mature, and senescent) and the stem were also collected for anatomical characterization. In addition, leaf samples were collected at three times of the day (6:00 am, 12:00 pm, and 6:00 pm), and immediately frozen in liquid nitrogen and stored at -80 ºC for further biochemical and molecular analyses.

Growth parameters

Stem length (cm), number of branches, dry mass (g), number of leaves, and leaf area (cm^2) were measured. For determination of leaf area, leaves were detached and fixed individually on white plasticized graph paper. Photographs were taken with a digital camera and images were processed using ImageJ software (Schneider et al., 2012). Dry weight (g) was obtained by oven-drying the plant material at 50°C for 72 h.

Gas exchange parameters

The net carbon assimilation rate (A_N), stomatal conductance (g_s), transpiration (E) and the instantaneous water use efficiency (WUE) calculated by the ratio A_N/E was evaluated with the aid of an infrared gas analyzer (LI-6400, Li-Cor Inc., Lincoln, Nebraska, EUA). Measurements were conducted after 1 h of illumination during the light period under PPFD of (1000 μmol m^{-2} s^{-1}). The reference CO_2 concentration was set at 400 μmol CO_2 mol^{-1} of air in plants under a[CO_2] and 800 μmol CO_2 mol^{-1} of air in plants under e[CO_2]. All measurements were performed using the 2 cm^2 leaf chamber at 25°C, and the leaf-to-air vapor pressure deficit was kept at 1.2-2.0 kPa, while the amount of blue light was set to 10% PPFD to optimize stomatal aperture. Respiration rates in the dark (R_d) was determined using the same equipment during the dark period, after 1 h from the end of the light period (Niinemets and Sack, 2006).

The responses of A_N to internal CO_2 concentration (Ci) (A_N/C_i curves) were performed at 1000 μmol m^{-2} s^{-1} at 25°C under ambient O_2. Briefly, the measurements started at the ambient CO_2 concentration (C_a) of 400 μmol mol^{-1} and once the steady state was reached, C_a was decreased stepwise to 50 μmol mol^{-1}. Upon completion of the measurements at low C_a, C_a was returned to 400 μmol mol^{-1} to restore the original A_N. Next, C_a was increased stepwise

to 1400 μmol mol^{-1} for a total of 13 different C_a values (Long and Bernacchi, 2003). Corrections for the leakage of CO_2 into and water vapor out of the leaf chamber of the LI-6400 were applied to all gas exchange data as described by Rodeghiero et al. (2007).

From A_N/C_i curves, the maximum carboxylation velocity (V_{cmax}), the maximum capacity for electron transport rate (J_{max}), and the use of triose phosphate (TPU) were calculated by fitting the mechanistic model of CO_2 assimilation (Farquhar et al., 1980), using the C_i based on temperature of kinetic parameters of Rubisco (Kc and Ko) (Walker et al., 2013), While, V_{cmax}, J_{max} and TPU were normalized to 25ºC using the temperature response equations from Sharkey et al. (2007).

Metabolite analysis

Leaf samples (second fully expanded leaf from the apex of plants) were harvested at three times of the day: 6:00 am (anti-morning), 12:00 pm (midday), and 6:00 pm (evening). The samples were flash frozen in liquid nitrogen, and subsequently ground and lyophilized for analysis. Approximately 10 mg lyophilized tissues were used for extraction with methanolic as described by Lisec et al. (2006). Photosynthetic pigments were determined as described by Porra et al. (1989) and anthocyanin by Neff and Chory (1998). Carbohydrates (starch, sucrose, glucose, and fructose) were evaluated as described by Fernie et al. (2001). Protein and total amino acid levels were analyzed as reported in Gibon et al. (2004). Proline content followed the methodology proposed by Bates et al. (1973), with some modifications described previously by Felipe et al. (2019b).

Other metabolites of interest were quantified by gas chromatography-mass spectrometry (GC-MS). Approximately 10 mg lyophilized leaf tissues was extracted in 1.5 mL of extraction solution (water:methanol:chloroform, 1:2.5:1 *v/v*) as described by Fiehn (2007), using 5 μM ribitol (Sigma-Aldrich) as the internal standard. The extract (400 μL) was dried in a vacuum concentrator and derivatized in two steps using the MPS Dual Head autosampler (Gerstel), as described by Gu et al. (2012). After incubation for 2 h at room temperature, the samples were analyzed as described previously (Shim et al., 2020) using the 5977B GC-MSD system (Agilent Technologies). The peaks were integrated using MassHunter Quantitative (v b08.00; Agilent Technologies). For relative quantification, metabolite peak areas were normalized to the corresponding dry weight and peak area of the internal standard (ribitol).

Enzyme analysis and lipid peroxidation

The enzymes catalase (CAT, EC 1.11.1.6), ascorbate peroxidase (APX, EC 1.11.1.11), superoxide dismutase (SOD, EC 1.15.1.1), and peroxidase oxidoreductase (POD, EC1.11.1.7) were quantifed. Briefly, 50 mg of macerated leaf samples were collected and extracted in 1 mL extraction medium containing 0.1 M potassium phosphate buffer, pH 6.8; 0.1 mM ethylenediaminetetraacetic acid; 1 mM phenylmethylsulfonyl fuoride and 1% (*w/v*) polyvinylpolypyrrolidone. Then, the sample was centrifuged at 16,000 *g* for 15 min at 4 °C, and the supernatant was removed and set aside on ice for enzyme assays plus protein determination (Bradford, 1976). CAT, APX, and POD activities were determined as proposed previously (Chance and Maehly, 1955; Havir and McHale, 1987; Nakano and Asada, 1981) and expressed as $\mu mol^{-1}\ min^{-1}\ mg^{-1}$ protein. SOD activity was measured as described earlier (Giannopolitis and Ries, 1977) and expressed as $U\ min^{-1}\ mg^{-1}$ protein, with 1 U being equivalent to the concentration of SOD required to inhibit 50% of nitro blue tetrazolium photoreduction.

Lipid peroxidation was determined based on the quantification of malondialdehyde (MDA), as proposed by por (Lima et al., 2002) with modifications. Extraction was performed by adding 1 mL of 1% trichloroacetic acid (TCA) to 50 mg of fresh and macerated leaf samples. The solution was vortexed and centrifuged at 12.000 *g* for 15 min at 4 °C, after which 125 µL of the supernatant were transferred to new tubes, along with 375 µL of 0.5% 2-thiobarbituric acid (*w/v*) in 20% TCA (*w/v*). The reaction proceeded for 30 min with shaking at 95°C, and was blocked by incubation in an ice bath. The supernatants were transferred to new tubes, centrifuged at 10.000 *g* for 10 min at 4°C, and read on a spectrophotometer at 532 and 600 nm. With the absorbance values, the means of the triplicates were obtained and the MDA concentration was determined by the equation of Heath and Packer (1968), expressing the results in nmol g^{-1} FW.

Quantification of 20E

The 20E quantification was performed according to the methodology described by Corrêa et al. (2015). Briefly, a methanolic extraction of macerated samples of leaves, stem and roots was performed. The determination of 20E was done using a Shimadzu Proeminence liquid chromatography system (Shimadzu, Kyoto, Japan) equipped with RP column (150 mm x 4,6 mm i.d., 5 µm particle size; C18 stationary phase) from Phenomenex (Torrance, CA)

and a Shimadzu SPD –M20A photodiode array detector (monitoring 246 nm). The mobile phase of 1:1 (*v/v*) methanol:water, the flow rate of 1.0 mL min^{-1}, injection of 20 μL of extract, and with reading at 245 nm for 15 min. A 20E standard (Sigma-Aldrich) solution was prepared to quantify a calibration curve (0-120 mg L^{-1}). 20E content was expressed by mg g^{-1} DW and 20E production by g.

Anatomical and histochemical characterization

For the anatomical studies, transverse sections of the midrib of leaves from three phenological stages (expanding, mature and senescent) and of stems from the midrib of the fourth internode were collected. Then, the samples were fixed in Karnovsky's solution (Karnovsky, 1964), composed of: 2.5% glutaraldehyde, 4.0% paraformaldehyde, 5 mM CaCl2, in 0.1M cacodylate buffer, pH 6.8, and kept refrigerated. After fxation, the samples were dehydrated in ethanolic series and included in acrylic resin (Historesin®, Leica Instruments, Wetzlar, Germany). Transverse sections (5 μm thickness) were obtained on an automated advance rotary microtome (RM2155, Leica Microsystems Inc., Buffalo Grove, IL, USA). For structural characterization, samples were stained in toluidine blue (pH 3.2) for 3 min (O'Brien and McCully, 1981). The sections were then mounted on glass slides with synthetic Permount® SP15-500 resin (Fisher Chemicals, Thermo Fisher Scientifc, Waltham, MA, USA) and observed under a light microscope.

For histochemical analyses, stem sections from the median region of the fourth internode were cut with a manual microtome (LPC, Rolemberg and Bhering, Belo Horizonte, Brazil). Stem sections were stained with 1% phloroglucinol and HCl (Wiesner's reaction) to detect lignin (Trabucco et al., 2013) and with Calcofluor White 0.01% (Hughes and McCully, 1975) in which β-1,3 and β-1,4 glucan bonds are stained blue-white. Images were captured on a light microscope (AX70 TRF; Olympus Optical, Tokyo, Japan) with a U-photo system, coupled to a digital color camera (Spot Insight 3.2.0; Diagnostic Instruments Inc., Sterling Heights, MI, USA) and microcomputer with the Spot Basic image capture program.

Transmission electron microscopy

For ultrastructural analysis, senescent leaf samples were fixed in glutaraldehyde solution (2.5%) in 0.1 M sodium cacodylate buffer (pH 7.0). Then, the samples were washed with 0.1 M sodium cacodylate buffer (pH 7.0) and post-fixed in 1% osmium tetroxide and contrasted with 0.5% uracil acetate. The samples were then dehydrated in increasing ethanol concentration series, infiltrated and polymerized in LR White resin (Sigma-Aldrich). Ultra-thin sections (60-80 nm thick) were obtained on an ultramicrotome Power Tome-X (RMC Products, Tucson, USA) and contrasted with uranyl acetate and lead citrate (Reynolds, 1963). The analyses were performed on a Zeiss EM 109 and Libra 120 transmission electron microscope (Carl Zeiss, Germany).

RNA extraction, cDNA synthesis, and quantitative PCR analysis

Total RNA was extracted of shoot samples using the TRI Reagent® (Sigma-Aldrich Co.) as recommended by the manufacturer. To remove contamination with genomic DNA, RNA was treated with DNase I (Thermo Scientific NanoDrop Technology, Wilmington, DE, USA). Then, cDNA was synthesized with the Super Script™ III kit (Invitrogen, Carlsbad, CA, USA). We evaluated the expression of genes belonging to the lignin biosynthesis pathway: cinnamate 4-hydroxylase (*PgC4H*), caffeoyl-CoA O-methyltransferase (*PgCCoAOMT*), cinnamoyl-CoA reductase (*PgCCR*), and cinnamyl alcohol dehydrogenase (*PgCAD*) obtained from the transcriptome of *P. glomerata* were evaluated (Batista et al., 2019a). The *glyceraldehyde-3-phosphate dehydrogenase* (*GAPDH*) gene was used for normalization (Batista et al., 2019b). Expression analyses were performed by real-time PCR on a CFX96 Touch™ device (BIO-RAD) using SYBR Green Master Mix (BIO-RAD), the reactions were performed with three biological replicates in duplicate technique each, in a reaction volume of 10 μL (4 μL of SYBR-Green, 1 μL (4 μM) of each primer, 3 μL of diethylpyrocarbonate-treated water and 1 μL (40 ng) of cDNA. The amplification conditions were performed in the following steps: 2 min at 50 ºC and 10 min at 95 ºC, followed by 40 cycles of 95 ºC for 16 s and 60 ºC for 60 s, and the dissociation curve from 60 to 95 ºC at 0.1 ºC s^{-1}. Transcript levels were determined using the $2^{-\Delta\Delta Ct}$ method (Livak and Schmittgen, 2001), with three biological replicates with at least two technical replicates each.

Protein extraction and digestion

Proteomic analyses were performed using freeze-dried and macerated leaf samples (three biological replicates, 60 mg DW each sample). The extraction was performed by the methodology described by Damerval et al. (1986), by suspending the samples in a buffer solution (10% (*w/v*) Trichloroacetic acid/acetone (Sigma-Aldrich) together with 20 mM of Dithiothreitol (DTT, GE Healthcare, Piscataway, NJ, USA), with subsequent vortex mixing (5 min, 8 °C). The solution was kept for 60 min at -20 °C and then centrifuged (16.000 *g*, 30 min, 4 °C). The pellets from the previous step were washed 3 times in acetone solution with DTT (20 mM) and centrifuged for 5 min each wash. Subsequently, the pellets were dried under vacuum, solubilized in a buffer composed of 7 M urea (GE Healthcare), 2 M thiourea (GE Healthcare), 2% Triton X-100 (GE Healthcare), 1% DTT, 1 mM phenylmethylsulfonyl fluoride (PMSF; Sigma-Aldrich), and 5 µM pepstatin (Sigma-Aldrich), and incubated for 30 min on ice. The samples were vortexed (16.000 *g*, 30 min, 8 °C), the supernatants were collected, and the protein concentration was measured using a 2-D Quant Kit (GE Healthcare). Before the trypsin digestion step, protein samples (100 µg from each biological replicate) were precipitated using the methanol/chloroform, and the samples were resuspended in a solution buffer (urea 7 M/thiourea 2 M). Protein digestion was performed by filter-aided sample preparation (FASP) methodology according to Reis et al. (2021). Then, the peptides and proteins were quantified through a NanoDrop 2000c spectrophotometer (Thermo Fisher Scientific, Waltham, MA, USA), at a wavelength of 205 nm. The peptides were stored at −80 °C prior to analyses.

Mass spectrometry analysis

Mass spectrometry was performed using a nanoAcquity UPLC connected to a Q-TOF SYNAPT G2-Si instrument (Waters, Manchester, UK) according to Passamani et al. (2020). Briefly, runs consisted of three biological replicates of 1 µg of digested peptides. During separation, samples were loaded onto the nanoAcquity UPLC M-Class Symmetry C18 5 µm trap column (180 µm × 20 mm) at 5 µl min^{-1} for 3 min and then onto the nanoAcquity M-Class HSS T3 1.8 µm analytical reversed-phase column (75 µm × 150 mm) at 400 nl min^{-1}, with a column temperature of 45°C. For peptide elution, a binary gradient was used, with mobile phase A consisting of water (Tedia; Fairfield, Ohio, USA) and 0.1% formic acid (Sigma-Aldrich) and mobile phase B consisting of acetonitrile (Sigma-Aldrich) and 0.1%

formic acid. The gradient elution started at 7% B, then ramped from 7 B to 40% B until 91.12 min, then ramped again from 40 B to 99.9% B until 92.72 min, then remained at 99.9% until 106.00 min, then decreased to 7% B until 106.1 min, and finally remained at 7% B until the end of run at 120 min. Mass spectrometry was performed in positive and resolution mode (V mode), at 35,000 FWHM, with ion mobility, and in data-independent acquisition mode (HDMSE). Human [Glu1]-fibrinopeptide B at 100 fmol μl^{-1} was used as an external calibrant, and lock mass acquisition was performed every 30 s. Mass spectra were acquired by MassLynx v 4.1 software.

Proteomic data analysis

Spectra processing and comparative analysis were performed according to Passamani et al. (2020). Spectra processing and database searching were performed using ProteinLynx Global Server (PLGS) software v. 3.0.2 (Waters). The Apex3D parameters were set to a low-energy threshold of 150 counts, an elevated-energy threshold of 50 counts, and an intensity threshold of 750 counts. In addition, the analysis settings included the following: one missed cleavage, minimum fragment ion per peptide equal to 3, minimum fragment ions per protein equal to 7, minimum peptide per protein equal to 2, automatic peptide and fragment tolerance, a fixed modification of carbamidomethyl and variable modifications of oxidation and phosphoryl. The false discovery rate (FDR) was set to a maximum of 1%. The proteomics data were processed against the *P. glomerata* data base (http://www.ncbi.nlm.nih.gov/biosample/8103044; Batista et al., 2019a). Comparative label-free quantification was performed using ISOQuant software v. 1.7 (Distler et al., 2014). Briefly, for ISOQuant the following parameters were used to identify proteins: a 1% FDR, a peptide score greater than six, a minimum peptide length of six amino acids, and at least two peptides per protein were required for label-free quantitation using the TOP3 approach, followed by the multidimensional normalized process within ISOQuant. The mass spectrometry proteomic data have been deposited with ProteomeXchange (Deutsch et al. 2019). Consortium via the PRIDE (Perez-Riverol et al. 2019) partner repository.

For comparative proteomic analysis, only proteins present in all three biological replications, or absent in all replicates (for unique proteins) were considered. Data were analyzed using Student's *t*-test ($P \leq 0.05$). Also, the criterion of Log_2 fold change (FC) was considered for the calculation of the differential accumulated proteins (DAPs), being

considered up-accumulated when Log_2 FC > 0.6 and down-accumulated when Log_2 FC < -0.6. Description and functional annotation were performed for the DAPs using OmicsBox software (https://www.biobam.com/omicsbox). The protein sequences were submitted to a Basic Local Alignment Search Tool (BLAST) search against the National Center for Biotechnology Information (NCBI) nonredundant green plant protein database (taxa: 33090, Viridiplantae). An analysis of the enrichment of biological processes and cellular components of DAPs was performed by Fisher's exact test (P < 0.01) using OmicsBox. A Kyoto Encyclopedia of Genes and Genomes (KEGG) enrichment pathway analysis between DAPs (P < 0.01) was performed.

Statistical analysis

The data was subject to a *t*-Student test to analyze the difference between the treatment ($P \leq 0.05$). A Pearson correlation analysis was also performed (*t*-Student; $P \leq 0.05$) for the variables that differed significantly. Positive and negative correlation coefficients (r) among the variables were classified as: 0.0–0.2, no correlation; 0.2–0.4, weak; 0.4–0.6, moderate; 0.6–0.8, strong; and 0.8–1.0, very strong. All analyses were performed using GENES software (Cruz, 2016).

RESULTS

Elevated CO_2 promoted greater biomass accumulation

After 21 days of culture in the OTCs (Fig. 1), the growth and development of *P. glomerata* were significantly different (Figs. 2 and 3). Compared to a[CO_2], e[CO_2] promoted a significant increase in leaf area (12%), number of leaves (18%), stem length (5%), leaves dry weight (19%), stems dry weight (26%) (Fig. 3 A-E), total dry weight (21%) (Fig. 3G), and total branches (24%) (Fig 3H). However, there was no significant difference in roots dry weight (Fig. 3F). A higher biomass allocation occurred in stems of plants grown under e[CO_2], whereas the same did not occur in the leaves and root (Fig. 3I).

Elevated CO_2 positively affects photosynthetic performance and efficient water use

We observed significant increment in photosynthetic rate (A_N) (33%) and instantaneous water use efficiency (WUE) (54%) in plants under e[CO_2] compared to a[CO_2] (Fig. 4A and E). Conversely, e[CO_2]-exposed plants significantly reduced stomatal conductance (g_S) (29%) and transpiration (E) (28%) (Fig. 4C and D). There was no significant difference in the dark respiration rate (R_d) (Fig. 4B). Plants under e[CO_2] showed better performance on the A_N/C_i curve, since A_N increased gradually with higher C_i (Fig. 4F). In addition, an increase (14%) in the use of phosphate trioses (TPU) was observed in e[CO_2] condition, but there was no significant difference in RuBisCO carboxylation rate (V_{cmax}), maximum electron transport rate (J*max*) and CO_2 compensation point (Fig. S1).

Primary metabolism is altered by elevated CO_2

Compared to a[CO_2], chlorophyll (Chl) content was significantly increased in plants under e[CO_2], Chl *a* (16%), Chl *b* (15%), total Chl (16%) (Fig. 5A-C), and carotenoid content (11%) (Fig. 5E). Regarding the Chl *a*/Chl *b* ratio and the anthocyanin content, there was no significant difference (Fig. 5D and F). We analyzed the metabolites glucose, fructose, sucrose, starch, free amino acids, and total protein at three periods of the day (anti-morning, midday, and evening) and did not observe a specific pattern among the treatments (Fig. 6). Plants

under e[CO_2] showed higher glucose (27%) and sucrose (24%) levels in the evening, but glucose levels were lower (41%) in the anti-morning (Fig. 6A and C). We also observed a reduction in starch (9%) and protein (37%) levels in the midday period (Fig. 6D and F). Regardless the period of the day, no statistical difference in fructose and free amino acid contents was detected (Fig. 6B and E).

In addition, we performed analyses of some metabolites of interest using GC-MS. These analyses allowed the identification and quantification of 13 metabolites (Table S1). Among these metabolites, 4 exhibited significantly different levels in plants under e[CO_2], aspartate, glutamate and glycerate showed reduced levels, while alanine higher levels (Fig. 7, Table S1).

Antioxidant enzymes and proline content is not affected by elevated CO_2

The activity of antioxidant enzymes (APX, CAT, POD, and SOD), MDA formation and proline content were not significantly influenced by [CO_2] (Fig. S2).

Elevated CO_2 negatively affects 20E content

In respect to a[CO_2], there was a significant reduction in 20E content in the stems (41%) and roots (38%) of plants under e[CO_2] (Fig. 8A). However, only stems displayed significant reduction (28%) in the production of this metabolite (Fig. 8B). There was no significant difference in 20E content of leaves, as well as in 20E production in leaves and roots (Fig. 8).

Elevated CO_2 promoted anatomical changes

There were no remarkable structural changes in the anatomy of expanding and mature leaves of plants grown under different [CO_2] conditions (Fig. 9A-H). The expanding leaves consist of juxtaposed cells with a dense nucleus, uniseriate epidermis with the presence of trichomes, a large central vascular bundle with parenchyma distributed along the main vein, subepidermal collenchyma on the adaxial side and the leaf lamina subdivided into palisade

and lacunar parenchyma (Fig. 9A-D). The mature leaves showed a similar morphology, but their cells were less juxtaposed with less dense nuclei as well (Fig. 91E-H). However, at the senescent phenological stage, a[CO_2] induced obvious anatomical changes in leaf tissues, with commitment of the integrity of epidermal and mesophyll cells, absence of collenchyma, and dismantling of the vascular system (Fig. 9I and J). Interestingly, under e[CO_2], the anatomical changes of senescent leaves were less drastic. We observed an intact vascular system, the presence of collenchyma, and the beginning of parenchymal cell disorganization (Fig. 9K and L). Furthermore, transmission electron microscopy revealed that the chloroplasts of plants under e[CO_2] had a lower degree of senescence (Fig. S3). Plants under a[CO_2] showed an increased lamellation pattern, coupled with a loose organization of the thylakoid membranes with wavy areas and intense expansions between them (Fig. S3).

In both [CO_2] conditions, the stems showed uniseriate epidermis, subepidermal collenchyma, and a strand of fibers above the vascular system (Fig. 10). Secondary growth was represented by the vascular cambium, which produces predominantly xylem (Fig. 10). The stems of plants on e[CO_2] had more differentiated vascular tissue, with greater vascular cambium activity and more pronounced vascular system (Fig. 10C-D). The reaction with phloroglucinol evidenced in plants under e[CO_2] the most intense coloration (reddish-purple) of the vascular bundles indicated strong lignification of the xylem and thickening of the cell wall in the interfascicular region, forming a continuous ring (Fig. 10E-H). However, staining with Calcofluor White did not indicate significant differences in cellulose deposition (Fig. 10I-P).

Elevated CO_2 modulated the expression of genes related to the lignin biosynthetic pathway

In the phenylpropanoid biosynthesis pathway, the expression of lignin-related genes was positively influenced by e[CO_2]. Compared to a[CO_2], *PgCAD*, *PgC4H* and *PgCCR* were upregulated (1.5-2.9 fold) in plants under e[CO_2] (Fig. 11A-C). The *PgCCoAOMT* gene showed no significant difference in its expression level (Fig. 11D).

Elevated CO_2 affects the proteomic profile

Proteomic analyses of *P. glomerata* plants under different [CO_2] revealed significant changes in the abundance of proteins. In total, 616 proteins were identified, of which 594 (96%) were found in plants in both [CO_2] (Fig. 12A, Table S2). Comparing e[CO_2]/a[CO_2] we observed 33 common differentially accumulated proteins (DAP), of which 10 proteins were up-accumulated, 11 proteins down-accumulated, 5 proteins unique to a[CO_2], and 7 proteins unique to e[CO_2] (Fig. 12A, Table S3).

KEGG analyses were performed and DAPs were identified in 17 different metabolic pathways (Fig. 12B, Table S4). By comparing e[CO_2]/a[CO_2], 14 metabolic pathways showed proteins up-accumulated, of which several are related to energy generation in plants, as Photosynthesis, Carbon fixation in photosynthetic organisms, Oxidative phosphorylation, Glycolysis - Gluconeogenesis, Fructose and mannose metabolism, Carbon metabolism, Starch and sucrose metabolism and Pentose phosphate and other metabolic pathways associated with Biosynthesis of aminoacids (e.g. phenylalanine and tyrosine) and secondary metabolites (Fig. 12B, Table S4). In addition, we observed 6 metabolic pathways that showed proteins down-accumulated, related to Aminoacid biosynthesis (e.g. cysteine and methionine), Secondary metabolites and Fatty acid and Biotin metabolism (Fig. 12B, Table S4).

Genetic ontology (GO) analyses of the DAPs were performed using OmicsBox software (Fig. 13). The proteins were identified and categorized into Biological Process and Cellular Component (Fig. 13). The analysis revealed that most of the proteins accumulated in e[CO_2] are related to biological processes of carbon metabolism and photosynthesis, as well as metabolic pathways (Fig. 13A). Concomitantly, DAPs were present predominantly in chloroplasts and their compartments (25), membrane (9), cytosol (9) and mitochondria (5), cellular components that are particularly important for photosynthesis and respiration (Fig. 13B).

DISCUSSION

To the best of our knowledge, this study is the first to investigate the impact of e[CO_2] in *P. glomerta* plants grown on OTC. Our data confirmed the hypothesis that e[CO_2] promotes higher photosynthetic performance and altered the production of primary and secondary metabolites. The e[CO_2] positively affected photosynthesis and water use efficiency, biomass accumulation, photosynthetic pigments, carbohydrate content, genes of the lignin synthesis pathway, and was able to induce changes in the proteomic profile. On the other hand, e[CO_2] promoted reduced total protein content and negatively regulated the production of some amino acids, and ultimately led to decreased 20E content and production.

In *P. glomerata*, as in other C3-type metabolism plants, an increase in [CO_2] generally results in an immediate increase in photosynthesis rate and reduction in respiration, favoring greater growth and biomass gain (Ehleringer and Bjorkman, 1977). The main reason for the increased photosynthetic rate (A_N) is that the key enzyme of this process, Ribulose-1,5-bisphosphate is quite sensitive to [CO_2] (Busch and Sage, 2017; Drake et al., 1997). Here we report that e[CO_2] did not affect dark respiration (R_d), but positively regulated A_N and Ribulose bisphosphate carboxylase/oxygenase (RuBisCO; cds.comp47860_c0_seq3) accumulation, and other proteins involved in the photosynthetic process, such as Photosystem I P700 apoprotein A2 (psaB) (cds.comp65786_c0_seq22) and Photosystem II 22 kDa protein (psbS) (cds.comp66564_c0_seq4) (Table S3 and S4). A very strong correlation was observed between A_N and RuBisCO (R= 0.83; P =1.11) and A_N and psbS (R= 0.96; P=0.31) (Fig. S4). The efficiency of photosystems I and II (PSI and PSII) is increased in e[CO_2] and correlates well with the rate of photosynthesis (Zhang et al., 2008). We observed from the A_N/C_i curve that in plants grown on e[CO_2] the A_N was significantly higher C_i above 400 µmol CO_2 mol^{-1}. Evidencing the plasticity and adaptability of *P. glomerata* to increased [CO_2] and possibly the higher efficiency of the photosynthetic apparatus of the plants under this condition.

Plant responses are species-specific and the immediate increase in A_N is not always linear with respect to an additional increase in [CO_2], as observed in radish, garlic, and soybean plants (Nackley et al., 2016; Usuda and Shimogawara, 1998; Zheng et al., 2019). At e[CO_2], the CO_2/O_2 ratio is increased; thus, the carboxylase activity of RuBisCO is predominantly over oxygenase activity, which consequently results in a reduction in the photorespiration rate (Bowes, 1991). One of the major metabolic fluxes of C3 plants is photorespiration (Sharkey and Sharkey, 1988), because to eliminate 2-phosphoglycolate

(2PG), a highly toxic molecule, plants consume ATP and reduce energy, while releasing previously fixed CO_2 (Walker et al., 2016). The photorespiratory cycle involves the participation of three cellular compartments (chloroplast, peroxisome, and mitochondria), and various intermediates, such as glycolate, glycine, serine, hydroxypyruvate, and glycerate (Dusenge et al., 2019). Therefore, these intermediates can be used to estimate the photorespiration rate (Dellero et al., 2021; Jolivet-Tournier and Gerster, 1984). In *P. glomerata* grown under e[CO_2] we did not observe a significant difference in glycine and serine content, but there was a 33% reduction in glycerate content (Table S1), we can infer that e[CO_2] is promoting reduced photorespiration in this species.

A significant reduction in g_S and E and a strong increase (54%) in WUE contributed to improved photosynthetic efficiency in *P. glomerata* under e[CO_2]. These discoveries are consistent with those of other species, as A_N and WUE generally increase in some C3 plants in e[CO_2] (Lawlor and Mitchell, 1991; Policy et al., 1993; Poorter et al., 2022). The changes in g_S and E were in a similar pattern, reduction of ±28.5%, as both depend on stomatal behavior, that is the implication this decrease is mainly due to the closure of stomata in e[CO_2] (Ainsworth and Rogers, 2007). Therefore, increasing [CO_2] reduces E and increases WUE (Pazzagli et al., 2016), the improvement in WUE (A_N/E) is attributed to the partial closure of stomata (Nackley et al., 2016). WUE is the main driver for improving agronomic or genetic traits of agricultural crops under a limited water regime (Blum, 2009), and several studies report positive effects of e[CO_2] on WUE in drought stress mitigation (Conley et al., 2001; Hatfield and Dold, 2019; Oliveira et al., 2016; Qiao et al., 2010).

Higher photosynthetic rates in plants under e[CO_2] can also be associated with an increased content of photosynthetic pigments. Here, we observed an increase in chlorophyll and carotenoid content in plants treated with e[CO_2], indicating that the biosynthesis of these pigments may be regulated by [CO_2] (Lu et al., 2020). Furthermore, A_N was strongly correlated with the total concentration of chlorophylls (R= 0.92; P =0.14) and carotenoids (R= 0.92; P=0.17) (Fig. S4). An increase in photosynthetic pigments is suggested to be an adaptation of plants to increase the efficiency of capturing radiant energy and consequently the photosynthetic process (Bhatt et al., 2010).

Plant growth under e[CO_2] usually results in accumulation of starch and soluble sugars, which can be explained by higher carbohydrate assimilation rates (Ainsworth and Long, 2005; De la Mata et al., 2012; De Souza et al., 2008; Moore et al., 1997). In *P. glomerata* under e[CO_2], increases in glucose and sucrose contents took place at evening, but

at anti-morning glucose contents lessened. We also observed a small reduction in starch content at midday. *P. glomerata* showed an absence of a pattern in carbohydrate production during different times of the day. Here, we identified pathways of carbohydrate metabolism with DAPs being positively regulated by e[CO_2], such as Glycolysis/Glyconeogenesis, Starch and Sucrose Metabolism, Fructose and Mannose Metabolism, Carbon Metabolism and Pentose Phosphate. The increased accumulation of the proteins in these pathways, such as Fructose-bisphosphate aldolase 3 (cds.comp19157_c0_seq1) and Glucose-6-phosphate isomerase 1 (cds.comp62838_c0_seq1) (Tables S3 and S4), reinforce the influence of e[CO_2] in increasing carbohydrate production. In an upcoming world of arisen CO_2 levels, increasing investment in carbon metabolism, with consequent accumulation of sugars, is an important component of plants to maximize photosynthesis and their production (Ainsworth and Bush, 2011).

In *P. glomerata*, e[CO_2] promoted a reduction in total protein content (at midday) and in the contents of amino acids, such as aspartate (Asp) and glutamate (Glu). Several studies have reported reduced nitrogen compound contents due to N deficiency in plants under e[CO_2] (Ebi et al., 2021; Keutgen et al., 1997; Kumari et al., 2015; Lee et al., 2020; Taub et al., 2008). One of the main causes for this change in N content is that e[CO_2] increases the rate of carbohydrate production and consequently increases the C/N ratios (Reich et al., 2006; Shi et al., 2016). The decline in N in plants can also occur by decreased assimilation of nitrate (NO_3^-) (Adavi and Sathee, 2021; Hocking and Meyer, 1991). Photorespiration stimulates NO_3^- assimilation in roots in C3 plants by increasing NADH availability in the cytosol (Andrews et al., 2019; Buchner et al., 2015). Possibly, lower rates of photorespiration in plants under e[CO_2] may result in less NO_3 reduction and as a consequence, reduced total N assimilation (Bloom et al. 2001, 2015).

Decreased N content in crops means that micro- and macronutrients will be less available for human nutrition, since plant proteins are the primary source of essential amino acids (Hildebrandt et al., 2015). The products of initial N assimilation, mainly the amino acids asparagine (Asn), glutamine (Gln), Asp and Glu, in addition to serving as substrates in protein biosynthesis, also function as energy donors via degradation in the Tricarboxylic Acid Cycle (TCA) (Coruzzi, 2003; Galili et al., 2016). Asn and Gln are metabolized to Asp and Glu; Glu is a nitrogen donor for the biosynthesis of essential amino acids via the Asp and aromatic amino acid pathways; Asp, on the other hand, is a metabolically reactive amino acid that serves as the nitrogen donor in numerous aminotransferase reactions and is the precursor to a

large family of amino acids (De la Torre et al., 2014; Erecihska et al., 1993; Galili, 2011; Zhu and Galili, 2003). Here we report the reduction in the relative content of Asp and Glu in *P. glomerata* plants under e[CO_2]. In cucumber leaves, e[CO_2] reduced L-glutamate content under normal water conditions, but its content was increased under severe drought stress, the authors believe that this response may be associated with the role of Glu in photosynthetic and osmotic adjustment (Li et al., 2018). Glu is a precursor of chlorophylls *a* and *b* (Hofgen et al., 1994) and is the main source of proline synthesis in response to osmotic stress (Wang et al., 2007). Thus, Glu and Asp are precursors to several other vital plant molecules, and a decline in the content of these amino acids could lead to serious damage to plants under stress conditions. In parallel, our study showed that e[CO_2] alone did not promote a difference in anthocyanin and proline contents, oxidative stress enzyme activity nor lipid peroxidation (MDA) (Fig. S2), indicating that e[CO_2] is not a stressor for *P. glomerata*.

Nitrogen limitation caused by e[CO_2] can also affect amino acid synthesis. Experiments with wheat showed that e[CO_2] induced a decrease in the total sulfur content of the grain, due to a decrease in the content of methionine (Met) and cysteine (Cys) (Fernando et al., 2012; Högy et al., 2009). In addition to the essential role of Met and Cys as a substrate for protein biosynthesis, Met is a precursor of the important enzyme cofactor S-adenosylmethionine (SAM) (Nikiforova et al., 2002). SAM serves as a carbon skeleton donor (methyl group) for synthesis of various molecules in plants, such as glutathione, ethylene, polyamines, fatty acids, and biotin (Wirtz and Droux, 2005). In our study, e[CO_2] negatively regulated the accumulation of the enzyme S-adenosylmethionine synthase (SAM-S; cds.comp54515_c0_seq1), which caused down regulation of the Met synthesis pathway (Tables S3 and S4). SAM-S catalyzes the formation of SAM from Met and ATP and performs the hydrolysis of tripolyphosphate to PP_i and P_i (Komoto et al., 2004). Met is easily converted into SAM, about 20% is incorporated into proteins while 80% is converted into SAM which comprises the end product of the Met synthesis pathway (Nikiforova et al., 2002).

We observed reduced biosynthesis of fatty acids and biotin by negative accumulation of the Enoyl-[acyl-carrier-protein] reductase [NADH] (ENR; cds.comp68161_c0_seq10) protein (Tables S3 and S4). There was a very strong correlation between SAM-S and ENR ($R = 0.97$; $P = 0.013$) (Fig. S4), so it may have a relationship with the reduction of SAM. Therefore, e[CO_2] leads to a reduction in the levels of amino acids, such as Met, precursors of the important biological compound SAM, essential for the synthesis of various plant defense-

related molecules such as ethylene and polyamines (Wirtz and Droux, 2005), affecting both the quality of human nutrition and plant development.

On the other hand, some amino acids can be increased in e[CO_2] and serve as precursors for the synthesis of secondary metabolites. Here we observe positive regulation of the synthesis pathways of phenylalanine (Phe) and tyrosine (Tyr) metabolism (Table S4). Both are aromatic amino acids that are precursors to several crucial plant compounds, such as lignin, anthocyanins, flavonoids, and tocopherols (Bonawitz and Chapple, 2010; Vogt, 2010; Winkel-Shirley, 2001). We identified the up-accumulation of macrophage migration inhibitory factor homolog isoform X2 NADH dehydrogenase [ubiquinone] iron-sulfur protein 7 (MIF; cds.comp50470_c0_seq1) (Tables S3 and S4), a phenylpyruvate tautomerase in plants grown in e[CO_2]. Phenylpyruvate tautomerase catalyzes the interconversion between 2-hydroxy-3-phenylpropanoate and phenylpyruvate (Rosengren et al., 1997; Sun et al., 2018). The phenylpyruvate pathway is an alternative pathway for Phe production in plants, but studies point out that the phenylpyruvate pathway can also coordinate Tyr catabolism, using a cytosolic aminotransferase of Tyr as an amino donor, thus linking the metabolism of these amino acids (Koper et al., 2022; Yoo et al., 2013). Thus, e[CO_2] seems to positively regulate the Phe and Tyr synthesis pathway by up accumulation of MIF.

The aromatic amino acids Phe and Tyr, regulate the metabolism of phenylpropanoids, resulting in the formation of lignin, one of the most important polymers in the plant cell. The influence of e[CO_2] on lignin content and expression levels of genes related to its synthesis (e.g. *PAL*, *C4H*, *4CL*, and *CCR*) is extensively reported in several species (Henry et al., 2005; Kasurinen et al., 2006; Shabbaj et al., 2021). Conversely, e[CO_2] also negatively regulated the expression of many lignin-related genes, leading to a decreased lignin deposition in secondary walls (Kasirajan et al., 2018; Ponniah et al., 2017; Sykes et al., 2015; Tu et al., 2010). Overall, the response to e[CO_2] to lignin accumulation and biosynthesis is inherent to each species. In *P. glomerata* grown in vitro in an enriched CO_2 atmosphere (1000 μL L^{-1}), several cell wall components showed an increase in their deposition. A gradual change in the deposition of hemicelluloses, and arabinogalactan proteins took place at 20 and 40 days, as well as at 30 days for lignin and cellulose (Louback et al., 2021).

In our study, e[CO_2] regulated three of the four analyzed genes of the lignin biosynthesis pathway. *PgCAD*, *PgC4H* and *PgCCR* were upregulated, whereas *PgCCoAOMT* remained unchanged by e[CO_2]. In agreement, the anatomical characterization of the stem of plants on e[CO_2] showed increased activity of the vascular cambium, which produces

predominantly xylem, evidencing increased secondary growth and consequently greater lignification of the cells. We believe that in plants grown under e[CO_2] the biomass accumulation and photosynthesis, may be related to higher lignin content. The correlation data reinforce this idea, the *PgCAD*, *PgC4H* and *PgCCR* genes strongly correlated with total dry mass (TDW) and A_N (Fig. S4). Therefore, the increased CO_2 supply can enhance carbon assimilation and consequently more metabolic energy can be channeled into lignin biosynthesis.

Here, there was no increase in lignin content in the leaves of plants under e[CO_2], as expected, because leaves of herbaceous plants have low lignin content (Kendall et al., 2019). Regarding leaf anatomy, no structural changes were observed in the expanding and mature leaves in relation to [CO_2], unlike the senescent leaves. In these, we observed that leaves from plants grown in a[CO_2] showed stronger senescence symptoms, such as greater disintegration of epidermal and mesophyll cells, when compared to e[CO_2]. We also verified that the ultrastructure of the chloroplasts corresponds with the anatomical characterization. The chloroplasts of the plants under a[CO_2] showed a higher degree of senescence (Fig. S3). In *P. glomeratra*, leaf senescence appears to be delayed in e[CO_2], and similar results have been reported elsewhere for other species (Buchner et al., 2015; Tipping and Murray, 1999; Tricker et al., 2004).

Although we observed a possible investment of skeleton C in the lignin increment in e[CO_2], conversely we reported a reduction in the secondary metabolite 20E. 20E is the major ecdysteroid found in insects, but its biological functions in plants are not yet fully elucidated (Guo et al., 2021; Jindra et al., 2013; Lin and Smagghe, 2019). The main hypothesis is that 20E is a protective compound against non-adapted phytophagous insects (Bakrim et al., 2008; Festucci-Buselli et al., 2008; Lafont et al., 1997). Studies have reported that plant resistance to some insects and pathogens is compromised when grown under e[CO_2], due to reduced secondary compound content (Ahammed et al., 2020; Li et al., 2019). We demonstrated that e[CO_2] did not affect 20E content and production in leaves, but reduced it in the stem and roots. It is still unclear the organ of synthesis and accumulation of this metabolite in *P. glomerata*, studies assume that 20E is produced in the leaves and accumulated in its roots (Dias et al., 2019; Neves et al., 2016), we also observed higher 20E content in the roots. Therefore, under the climate change scenario, especially because of the increase in atmospheric CO_2 concentration, the morphophysiology and chemical composition of plants are affected, altering their primary and secondary metabolism.

CONCLUSION

Overall, our data show that in *P. glomerata* e[CO_2] led to increased photosynthesis rate, improved water use efficiency, favored higher growth and biomass gain. At the same time, e[CO_2] promoted an increase in photosynthetic pigments, reflected in improved photosynthetic efficiency, and consequently greater accumulation of glucose and sucrose at evening. At the proteomic level, CO_2-enrichment also altered primary metabolism, and 33 common DAPs were identified, mainly related to carbohydrate and energy metabolism (e.g., RuBisCO, psaB, and psbS). On the other hand, despite the higher C gain, *P. glomerata* plants under e[CO_2] show reduced total protein content and negatively regulated the production of some amino acids (e.g. Asp and Glu). We observed in plants under e[CO_2] positive regulation in three genes (*PgCAD*, *PgC4H* and *PgCCR*) and two amino acids (Phe and Tyr) that regulate the biosynthesis pathway of phenylpropanoids, a precursor mainly of lignin. This along with the increased lignification of the stem reinforces the hypothesis that CO_2-enrichment favors lignin accumulation. In contrast, e[CO_2] promoted a reduction in 20E content and production, evidencing the plasticity of response of *P. glomerata* to changes in abiotic conditions. Thus, the cultivation of *P. glomerata* plants in e[CO_2] may represent a strategy to obtain plants with higher biomass, as well as to alter the content of plant defense compounds. Finally, this work opens possibilities and contributes to elucidate the morphophysiological, biochemical and molecular responses of *P. glomerata* to climate change, especially in relation to e[CO_2].

REFERENCES

Adavi, S. B., Sathee, L. (2021). Elevated CO_2 alters tissue balance of nitrogen metabolism and downregulates nitrogen assimilation and signalling gene expression in wheat seedlings receiving high nitrate supply. *Protoplasma*, *258*(1), 219–233. https://doi.org/10.1007/s00709-020-01564-3

Ahammed, G. J., Li, X., Liu, A., Chen, S. (2020). Physiological and defense responses of tea plants to elevated CO_2: A Review. *Frontiers in Plant Science*, 11, 305 https://doi.org/10.3389/fpls.2020.00305

Ainsworth, E. A., Bush, D. R. (2011). Carbohydrate export from the leaf: A highly regulated process and target to enhance photosynthesis and productivity. *Plant Physiology*, *155*(1), 64–69. https://doi.org/10.1104/pp.110.167684

Ainsworth, E. A., Long, S. P. (2005). What have we learned from 15 years of free-air CO_2 enrichment (FACE)? A meta-analytic review of the responses of photosynthesis, canopy properties and plant production to rising CO_2. *New Phytologist*, 165(2), 351–372. https://doi.org/10.1111/j.1469-8137.2004.01224.x

Ainsworth, E. A., Rogers, A. (2007). The response of photosynthesis and stomatal conductance to rising [CO_2]: Mechanisms and environmental interactions. *Plant, Cell and Environment*, *30*(3), 258–270. https://doi.org/10.1111/j.1365-3040.2007.01641.x

Al Jaouni, S., Saleh, A. M., Wadaan, M. A. M., Hozzein, W. N., Selim, S., AbdElgawad, H. (2018). Elevated CO_2 induces a global metabolic change in basil (*Ocimum basilicum* L.) and peppermint (*Mentha piperita* L.) and improves their biological activity. *Journal of Plant Physiology*, *224*, 121–131. https://doi.org/10.1016/j.jplph.2018.03.016

Ali, M. B., Eun, J. H., Paek, K. Y. (2005). CO_2-induced total phenolics in suspension cultures of *Panax ginseng* C. A. Mayer roots: Role of antioxidants and enzymes. *Plant Physiology and Biochemistry*, *43*(5), 449–457. https://doi.org/10.1016/j.plaphy.2005.03.005

Almuhayawi, M. S., Hassan, A. H. A., Al Jaouni, S. K., Alkhalifah, D. H. M., Hozzein, W. N., Selim, S., AbdElgawad, H., Khamis, G. (2021). Influence of elevated CO_2 on nutritive value and health-promoting prospective of three genotypes of Alfalfa sprouts (*Medicago sativa*). *Food Chemistry*, *340*, 128147. https://doi.org/10.1016/j.foodchem.2020.128147

Andrews, M., Condron, L. M., Kemp, P. D., Topping, J. F., Lindsey, K., Hodge, S., Raven, J.

A. (2019). Elevated CO_2 effects on nitrogen assimilation and growth of C3 vascular plants are similar regardless of N-form assimilated. *Journal of Experimental Botany*, *70*(2), 683–690. https://doi.org/10.1093/jxb/ery371

Avila, R. T., de Almeida, W. L., Costa, L. C., Machado, K. L. G., Barbosa, M. L., de Souza, R. P. B., Martino, P. B., Juárez, M. A. T., Marçal, D. M. S., Martins, S. C. V., Ramalho, J. D. C., DaMatta, F. M. (2020). Elevated air [CO_2] improves photosynthetic performance and alters biomass accumulation and partitioning in drought-stressed coffee plants. *Environmental and Experimental Botany*, *177*, 104137. https://doi.org/10.1016/j.envexpbot.2020.104137

Bakrim, A., Maria, A., Sayah, F., Lafont, R., Takvorian, N. (2008). Ecdysteroids in spinach (*Spinacia oleracea* L.): Biosynthesis, transport and regulation of levels. *Plant Physiology and Biochemistry*, *46*(10), 844–854. https://doi.org/10.1016/j.plaphy.2008.06.002

Bates, L. S., Waldren, R. P., Teare, I. D. (1973). Rapid determination of free proline for water-stress studies. *Plant and Soil*, *39*(1), 205–207. https://doi.org/10.1007/BF00018060

Batista, D. S., Dias, L. L. C., Rêgo, M. M., Saldanha, C. W., Otoni, W. C. (2017). Flask sealing on in vitro seed germination and morphogenesis of two types of ornamental pepper explants. *Ciência Rural*, *47*(3). https://doi.org/10.1590/0103-8478cr20150245

Batista, D. S., Koehler, A. D., Romanel, E., Souza, V. C., Silva, T. D., Almeida, M. C., Maciel, T. E. F., Ferreira, P. R. B., Felipe, S. H. S., Saldanha, C. W., Maldaner, J., Dias, L. L. C., Festucci-Buselli, R. A., Otoni, W. C. (2019a). *De novo* assembly and transcriptome of *Pfaffia glomerata* uncovers the role of photoautotrophy and the P450 family genes in 20-hydroxyecdysone production. *Protoplasma*, *256*(3), 601–614. https://doi.org/10.1007/s00709-018-1322-1

Batista, D. S., Moreira, V. S., Felipe, S. H. S., Fortini, E. A., Silva, T. D., Chagas, K., Louback, E., Romanel, E., Costa, M. G. C., Otoni, W. C. (2019b). Reference gene selection for qRT-PCR in Brazilian-ginseng [*Pfaffia glomerata* (Spreng.) Pedersen] as affected by various abiotic factors. *Plant Cell, Tissue and Organ Culture*, *138*(1), 97–107. https://doi.org/10.1007/s11240-019-01606-6

Bernardy, K., Farias, J. G., Pereira, A. S., Dorneles, A. O. S., Bernardy, D., Tabaldi, L. A., Neves, V. M., Dressler, V. L., Nicoloso, F. T. (2020). Plants' genetic variation approach applied to zinc contamination: secondary metabolites and enzymes of the antioxidant system in *Pfaffia glomerata* accessions. *Chemosphere*, *253*, 126692.

https://doi.org/10.1016/j.chemosphere.2020.126692

Bhatt, R. K., Baig, M. J., Tiwari, H. S. (2010). Elevated CO_2 influences photosynthetic characteristics of *Avena sativa* L. cultivars. *Journal of Environmental Biology, 31*(5) 813-818.

Bisbis, M. B., Gruda, N., Blanke, M. (2018). Potential impacts of climate change on vegetable production and product quality – A review. *Journal of Cleaner Production*, *170*, 1602–1620. https://doi.org/10.1016/j.jclepro.2017.09.224

Bloom, A. J. (2015). Photorespiration and nitrate assimilation: A major intersection between plant carbon and nitrogen. *Photosynthesis Research*, *123*(2), 117–128. https://doi.org/10.1007/s11120-014-0056-y

Bloom, A. J., Smart, D. R., Nguyen, D. T., Searles, P. S. (2001). Nitrogen assimilation and growth of wheat under elevated carbon dioxide. *Proceedings of the National Academy of Sciences*, *99*(3), 1730-1735. https://doi.org/10.1073/pnas.022627299

Blum, A. (2009). Effective use of water (EUW) and not water-use efficiency (WUE) is the target of crop yield improvement under drought stress. *Field Crops Research,* 112(2–3), 119–123. https://doi.org/10.1016/j.fcr.2009.03.009

Bonawitz, N. D., Chapple, C. (2010). The genetics of lignin biosynthesis: Connecting genotype to phenotype. *Annual Review of Genetics*, 44, 337–363. https://doi.org/10.1146/annurev-genet-102209-163508

Bowes, G. (1991). Growth at elevated CO_2: photosynthetic responses mediated through Rubisco. *Plant, Cell and Environment*, *14*(8), 795–806. https://doi.org/10.1111/j.1365-3040.1991.tb01443.x

Bradford, M. M. (1976). A rapid and sensitive method for the quantitation of microgram quantities of protein utilizing the principle of protein-dye binding. *Analytical Biochemistry*, *72*(1–2), 248–254. https://doi.org/10.1016/0003-2697(76)90527-3

Brito, F. A. L., Pimenta, T. M., Henschel, J. M., Martins, S. C. V., Zsögön, A., Ribeiro, D. M. (2020). Elevated CO_2 improves assimilation rate and growth of tomato plants under progressively higher soil salinity by decreasing abscisic acid and ethylene levels. *Environmental and Experimental Botany*, *176*, 104050. https://doi.org/10.1016/j.envexpbot.2020.104050

Buchner, P., Tausz, M., Ford, R., Leo, A., Fitzgerald, G. J., Hawkesford, M. J., Tausz-Posch, S. (2015). Expression patterns of C- and N-metabolism related genes in wheat are changed during senescence under elevated CO_2 in dry-land agriculture. *Plant Science*,

236, 239–249. https://doi.org/10.1016/j.plantsci.2015.04.006

Busch, F. A., Sage, R. F. (2017). The sensitivity of photosynthesis to O_2 and CO_2 concentration identifies strong Rubisco control above the thermal optimum. *New Phytologist*, *213*(3), 1036–1051. https://doi.org/10.1111/nph.14258

Chance, B., Maehly, A. C. (1955). Assay of catalases and peroxidases, *Methods in Enzymology,* 11,764–775. https://doi.org/10.1016/S0076-6879(55)02300-8

Chang, J. dong, Mantri, N., Sun, B., Jiang, L., Chen, P., Jiang, B., Jiang, Z., Zhang, J., Shen, J., Lu, H., Liang, Z. (2016). Effects of elevated CO_2 and temperature on *Gynostemma pentaphyllum* physiology and bioactive compounds. *Journal of Plant Physiology*, *196*, 41–52. https://doi.org/10.1016/j.jplph.2016.02.020

Chumley, H., Hewlings, S. (2020). The effects of elevated atmospheric carbon dioxide [CO_2] on micronutrient concentration, specifically iron (Fe) and zinc (Zn) in rice; a systematic review. *Journal of Plant Nutrition*, 43(10), 1571–1578). https://doi.org/10.1080/01904167.2020.1739303

Conley, M. M., Kimball, B. A., Brooks, T. J., Pinter, P. J., Hunsaker, D. J., Wall, G. W., Adam, N. R., Lamorte, R. L., Matthias, A. D., Thompson, T. L., Leavitt, S. W., Ottman, M. J., Cousins, A. B., Triggs, J. M. (2001). CO_2 enrichment increases water-use efficiency in sorghum. *New Phytologist*, *151*, 407–412.

Corrêa, J. P. O., Vital, C. E., Pinheiro, M. V. M., Batista, D. S., Azevedo, J. F. L., Saldanha, C. W., da Cruz, A. C. F., DaMatta, F. M., Otoni, W. C. (2015). In vitro photoautotrophic potential and ex vitro photosynthetic competence of *Pfaffia glomerata* (Spreng.) Pedersen accessions. *Plant Cell, Tissue and Organ Culture*, *121*(2), 289–300. https://doi.org/10.1007/s11240-014-0700-4

Coruzzi, G. M. (2003). Primary N-assimilation into Amino Acids in Arabidopsis. *The Arabidopsis Book*, *2*, e0010. https://doi.org/10.1199/tab.0010

Cruz, C. D. (2016). Genes Software – extended and integrated with the R, Matlab and Selegen. *Acta Scientiarum. Agronomy*, *38*(4), 547. https://doi.org/10.4025/actasciagron.v38i3.32629

DaMatta, F. M., Avila, R. T., Cardoso, A. A., Martins, S. C. V., Ramalho, J. C. (2018). Physiological and agronomic performance of the coffee crop in the context of climate change and global warming: A Review. *Journal of Agricultural and Food Chemistry*, *66*(21), 5264–5274. https://doi.org/10.1021/acs.jafc.7b04537

Damerval, C., De Vienne, D., Zivy, M., Thiellement, H. (1986). Technical improvements in

two-dimensional electrophoresis increase the level of genetic variation detected in wheat-seedling proteins. *Electrophoresis*, *7*(1), 52–54. https://doi.org/10.1002/elps.1150070108

De la Mata, L., Cabello, P., De la Haba, P., Agüera, E. (2012). Growth under elevated atmospheric CO_2 concentration accelerates leaf senescence in sunflower (*Helianthus annuus* L.) plants. *Journal of Plant Physiology*, *169*(14), 1392–1400. https://doi.org/10.1016/j.jplph.2012.05.024

De la Torre, F., El-Azaz, J., Ávila, C., Cánovas, F. M. (2014). Deciphering the role of aspartate and prephenate aminotransferase activities in plastid nitrogen metabolism. *Plant Physiology*, *164*(1), 92–104. https://doi.org/10.1104/pp.113.232462

De Souza, A. P., Gaspar, M., Da Silva, E. A., Ulian, E. C., Waclawovsky, A. J., Nishiyama, M. Y., Dos Santos, R. V., Teixeira, M. M., Souza, G. M., Buckeridge, M. S. (2008). Elevated CO_2 increases photosynthesis, biomass and productivity, and modifies gene expression in sugarcane. *Plant, Cell and Environment*, *31*(8), 1116–1127. https://doi.org/10.1111/j.1365-3040.2008.01822.x

Dellero, Y., Mauve, C., Jossier, M., Hodges, M. (2021). The impact of photorespiratory glycolate oxidase activity on *Arabidopsis thaliana* leaf soluble amino acid pool sizes during acclimation to low atmospheric CO_2 concentrations. *Metabolites*, *11*(8), 501. https://doi.org/10.3390/metabo11080501

Deutsch, E. W., Bandeira, N., Sharma, V., Perez-Riverol, Y., Carver, J. J., Kundu, D. J., García-Seisdedos, D., Jarnuczak, A. F., Hewapathirana, S., Pullman, B. S., Wertz, J., Sun, Z., Kawano, S., Okuda, S., Watanabe, Y., Hermjakob, H., MacLean, B., MacCoss, M. J., Zhu, Y., Ishihama, Y., Vizcaíno, J. A. (2020). The ProteomeXchange consortium in 2020: enabling 'big data'approaches in proteomics. *Nucleic Acids Research*, *48*(D1), D1145-D1152. https://doi.org/10.1093/nar/gkz984

Dias, F. C. R., Martins, A. L. P., Melo, F. C. S. A., Cupertino, M. C., Gomes, M. L. M., Oliveira, J. M., Damasceno, E. M., Silva, J., Otoni, W. C., da Matta, S. L. P. (2019). Hydroalcoholic extract of *Pfaffia glomerata* alters the organization of the seminiferous tubules by modulating the oxidative state and the microstructural reorganization of the mice testes. *Journal of Ethnopharmacology*, *233*, 179–189. https://doi.org/10.1016/j.jep.2018.12.047

Dinan, L. (2001). Phytoecdysteroids: Biological aspects. *Phytochemistry*, *57*, 325–339. https://doi.org/10.1016/S0031-9422(01)00078-4

Dinan, L., Lafont, R. (2006). Effects and applications of arthropod steroid hormones (ecdysteroids) in mammals. *Journal of Endocrinology*, *191*(1), 1–8. https://doi.org/10.1677/joe.1.06900

Distler, U., Kuharev, J., Navarro, P., Levin, Y., Schild, H., Tenzer, S. (2014). Drift time-specific collision energies enable deep-coverage data-independent acquisition proteomics. *Nature Methods*, *11*(2), 167–170. https://doi.org/10.1038/nmeth.2767

Dong, J., Gruda, N., Lam, S. K., Li, X., Duan, Z. (2018). Effects of elevated CO_2 on nutritional quality of vegetables: A review. *Frontiers in Plant Science*, 9, 924. https://doi.org/10.3389/fpls.2018.00924

Drake, B. G., Gonzàlez-Meler, M. A., Long, S. P. (1997). More efficient plants: A consequence of rising atmospheric CO_2? *Annual Review of Plant Physiology and Plant Molecular Biology*, *48*, 609-39.

Dusenge, M. E., Duarte, A. G., Way, D. A. (2019). Plant carbon metabolism and climate change: elevated CO_2 and temperature impacts on photosynthesis, photorespiration and respiration. *New Phytologist*, 221(1), 32–49). https://doi.org/10.1111/nph.15283

Ebi, K. L., Anderson, C. L., Hess, J. J., Kim, S. H., Loladze, I., Neumann, R. B., Singh, D., Ziska, L., Wood, R. (2021). Nutritional quality of crops in a high CO_2 world: An agenda for research and technology development. *Environmental Research Letters*, *16*(6), 064045. https://doi.org/10.1088/1748-9326/abfcfa

Ehleringer, J., Bjorkman, O. (1977). Quantum yields for CO_2 uptake in C3 and C4 plants dependence on temperature, CO_2, and O_2 concentration'. *Plant Physiology*, *59*(1), 86-90. https://doi.org/10.1104/pp.59.1.86

Erecihska, M., Nelson, D. P. D., Nissim, I., Yudkoff, M., Erecihska, M. (1993). Cerebral aspartate utilization: Near-equilibrium relationships in aspartate aminotransferase reaction. *Journal of Neurochemistry*, *60*(5), 1696-1706. https://doi.org/10.1111/j.1471-4159.1993.tb13393.x

Farquhar, G. D., Caemmerer, S. von, Berry, J. A. (1980). A Biochemical model of photosynthetic CO_2 assimilation in leaves of C3 species. *Planta*, *149*(1), 78–90. https://doi.org/23374770

Felipe, S. H. S., Batista, D. S., Chagas, K., Correia, L. N. F., Silva, T. D., Fortini, E. A., Silva, P. O., Otoni, W. C. (2019a). Accessions of Brazilian ginseng (*Pfaffia glomerata*) with contrasting anthocyanin content behave differently in growth, antioxidative defense, and 20-hydroxyecdysone levels under UV-B radiation. *Protoplasma*, *256*(6), 1557–1571.

https://doi.org/10.1007/s00709-019-01400-3

Felipe, S. H. S., Batista, D. S., Vital, C. E., Chagas, K., Silva, P. O., Silva, T. D., Fortini, E. A., Correia, L. N. F., Avila, R. T., Maldaner, J., Festucci-Buselli, R. A., DaMatta, F. M., Otoni, W. C. (2019b). Salinity-induced modifications on growth, physiology and 20-hydroxyecdysone levels in Brazilian-ginseng [*Pfaffia glomerata* (Spreng.) Pedersen]. *Plant Physiology and Biochemistry*, *140*, 43–54. https://doi.org/10.1016/j.plaphy.2019.05.002

Fernando, N., Panozzo, J., Tausz, M., Norton, R., Fitzgerald, G., Seneweera, S. (2012). Rising atmospheric CO_2 concentration affects mineral nutrient and protein concentration of wheat grain. *Food Chemistry*, *133*(4), 1307–1311. https://doi.org/10.1016/j.foodchem.2012.01.105

Fernie, A. R., Roscher, A., Ratcliffe, R. G., Kruger, N. J. (2001). Fructose 2,6-bisphosphate activates pyrophosphate: fructose-6-phosphate 1-phosphotransferase and increases triose phosphate to hexose phosphate cycling in heterotrophic cells. *Planta*, *212*(2), 250–263. https://doi.org/10.1007/s004250000386

Ferreira, P. R. B., da Cruz, A. C. F., Batista, D. S., Nery, L. A., Andrade, I. G., Rocha, D. I., Felipe, S. H. S., Koehler, A. D., Nunes-Nesi, A., Otoni, W. C. (2019). CO_2 enrichment and supporting material impact the primary metabolism and 20-hydroxyecdysone levels in Brazilian ginseng grown under photoautotrophy. *Plant Cell, Tissue and Organ Culture*, *139*(1), 77–89. https://doi.org/10.1007/s11240-019-01664-w

Festucci-Buselli, R. A., Contim, L. A. S., Barbosa, L. C. A., Stuart, J., Otoni, W. C. (2008). Biosynthesis and potential functions of the ecdysteroid 20-hydroxyecdysone - A review. *Botany*, *86*(9), 978–987. https://doi.org/10.1139/B08-049

Fiehn, O. (2007). Validated high quality automated metabolome analysis of *Arabidopsis thaliana* leaf disks. *Concepts in Plant Metabolomics*, 1–18. Springer Netherlands. https://doi.org/10.1007/978-1-4020-5608-6_1

Fortini, E. A., Batista, D. S., Castro, K. M., Silva, T. D., Felipe, S. H. S., Correia, L. N. F., Chagas, K., Farias, L. M., Leite, J. P. V., Otoni, W. C. (2020). Photoperiod modulates growth and pigments and 20-hydroxyecdysone accumulation in Brazilian ginseng [*Pfaffia glomerata* (Spreng.) Pedersen] grown in vitro. *Plant Cell, Tissue and Organ Culture*, *142*(3), 595–611. https://doi.org/10.1007/s11240-020-01886-3

Franco, R. R., Almeida Takata, L., Chagas, K., Justino, A. B., Saraiva, A. L., Goulart, L. R., Melo Rodrigues Ávila, V., Otoni, W. C., Espindola, F. S., Silva, C. R. (2021). A 20-

hydroxyecdysone-enriched fraction from *Pfaffia glomerata* (Spreng.) pedersen roots alleviates stress, anxiety, and depression in mice. *Journal of Ethnopharmacology*, *26*, 113599. https://doi.org/10.1016/j.jep.2020.113599

Gairola, S., Mohd Shariff, N., Bhatt, A., Prakash Kala, C. (2010). Influence of climate change on production of secondary chemicals in high altitude medicinal plants: Issues needs immediate attention. *Journal of Medicinal Plants Research*, *4*(18), 1825–1829. https://doi.org/10.5897/JMPR10.354

Galili, G. (2011). The aspartate-family pathway of plants: Linking production of essential amino acids with energy and stress regulation. *Plant Signaling and Behavior*, 6(2), 192–195. https://doi.org/10.4161/psb.6.2.14425

Galili, G., Amir, R., Fernie, A. R. (2016). The regulation of essential amino acid synthesis and accumulation in plants. *Annual Review of Plant Biology*, *67*, 153–178. https://doi.org/10.1146/annurev-arplant-043015-112213

Gasparini, K., Costa, L. C., Brito, F. A. L., Pimenta, T. M., Cardoso, F. B., Araújo, W. L., Zsögön, A., Ribeiro, D. M. (2019). Elevated CO_2 induces age-dependent restoration of growth and metabolism in gibberellin-deficient plants. *Planta*, *250*(4), 1147–1161. https://doi.org/10.1007/s00425-019-03208-0

Giannopolitis, C. N., Ries, S. K. (1977). Superoxide Dismutases. *Plant Physiology*, *59*(2), 309–314. https://doi.org/10.1104/pp.59.2.309

Gibon, Y., Bläsing, O. E., Palacios-Rojas, N., Pankovic, D., Hendriks, J. H. M., Fisahn, J., Höhne, M., Günther, M., Stitt, M. (2004). Adjustment of diurnal starch turnover to short days: Depletion of sugar during the night leads to a temporary inhibition of carbohydrate utilization, accumulation of sugars and post-translational activation of ADP-glucose pyrophosphorylase in the followin. *The Plant Journal*, *39*(6), 847–862. https://doi.org/10.1111/j.1365-313X.2004.02173.x

Gomes, M. P., Marques, T. C. L. L. S. e. M., Soares, A. M. (2013). Cadmium effects on mineral nutrition of the Cd-hyperaccumulator *Pfaffia glomerata*. *Biologia*, *68*(2), 223–230. https://doi.org/10.2478/s11756-013-0005-9

Gu, J., Weber, K., Klemp, E., Winters, G., Franssen, S. U., Wienpahl, I., Huylmans, A.-K., Zecher, K., Reusch, T. B. H., Bornberg-Bauer, E., Weber, A. P. M. (2012). Identifying core features of adaptive metabolic mechanisms for chronic heat stress attenuation contributing to systems robustness. *Integrative Biology*, *4*(5), 480. https://doi.org/10.1039/c2ib00109h

Guo, S., Tian, Z., Wu, Q. W., King-Jones, K., Liu, W., Zhu, F., Wang, X. P. (2021). Steroid hormone ecdysone deficiency stimulates preparation for photoperiodic reproductive diapause. *PLoS Genetics*, *17*(2), e1009352. https://doi.org/10.1371/JOURNAL.PGEN.1009352

Gupta, D. K., Huang, H. G., Nicoloso, F. T., Schetinger, M. R., Farias, J. G., Li, T. Q., Razafindrabe, B. H. N., Aryal, N., Inouhe, M. (2013). Effect of Hg, As and Pb on biomass production, photosynthetic rate, nutrients uptake and phytochelatin induction in *Pfaffia glomerata*. *Ecotoxicology*, *22*(9), 1403–1412. https://doi.org/10.1007/s10646-013-1126-1

Hatfield, J. L., Dold, C. (2019). Water-use efficiency: Advances and challenges in a changing climate. *Frontiers in Plant Science*, *10*, 103. https://doi.org/10.3389/fpls.2019.00103

Havir, E. A., McHale, N. A. (1987). Biochemical and developmental characterization of multiple forms of catalase in tobacco leaves. *Plant Physiology*, *84*(2), 450–455. https://doi.org/10.1104/pp.84.2.450

Heath, R. L., Packer, L. (1968). Photoperoxidation in isolated chloroplasts. *Archives of Biochemistry and Biophysics*, *125*(1), 189–198. https://doi.org/10.1016/0003-9861(68)90654-1

Henry, H. A. L., Cleland, E. E., Field, C. B., Vitousek, P. M. (2005). Interactive effects of elevated CO_2, N deposition and climate change on plant litter quality in a California annual grassland. *Oecologia*, *142*(3), 465–473. https://doi.org/10.1007/s00442-004-1713-1

Hildebrandt, T. M., Nunes Nesi, A., Araújo, W. L., Braun, H. P. (2015). Amino acid catabolism in plants. *Molecular Plant*, 8(11), 1563–1579. https://doi.org/10.1016/j.molp.2015.09.005

Hocking, P. J., Meyer, C. P. (1991). Carbon dioxide enrichment decreases critical nitrate and nitrogen concentrations in wheat. *Journal of Plant Nutrition*, *14*(6), 571–584. https://doi.org/10.1080/01904169109364225

Hofgen, R., Axelsent, K. B., Gamini Kannangara, C., Schottke, I., Pohlenz, H. D., Willmitzert, L., Grimmu, B., Von Wettsteint, D. (1994). Plant Biology A visible marker for antisense mRNA expression in plants: Inhibition of chlorophyll synthesis with a glutamate-1-semialdehyde aminotransferase anti'sense gene. *Proceedings of the National Academy of Sciences*, *91*(5), 1726-1730. https://doi.org/10.1073/pnas.91.5.172

Högy, P., Wieser, H., Köhler, P., Schwadorf, K., Breuer, J., Franzaring, J., Muntifering, R.,

Fangmeier, A. (2009). Effects of elevated CO_2 on grain yield and quality of wheat: Results from a 3-year free-air CO_2 enrichment experiment. *Plant Biology*, *11*(1), 60–69. https://doi.org/10.1111/j.1438-8677.2009.00230.x

Houshmandfar, A., Fitzgerald, G. J., Tausz, M. (2015). Elevated CO_2 decreases both transpiration flow and concentrations of Ca and Mg in the xylem sap of wheat. *Journal of Plant Physiology*, *174*, 157–160. https://doi.org/10.1016/j.jplph.2014.10.008

Hozzein, W. N., Saleh, A. M., Habeeb, T. H., Wadaan, M. A. M., Elgawad, H. (2020). CO_2 treatment improves the hypocholesterolemic and antioxidant properties of fenugreek seeds. *Food Chemistry*, *308,* 125661. https://doi.org/10.1016/j.foodchem.2019.125661

IPCC (2022). Global Warming of 1.5°C. An IPCC Special Report on the impacts of global warming of 1.5°C above pre-industrial levels and related global greenhouse gas emission pathways, in the context of strengthening the global response to the threat of climate change. Cambridge University Press. https://doi.org/10.1017/9781009157940

Hughes, J., McCull, M. E. (1975). The use of an optical brightener in the study of plant structure. *Stain Technology 50:1037–1041*

Jaafar, H. Z. E., Ibrahim, M. H., Karimi, E. (2012). Phenolics and flavonoids compounds, phenylanine ammonia lyase and antioxidant activity responses to elevated CO_2 in *Labisia pumila* (Myrisinaceae). *Molecules*, *17*(6), 6331–6347. https://doi.org/10.3390/molecules17066331

Jindra, M., Palli, S. R., Riddiford, L. M. (2013). The juvenile hormone signaling pathway in insect development. *Annual Review of Entomology*, 58, 181–204. https://doi.org/10.1146/annurev-ento-120811-153700

Jolivet-Tournier, P., Gerster, R. (1984). Incorporation of oxygen into glycolate, glycine, and serine during photorespiration in maize leaves. *Plant Physiology*, *74*(1), 108-111. https://doi.org/10.1104/pp.74.1.108

Karnovsky, M. J. (1964). A formaldehyde-glutaraldehyde fixative of high osmolality for use in electron microscopy. *The Journal of Cell Biology*, 7, 1A-149A https://www.researchgate.net/publication/244955881

Kasirajan, L., Hoang, N. V., Furtado, A., Botha, F. C., Henry, R. J. (2018). Transcriptome analysis highlights key differentially expressed genes involved in cellulose and lignin biosynthesis of sugarcane genotypes varying in fiber content. *Scientific Reports*, *8*(1), 11612. https://doi.org/10.1038/s41598-018-30033-4

Kasurinen, A., Riikonen, J., Oksanen, E., Vapaavuori, E., Holopainen, T. (2006). Chemical

composition and decomposition of silver birch leaf litter produced under elevated CO_2 and O_3. *Plant and Soil*, *282*(1–2), 261–280. https://doi.org/10.1007/s11104-005-6026-6

Kendall, I. P., Woodward, P., Clark, J. P., Styring, A. K., Hanna, J. V., Evershed, R. P. (2019). Compound-specific $\delta^{15}N$ values express differences in amino acid metabolism in plants of varying lignin content. *Phytochemistry*, *161*, 130-138. https://doi.org/10.1016/j.phytochem.2019.01.012

Keutgen, N., Chen, K., Lenz, F. (1997). Responses of strawberry leaf photosynthesis, chlorophyll fluorescence and macronutrient contents to elevated CO_2. *Journal of Plant Physiology*, *150*(4), 395–400. https://doi.org/10.1016/S0176-1617(97)80088-0

Komoto, J., Yamada, T., Takata, Y., Markham, G. D., Takusagawa, F. (2004). Crystal structure of the S-adenosylmethionine synthetase ternary complex: A novel catalytic mechanism of S-adenosylmethionine synthesis from ATP and Met. *Biochemistry*, *43*(7), 1821–1831. https://doi.org/10.1021/bi035611t

Koper, K., Han, S.-W., Pastor, D. C., Yoshikuni, Y., Maeda, H. A. (2022). Evolutionary origin and functional diversification of aminotransferases. *Journal of Biological Chemistry*, 102122. https://doi.org/10.1016/j.jbc.2022.102122

Kumari, S., Agrawal, M., Singh, A. (2015). Effects of ambient and elevated CO_2 and ozone on physiological characteristics, antioxidative defense system and metabolites of potato in relation to ozone flux. *Environmental and Experimental Botany*, *109*, 276–287. https://doi.org/10.1016/j.envexpbot.2014.06.015

Lafont, R., Blais, C., Dauphin-Villemant, C., Garcia, M., Lachaise, F., Sommé-Martin, G. (1997). Ecdysteroids and related molecules in animals and plants. *Archives of Insect Biochemistry and Physiology*, *35*, 3–20.

Lawlor, D. W., Mitchell, R. A. C. (1991). The effects of increasing CO_2 on crop photosynthesis and productivity: a review of field studies. *Cell and Environment, 14*(8), 807–818. https://doi.org/10.1111/j.1365-3040.1991.tb01444.x

Lee, Y. H., Sang, W. G., Baek, J. K., Kim, J. H., Shin, P., Seo, M. C., Cho, J. Il. (2020). The effect of concurrent elevation in CO_2 and temperature on the growth, photosynthesis, and yield of potato crops. *PLoS ONE*, *15*(10), e0189308. https://doi.org/10.1371/journal.pone.0241081

Li, L., Wang, M., Pokharel, S. S., Li, C., Parajulee, M. N., Chen, F., Fang, W. (2019). Effects of elevated CO_2 on foliar soluble nutrients and functional components of tea, and population dynamics of tea aphid, *Toxoptera aurantii*. *Plant Physiology and*

Biochemistry, *145*, 84–94. https://doi.org/10.1016/j.plaphy.2019.10.023

Li, M., Li, Y., Zhang, W., Li, S., Gao, Y., Ai, X., Zhang, D., Liu, B., Li, Q. (2018). Metabolomics analysis reveals that elevated atmospheric CO_2 alleviates drought stress in cucumber seedling leaves. *Analytical Biochemistry*, *559*, 71–85. https://doi.org/10.1016/j.ab.2018.08.020

Li, P., Li, H., Zong, Y., Li, F. Y., Han, Y., Hao, X. (2017). Photosynthesis and metabolite responses of *Isatis indigotica* Fortune to elevated [CO_2]. *The Crop Journal*, *5*(4), 345–353. http://dx.doi.org/10.1016/j.cj.2017.03.007

Lin, X., Smagghe, G. (2019). Roles of the insulin signaling pathway in insect development and organ growth. *Peptides*, *122,* 169923. https://doi.org/10.1016/j.peptides.2018.02.001

Lisec, J., Schauer, N., Kopka, J., Willmitzer, L., Fernie, A. R. (2006). Gas chromatography mass spectrometry-based metabolite profiling in plants. *Nature Protocols*, *1*(1), 387–396. https://doi.org/10.1038/nprot.2006.59

Livak, K. J., Schmittgen, T. D. (2001). Analysis of relative gene expression data using real-time quantitative PCR and the $2^{-\Delta\Delta CT}$ Method. *Methods*, *25*(4), 402–408. https://doi.org/10.1006/meth.2001.1262

Louback, E., Batista, D. S., Pereira, T. A. R., Mamedes-Rodrigues, T. C., Silva, T. D., Felipe, S. H. S., Rocha, D. I., Steinmacher, D. A., Otoni, W. C. (2021). CO_2 enrichment leads to altered cell wall composition in plants of *Pfaffia glomerata* (Spreng.) Pedersen (Amaranthaceae). *Plant Cell, Tissue and Organ Culture*, *145*(3), 603–613. https://doi.org/10.1007/s11240-021-02031-4

Lima, A. L. S., Damatta, F. M., Pinheiro, H. A., Totola, M. R., Loureiro, M. E. (2002). Photochemical responses and oxidative stress in two clones of *Coffea canephora* under water deficit conditions. *Environmental and Experimental Botany*, *47*(3), 239-247. https://doi.org/10.1016/S0098-8472(01)00130-7

Lu, Y., Li, D., Li, L., Belwal, T., Xu, Y., Lin, X., Duan, Z., Luo, Z. (2020). Effects of elevated CO_2 on pigment metabolism of postharvest mandarin fruit for degreening. *Food Chemistry*, *318*(15)*,* 126462. https://doi.org/10.1016/j.foodchem.2020.126462

Madan, P., Jagadish, S. V. K., Craufurd, P. Q., Fitzgerald, M., Lafarge, T., Wheeler, T. R. (2012). Effect of elevated CO_2 and high temperature on seed-set and grain quality of rice. *Journal of Experimental Botany*, *63*(10), 3843–3852. https://doi.org/10.1093/jxb/ers077

Marchioretto, M. S., Miotto, S. T. S., Siqueira, C. De. (2010). O gênero *Pfaffia* Mart.

(Amaranthaceae) no Brasil Maria. *Hoehnea*, *37*(3), 461–511. https://doi.org/10.1590/S2236-89062010000300004

Matimati, I., Verboom, G. A., Cramer, M. D. (2014). Nitrogen regulation of transpiration controls mass-flow acquisition of nutrients. *Journal of Experimental Botany*, *65*(1), 159–168. https://doi.org/10.1093/jxb/ert367

Moore, B. D., Palmquist, D. E., Seemann, J. R. (1997). Influence of plant growth at high co_2 concentrations on leaf content of ribulose-1,5-bisphosphate carboxylase/oxygenase and intracellular distribution of soluble carbohydrates in tobacco, snapdragon, and parsley. *Plant Physiology*, *115*(1), 241–248. https://doi.org/10.1104/pp.115.1.241

Moura, C. L., Casemiro, L. A., Martins, C. H. G., Cunha, W. R., Silva, M. L. de A., Cury, A. H. V. (2011). Evaluation of the antimicrobial activity of the plant species *Pfaffia glomerata* against oral pathogens. *Investigação*, *11*, 24–28. https://doi.org/10.26843/investigacao.v11i2.500

Murashige, T., Skoog, F. (1962). A revised medium for rapid growth and bio assays with tobacco tissue cultures. *Physiologia Plantarum*, *15*(3), 473–497. https://doi.org/10.1111/j.1399-3054.1962.tb08052.x

Nackley, L. L., Jeong, J. H., Oki, L. R., Kim, S.-H. (2016). Photosynthetic acclimation, biomass allocation, and water use efficiency of garlic in response to carbon dioxide enrichment and nitrogen fertilization. *Journal of the American Society for Horticultural Science*, *141*(4), 373-380. https://doi.org/10.21273/JASHS.141.4.373

Nakagawa, Y., Henrich, V. C. (2009). Arthropod nuclear receptors and their role in molting. *FEBS Journal,* 276(21), 6128–6157. https://doi.org/10.1111/j.1742-4658.2009.07347.x

Nakano, Y., Asada, K. (1981). Hydrogen peroxide is scavenged by ascorbate-specific peroxidase in spinach chloroplasts. *Plant and Cell Physiology*, *22*, 867–880. https://doi.org/10.1093/oxfordjournals.pcp.a076232

Neff, M. M., Chory, J. (1998). Genetic interactions between phytochrome A, phytochrome B, and cryptochrome 1 during *Arabidopsis* development 1. *Plant Physiology*, *118*(1), 27–35. https://doi.org/10.1104/pp.118.1.27

Neto, A. G., Costa, J. M. L. C., Belati, C. C., Vinhólis, A. H. C., Possebom, L. S., Da Silva Filho, A. A., Cunha, W. R., Carvalho, J. C. T., Bastos, J. K., E Silva, M. L. A. (2005). Analgesic and anti-inflammatory activity of a crude root extract of *Pfaffia glomerata* (Spreng) Pedersen. *Journal of Ethnopharmacology*, *96*(1–2), 87–91. https://doi.org/10.1016/j.jep.2004.08.035

Neves, C. S., Gomes, S. S. L., Santos, T. R. do., de Almeida, M. M., de Souza, Y. O., Garcia, R. M. G., Otoni, W. C., Chedier, L. M., Raposo, N. R. B., Viccini, L. F., de Campos, J. M. S. (2016). "Brazilian ginseng" (*Pfaffia glomerata* Spreng. Pedersen, Amaranthaceae) methanolic extract: cytogenotoxicity in animal and plant assays. *South African Journal of Botany*, *106*, 174–180. https://doi.org/10.1016/j.sajb.2016.07.003

Niinemets, Ü., Sack, L. (2006). Structural determinants of leaf light-harvesting capacity and photosynthetic potentials. *Progress in Botany*, *67*, 385–419. https://doi.org/10.1007/3-540-27998-9_17

Nikiforova, V., Kempa, S., Zeh, M., Maimann, S., Kreft, O., Casazza, A. P., Riedel, K., Tauberger, E., Hoefgen, R., Hesse, H. (2002). Engineering of cysteine and methionine biosynthesis in potato. *Amino Acids*, *22*(3), 259-278. https://doi.org/10.1007/s007260200013

O'Brien, T. P., McCully, M. E. (1981). *The study of plant structure principles and selected methods.* Termarcarphi Pty. Ltd., Melbourne, *581*(4).

Oliveira, V. F., Silva, E. A., Carvalho, M. A. M. (2016). Elevated CO_2 atmosphere minimizes the effect of drought on the Cerrado species *Chrysolaena obovata. Frontiers in Plant Science*, *7*, 810. https://doi.org/10.3389/fpls.2016.00810

Passamani, L. Z., Reis, R. S., Vale, E. M., Sousa, K. R., Aragão, V. P. M., Santa-Catarina, C., Silveira, V. (2020). Long-term culture with 2,4-dichlorophenoxyacetic acid affects embryogenic competence in sugarcane callus via changes in starch, polyamine and protein profiles. *Plant Cell, Tissue and Organ Culture*, *140*(2), 415–429. https://doi.org/10.1007/s11240-019-01737-w

Pazzagli, P. T., Weiner, J., Liu, F. (2016). Effects of CO_2 elevation and irrigation regimes on leaf gas exchange, plant water relations, and water use efficiency of two tomato cultivars. *Agricultural Water Management*, *169*, 26–33. https://doi.org/10.1016/j.agwat.2016.02.015

Pereira, A. S., Dorneles, A. O. S., Bernardy, K., Sasso, V. M., Bernardy, D., Possebom, G., Rossato, L. V., Dressler, V. L., Tabaldi, L. A. (2018). Selenium and silicon reduce cadmium uptake and mitigate cadmium toxicity in *Pfaffia glomerata* (Spreng.) Pedersen plants by activation antioxidant enzyme system. *Environmental Science and Pollution Research*, *25*(19), 18548–18558. https://doi.org/10.1007/s11356-018-2005-3

Perez-Riverol, Y., Csordas, A., Bai, J., Bernal-Llinares, M., Hewapathirana, S., Kundu, D. J., Inuganti, A., Griss, J., Mayer, G., Eisenacher, M., Pérez, E., Uszkoreit, J., Pfeuffer, J.,

Sachsenberg, T., Yılmaz, S., Tiwary, S., Cox, J., Audain, E., Walzer, M., Jarnuczak, A. F., Ternent, T. T., Brazma, A., Vizcaíno, J. A. (2019). The PRIDE database and related tools and resources in 2019: improving support for quantification data. *Nucleic Acids Research*, *47*(D1), D442-D450. https://doi.org/10.1093/nar/gky1106

Policy, H. W., Johnson, H. B., Marinot, B. D., Mayeux, H. S. (1993). Increase in C3 plant water-use efficiency and biomass over Glacial to present CO_2 concentrations. *Nature*, *361*(6407), 61–64. https://doi.org/10.1038/361061a0

Ponniah, S. K., Shang, Z., Akbudak, M. A., Srivastava, V., Manoharan, M. (2017). Down-regulation of hydroxycinnamoyl CoA: shikimate hydroxycinnamoyl transferase, cinnamoyl CoA reductase, and cinnamyl alcohol dehydrogenase leads to lignin reduction in rice (*Oryza sativa* L. ssp. japonica cv. Nipponbare). *Plant Biotechnology Reports*, *11*(1), 17–27. https://doi.org/10.1007/s11816-017-0426-y

Poorter, H., Knopf, O., Wright, I. J., Temme, A. A., Hogewoning, S. W., Graf, A., Cernusak, L. A., Pons, T. L. (2022). A meta-analysis of responses of C3 plants to atmospheric CO_2: dose–response curves for 85 traits ranging from the molecular to the whole-plant level. *New Phytologist*, *233*(4), 1560–1596. https://doi.org/10.1111/nph.17802

Porra, R. J., Thompson, W. A., Kriedemann, P. E. (1989). Determination of accurate extinction coefficients and simultaneous equations for assaying chlorophylls *a* and *b* extracted with four different solvents: verification of the concentration of chlorophyll standards by atomic absorption spectroscopy. *Biochimica et Biophysica Acta (BBA) - Bioenergetics*, *975*(3), 384–394. https://doi.org/10.1016/S0005-2728(89)80347-0

Qiao, Y., Zhang, H., Dong, B., Shi, C., Li, Y., Zhai, H., Liu, M. (2010). Effects of elevated CO_2 concentration on growth and water use efficiency of winter wheat under two soil water regimes. *Agricultural Water Management*, *97*(11), 1742–1748. https://doi.org/10.1016/j.agwat.2010.06.007

Reich, P. B., Hungate, B. A., Luo, Y. (2006). Carbon-nitrogen interactions in terrestrial ecosystems in response to rising atmospheric carbon dioxide. *Source: Annual Review of Ecology, Evolution, and Systematics*, *37*, 611–636. https://doi.org/10.2307/annurev.ecolsys.37.091305.30000023

Reis R.S., Vale E.M., Sousa K.R., Santa-Catarina C., Silveira, V. (2021) Pretreatment free of 2,4-dichlorophenoxyacetic acid improves the diferentiation of sugarcane somatic embryos by afecting the hormonal balance and the accumulation of reserves. *Plant Cell Tissue and Organ Culture,* 145:101–115. https://doi.org/10.1007/ s11240-020-01995-z

Reynolds, E. S. (1963). The use of lead citrate at high ph as an electron-opaque stain in electron microscopy. *Journal of Cell Biology*, *17*(1), 208–212. https://doi.org/10.1083/jcb.17.1.208

Rodeghiero, M., Niinemets, Ü., Cescatti, A. (2007). Major diffusion leaks of clamp-on leaf cuvettes still unaccounted: how erroneous are the estimates of Farquhar et al. model parameters? *Plant, Cell & Environment*, *30*(8), 1006–1022. https://doi.org/10.1111/j.1365-3040.2007.001689.x

Rosengren, E., Aman, P., Thelin, S., Hansson, C., Ahlfors, S., Björk, P., Jacobsson, L., Rorsman, H. (1997). The macrophage migration inhibitory factor MIF is a phenylpyruvate tautomerase. *FEBS 19409 FEBS Letters*, *417*(1), 85-88. https://doi.org/10.1016/S0014-5793(97)01261-1

Saldanha, C. W., Otoni, C. G., Notini, M. M., Kuki, K. N., da Cruz, A. C. F., Neto, A. R., Dias, L. L. C., Otoni, W. C. (2013). A CO_2-enriched atmosphere improves in vitro growth of Brazilian ginseng [*Pfaffia glomerata* (Spreng.) Pedersen]. *In Vitro Cellular & Developmental Biology - Plant*, *49*(4), 433–444. https://doi.org/10.1007/s11627-013-9529-5

Saldanha, C. W., Otoni, C. G., Rocha, D. I., Cavatte, P. C., Detmann, K. da S. C., Tanaka, F. A. O., Dias, L. L. C., DaMatta, F. M., Otoni, W. C. (2014). CO_2-enriched atmosphere and supporting material impact the growth, morphophysiology and ultrastructure of in vitro Brazilian-ginseng [*Pfaffia glomerata* (Spreng.) Pedersen] plantlets. *Plant Cell, Tissue and Organ Culture*, *118*(1), 87–99. https://doi.org/10.1007/s11240-014-0464-x

Schneider, C., Rasband, W., Eliceiri, K. (2012). NIH Image to ImageJ: 25 years of image analysis. *Nature Methods*, *9*(7), 671–675. https://doi.org/10.1038/nmeth .2089

Shabbaj, I. I., Elgawad, H., Tammar, A., Alsiary, W. A., Madany, M. M. Y. (2021). Future climate CO_2 can harness ROS homeostasis and improve cell wall fortification to alleviate the hazardous effect of *Phelipanche infection* in pea seedlings. *Plant Physiology and Biochemistry*, *166*, 1131–1141. https://doi.org/10.1016/j.plaphy.2021.07.020

Sharkey, T. D., Bernacchi, C. J., Farquhar, G. D., Singsaas, E. L. (2007). Fitting photosynthetic carbon dioxide response curves for C3 leaves. *Plant, Cell & Environment*, *30*(9), 1035–1040. https://doi.org/10.1111/j.1365-3040.2007.01710.x

Sharkey, T. D. (1988). Estimating the rate of photorespiration in leaves. *Physiologia Plantarum*, *73*(1), 147-152. https://doi.org/10.1111/j.1399-3054.1988.tb09205.x

Shi, Z., Yang, Y., Zhou, X., Weng, E., Finzi, A. C., Luo, Y. (2016). Inverse analysis of

coupled carbon-nitrogen cycles against multiple datasets at ambient and elevated CO_2. *Journal of Plant Ecology*, *9*(3), 285–295. https://doi.org/10.1093/jpe/rtv059

Shim, S. H., Lee, S. K., Lee, D. W., Brilhaus, D., Wu, G., Ko, S., Lee, C. H., Weber, A. P. M., Jeon, J. S. (2020). Loss of function of rice plastidic glycolate/glycerate translocator 1 impairs photorespiration and plant growth. *Frontiers in Plant Science*, *10,* 1726. https://doi.org/10.3389/fpls.2019.01726

Silva, T. D., Batista, D. S., Castro, K. M., Fortini, E. A., Felipe, S. H. S., Fernandes, A. M., Sousa, R. M. J., Chagas, K., Silva, J. V. S., Correia, L. N. F., Torres-Silva, G., Farias, L. M., Otoni, W. C. (2020b). Irradiance-driven 20-hydroxyecdysone production and morphophysiological changes in *Pfaffia glomerata* plants grown in vitro. *Protoplasma*, *258*(1), 151–167. https://doi.org/10.1007/s00709-020-01558-1

Silva, T. D., Batista, D. S., Fortini, E. A., Castro, K. M. , Felipe, S. H. S., Fernandes, A. M., Sousa, R. M. J., Chagas, K., Silva, J. V. S. , Correia, L. N. F., Farias, L. M., Leite, J. P. V., Rocha, D. I., Otoni, W. C. (2020a). Blue and red light affects morphogenesis and 20-hydroxyecdisone content of in vitro *Pfaffia glomerata* accessions. *Journal of Photochemistry and Photobiology B: Biology*, *203*, 111761. https://doi.org/10.1016/j.jphotobiol.2019.111761

Soares, J. C., Santos, C. S., Carvalho, S. M. P., Pintado, M. M., Vasconcelos, M. W. (2019). Preserving the nutritional quality of crop plants under a changing climate: importance and strategies. *Plant and Soil*, *443*(1–2), 1–26. https://doi.org/10.1007/s11104-019-04229-0

Sun, Q., Su, F., Wang, T., Ding, Z. (2018). The transcriptome properties of reeds under cadmium stress in Liaohe Estuary wetland. *South African Journal of Botany*, *116*, 200–206. https://doi.org/10.1016/j.sajb.2018.03.012

Sykes, R. W., Gjersing, E. L., Foutz, K., Rottmann, W. H., Kuhn, S. A., Foster, C. E., Ziebell, A., Turner, G. B., Decker, S. R., Hinchee, M. A. W., Davis, M. F. (2015). Down-regulation of p-coumaroyl quinate/shikimate 3′-hydroxylase (C3′H) and cinnamate 4-hydroxylase (C4H) genes in the lignin biosynthetic pathway of *Eucalyptus urophylla* × *E. grandis* leads to improved sugar release. *Biotechnology for Biofuels*, *8*(1), 128. https://doi.org/10.1186/s13068-015-0316-x

Taub, D. R., Miller, B., Allen, H. (2008). Effects of elevated CO_2 on the protein concentration of food crops: A meta-analysis. *Global Change Biology*, *14*(3), 565–575. https://doi.org/10.1111/j.1365-2486.2007.01511.x

Terrer, C., Phillips, R. P., Hungate, B. A., Rosende, J., Pett-Ridge, J., Craig, M. E., van Groenigen, K. J., Keenan, T. F., Sulman, B. N., Stocker, B. D., Reich, P. B., Pellegrini, A. F. A., Pendall, E., Zhang, H., Evans, R. D., Carrillo, Y., Fisher, J. B., Van Sundert, K., Vicca, S., Jackson, R. B. (2021). A trade-off between plant and soil carbon storage under elevated CO_2. *Nature*, *591*(7851), 599–603. https://doi.org/10.1038/s41586-021-03306-8

Tipping, C., Murray, D. R. (1999). Effects of elevated atmospheric CO_2 concentration on leaf anatomy and morphology in *Panicum* species representing different photosynthetic modes. *International Journal of Plant Sciences*, *160*(6), 1063–1073. https://doi.org/10.1086/314201

Trabucco, G. M., Matos, D. A., Lee, S. J., Saathoff, A. J., Priest, H. D., Mockler, T. C., Sarath, G., Hazen, S. P. (2013). Functional characterization of cinnamyl alcohol dehydrogenase and caffeic acid O-methyltransferase in *Brachypodium distachyon*. *BMC Biotechnology*, *13*(1), 61. https://doi.org/10.1186/1472-6750-13-61

Tricker, P. J., Calfapietra, C., Kuzminsky, E., Puleggi, R., Ferris, R., Nathoo, M., Pleasants, L. J., Alston, V., De Angelis, P., Taylor, G. (2004). Long-term acclimation of leaf production, development, longevity and quality following 3 yr exposure to free-air CO_2 enrichment during canopy closure in *Populus*. *New Phytologist*, *162*(2), 413–426. https://doi.org/10.1111/j.1469-8137.2004.01057.x

Tsukagoshi, Y., Ohyama, K., Seki, H., Akashi, T., Muranaka, T., Suzuki, H., Fujimoto, Y. (2016). Functional characterization of CYP71D443, a cytochrome P450 catalyzing C-22 hydroxylation in the 20-hydroxyecdysone biosynthesis of *Ajuga* hairy roots. *Phytochemistry*, *127*, 23–28. https://doi.org/10.1016/j.phytochem.2016.03.010

Tu, Y., Rochfort, S., Liu, Z., Ran, Y., Griffith, M., Badenhorst, P., Louie, G. V., Bowman, M. E., Smith, K. F., Noel, J. P., Mouradov, A., Spangenberg, G. (2010). Functional analyses of caffeic acid O-methyltransferase and cinnamoyl-CoA-reductase genes from perennial ryegrass (*Lolium perenne*). *The Plant Cell*, *22*(10), 3357–3373. https://doi.org/10.1105/tpc.109.072827

Usuda, H., Shimogawara, K. (1998). The effects of increased atmospheric carbon dioxide on growth, carbohydrates, and photosynthesis in radish, *Raphanus sativus*. *Plant Cell Physiol*, *39*(1), 1–7. https://academic.oup.com/pcp/article/39/1/1/2756923

Vogt, T. (2010). Phenylpropanoid biosynthesis. *Molecular Plant*, 3(1), 2–20. https://doi.org/10.1093/mp/ssp106

Walker, B., Ariza, L. S., Kaines, S., Badger, M. R., Cousins, A. B. (2013). Temperature response of in vivo Rubisco kinetics and mesophyll conductance in *Arabidopsis thaliana*: Comparisons to Nicotiana tabacum. *Plant, Cell and Environment*, *36*(12), 2108–2119. https://doi.org/10.1111/pce.12166

Walker, B. J., Vanloocke, A., Bernacchi, C. J., Ort, D. R. (2016). The Costs of Photorespiration to Food Production Now and in the Future. *Annual Review of Plant Biology*, 67, 107–129. https://doi.org/10.1146/annurev-arplant-043015-111709

Wang, Z. Q., Yuan, Y. Z., Ou, J. Q., Lin, Q. H., Zhang, C. F. (2007). Glutamine synthetase and glutamate dehydrogenase contribute differentially to proline accumulation in leaves of wheat (*Triticum aestivum*) seedlings exposed to different salinity. *Journal of Plant Physiology*, *164*(6), 695–701. https://doi.org/10.1016/j.jplph.2006.05.001

Winkel-Shirley, B. (2001). Flavonoid Biosynthesis. A colorful model for genetics, biochemistry, cell biology, and biotechnology. *Plant Physiology*, *126*(2), 485-493. https://doi.org/10.1104/pp.126.2.485

Wirtz, M., Droux, M. (2005). Synthesis of the sulfur amino acids: Cysteine and methionine. *Photosynthesis Research, 86*(3), 345–362. https://doi.org/10.1007/s11120-005-8810-9

Yi, Z., Li, S., Liang, Y., Zhao, H., Hou, L., Yu, S., Ahammed, G. J. (2018). Effects of exogenous spermidine and elevated CO_2 on physiological and biochemical changes in tomato plants under iso-osmotic salt stress. *Journal of Plant Growth Regulation*, *37*(4), 1222–1234. https://doi.org/10.1007/s00344-018-9856-1

Yoo, H., Widhalm, J. R., Qian, Y., Maeda, H., Cooper, B. R., Jannasch, A. S., Gonda, I., Lewinsohn, E., Rhodes, D., Dudareva, N. (2013). An alternative pathway contributes to phenylalanine biosynthesis in plants via a cytosolic tyrosine:phenylpyruvate aminotransferase. *Nature Communications*, *4*(1), 1–11. https://doi.org/10.1038/ncomms3833

Zhang, H., Xie, X., Kim, M.-S., Kornyeyev, D. A., Holaday, S., Paré, P. W. (2008). Soil bacteria augment *Arabidopsis* photosynthesis by decreasing glucose sensing and abscisic acid levels in planta. *The Plant Journal*, *56*(2), 264–273. https://doi.org/10.1111/j.1365-313X.2008.03593.x

Zheng, Y., Li, F., Hao, L., Yu, J., Guo, L., Zhou, H., Ma, C., Zhang, X., Xu, M. (2019). Elevated CO_2 concentration induces photosynthetic down-regulation with changes in leaf structure, non-structural carbohydrates and nitrogen content of soybean. *BMC Plant Biology*, *19*(1), 1–18. https://doi.org/10.1186/s12870-019-1788-9

Zhu, X., Galili, G. (2003). Increased lysine synthesis coupled with a knockout of its catabolism synergistically boosts lysine content and also transregulates the metabolism of other amino acids in *Arabidopsis* seeds. *Plant Cell*, *15*(4), 845–853. https://doi.org/10.1105/tpc.009647

FIGURES

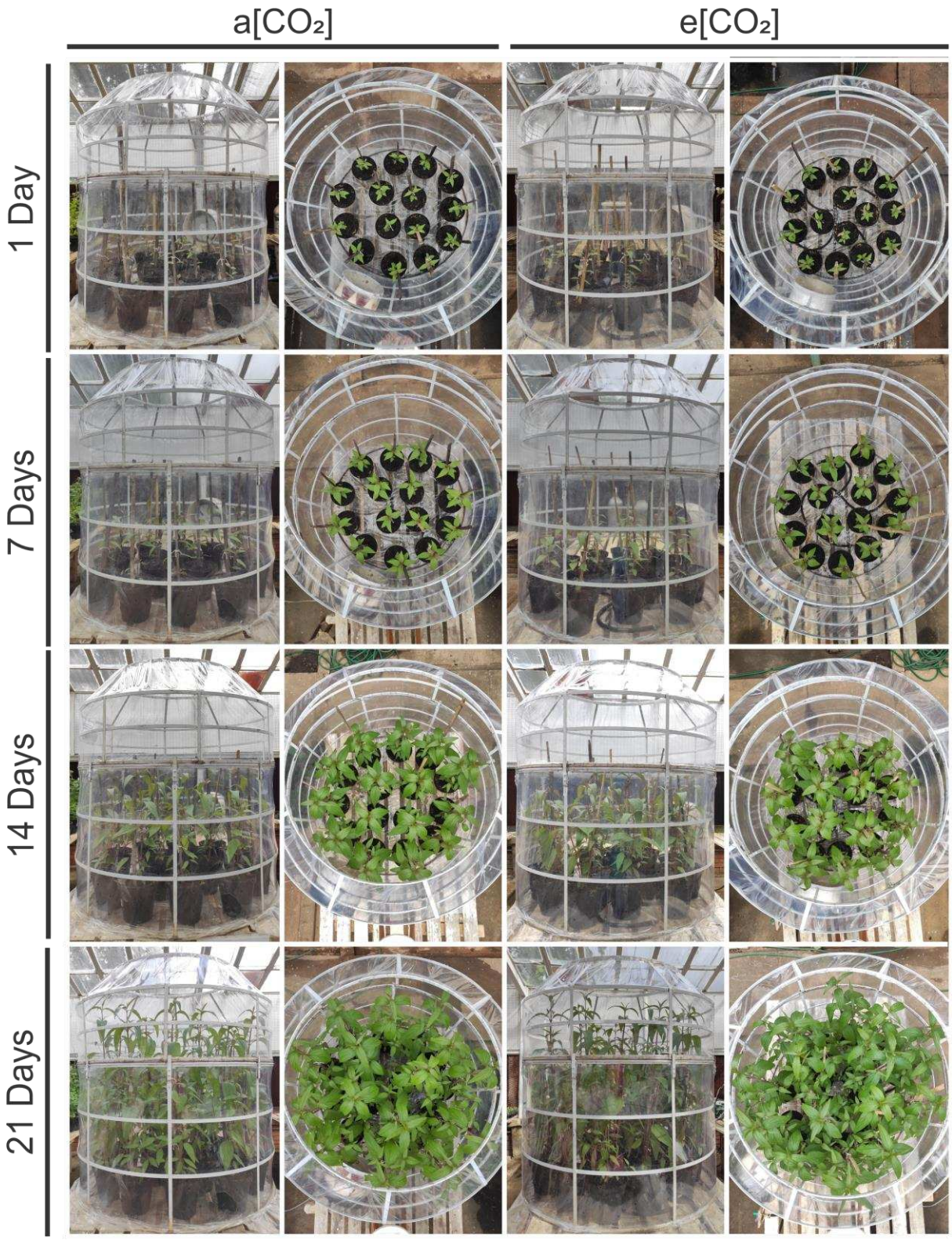

Fig. 1. Overview of CO_2-enriched experiment conducted with Brazilian ginseng (*Pffafia glomerata*) at two CO_2 concentrations: ambient (a[CO_2]) and elevated (e[CO_2]) in open top chambers under greenhouse conditions.

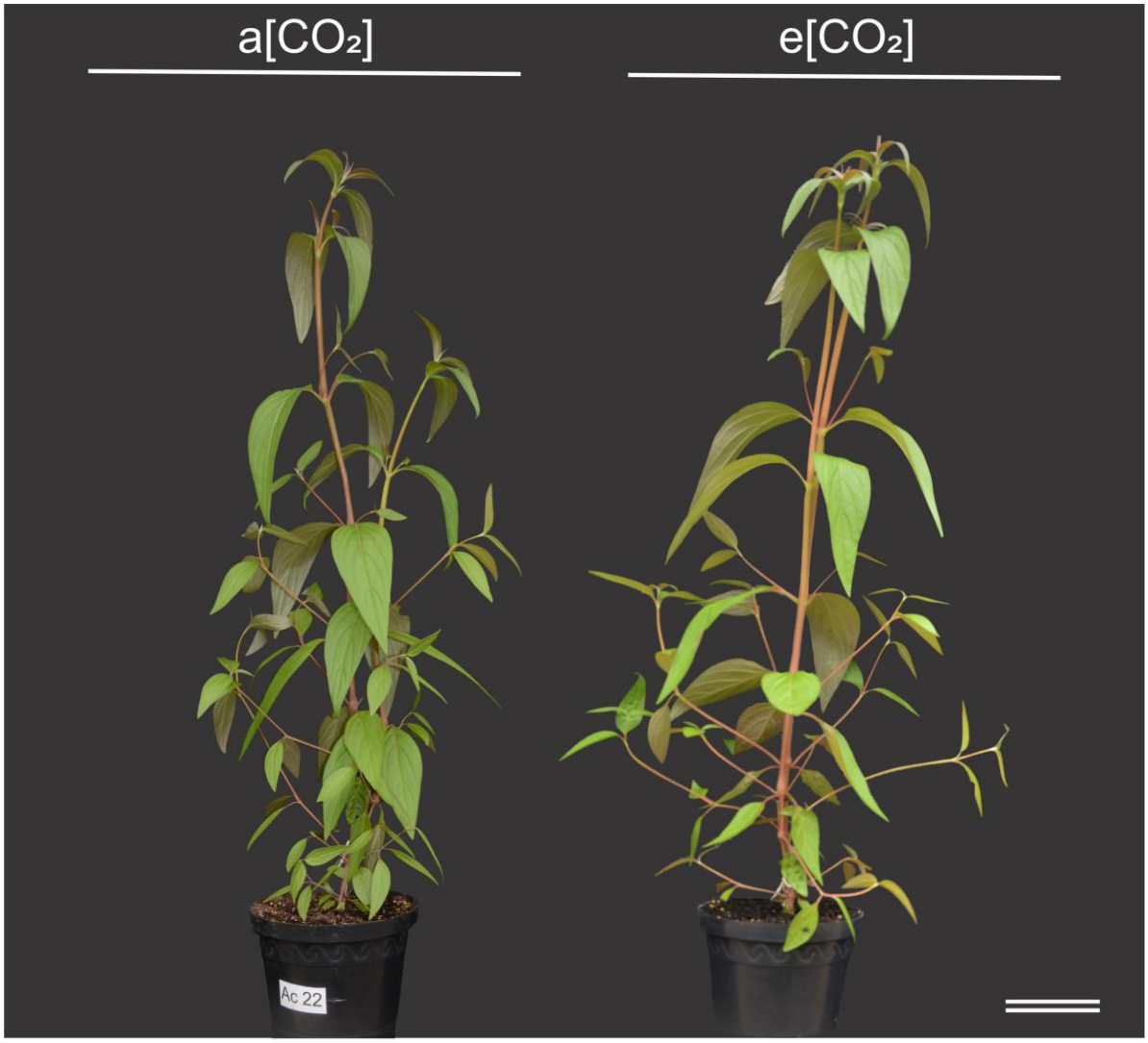

Fig. 2. Visual aspect of *P. glomerata* plants, accession 22 cultivated for 21 days under ambient (a[CO_2]) and elevated (e[CO_2]) CO_2 concentration. Bar = 10 cm.

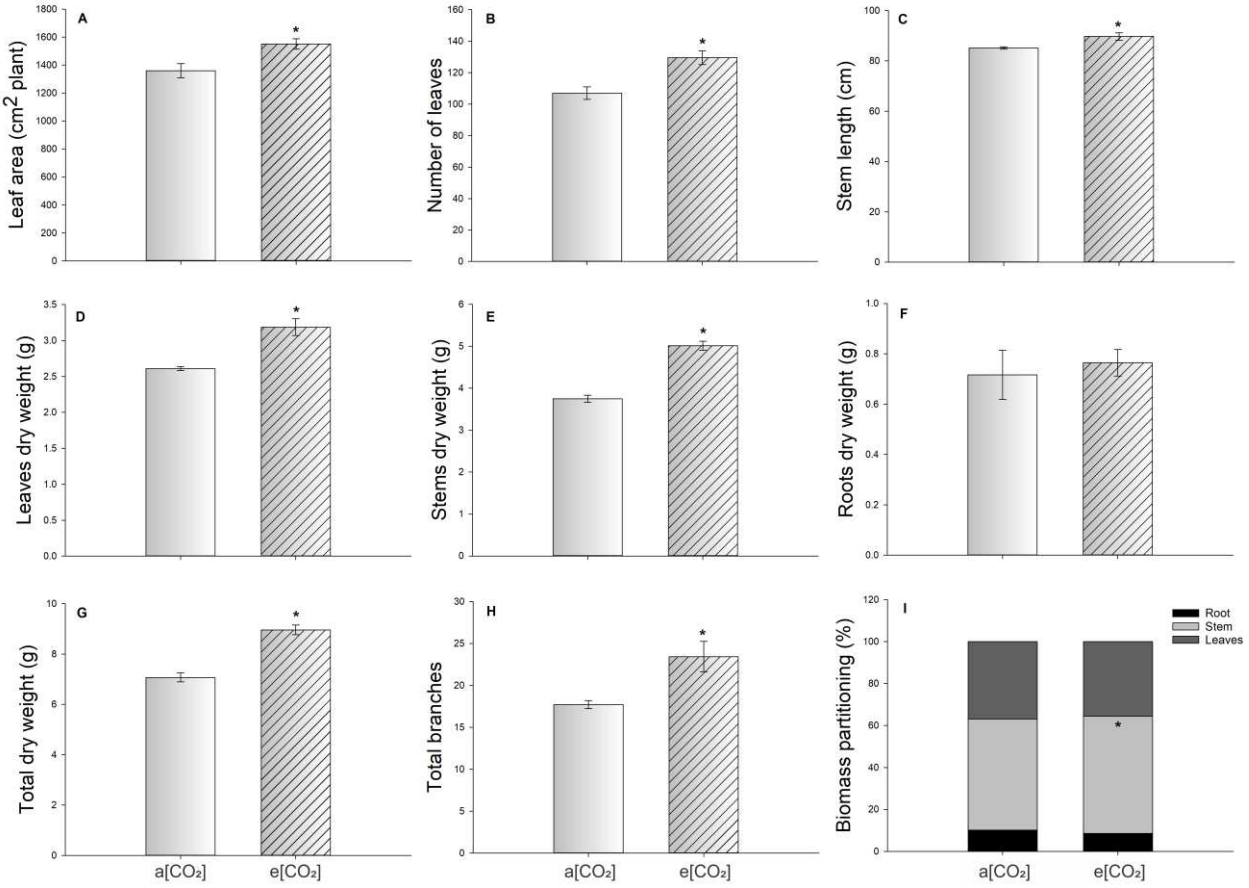

Fig. 3. Variation of biometric parameters in *P. glomerata* plants cultivated for 21 days under ambient (a[CO_2]) and elevated (e[CO_2]) CO_2 concentration. (**A**) Leaf area (cm^2); (**B**) number of leaves; (**C**) stem length (cm); (**D**) leaves dry weight (g); (**E**) stem dry weight (g); (**F**) root dry weight (g); (**G**) total dry weight (g); (**H**) total branches; and (**I**) biomass partitioning (%) which bars represent the percentage of the total dry weight of each organ. Values are presented as means (n=7) ± standard error. Asterisks indicate significant difference (*t*-Student; $P \leq 0.05$).

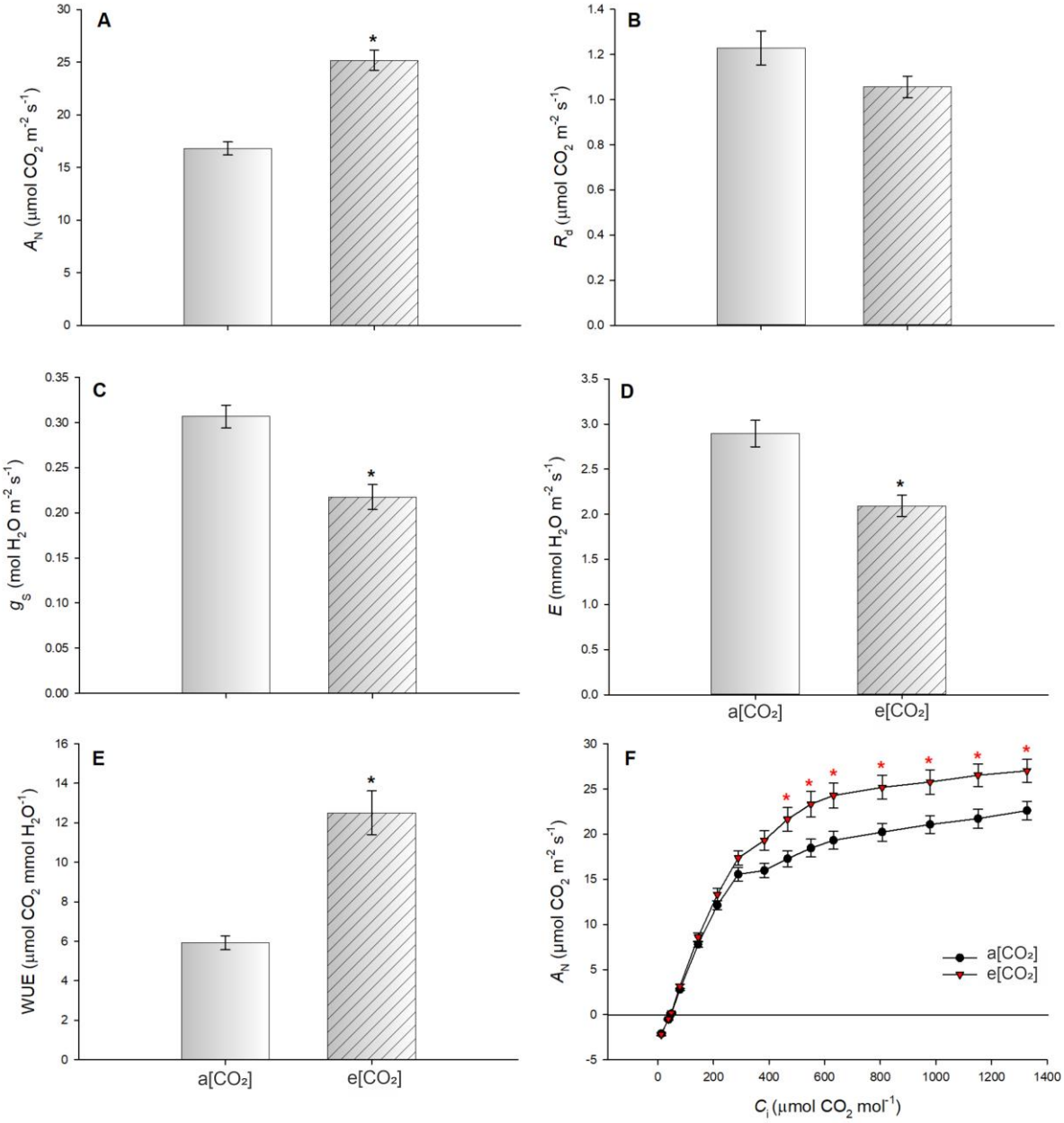

Fig. 4. Alteration in gas exchange parameter of leaves of *P. glomerata* plants cultivated for 21 days under ambient (a[CO_2]) and elevated (e[CO_2]) CO_2 concentration. (**A**) Net CO_2 net assimilation rate (A_N); (**B**) dark respiration rate (R_d); (**C**) Stomatal conductance (g_S); (**D**) Transpiration rate (E); (**E**) instantaneous water use efficiency (WUE); and (**F**) net photosynthesis (A) curves in response to internal (C_i) CO_2 concentration. Values are presented as means (n=5) ± standard error. Asterisks indicate significant difference (*t*-Student; $P \leq 0.05$).

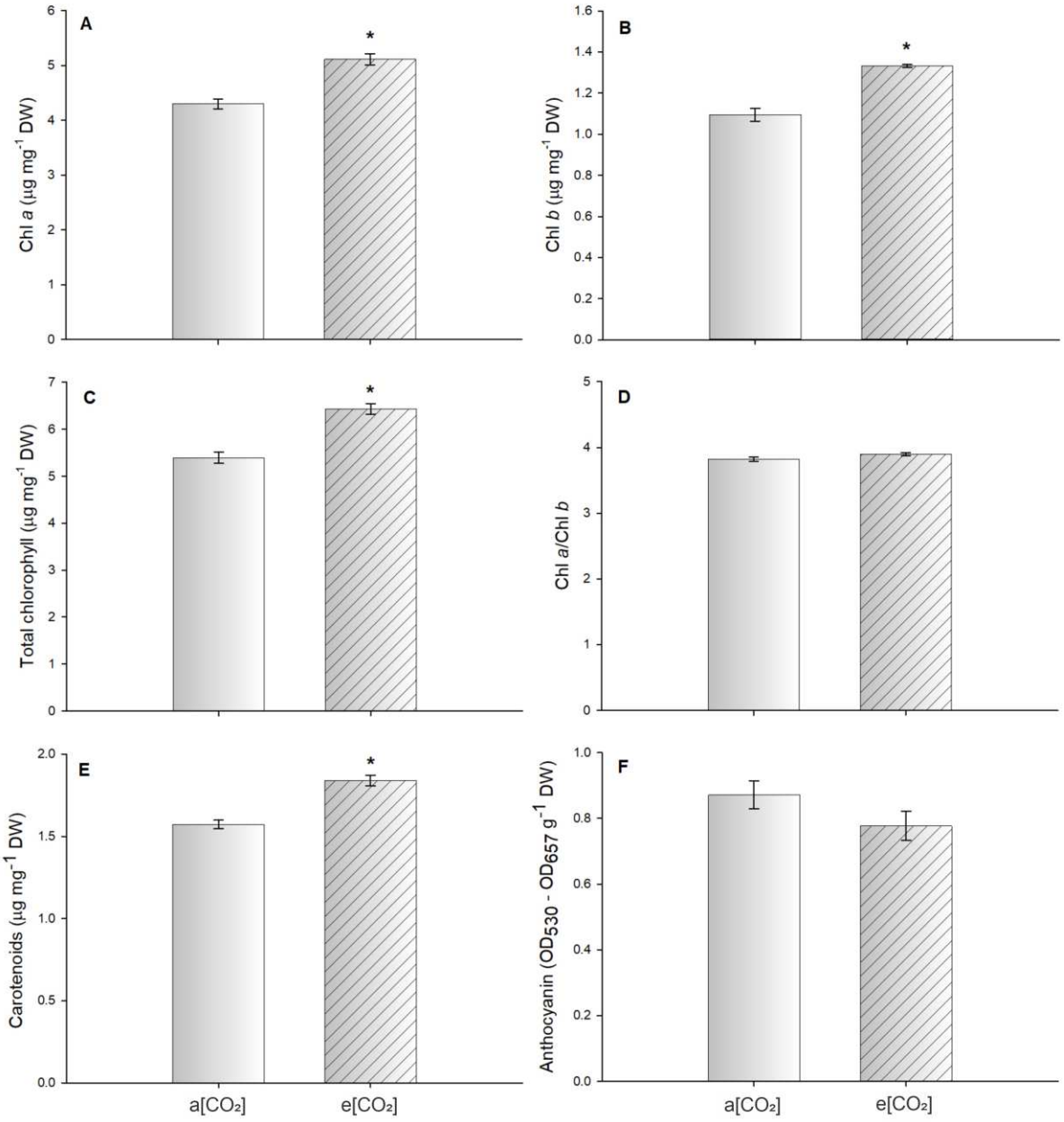

Fig. 5. Pigment content in leaves of *P. glomerata* plants cultivated for 21 days under ambient (a[CO_2]) and elevated (e[CO_2]) CO_2 concentration. (**A**) Chlorophyll *a* (Chl *a*); (**B**) chlorophyll *b* (Chl *b*); (**C**) total chlorophyll; (**D**) chlorophyll *a* and chlorophyll *b* ratio (Chl *a*/Chl *b*); (**E**) carotenoids; and (**F**) anthocyanin. Values are presented as means (n=5) ± standard error. Asterisks indicate significant difference (*t*-Student; $P \leq 0.05$).

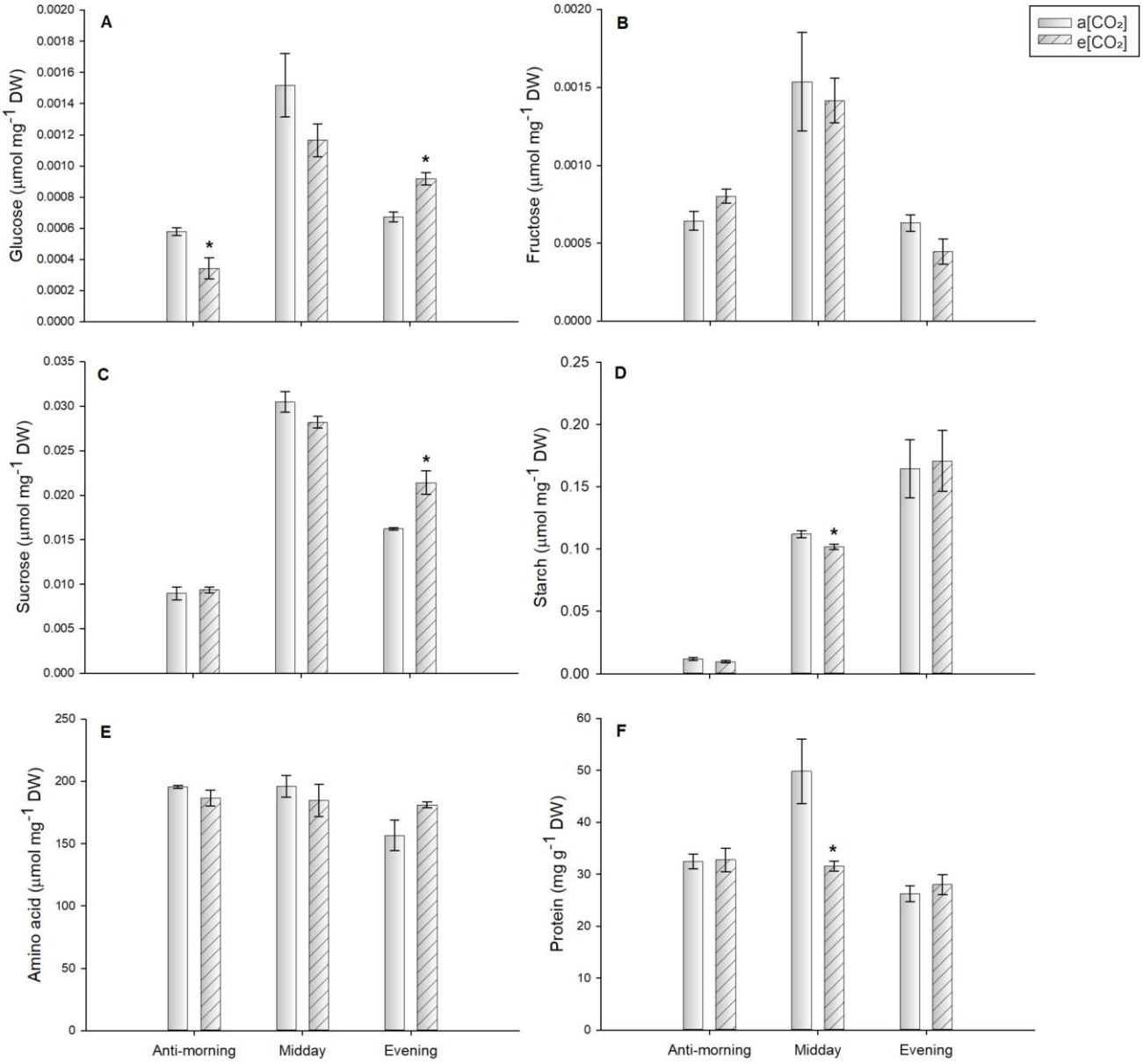

Fig. 6. Changes in metabolite contents involved in carbon metabolism in leaves of *P. glomerata* plants cultivated for 21 days under ambient (a[CO_2]) and elevated (e[CO_2]) CO_2 concentration. (**A**) Glucose; (**B**) fructose; (**C**) sucrose; (**D**) starch; (**E**) amino acid; and (**F**) protein. Values are presented as means (n=4) ± standard error. Asterisks indicate significant difference (*t*-Student; $P \leq 0.05$) in relation to plants grown under a[CO_2] within the same collection time.

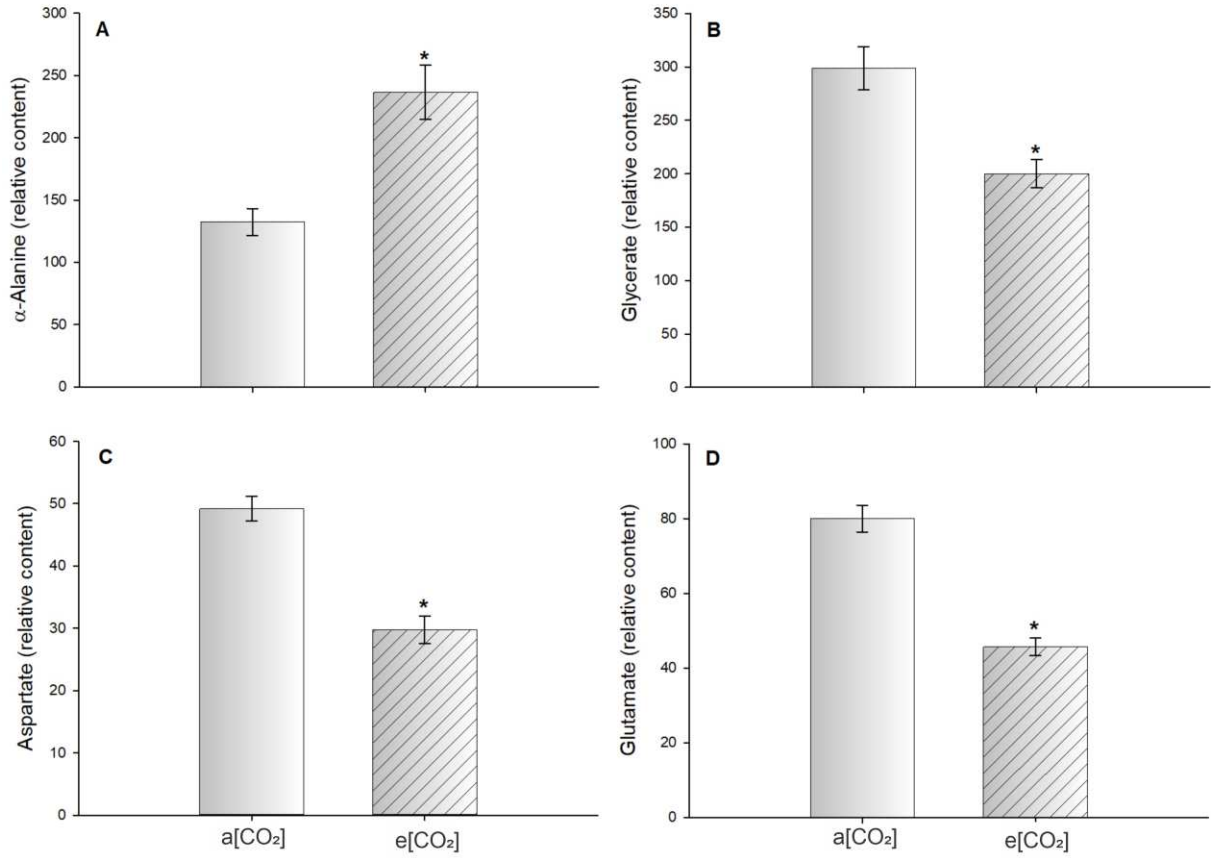

Fig. 7. Relative metabolite content from GC-MS in leaves of *P. glomerata* plants cultivated for 21 days under ambient (a[CO_2]) and elevated (e[CO_2]) CO_2 concentration. (**A**) α-Alanine; (**B**) Glycerate; (**C**) Aspartate; (**D**) Glutamate. Values are presented as means (n=5) ± standard error. Asterisks indicate significant difference (*t*-Student; $P \leq 0.05$).

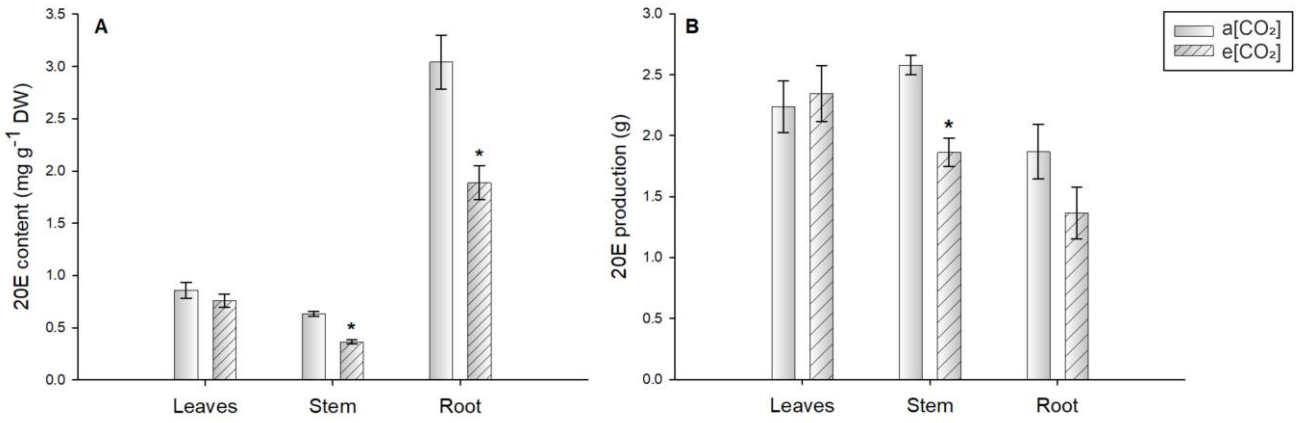

Fig. 8. 20-hydroxyecdysone (20E) content of *P. glomerata* plants cultivated for 21 days under ambient (a[CO_2]) and elevated (e[CO_2]) CO_2 concentration. (**A**) 20E content in leaves, stem and root; and (**B**) 20E production in leaves, stem and root. Values are presented as means (n=6) ± standard error. Asterisks indicate significant difference (*t*-Student; $P \leq 0.05$) in relation to plants grown under a[CO_2] within the same organ type.

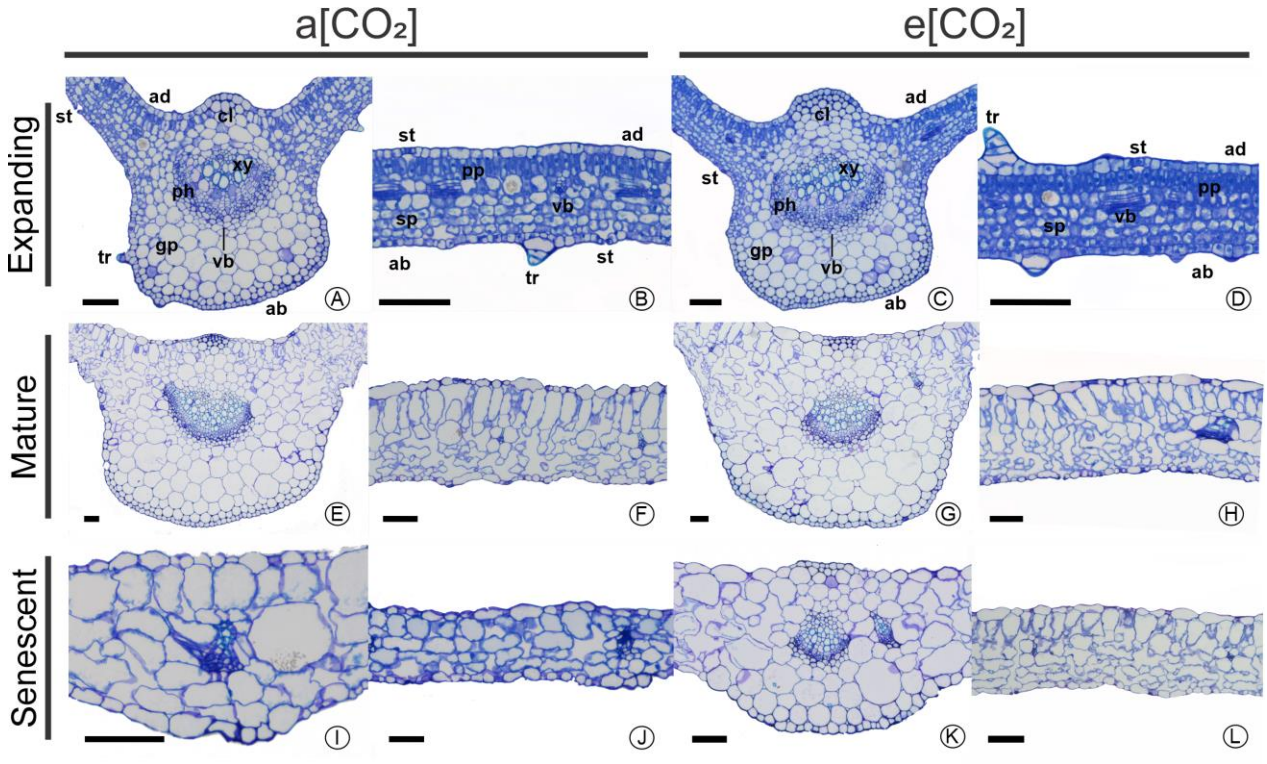

Fig. 9. Leaf midrib cross-sections of *P. glomerata* plants cultivated for 21 days under ambient (a[CO_2]) and elevated (e[CO_2]) CO_2 concentration. (**A-D**) Expanding leaf; (**E-H**) mature leaf; and (**I-L**) senescent leaf. *Abbreviations:* ab, abaxial epidermis; ad, adaxial epidermis; cl, collenchyma; gp, ground parenchyma; ph, phloem; pp, palisade parenchyma; sp, spongy parenchyma; st, stomata; tr, trichome; x, xylem; vb, vascular bundle. Bar = 200 µm.

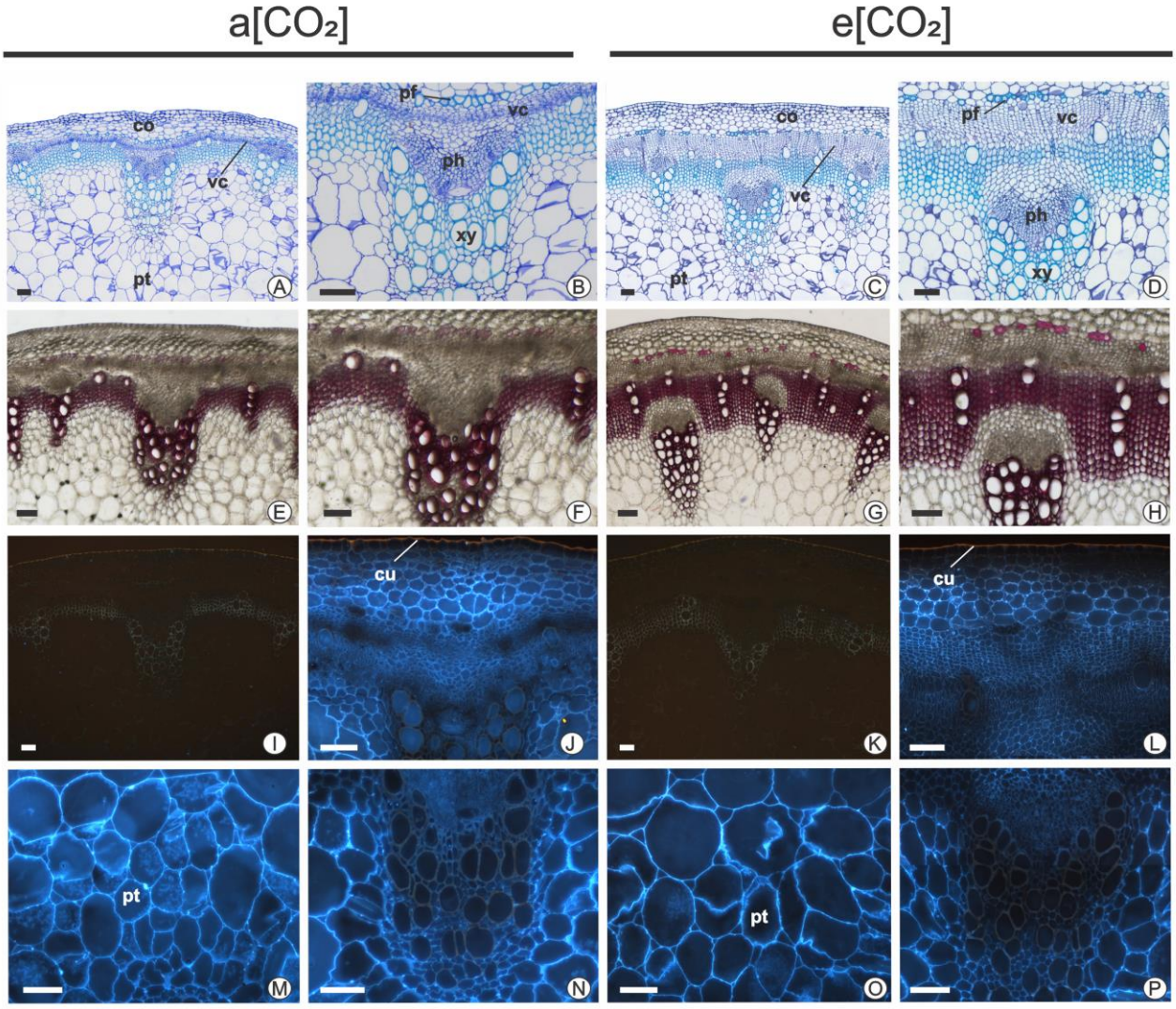

Fig. 10. Stem cross-sections of *P. glomerata* plants cultivated for 21 days under ambient (a[CO_2]) and elevated (e[CO_2]) CO_2 concentration, and stained with the following reagents: (**A-D**) Toluidine blue; (**E-H**) Phloroglucin; and (**I-P**) Calcofluor White. Abbreviations: co, collenchyma; cu, cuticle; pf, perivascular fibers; ph, phloem; pt, pith; x, xylem; vc, vascular cambium. Bar = 200 µm.

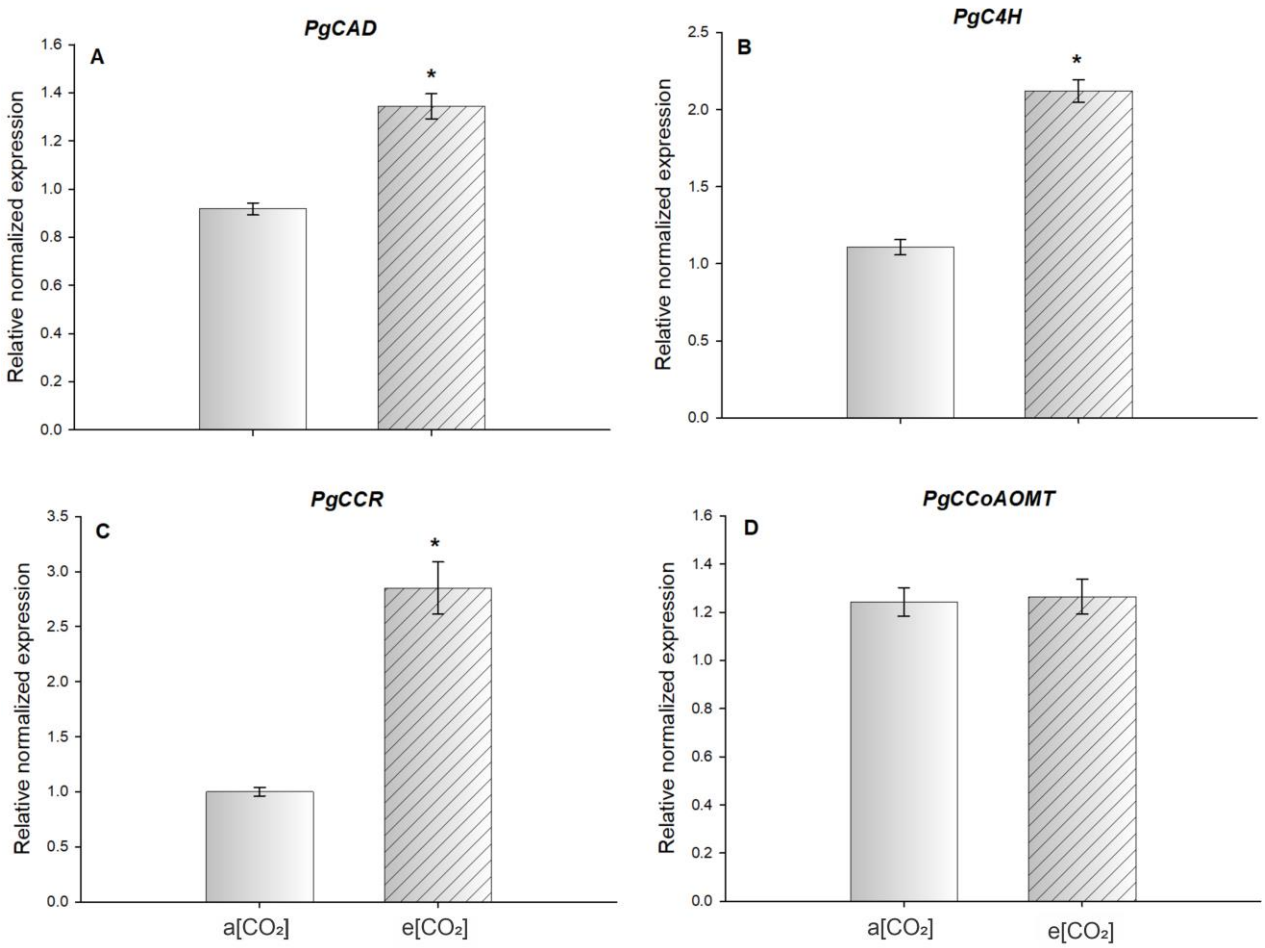

Fig. 11. Relative expression of lignin synthesis pathway genes of *P. glomerata* plants cultivated for 21 days under ambient (a[CO_2]) and elevated (e[CO_2]) CO_2 concentration. (A) *PgCAD*; (B) *PgC4H*; (C) *PgCCR*; ans (D) *PgCCoAOMT*. Expression was normalized by the glyceraldehyde-3-phosphate dehydrogenase gene. Values are presented as means (n=3) ± standard error. Asterisks indicate significant difference (*t*-Student; $P \leq 0.05$).

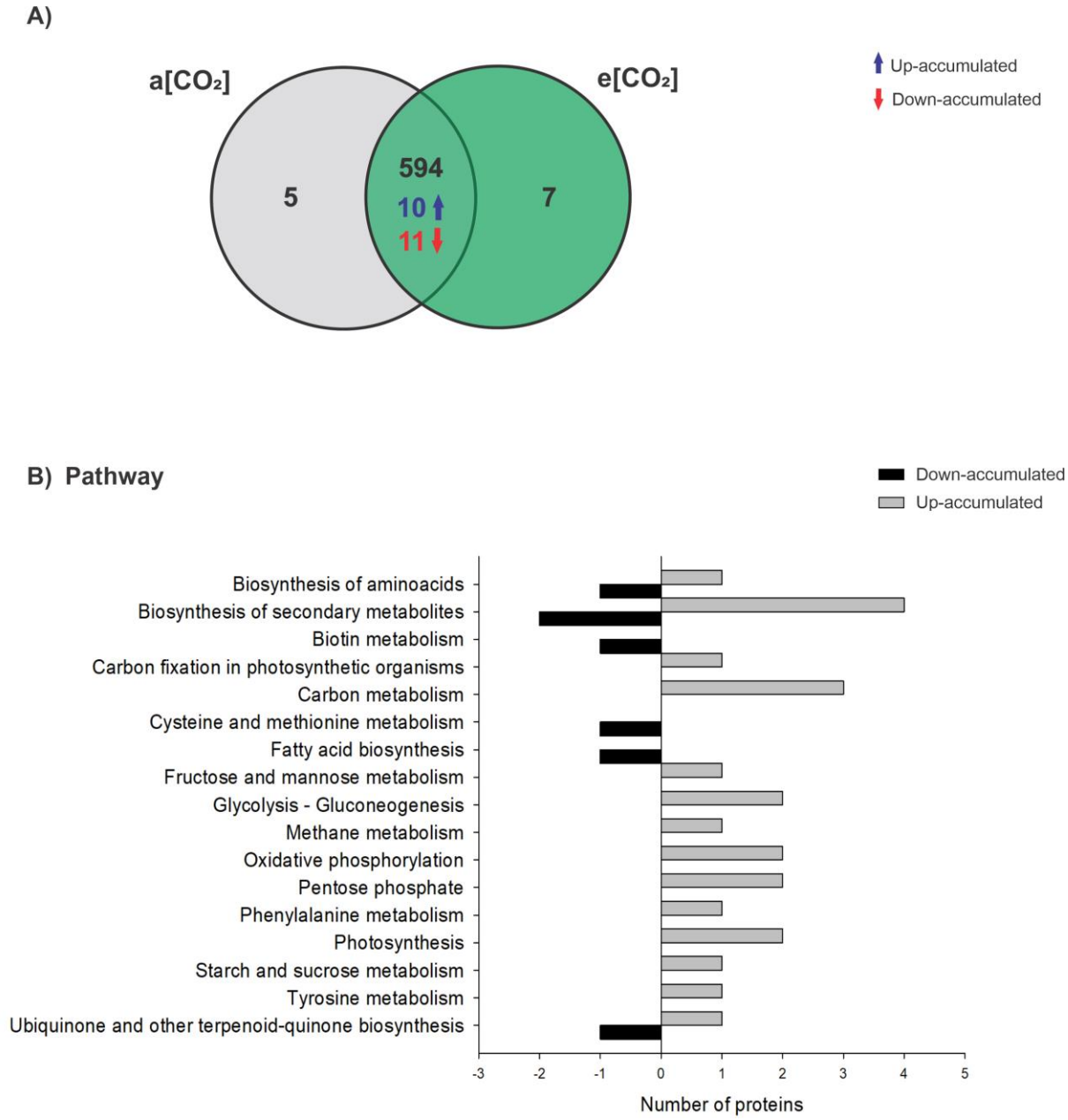

Fig. 12. Analysis of differentially accumulated proteins (DAP) in leaves of *P. glomerata* plants in the comparison e[CO_2]/a[CO_2]. **(A)** Venn diagram showing common DAP proteins; and **(B)** pathway enrichment analysis revealed by KEGG analyzes (Kyoto Encyclopedia of Genes and Genomes).

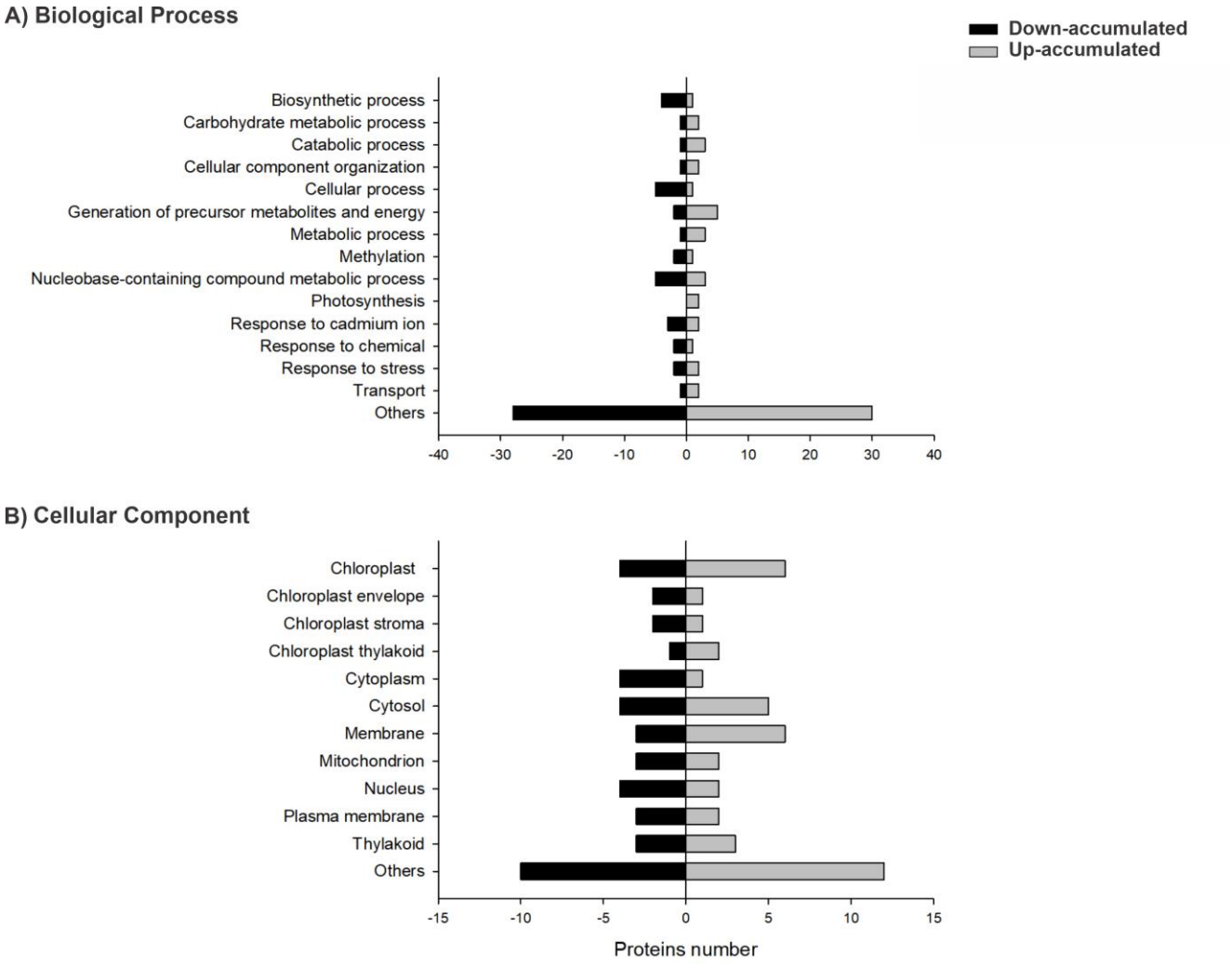

Fig. 13. Functional classification based on the gene ontology (GO) of differentially accumulated proteins in leaves of *P. glomerata* plants in the comparison e[CO_2]/a[CO_2]. (**A**) Biological process; and (**B**) cellular component. Processes and components identified as Others correspond to all the other GO terms added together.

SUPPLEMENTARY MATERIAL

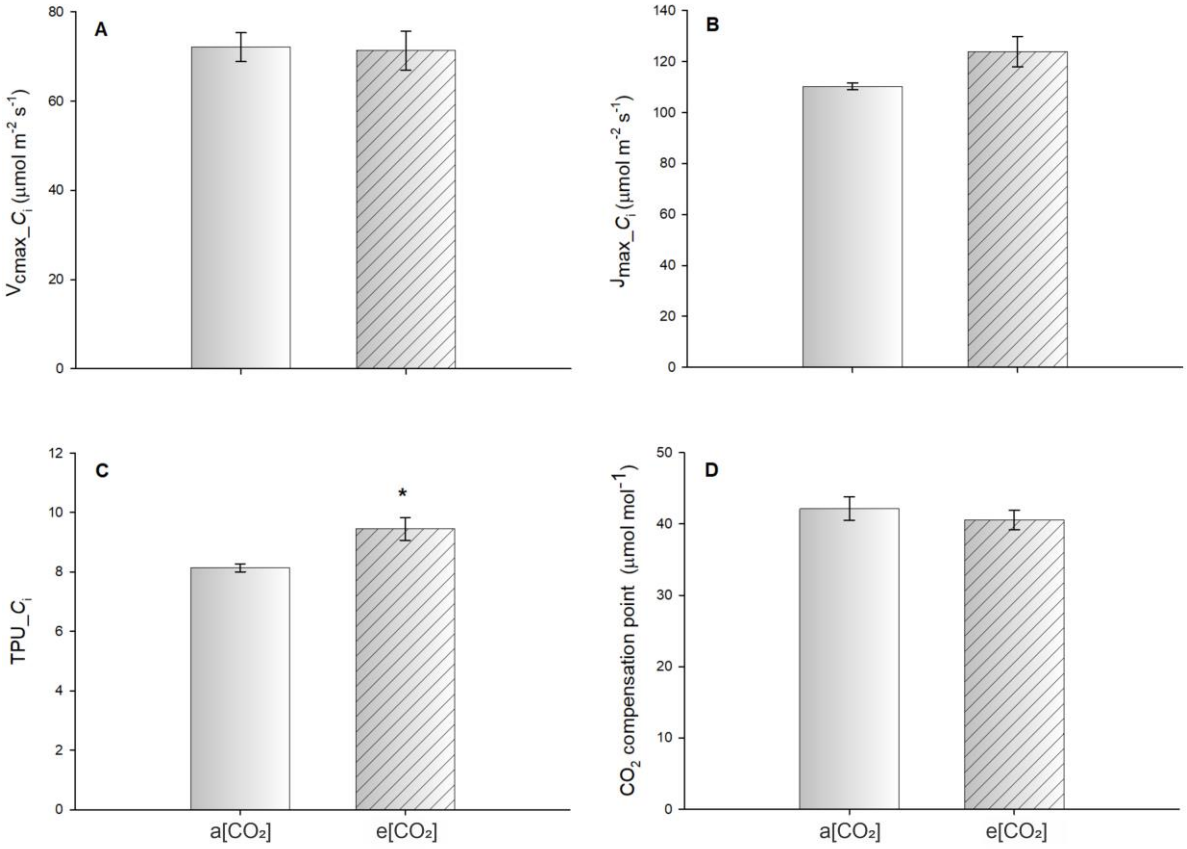

Fig. S1. Alteration in gas exchange parameters in leaves of *P. glomerata* plants cultivated for 21 days under ambient (a[CO_2]) and elevated (e[CO_2]) CO_2 concentration. (**A**) Maximum carboxylation velocity (V_{cmax_Ci}); (**B**) maximum electron transport rate (J_{max_Ci}); (**C**) use of triose phosphate ($TPU_{\_Ci}$); and (**D**) CO_2 compensation point. Values are presented as means (n=6) ± standard error. Asterisks indicate significant difference (*t*-Student; $P \leq 0.05$).

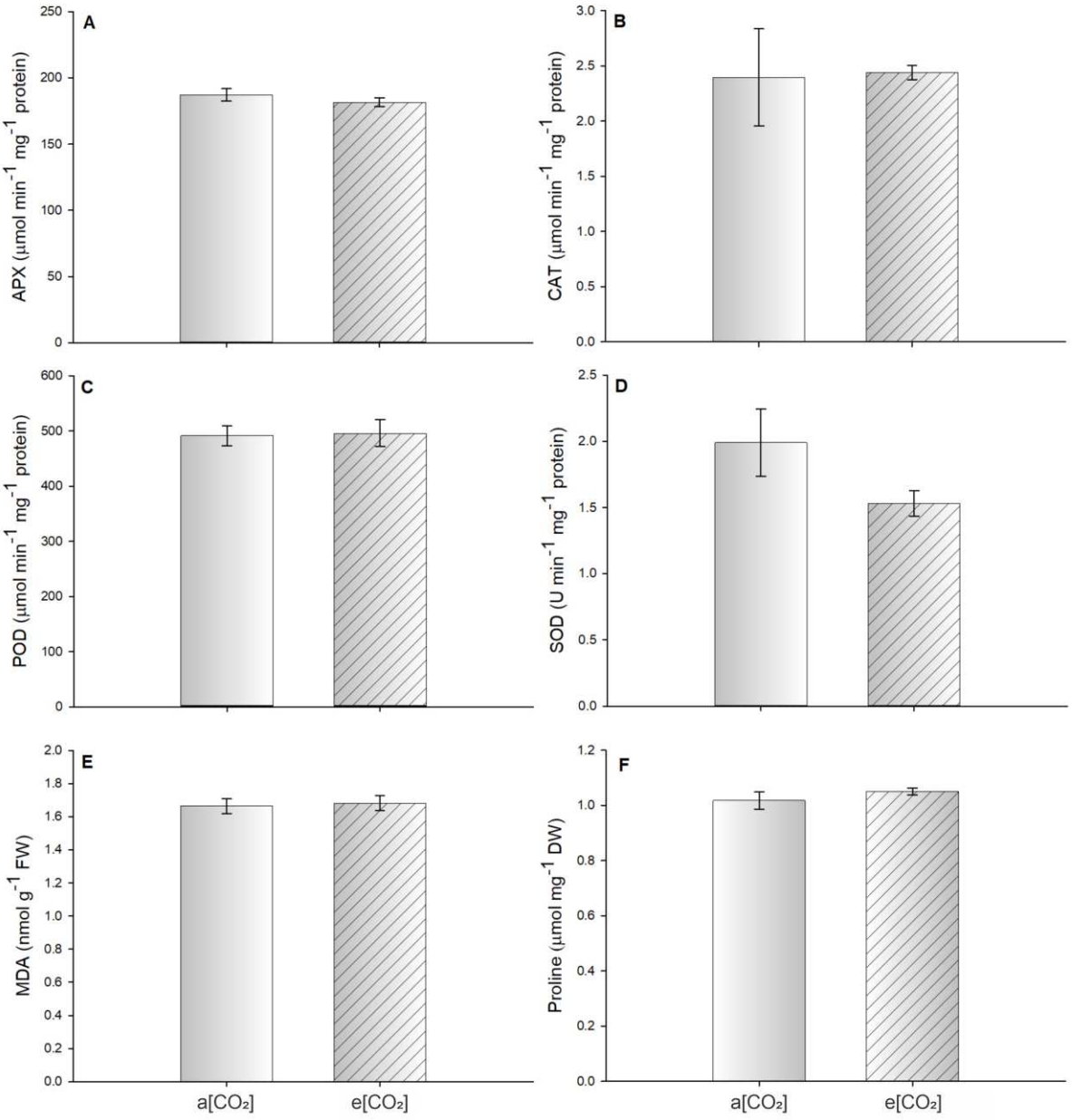

Fig. S2. Enzymes activity involved in antioxidative and malonaldehyde (MDA) and proline content in leaves of *P. glomerata* plants cultivated for 21 days under ambient (a[CO_2]) and elevated (e[CO_2]) CO_2 concentration. (**A**) ascorbate peroxidase (APX); (**B**) Catalase (CAT); (**C**) peroxidases (POD); (**D**) superoxide dismutase (SOD); (**E**) malonaldehyde (MDA); and (**F**) proline. Values are presented as means (n=6) ± standard error. The values of plants under e[CO_2] do not show significantly different (*t*-Student; $P \leq 0.05$).

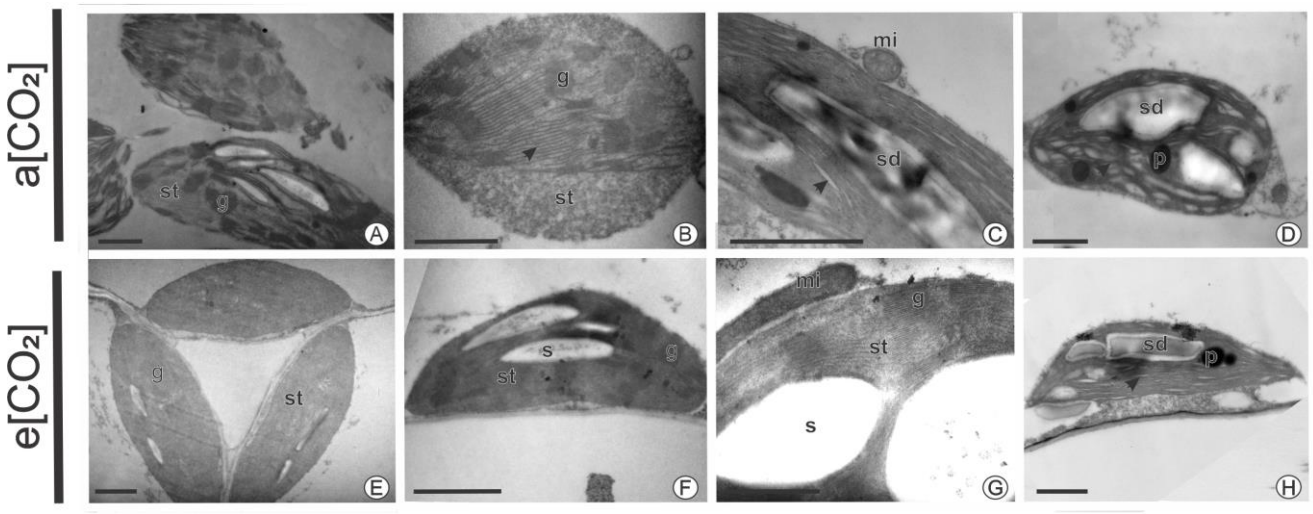

Fig. S3. Chloroplast ultrastructure of senescent leaves of *P. glomerata* plants cultivated for 21 days under ambient (a[CO_2]) and elevated (e[CO_2]) CO_2 concentration.Transmission Electron Microscopy. (**A-D**) Plants grown in a[CO_2]; and (**E-H**) Plants grown in e[CO_2]. *Abbreviations*: g, grana; mi, mitochondria; p, plastoglobuli; s, starch grain; sd, starch degradation; st, stroma thylakoids; arrowhead, ripples in chloroplast internal membranes. Bars = 1.0 µm.

Fig. S4. Pearson correlation coefficients between the variables analyzed in *P. glomerata* plants cultivated for 21 days under ambient (a[CO_2]) and elevated (e[CO_2]) CO_2 concentration. Apreviations: **LA**, leaf area; **TDW**, total dry weight; A_N, net photosynthetic rate; g_s, stomatal conductance; ***E***, transpiration; **WUE**, water use efficiency; **Car**, carotenoids; **TChl**, total chlorophylls; **Gluc**, glucose; **Suc**, sucrose; **Sta**, starch; **TProt**, total proteins; **Asp**, aspartate; **Glu**, glutamate; **Gly**, glycerate; **Ala**, alanine; **20E S**, 20E content of stem; **20E R**, 20E content of root; ***PgCAD***, cinnamyl alcohol dehydrogenase; ***PgC4H***, cinnamate 4-hydroxylase; ***PgCCR***, cinnamoyl-CoA reductase; **SAM-S**, S-adenosylmethionine synthase; **MSBQ**, 2-methyl-6-phytyl-1,4-hydroquinone methyltransferase; **ENR**, Enoyl-acyl-carrier-protein reductase NADH; **FBA**, Fructose-bisphosphate aldolase; **GPI**, Glucose-6-phosphate isomerase; **RuBiCO**, Ribulose bisphosphate carboxylase/oxygenase; **psaB**, Photosystem I P700 apoprotein A2; **psbS**, Photosystem II 22 kDa protein; and **MIF**, Macrophage migration inhibitory factor homolog isoform X2.

https://ufvcv-my.sharepoint.com/:i:/g/personal/tatiane_dulcineia_ufv_br/EdFt-GjliThMmDDkso-UxCYBgpdHdLIjR7B6t7pfhzVYvQ?e=IkBgqv

Table S1. Relative metabolite content in leaves of *P. glomerata* plants cultivated for 21 days under ambient (a[CO_2]) and elevated (e[CO_2]) CO_2 concentration. Means indicated in bold differ statistically from plants under a[CO_2] (*t*-Student; $P \leq 0.05$). Values are presented as means (n=5) ± standard error.

Metabolite	**a[CO_2]**	**e[CO_2]**
α-Alanine	132.40	**236.55**
Aspartate	49.21	**29.75**
Fructose	125.03	127.84
Glucose	56.12	47.87
Glutamate	79.99	**45.70**
Glycerate	298.64	**200.04**
Glycine	192.86	122.22
Malate	20.59	21.87
Oxoproline	489.09	403.39
Serine	50.65	58.90
Threonate	142.86	125.52
Valine	18.19	19.54
Myoinositol	178.35	178.59

Table S2. Complete list of identified proteins, functional protein annotations, and configuration parameters of *P. glomerata* plants cultivated for 21 days under ambient (a[CO_2]) and elevated (e[CO_2]) CO_2 concentration. The *t*-test and Log2 Fold change (FC) was used to calculate the differential protein abundance, being considered up accumulated when Log2 FC > 0.6 and down-accumulated when Log2 FC < -0.6.

https://ufvcv-my.sharepoint.com/:x:/g/personal/tatiane_dulcineia_ufv_br/ETBz7WHfF6RBiR_LJduiZAgBD8XUmZfZKKC3F3mYpNeI3w?e=mi6YlL

Table S3. Complete list of identified common differentially accumulated proteins of *P. glomerata* plants cultivated for 21 days under ambient (a[CO_2]) and elevated (e[CO_2]) CO_2 concentration. The *t*-test and Log2 Fold change (FC) was used to calculate the differential protein abundance, being considered up accumulatedwhen Log2 FC > 0.6 and down-accumulated when Log2 FC < -0.6.

ID	Description	Max score	Reported peptides	Average		t-Test	log_2 of Fold Change	Differential accumulation
				a[CO_2]	e[CO_2]	e[CO_2]/ a[CO_2]		
cds.comp48047_c0_seq1	33 kDa ribonucleoprotein, chloroplastic-like	828.24	2	68173	37830	0.00376	-0.85	DOWN
cds.comp54515_c0_seq1	S-adenosylmethionine synthase 1	4161.31	4	3875	1823	0.00527	-1.09	DOWN
cds.comp18001_c0_seq2	14 kDa zinc-binding protein	1270.99	4	65159	35568	0.04427	-0.87	DOWN
cds.comp62072_c0_seq1	Nuclear poly(A) polymerase 1	3381.16	11	216410	115808	0.04491	-0.90	DOWN
cds.comp62374_c0_seq1	2-methyl-6-phytyl-1,4-hydroquinone methyltransferase, chloroplastic	3983.11	7	237888	76534	0.01097	-1.64	DOWN
cds.comp65506_c0_seq1	Stromal 70 kDa heat shock-related protein, chloroplastic-like	2829.16	10	11446	6541	0.04744	-0.81	DOWN
cds.comp26213_c0_seq1	Glutaredoxin	3130.80	3	78522	47414	0.02436	-0.73	DOWN
cds.comp68161_c0_seq10	Enoyl-[acyl-carrier-protein] reductase [NADH], chloroplastic-like	1239.57	6	49728	25776	0.00082	-0.95	DOWN
	ATP-dependent Clp protease ATP-binding subunit	1286.61	14	117960	63141	0.02213	-0.90	DOWN

cds.comp68883_c0_seq2	ClpA homolog CD4B, chloroplastic							
cds.comp69250_c0_seq1	UPF0664 stress-induced protein C29B12.11c	1143.21	2	265984	100480	0.01692	-1.40	DOWN
cds.comp43203_c1_seq2	14-3-3-like protein GF14 kappa	4205.69	4	2791	1254	0.01291	-1.15	DOWN
cds.comp62531_c1_seq6	14-3-3-like protein A	6298.04	9	2411	-	-	-	Unique a[CO_2]
cds.comp65814_c2_seq1	Tubulin beta-4 chain-like	5368.32	10	27725	-	-	-	Unique a[CO_2]
cds.comp66421_c0_seq1	5-methyltetrahydropteroyltriglutamate--homocysteine methyltransferase-like	5540.94	4	8743	-	-	-	Unique a[CO_2]
cds.comp66736_c0_seq2	Pyrophosphatase	3149.91	5	39924	-	-	-	Unique a[CO_2]
cds.comp43136_c0_seq1	Fructose-bisphosphate aldolase 3, chloroplastic	2824.97	3	9401	-	-	-	Unique a[CO_2]
cds.comp47860_c0_seq3	Ribulose bisphosphate carboxylase/oxygenase	3028.79	5	73880	114102	0.04193	0.63	UP
cds.comp50470_c0_seq1	Macrophage migration inhibitory factor homolog isoform X2	1777.62	3	28830	158651	0.00171	2.46	UP
cds.comp54155_c0_seq1	NADH dehydrogenase [ubiquinone] iron-sulfur protein 7, mitochondrial	3981.57	2	17425	32118	0.02149	0.88	UP
cds.comp54948_c0_seq1	14-3-3-like protein	5780.14	14	58112	112057	0.02467	0.95	UP
	Probable serine/threonine-protein kinase kinX isoform	2523.20	12	68092	125216	0.02857	0.88	UP

cds.comp59822_c0_seq2	X2							
cds.comp65814_c1_seq2	Tubulin beta chain-like	5164.57	4	11480	28288	0.04230	1.30	UP
cds.comp66564_c0_seq4	Photosystem II 22 kDa protein, chloroplastic	7429.89	14	74543	169190	0.00156	1.18	UP
cds.comp66736_c0_seq1	Pyrophosphate-energized vacuolar membrane proton pump	3692.76	8	37632	94356	0.00399	1.33	UP
cds.comp66837_c0_seq1	Luminal-binding protein 5	2711.63	4	21575	36687	0.00452	0.77	UP
cds.comp68986_c0_seq1	TATA-binding protein-associated factor 2N-like isoform X1	16813.05	7	142675	271695	0.02265	0.93	UP
cds.comp58958_c0_seq1	Thioredoxin F-type, chloroplastic-like	4343.83	3	-	4730	-	-	Unique e[CO_2]
cds.comp19157_c0_seq1	Fructose-bisphosphate aldolase 3, chloroplastic	1573.45	2	-	19531	-	-	Unique e[CO_2]
cds.comp62374_c0_seq3	2-methyl-6-phytyl-1,4-hydroquinone methyltransferase, chloroplastic	4029.00	6	-	160108	-	-	Unique e[CO_2]
cds.comp62838_c0_seq1	Glucose-6-phosphate isomerase 1, chloroplastic	1786.24	3	-	39016	-	-	Unique e[CO_2]
cds.comp65786_c0_seq22	Photosystem I P700 apoprotein A2	4095.92	9	-	785	-	-	Unique e[CO_2]
cds.comp28520_c0_seq1	28 kDa ribonucleoprotein, chloroplastic-like	1649.18	3	-	7152	-	-	Unique e[CO_2]
cds.comp41909_c0_seq1	14-3-3-like protein D	1631.19	6	-	3787	-	-	Unique e[CO_2]

Table S4. Complete list of identified pathway and their respective differentially accumulated proteins in *P. glomerata* plants cultivated for 21 days under ambient (a[CO_2]) and elevated (e[CO_2]) CO_2 concentration.

Pathway	**Up-accumulated**	**Down-accumulated**
Biosynthesis of aminoacids	- Fructose-bisphosphate aldolase 3, chloroplastic	- S-adenosylmethionine synthase 1
Biosynthesis of secondary metabolites	- 2-methyl-6-phytyl-1,4-hydroquinone methyltransferase, chloroplastic; - Ribulose bisphosphate carboxylase/oxygenase - Fructose-bisphosphate aldolase 3, chloroplastic - Glucose-6-phosphate isomerase 1, chloroplastic	- 2-methyl-6-phytyl-1,4-hydroquinone methyltransferase, chloroplastic - S-adenosylmethionine synthase 1
Biotin metabolism		- Enoyl-acyl-carrier-protein reductase NADH
Carbon fixation in photosynthetic organisms	- Fructose-bisphosphate aldolase 3, chloroplastic	
Carbon metabolism	- Ribulose bisphosphate carboxylase/oxygenase - Fructose-bisphosphate aldolase 3, chloroplastic - Glucose-6-phosphate isomerase 1, chloroplastic	
Cysteine and methionine metabolism		- S-adenosylmethionine synthase
Fatty acid biosynthesis		- Enoyl-acyl-carrier-protein reductase NADH
Fructose and mannose metabolism	- Fructose-bisphosphate aldolase 3, chloroplastic	
Glycolysis - Gluconeogenesis	- Fructose-bisphosphate aldolase 3, chloroplastic - Glucose-6-phosphate isomerase 1, chloroplastic	

Methane metabolism	- Fructose-bisphosphate aldolase 3, chloroplastic	
Oxidative phosphorylation	- NADH dehydrogenase [ubiquinone] iron-sulfur protein 7, mitochondrial - Pyrophosphate-energized vacuolar membrane proton pump	
Pentose phosphate	- Fructose-bisphosphate aldolase 3, chloroplastic - Glucose-6-phosphate isomerase 1, chloroplastic	
Phenylalanine metabolism	- Macrophage migration inhibitory factor homolog isoform X2	
Photosynthesis	- Photosystem I P700 apoprotein A2 - Photosystem II 22 kDa protein, chloroplastic	
Starch and sucrose metabolism	- Glucose-6-phosphate isomerase 1, chloroplastic	
Tyrosine metabolism	- Macrophage migration inhibitory factor homolog isoform X2	
Ubiquinone and other terpenoid-quinone biosynthesis	- 2-methyl-6-phytyl-1,4-hydroquinone methyltransferase, chloroplastic	- 2-methyl-6-phytyl-1,4-hydroquinone methyltransferase, chloroplastic

CHAPTER 2

Impact of elevated CO_2 and drought stress on morphophysiology and biosynthesis of 20-hydroxyecdysone in *Pfaffia glomerata* [(Spreng.) Pedersen]

Abstract

Abiotic stresses, such as heat, salinity, and drought, are becoming an increasing concern due to the threats of global warming. Furthermore, the atmospheric concentration of carbon dioxide ([CO_2]) has been rising in recent decades. Drought is one of the main limiting factors in plant growth and productivity, but several studies have demonstrated the mitigating effect of elevated [CO_2] (e[CO_2]) on drought stress. Here, we evaluated the effects of e[CO_2] combined with drought stress on morphophysiological responses and 20-hydroxyecdysone (20E) production in *Pfaffia glomerata*. Our data showed that e[CO_2], reduced water loss in leaves, reflected in lower *g*s and less negative water potentials, resulting in higher water use efficiency through amplification of drought stress. However, photosynthesis and growth parameters decreased due to water restriction, independent of [CO_2]. Furthermore, drought altered primary and secondary metabolism in *P. glomerata* plants. While in e[CO_2] the plants invested in osmoregulatory metabolites, such as soluble sugars (glucose, fructose, sucrose, and myo-inositol), malate, free amino acids and glutamate, osmotic adjustment in plants under ambient [CO_2] (a[CO_2]) was subtle. On the other hand, plants grown in the combination of e[CO_2] and drought show a reduction in photosynthetic pigment content, total protein and in the amino acids alanine and aspartate relative to their well-watered control. Comparative proteomic analysis revealed 405 common differentially accumulated proteins (DAPs) involved in 19 metabolic pathways, most of them related to porphyrin metabolism, carbon metabolism, biosynthesis of amino acids, and biosynthesis of cofactors. Under drought condition e[CO_2] delayed or eliminated many DAPs, mainly related to biological stress response processes (e.g. glutathione metabolic process and response to oxidative stress) compared to plants in a[CO_2]. In addition, other mechanisms of drought tolerance commonly expected in plants were observed under a[CO_2] and not in e[CO_2], such as increased root/shoot ratio, advance in secondary growth of the stem, and increase in anthocyanin content. Similar drought response strategies were found in both [CO_2], such as increment in CAT and SOD enzyme activity and increase in 20E content. Although, only e[CO_2] favored increased 20E production, overcoming the biomass limitation caused by drought. Comparing

the e[CO_2] and drought treatment with its well-watered control we report up-accumulation of the cytochrome P450 CYP72A219-like protein, so we believe in a possible relation of this protein to 20E biosynthesis. Lastly, e[CO_2] combined with drought showed to be a favorable environment to improve 20E production in *P. glomerata*.

Keywords: Brazilian ginseng. Climatic changes. Phytoecdysteroids. Proteomics. Water stress.

INTRODUCTION

The rising atmospheric concentration of carbon dioxide ([CO_2]) associated with increasing surface temperatures is considered one of the main driving forces of global climate change. By the end of this century, [CO_2] is expected to reach about 800 ppm (IPCC, 2022). CO_2 is the primary substrate for the photosynthesis and growth of C3 plants, and an increase in its concentration affects the physiological and biochemical processes of the plants (Prasad et al., 2009). For example, it is known that elevated [CO_2] (e[CO_2]) can increase intercellular carboxylation, and consequently increase net photosynthetic rate (A_N) and reduce photorespiration, improving crop yield (Ainsworth and Long, 2005; Bowes, 1991; Lemonnier and Ainsworth, 2018). In addition, e[CO_2] decreases stomatal conductance (*g*s) and transpiration (*E*), often contributing to increase water use efficiency (WUE) in plants (Pazzagli et al., 2016; Qiao et al., 2010; Varga et al., 2017). e[CO_2] can also lead to increased levels of soluble sugar and starch (De la Mata et al., 2012; De Souza et al., 2008; Sun et al., 2012) and in the increase of compounds (e.g. flavonoids, ascorbate, glutamate, and lignin) and antioxidant enzymes (e.g. POD, CAT and SOD) (Al Jaouni et al., 2018; Almuhayawi et al., 2021; Kumari et al., 2015). However, studies have shown that e[CO_2] alters the mineral balance of plants, mainly due to indirectly limiting the uptake of nutrients, especially nitrogen (N), by reducing transpiration, affecting the growth and chemical composition of plants (Dong et al., 2018; Houshmandfar et al., 2015; Taub et al., 2008).

The global warming is not an isolated consequence of increase in [CO_2] emission, abiotic stresses such as heat, frost, salinity and drought occur simultaneously with climate change (Mehmood et al., 2020; Soares et al., 2019). The combination of different abiotic stresses leads to complex plant responses that cannot be deduced separately (Prasch and Sonnewald, 2013). Drought stress is a relevant restricting factor to plant growth and development (Dusenge et al., 2019; Hatfield and Dold, 2019; Le Gall et al., 2015; Xu et al., 2016). Under drought stress, plants can suppress a number of physiological processes, such as A_N, *g*s and *E*, reduce pigment content, growth and biomass accumulation (Bodner et al., 2015; Fathi and Tari, 2016; Hossain et al., 2016).

Several recent studies show that e[CO_2] mitigates damages caused by drought stress. The e[CO_2] often reduces *gs* by improving WUE, leading to important implications for the water balance of plants under drought, such as increased vapor-pressure deficit (VPD) and reduced *E* (Birami, Nägele, et al., 2020; Houshmandfar et al., 2015; Qiao et al., 2010). In

coffee plants, the association of drought stress with e[CO_2] promoted higher water potentials, in parallel with higher hydraulic conductance and *E* (Avila et al., 2020). One of the first responses of plants minimizing excessive water loss during soil drought is increasing leaf abscisic acid (ABA) levels, due to its role in regulating stomatal closure, and consequently, *g*s (Aroca et al., 2006; Li et al., 2020a; Zhang et al., 2019). Therefore, ABA and e[CO_2] induce rapid stomatal closure, but the mechanisms of how this signal occurs remain unclear. Studies point to a model in which the rapid transduction of the CO_2 signal leading to stomatal closure occurs via an ABA-independent pathway (Hsu et al., 2018; Zhang et al., 2020).

Increased intercellular CO_2 concentration (C_i) in plants under e[CO_2] compensate for the CO_2 restriction caused by decreased *g*s under drought stress (Morison and Gifford, 1983). In *Arabidopsis thaliana*, e[CO_2] significantly mitigated the impact of drought and heat, although it reduced biomass and inhibited photosynthesis, e[CO_2] positively regulated antioxidant defense metabolites and reduced photorespiration (Zinta et al., 2014). The e[CO_2] can alleviate the adverse effect of drought by accumulating osmoregulatory compounds, such as carbohydrates and amino acids, leading to increased cellular osmotic potential and improving the water balance of plants (Dong et al., 2015; Vivin et al., 1996). In addition, several classes of secondary metabolites can be regulated by e[CO_2] during abiotic stress, such as alkaloids, phenols, flavonoids, terpenes, and steroids (Hozzein et al., 2020; Li et al., 2017; Ramakrishna and Ravishankar, 2013; Roy and Mathur, 2021).

The 20-hydroxyecdysone (20E), alongside the juvenile hormone mediates developmental transitions in insects and other arthropods (Guo et al. 2021; Jindra et al. 2013; Lin and Smagghe 2019; Riddiford et al. 2003). In a select group of plants, 20E is a secondary metabolite and little is known about its biological functions. The main hypothesis is that 20E is a protective compound against non-adapted phytophagous insects (Bakrim et al., 2008; Festucci-Buselli et al., 2008; Lafont, 1997). After these insects feed on 20E producing plants there will be a deregulation of their endocrine system, affecting their larval development by anticipating the ecdysis process, possibly causing the death of the larvae (Dinan et al., 2020; Rharrabe et al. 2010). Therefore, phytoecdysteroids act as protection against phytophagous invertebrates, and can be an excellent substitute for synthetic insecticides (Chaubey, 2018).

In addition, 20E has many beneficial effects in mammals, including humans, such as fighting gastric problems, rheumatism, diabetes, anti-inflammatory, and analgesic action, antimicrobial action, muscle tonic, antimutagenic, aphrodisiac, and other herbal properties related to 20E (Almeida et al., 2017; Buniam et al., 2020; Dinan et al., 2021; Franco et al.,

2021; Neto et al., 2005; Neves et al., 2016). Among the 20E-producing plants is *Pfaffia glomerata* (Amaranthaceae), known as Brazilian ginseng (Nascimento et al., 2007). Herbaceous species native to South America, widely distributed in Brazil, especially in regions with riparian vegetation and river floodplains (Marchioretto et al., 2010). Therefore, due to the medicinal and economic interest of *P. glomerata*, more studies are needed to provide a better understanding of the secondary metabolism of this species.

Several studies demonstrate that 20E production in *P. glomerata* can be modulated by in vitro culture conditions (Corrêa et al., 2015; Fortini et al., 2020; Iarema et al., 2012; Saldanha et al., 2013; Silva et al., 2019; Silva et al., 2020; Silva et al., 2021). However, little is known about the physiological and molecular mechanisms that regulate 20E biosynthesis in plants (Tsukagoshi et al., 2016). Studies have validated the participation of the cytochrome P450 gene family in the biosynthetic route of ecdysteroids in plants (Batista et al., 2019; Janeczko et al., 2021; Lei et al., 2018; Park et al., 2020; Wang et al., 2018). In *P. glomerata*, the *Halloween-genes Spook* and *Phantom*, previously described as regulators of 20E biosynthesis in insects, were identified, and the expression level of these two genes can be regulated by abiotic stress conditions (Batista et al., 2019). Felipe et al. (2019a,b) showed that ultraviolet-B radiation and moderate salt stress promoted an increase in 20E content and up-regulated these genes in *P. glomerata* plants.

Given the above and aware that enrichment of [CO_2] in vitro leads to morphophysiological changes in *P. glomerata* (Ferreira et al., 2019; Louback et al., 2021; Saldanha et al., 2013, 2014) and that 20E can be modulated by abiotic stresses (Felipe et al., 2019a,b; Fortini et al., 2022). Here, we raise the following hypotheses: (i) CO_2-enrichment associated with drought stress can lead to changes in morphophysiology and 20E content; and (ii) CO_2-enrichment is able to mitigate the effects of drought stress. Thus, the objective of the work was to evaluate the effects of elevated CO_2 and drought on the morphology and production of 20E in *P. glomerata*.

MATERIALS AND METHODS

Plant material and experimental design

Pfaffia glomerata plants (Accession 22) came from a germplasm bank of the Plant Tissue Culture Laboratory (LCT-II, BIOAGRO, Universidade Federal de Viçosa). Voucher material was deposited at the Leopoldo Krieger Herbarium (UFJF, Juiz de Fora, MG, Brazil) under code number CESJ 63317. Access to the genetic material (permission number AA2A367) was granted by the Brazilian National System for the Management of Genetic Heritage and Associated Traditional Knowledge (SISGEN), in accordance with existing Brazilian biodiversity legislation.

Nodal segments (≈ 1.5 cm) without leaves of *P. glomerata* were grown in vitro on MS medium (Murashige and Skoog, 1962), supplemented with vitamins, and myo-inositol (100 mg L^{-1}) (Sigma-Aldrich Co, St Louis, MO, USA), and solidified with 5.5 g L^{-1} agar (PhytoTechnology Laboratories®, KS, USA). The flasks were closed with rigid polypropylene lids with two holes of 10 mm covered by two 0.45 μm-pore hydrophobic fluoropore polytetrafluoroethylene membranes (MilliSeal AVS-045 Air Vent, Tokyo, Japan), with the CO_2 exchange rate of 25 μL L^{-1} s^{-1} (Batista et al., 2017). The cultures were maintained at 25 ± 2 °C, under 60 μmol m^{-2} s^{-1} irradiance and 16 h light photoperiod for 30 days.

After the in vitro culture, plants were acclimatized for 7 days in 300 mL plastic cups (COPOBRAS, São Ludgero, SC, Brazil). Then, they were transplanted into plastic pots with 2 kg of commercial substrate Tropstrato HT® (Vida Verde, Mogi Mirim, Brazil) and the plants were grown in a greenhouse (average temperature 21/12 ± 2 °C, day/night; naturally fluctuating air humidity and photosynthetic photon flux density (PPFD)) for another 7 days. Subsequently, plantlets were transferred to open top chambers (OTC), 1.15 m in diameter and 1.40 m in height, and subjected to ambient CO_2 concentration (a[CO_2], ≈ 400 μmol mol^{-1}); or elevated CO_2 (e[CO_2], ≈ 800 μmol mol^{-1}). During the first 14 days of cultivation, all plants were regularly irrigated to maintain soil water at field capacity. CO_2 fumigation was accomplished from 06:00 to 18:00 h and was checked daily the [CO_2], temperature, and humidity using portable CO_2 sensors (model CO277, Akso Produtos Eletrônicos, São Leopoldo, Brazil).

To evaluate the influence of CO_2-enrichment associated with drought stress, plants were subjected to four combinations of treatments: (**I**) a[CO_2] and well-watered (a[CO_2]WW); (**II**) e[CO_2] and well-watered (e[CO_2]WW); (**III**) a[CO_2] and drought stressed (a[CO_2]D); and

(**IV**) e[CO_2] and drought stressed (e[CO_2]D). Therefore, plants in treatments **I** and **II** were irrigated until the end of the experiment, while irrigation has been suspended completely for plants in treatments **III** and **IV**. During the greenhouse cultivation (41 days in total, being 21 days of acclimation and 20 days of experiment), the plants were fertilized on days 1 and 15 with 5.5 g NPK - 15:09:12 (Osmocote® Plus, São Paulo, Brazil). The experiment was conducted in the winter period from June to August 2021.

The experimental was designed in a completely randomized design, in a 2x2 factorial scheme, corresponding to two [CO_2] (ambient and elevated) and two water regimes (well-watered and drought stress), as detailed above. Each treatment was composed of one OTC, with 15 repetitions each, totaling 60 plants in the experiment. The evaluations were started when the water potential of at least 50% of the plants in treatment **III** reached the water potential of -0.7 MPa (on the 19th day). After 20 days of the establishment of drought stress, growth variables, photosynthetic parameters, hyperspectral data, water potential, and leaf water loss were evaluated. Leaf, stem and root sections were collected for anatomy. In addition, leaf samples were collected at three times of the day (6:00 am, 12:00 pm, and 6:00 pm), and immediately frozen in liquid nitrogen and stored at -80 ºC for later biochemical and molecular analyses.

Plant water status

Plant water status was determined throughout the experiment by means of a Scholander-type pressure chamber (model 1000, PMS Instruments, Albany, NY, USA) in the early anti-morning (Ψam) and at midday (Ψmd). The first pair of leaves fully expanded from the apex to the base was cut at the petiole insertion and immediately placed in the chamber for measurement of the water potential (Ψw) (Scholander et al., 1964). The results were expressed in MPa.

Determination of water loss in detached leaf

To determine water loss, the leaves were detached, kept on plates with the abaxial side facing up, and the weights were measured on a precision analytical balance at 15 min intervals over a 4 h period. Subsequently, water loss was calculated as the percentage of fresh weight loss, relative to the initial fresh weight (Araújo et al., 2011).

Growth analysis

Stem length (cm), largest root length (cm), total dry weight (g), leaf number, leaf area (cm^2) were measured. For determination of leaf area, leaves were detached and fixed individually on white plasticized graph paper. Photographs were taken with a digital camera and images were processed using ImageJ software (Schneider et al., 2012). Dry weight (g) was obtained by oven-drying the plant material at 50°C for 72 h.

Gas exchange parameters

The net carbon assimilation rate (A_N), stomatal conductance (g_s), transpiration (E), internal CO_2 concentration (C_i), and the instantaneous water use efficiency (WUE) calculated by the ratio A_N/E was evaluated with the aid of an infrared gas analyzer (LI-6400, Li-Cor Inc., Lincoln, Nebraska, USA). Measurements were conducted after 1 h of illumination during the light period under PPFD of (1000 μmol m^{-2} s^{-1}). The reference CO_2 concentration was set at 400 μmol CO_2 mol^{-1} of air in plants under a[CO_2] and 800 μmol CO_2 mol^{-1} of air in plants under e[CO_2]. All measurements were performed using the 2 cm^2 leaf chamber at 25°C, and the leaf-to-air vapor pressure deficit was kept at 1.2-2.0 kPa, while the amount of blue light was set to 10% PPFD to optimize stomatal aperture.

Hyperspectral data collection

Leaf spectral were collected using a FieldSpec®4 Hi-Res spectroradiometer (Analytical Spectral Devices, Boulder, CO, USA), coupled with an ASD Contact Probe with 10 mm in diameter as described by Fernandes et al. (2020). A leaf clip (Analytical Spectral Devices, Boulder, CO, USA) was used in the plant analysis to ensure orthogonal data free of atmospheric effects (Amaral et al., 2018; Meerdink et al., 2016). Each measurement was taken at a single point on the adaxial side of the leaves, at the middle lobe, excluding the median vein. Black and white (Spectralon®, Labsphere Inc. - North Sutton, NH, USA) artificial targets were used to optimize the equipment and automatically obtain reflectance values (wavelengths of 350-2500 nm) and the spectral resolution of the target bands was measured as described by Danner et al. (2015). The collected measurements were used to calculate different vegetation indexes (Table 1).

Metabolite analysis

Leaf samples (second fully expanded leaf from the apex of plants) were harvested at three times of the day: 6:00 am (anti-morning), 12:00 pm (midday), and 6:00 pm (evening). The samples were flash frozen in liquid nitrogen, and subsequently ground and lyophilized for analysis. Approximately 10 mg lyophilized tissues were used for extraction with methanolic as described by Lisec et al. (2006). Photosynthetic pigments were determined as described by Porra et al. (1989) and anthocyanin by Neff and Chory (1998). Carbohydrates (starch, sucrose, glucose, and fructose) were evaluated as described by Fernie et al. (2001). Protein and total amino acid levels were analyzed as reported in Gibon et al. (2004). Malate content was determined as previously described by Nunes-Nesi et al. (2007). Proline content followed the methodology proposed by Bates et al. (1973), with some modifications described previously by Felipe et al. (2019b).

Other metabolites of interest were quantified by gas chromatography-mass spectrometry (GC-MS). Approximately 10 mg lyophilized leaf tissues was extracted in 1.5 mL of extraction solution (water:methanol:chloroform, 1:2.5:1 v/v) as described by Fiehn (2007), using 5 µM ribitol (Sigma-Aldrich) as the internal standard. The extract (400 µL) was dried in a vacuum concentrator and derivatized in two steps using the MPS Dual Head autosampler (Gerstel), as described by Gu et al. (2012). After incubation for 2 h at room temperature, the samples were analyzed as described previously (Shim et al., 2020) using the 5977B GC-MSD system (Agilent Technologies). The peaks were integrated using MassHunter Quantitative (v b08.00; Agilent Technologies). For relative quantification, metabolite peak areas were normalized to the corresponding dry weight and peak area of the internal standard (ribitol). For comparative analysis of primary metabolites, a heatmap was constructed using the Log2 Fold change (FC) criterion, and metabolite was considered accumulated when Log2 FC > 0.6 and accumulated when Log2 FC < -0.6. Red, down-accumulated and Blue, up-accumulated.

Enzyme analysis and lipid peroxidation

The enzymes catalase (CAT, EC 1.11.1.6), ascorbate peroxidase (APX, EC 1.11.1.11), superoxide dismutase (SOD, EC 1.15.1.1), and peroxidase oxidoreductase (POD, EC1.11.1.7) were quantifed. Briefly, 50 mg of macerated leaf samples were collected and extracted in 1 mL extraction medium containing 0.1 M potassium phosphate buffer, pH 6.8; 0.1 mM

ethylenediaminetetraacetic acid; 1 mM phenylmethylsulfonyl fuoride and 1% (*w/v*) polyvinylpolypyrrolidone. Then, the sample was centrifuged at 16,000 *g* for 15 min at 4 °C, and the supernatant was removed and set aside on ice for enzyme assays plus protein determination (Bradford, 1976). CAT, APX, and POD activities were determined as proposed previously (Chance and Maehly, 1955; Havir and McHale, 1987; Nakano and Asada, 1981) and expressed as $\mu mol^{-1}\ min^{-1}\ mg^{-1}$ protein. SOD activity was measured as described earlier (Giannopolitis and Ries, 1977) and expressed as $U\ min^{-1}\ mg^{-1}$ protein, with 1 U being equivalent to the concentration of SOD required to inhibit 50% of nitro blue tetrazolium photoreduction.

Lipid peroxidation was determined based on the quantification of malondialdehyde (MDA), as proposed by por (Lima et al., 2002) with modifications. Extraction was performed by adding 1 mL of 1% trichloroacetic acid (TCA) to 50 mg of fresh and macerated leaf samples. The solution was vortexed and centrifuged at 12.000 *g* for 15 min at 4 °C, after which 125 µL of the supernatant were transferred to new tubes, along with 375 µL of 0.5% 2-thiobarbituric acid (*w/v*) in 20% TCA (*w/v*). The reaction proceeded for 30 min with shaking at 95°C, and was blocked by incubation in an ice bath. The supernatants were transferred to new tubes, centrifuged at 10.000 *g* for 10 min at 4°C, and read on a spectrophotometer at 532 and 600 nm. With the absorbance values, the means of the triplicates were obtained and the MDA concentration was determined by the equation of Heath and Packer (1968), expressing the results in $nmol\ g^{-1}$ FW.

Quantification of 20E

The 20E quantification was performed according to the methodology described by Corrêa et al. (2015). Briefly, a methanolic extraction of macerated samples of leaves, stem and roots was performed. The determination of 20E was done using a Shimadzu Proeminence liquid chromatography system (Shimadzu, Kyoto, Japan) equipped with RP column (150 mm x 4,6 mm i.d., 5 µm particle size; C18 stationary phase) from Phenomenex (Torrance, CA) and a Shimadzu SPD –M20A photodiode array detector (monitoring 246 nm). The mobile phase of 1:1 (*v/v*) methanol:water, the flow rate of 1.0 mL min^{-1}, injection of 20 µL of extract, and with reading at 245 nm for 15 min. A 20E standard (Sigma-Aldrich) solution was prepared to quantify a calibration curve (0-120 mg L^{-1}). 20E content was expressed by mg g^{-1} DW and 20E production by g.

Anatomical characterization

For the anatomical assessments, transverse sections of the midrib of leaves from three phenological stages, expanding, mature and senescent, and of stems from the midrib of the fourth internode. The samples were fixed in Karnovsky's solution (Karnovsky, 1964), composed of: 2.5% glutaraldehyde, 4.0% paraformaldehyde, 5 mM $CaCl_2$, in 0.1M cacodylate buffer, pH 6.8, and kept refrigerated. After fxation, the samples were dehydrated in ethanolic series and included in acrylic resin (Historesin®, Leica Instruments, Wetzlar, Germany). Transverse sections (5 μm thickness) were obtained on an automated advance rotary microtome (RM2155, Leica Microsystems Inc., Buffalo Grove, IL, USA). For structural characterization, samples were stained in toluidine blue (pH 3.2) for 3 min (O'Brien and McCully, 1981). The sections were then mounted on glass slides with synthetic Permount® SP15-500 resin (Fisher Chemicals, Thermo Fisher Scientifc, Waltham, MA, USA) and observed under a light microscope. Images were captured on a light microscope (AX70 TRF; Olympus Optical, Tokyo, Japan) with a U-photo system, coupled to a digital color camera (Spot Insight 3.2.0; Diagnostic Instruments Inc., Sterling Heights, MI, USA) and microcomputer with the Spot Basic image capture program.

Protein extraction and digestion

Proteomic analyses were performed using freeze-dried and macerated leaf samples (three biological replicates, 60 mg DW each sample). The extraction was performed by the methodology described by Damerval et al. (1986), by suspending the samples in a buffer solution (10% (*w/v*) Trichloroacetic acid/acetone (Sigma-Aldrich) together with 20 mM of Dithiothreitol (DTT, GE Healthcare, Piscataway, NJ, USA), with subsequent vortex mixing (5 min, 8 °C). The solution was kept for 60 min at -20 °C and then centrifuged (16.000 *g*, 30 min, 4 °C). The pellets from the previous step were washed 3 times in acetone solution with DTT (20 mM) and centrifuged for 5 min each wash. Subsequently, the pellets were dried under vacuum, solubilized in a buffer composed of 7 M urea (GE Healthcare), 2 M thiourea (GE Healthcare), 2% Triton X-100 (GE Healthcare), 1% DTT, 1 mM phenylmethylsulfonyl fluoride (PMSF; Sigma-Aldrich), and 5 μM pepstatin (Sigma-Aldrich), and incubated for 30 min on ice. The samples were vortexed (16.000 *g*, 30 min, 8 °C), the supernatants were collected, and the protein concentration was measured using a 2-D Quant Kit (GE

Healthcare). Before the trypsin digestion step, protein samples (100 µg from each biological replicate) were precipitated using the methanol/chloroform, and the samples were resuspended in a solution buffer (urea 7 M/thiourea 2 M). Protein digestion was performed by filter-aided sample preparation (FASP) methodology according to Reis et al. (2021). Then, the peptides and proteins were quantified through a NanoDrop 2000c spectrophotometer (Thermo Fisher Scientific, Waltham, MA, USA), at a wavelength of 205 nm. The peptides were stored at −80 °C prior to analyses.

Mass spectrometry analysis

Mass spectrometry was performed using a nanoAcquity UPLC connected to a Q-TOF SYNAPT G2-Si instrument (Waters, Manchester, UK) according to Passamani et al. (2020). Briefly, runs consisted of three biological replicates of 1 µg of digested peptides. During separation, samples were loaded onto the nanoAcquity UPLC M-Class Symmetry C18 5 µm trap column (180 µm × 20 mm) at 5 µl min^{-1} for 3 min and then onto the nanoAcquity M-Class HSS T3 1.8 µm analytical reversed-phase column (75 µm × 150 mm) at 400 nl min^{-1}, with a column temperature of 45°C. For peptide elution, a binary gradient was used, with mobile phase A consisting of water (Tedia; Fairfield, Ohio, USA) and 0.1% formic acid (Sigma-Aldrich) and mobile phase B consisting of acetonitrile (Sigma-Aldrich) and 0.1% formic acid. The gradient elution started at 7% B, then ramped from 7 B to 40% B until 91.12 min, then ramped again from 40 B to 99.9% B until 92.72 min, then remained at 99.9% until 106.00 min, then decreased to 7% B until 106.1 min, and finally remained at 7% B until the end of run at 120 min. Mass spectrometry was performed in positive and resolution mode (V mode), at 35,000 FWHM, with ion mobility, and in data-independent acquisition mode (HDMSE). Human [Glu1]-fibrinopeptide B at 100 fmol $µl^{-1}$ was used as an external calibrant, and lock mass acquisition was performed every 30 s. Mass spectra were acquired by MassLynx v 4.1 software.

Proteomic data analysis

Spectra processing and comparative analysis were performed according to Passamani et al. (2020). Spectra processing and database searching were performed using ProteinLynx Global Server (PLGS) software v. 3.0.2 (Waters). The Apex3D parameters were set to a low-

energy threshold of 150 counts, an elevated-energy threshold of 50 counts, and an intensity threshold of 750 counts. In addition, the analysis settings included the following: one missed cleavage, minimum fragment ion per peptide equal to 3, minimum fragment ions per protein equal to 7, minimum peptide per protein equal to 2, automatic peptide and fragment tolerance, a fixed modification of carbamidomethyl and variable modifications of oxidation and phosphoryl. The false discovery rate (FDR) was set to a maximum of 1%. The proteomics data were processed against the *P. glomerata* data base (http://www.ncbi.nlm.nih.gov/biosample/8103044; Batista et al., 2019a). Comparative label-free quantification was performed using ISOQuant software v. 1.7 (Distler et al., 2014). Briefly, for ISOQuant the following parameters were used to identify proteins: a 1% FDR, a peptide score greater than six, a minimum peptide length of six amino acids, and at least two peptides per protein were required for label-free quantitation using the TOP3 approach, followed by the multidimensional normalized process within ISOQuant. The mass spectrometry proteomic data have been deposited with ProteomeXchange (Deutsch et al. 2019). Consortium via the PRIDE (Perez-Riverol et al. 2019) partner repository.

For comparative proteomic analysis, only proteins present in all three biological replications, or absent in all replicates (for unique proteins) were considered. Data were analyzed using Student's *t*-test ($P \leq 0.05$). Also, the criterion of Log_2 fold change (FC) was considered for the calculation of the differential accumulated proteins (DAPs), being considered up-accumulated when Log_2 FC > 0.6 and down-accumulated when Log_2 FC < -0.6. Description and functional annotation were performed for the DAPs using OmicsBox software (https://www.biobam.com/omicsbox). The protein sequences were submitted to a Basic Local Alignment Search Tool (BLAST) search against the National Center for Biotechnology Information (NCBI) nonredundant green plant protein database (taxa: 33090, Viridiplantae). An analysis of the enrichment of biological processes and cellular components of DAPs was performed by Fisher's exact test ($P < 0.01$) using OmicsBox. A Kyoto Encyclopedia of Genes and Genomes (KEGG) enrichment pathway analysis between DAPs ($P < 0.01$) was performed.

Statistical analysis

Data were subjected to analysis of variance and means were compared by Tukey's test ($P \leq 0.05$). A Pearson correlation analysis was performed followed by *t*-test ($P \leq 0.05$) was

performed between vegetative indices and physiological and biochemical variables. Positive and negative correlation coefficients (r) among the variables were classified as: 0.0–0.2, no correlation; 0.2–0.4, weak; 0.4–0.6, moderate; 0.6–0.8, strong; and 0.8–1.0, very strong. All analyses were performed using GENES software (Cruz, 2016).

RESULTS

Elevated CO_2 improved water use efficiency under drought condition

Plants of *P. glomerata* grown under ambient (a[CO_2]) and elevated (e[CO_2]) CO_2 concentration and of well-watered (WW) and drought-stressed (D) (Fig. 1). As expected, after imposition of drought we observed dramatic reductions in A_N (78 and 73%), *g*s (91 and 92%), *E* (86 and 92%) and C_i (27 and 48%) (Fig. 2A-D) in plants grown under a[CO_2] and e[CO_2], respectively, compared to well-watered controls. Conversely, e[CO_2] clearly improved water use efficiency (WUE), as calculated by the A_N/E ratio, mainly by reducing *E* in plants under drought. We observed an increase of approximately 66% in WUE (Fig. 2E) of plants exposed to e[CO_2]D compared to their well-watered control; whereas for a[CO_2] we observed no statistical difference in WUE. In respect to plants under drought, we found that e[CO_2] promoted a greater reduction in *g*s (56%) (Fig. 2B) and increase in C_i (29%) (Fig. 2D) compared to plants in a[CO_2].

Elevated CO_2 delayed the decrease in water potential under drought conditions

The water status of the plants was determined at anti-morning (Ψam) and midday (Ψmd) for 20 days, until the plants in the a[CO_2]D treatment reached Ψmd of -0.7 MPa (Fig. 3B). Both Ψam and Ψmd were lower (±1.5 – 4-fold) in water-stressed plants than in well-watered individuals, regardless of CO_2 (Fig. 3A-D). After 20 days of stress, plants in the exposed a[CO_2]D reached water potentials of -0.46 MPa at anti-morning (Fig. 3C) and -0.73 MPa at midday (Fig. 3D). Whereas in the plants of the exposed e[CO_2]D the water potentials were less negative, Ψam= -0.35 MPa (Fig. 3C) and Ψmd= -0.53 Mpa (Fig. 3D). Therefore, the water potentials of plants under e[CO_2]D were on average 25% less negative compared to plants in the exposed a[CO_2]D.

In relation to water loss in detached leaves, we observed that within the first 15 min the plants under a[CO_2]D already showed significantly lower percentage water loss compared to their well-watered control; whereas in e[CO_2]D, this difference only occurred after 45 min (Fig. 3E). Leaf water loss in drought-stressed plants remained relatively constant after 4 h of analyses, being approximately 12% and 20% lower in plants under a[CO_2] and e[CO_2], respectively, relative to their well-watered controls (Fig. 3E). A Pearson correlation analyses

revealed a very strong negative correlation (R= -0.9; *P*= 0.00000351) between plant water potential and leaf water loss (Fig. 3F). Therefore, we observed that the more negative the water potential, the lower the water loss in the leaves and vice versa.

Drought stress affected growth independently of [CO_2]

After 20 days of drought imposition, the growth of *P. glomerata* was drastically affected (Fig. 1, Table 2). Compared with well-watered plants, we observed that plants grown on a[CO_2] and e[CO_2] under drought stress showed, respectively, a significant reduction in leaf area (71 and 66%), leaf number (27 and 36%), stem length (30 and 30%), root length (29 and 14%), and total dry weight (15 and 27%) (Table 2). In plants under drought, a[CO_2] favored more biomass accumulation in the roots (17%) and increased root/shoot ratio (28%); whereas under e[CO_2] plants invested more biomass accumulation in the stem (25%) (Table 2). Conversely, biomass partitioning in leaves did not differ significantly between drought (Table 2). Only when we compared the drought treatments with their respective irrigated controls, that there was a reduction in leaf biomass partitioning of approximately 31% in both [CO_2] (Table 2).

Drought promoted anatomical changes

There were no remarkable anatomical structural changes in the leaf anatomy of the plants under different [CO_2] and irrigation condition (Fig. 4A-H). The leaves consist of uniseriate epidermis, large central vascular bundle with parenchyma distributed along the main vein, subepidermal collenchyma on the adaxial side and the lamina subdivided into palisade and lacunar parenchyma (Fig. 4A-H). However, drought promoted changes in stems and roots anatomy (Fig. 4I-X). In general, the stems presented uniseriate epidermis, subepidermal collenchyma, and a fiber thread above the vascular system and thickening of the cell wall in the interfascicular region, forming a continuous ring (Fig. 4I-P). Secondary growth was represented by the vascular cambium, which produces predominantly xylem (Fig. 4I-P). Furthermore, there is a marked difference in the stems of the plants under a[CO_2]D, where more more differentiated vascular tissue can be observed, with greater vascular cambium activity and pronounced secondary xylem (Fig. 4K,L). Overall, cross sections of the roots showed irregularly shaped uniseriate epidermis, cortex with rounded and juxtaposed

cells, well-developed vascular cambium, with a predominance of vessel elements (Fig. 4Q-X). Regardless the [CO_2], we observed in the roots of the plants under drought an increase in the number of vessel elements of the central vascular bundle (Fig. 4S,T,W,X).

Changes in primary metabolism occurred in response to [CO_2] and drought stress

The e[CO_2] decreases photosynthetic pigments and anthocyanins contents in plants under drought (Fig. 5). We observed significant reduction in the content of Chl *a* (26%), Chl *b* (34%), total Chl (25%), Chl *a*/ Chl *b* ratio (7%) (Fig. 5A-D), carotenoids (24%) (Fig. 5E) and anthocyanins (36%) (Fig. 5F) in plants exposed to e[CO2]D compared to th well-watered counterpart. In contrast, a[CO_2]D did not promote significant changes in chlorophyll and carotenoid levels (Fig. 5A-E), but doubled the content of anthocyanins (Fig. 5F) relative to its well-watered control.

We analyzed the metabolites glucose, fructose, sucrose, starch, free amino acids, and total protein at three periods of the day (anti-morning, midday, and evening) and did not observe a specific pattern among the treatments (Fig. 6). Plants grown under e[CO_2]D displyed increased levels of osmolites in the three periods of the day, such as glucose (78-95%; Fig. 6A), fructose (73-93%; Fig. 6B) and sucrose (24-50%; Fig. 6C), in parallel with the content of free amino acids which increased at midday (37%) and at evening (86%) (Fig. 6E), in comparison with their irrigated control. In contrast, plants under a[CO_2]D showed a reduction in glucose (62%) and fructose (62%) (Fig. 6A-B) at evening and sucrose (24%) (Fig. 6C) at midday, relative to a[CO_2]WW. Regarding amino acid levels they increased in the early anti-morning (25%) and evening (56%) and decreased at midday (38%), as compared to their irrigated control (Fig. 6E). We did not observe any specific pattern of change in starch and total protein content in relation to [CO_2] and water condition. Except for the reduction in starch levels at midday (38%) and evening (51%) (Fig. 6D) and total protein at evening (24%) (Fig. 6F) in plants exposed to a[CO_2]D and reduced total protein at anti-morning (32%) (Fig. 6F) in plants under e[CO_2]D, compared to their well-watered controls.

Furthermore, we analyzed 9 metabolites (alanine, aspartate, glycerate, glycine, glutamate, myo-inositol, serine, threonate, and valine) using GC-MS and evaluated the malate and proline contents in the sampling performed at midday (Fig. 7, Fig. S1). Plants exposed to e[CO_2]D showed a reduction in the contents of alanine (66%), aspartate (73%), glycerate (40%) (Fig. 7A-C) and threonate (30%) (Fig. 7H), and increase in the levels of glutamate

(74%), myoinositol (32%) (Fig. 7E, F), malate (30%) (Fig. 7J), serine (65%) (Fig. 7G), and valine (64%) (Fig. 7I). There was no statistical difference for glycine and proline contents (Fig. 7D, K), compared to its well-watered control. On the other hand, plants under a[CO_2]D showed little difference in the levels of these metabolites. We observed decreased glycine (66%) (Fig. 7D) and threonate (20%) (Fig. 7H) contents and increased malate (23%) (Fig. 7J), the other metabolites did not differ significantly compared to their well-watered control.

Drought promotes increased antioxidant enzyme activity

Activity of antioxidant enzymes (APX, CAT, POD and SOD) and MDA formation were significantly influenced by drought and [CO_2] (Fig. 8). We observed in the plants under a[CO_2]D increased CAT (54%) (Fig. 8B) and SOD (30%) (Fig. 8D) activity, but there was a reduction in POD (32%) (Fig. 8C) compared to their well-watered control. However, in plants grown in e[CO_2]D there was a significant increase in APX (37%) (Fig. 8A) and CAT (57%) (Fig. 8B) activity, which was accompanied by higher MDA formation (50%) (Fig. 8E), relative to their well-watered counterparts. No statistical difference was detected for APX and MDA in the plants under a[CO_2]D and neither in POX and SOD activity in plants exposed to e[CO_2]D (Fig. 8).

Elevated [CO_2] associated with drought positively affects 20E contente

Drought induced an increase in 20E content in both [CO2], being more relevant in plants under e[CO_2] (Fig. 9). Curiously, only when plants under e[CO_2] were associated with drought did this increase occur, in the e[CO_2]WW treatment there was a reduction in 20E content (Fig. 9). In respect to a[CO_2]D, there was a significant increase in 20E content in leaves (65%) (Fig. 9A) and stem (25%) (Fig. 9C) and a decrease in 20E content in roots (20%) (Fig. 9E) and in its production in stem (38%) (Fig. 9D), we observed no significant difference in production in leaves (Fig. 9B) and roots (Fig. 9F) compared to their well-watered control. In contrast, in plants under e[CO_2]D there was a significant increase in 20E content and production in leaves (71 and 64%) (Fig. 9A, B), stem (47 and 28%) (Fig. 9C, D) and roots (53 and 55%) (Fig. 9E, F), respectively, relative to their well-watered control.

Drought and [CO2] affects the proteomic profile

Proteomic profiling of *P. glomerata* plants under different [CO_2] and irrigation condition revealed significant changes in protein abundance. In total, 1040 proteins were identified, of which 921 (89%) were found in plants of the four treatments: a[CO_2]WW; a[CO_2]D; e[CO_2]WW; and e[CO_2]D (Fig. S2; Table S1). We observed 405 differentially accumulated proteins (DAPs) (Fig. 10A, B). Comparisons between a[CO_2]D/ a[CO_2]WW, e[CO_2]D/ e[CO_2]WW, e[CO_2]D/ a[CO_2]D, and e[CO_2]WW/ a[CO_2]WW revealed 96, 24, 10, and 17 up-accumulated proteins, respectively (Fig. 10A). Regarding negatively regulated proteins, comparisons between a[CO_2]D/ a[CO_2]WW, e[CO_2]D/ e[CO_2]WW, e[CO_2]D/ a[CO_2]D, and e[CO_2]WW/ a[CO_2]WW revealed 68, 37, 4, and 1 down-accumulated proteins, respectively (Fig. 10B).

KEGG analyses were performed, and DAPs were identified in 19 different metabolic pathways of plants (Fig. 10C, Table S2). In comparing a[CO_2]D/ a[CO_2]WW, 18 metabolic pathways showed up-accumulated and 18 down-accumulated proteins (Fig. 10C, Table S2). The largest groups observed were carbon metabolism (25 proteins); porphyrin metabolism (18 proteins); ribosome (17 proteins); amino acid biosynthesis (16 proteins); cofactor biosynthesis (14 proteins); ascorbate and aldarate (11 proteins); and tricarboxylic acid (TCA) (10 proteins) (Fig. 10C, Table S2). Whereas in comparing e[CO_2]D / e[CO_2]WW, 14 metabolic pathways showed up-accumulated and 13 down-accumulated proteins, mainly related to porphyrin metabolism (17 proteins); amino acid biosynthesis (13 proteins); and cofactor biosynthesis (12 proteins) (Fig. 10C, Table S2). In the other comparisons we identified few differentially accumulated pathways, in e[CO_2]D / a[CO_2]D 4 metabolic pathways showed up-accumulated and 5 down-accumulated proteins, these are processing of proteins in endoplasmic reticulum (4 proteins); amino acid biosynthesis (3 proteins); porphyrin metabolism (3 proteins); alanine, aspartate, and glutamate metabolism (1 protein); ascorbate and aldarate metabolism (1 protein); cofactor biosynthesis (1 protein); and carbon metabolism (1 protein) (Fig. 10C, Table S2). Finally, in the e[CO_2]WW/ a[CO_2]WW comparison 11 metabolic pathways showed up-accumulated and 5 down-accumulated proteins, mainly related to carbon metabolism (6 proteins); amino acid biosynthesis (3 proteins); cofactor biosynthesis (3 proteins); and porphyrin metabolism (3 proteins) (Fig. 10C, Table S2).

Gene Ontology (GO) analysis of the DAPs were performed using the software OmicsBox. The proteins were identified and categorized in biological process, molecular function and cellular component (Fig. 11, Table S3). The analysis revealed that most of the

up-accumulated proteins are related to biological processes in response to water stress, such as response to abiotic stimulus (32 proteins); response to oxidative stress (25 proteins); response to abscisic acid (22 proteins); oxidative cell detoxification (21 proteins); and response to water deprivation (20 proteins) (Fig. 11). The DAPs mainly displayed the molecular function of catalytic activity (310 proteins); transporter activity (60 proteins); and hydrolysis activity (43 proteins) (Fig. 11). We found predominantly up-accumulated DAPs present in mitochondria (148 proteins) and in the cell wall (63 proteins), cellular components particularly important in the response to oxidative damage and in the physical protection of cells (Fig. 11).

Hyperspectral data are strongly related to physiological responses to drought and [CO_2]

The intact leaves of *P. glomerata* showed marked differences in the mean reflectance spectrum, showed the separation of the four treatments (Fig. 12). The spectral reflectance is characterized by the presence of leaf pigments (± 350-800nm), structural compounds (± 1500-1800 and 2000-2350 nm) and water absorption (± 970-2500 nm) (Fig. 12).

We analyzed narrow-band vegetation index related to pigments (ARI, AChl, BNb, CARI, CRI1, CRI2 and PSRI), efficient light use (PRI), water (MSI) and stress (WBI) (Tables 3 and S1). In plants under e[CO_2]D, we observed a significant reduction in pigment indices ARI, BNb, CRI1, CRI2 and PSRI relative to their irrigated control (Table 3). These data corroborate with the biochemical analysis of the pigments (Fig. 5). Moderate positive correlations were found between anthocyanin content and the ARI index (R= 0.67, *P*= 0.000376) and between the BNb index with carotenoid content (R= 0.41, *P*= 0.0469), total chlorophyll (R= 0.45, *P*= 0.0276), and chl *a* (R= 0.45, *P*= 0.0250) (Fig. S3). However, we observed in plants exposet to e[CO_2]D a significant increase in Achl and CARI indices compared to their irrigated control (Table 3). The CARI index correlated negatively with the contents of carotenoid (R= -0.52, *P*= 0.00868), total chlorophyll (R= -0.56, *P*= 0.00423), chl *a* (R= -0.58, *P*= 0.00317) and chl *b* (R= -0.48, *P*= 0.0188) (Fig. S3). In plants under [CO_2]D only the CARI index differed significantly from the well-watered control (Table 3). This also corroborates with the data for chlorophylls and carotenoids, which did not differ under a[CO_2] (Fig. 5). On the other hand, we verified in the plants exposed to a[CO_2]D reduction in the PRI and WBI indices and an increase in the MSI index, but we observed no significant difference in these indices in the plants under e[CO_2]D compared to their well-watered controls (Table

3). That is, drought in plants in a[CO_2] induced reduction in efficient light use and water content and promoted increased stress, this did not occur in e[CO_2].

Given the above, we analyzed the MSI, WBI and PRI indices separately in each leaf pair and correlated them with physiological data, such as water potential (Ψmd), leaf water loss and photosynthetic rate (A_N) (Fig. 13). Regarding the MSI, we observed in well irrigated plants that the younger the leaf the higher the MSI, while in plants under drought the MSI is higher than in well irrigated plants and similar between leaf pairs, regardless of the [CO_2] (Fig. 13A). We found a strong positive correlation between MSI and Ψmd (R= 0.681, *P*= 0.00372), that is the higher the MSI index, the more negative the Ψmd (Fig. 13D). Conversely, we observed strong negative correlation between MSI and PRI (R= -0.754, *P*= 0.0000213), the higher the MSI, the lower the PRI (Fig. 13G). In respect the water band index WBI, in general we found that the older the leaf the higher the WBI, moreover in stressed plants the WBI is lower than in well irrigated plants (Fig. 13B). The WBI index correlated positively with leaf water loss (R= 0.683, *P*= 0.00356) and with PRI (R= 0.77, *P*= 0.0000107) (Fig. 13E, H). Similar to what we observed in WBI, we verified in PRI that the older the leaf the higher the PRI and in plants under drought the PRI is lower than in well-watered plants (Fig. 13C). Finally, we observed a positive correlation between PRI and A_N (R= 0.526, *P*=0.0365) and PRI and leaf water loss (R= 0.633, *P*= 0.00849) (Fig. 13F, I).

DISCUSSION

We analyzed the morphophysiological and molecular responses of *P. glomerata* grown in e[CO_2] associated with drought stress. Here we demonstrate that e[CO_2] mitigate the impacts of drought stress by reducing g_S and increasing *Ci*. Although water deficit reduced A_N and *E*, a positive response was observed in WUE (A_N/E) of plants under e[CO_2]D, the same did not occur in a[CO_2]. We observed in the plants exposed to e[CO_2]D less negative water potentials and greater leaf water loss, an indication that these plants had more water available for their growth and development. In fact, in drought conditions, dramatic drops in A_N and growth are generally expected, as we reported here. However, comparing the plants under drought in e[CO_2] and a[CO_2], we observed higher dry weight accumulation and biomass partitioning changes in the plants in e[CO_2]. Furthermore, plants under drought showed distinct stress response mechanisms depending on [CO_2], such as changes in energy (carbon) allocation to primary and/or secondary metabolites. For example, plants in a[CO_2]D invested more in biomass partitioning toward the roots and increased the contents of anthocyanins; whereas plants exposed to e[CO_2]D invested more in osmoregulatory metabolites (e.g. sugars and amino acids). Our findings revealed that drought positively affected antioxidant enzyme activity and 20E content in both [CO_2]. However, e[CO_2] has enhanced the content and output of 20E.

WUE is an efficient physiological parameter for selection of more drought resistant crops (Hatfield and Dold, 2019). Along with higher WUE (+66%), a reduction in g_S and less negative water potential were observed in plants under e[CO_2]D. Studies with coffee, blackberry, tomato and wheat corroborate our data (Avila et al., 2020; Liu et al., 2019; Nackley et al., 2016; Pazzagli et al., 2016; Qiao et al., 2010). The WUE response at the leaf level is directly related to the physiological processes controlling CO_2 and H_2O gradients and stomatal closure is induced to maintain the integrity of the water transport system (Birami et al., 2020; Hatfield and Dold, 2019). In plants subjected to drought stress and e[CO_2] one of the main reasons for the increase in WUE is that the reduction in A_N is smaller than the reduction in *E* or *g*s (Earl, 2002; Lawson and Blatt, 2014).

Under drought stress conditions, a reduction in A_N is generally expected, and may also be associated with a reduction in photosynthetic pigment content. Here, we observed a reduction in chlorophyll and carotenoid content in plants exposed to e[CO_2]D, the same was not observed in plants under a[CO_2]D, indicating that the biosynthesis or degradation of these pigments may be regulated by the level of CO_2 (Dhami et al., 2018; Li et al., 2019; Song et

al., 2020). The reduction in the content of these pigments may be related to the negative regulation of the porphyrin pathway, such as by down-accumulation of chloroplast proteins magnesium-chelatase subunit ChlI (cds.comp53297_c0_seq1), magnesium-chelatase subunit ChlD (cds.comp49351_c0_seq1), and delta-aminolevulinic acid dehydratase 1 (cds.comp17367_c0_seq1) (Tables S1 and S2) (Hu et al., 1998; Luo et al., 2012; Prasad and Prasad, 1987; Zhang et al., 2006). The lower photosynthetic pigment content results in decreased light absorption, which in turn reduces the potentially damaging warming effect of high solar radiation on dry plants whose stomata are closed (Havaux and Tardy, 1999). Collectively, our results suggest that the characteristic reduction in photosynthetic pigments in *P. glomerata* under e[CO_2]D may be related to its adaptation to drought.

In this study, we investigated the potential of hyperspectral analyses to detect changes in physiological and biochemical aspects of *P. glomerata* leaves exposed to e[CO_2] and drought conditions. The reflectance indices BNb, CRI1, CRI2, ARI and PSRI correlated with the biochemical analyses of chlorophyll, carotenoids and anthocyanins, we observed a reduction of these indices and pigments, in plants under e[CO_2]D. Fernandes et al. (2020) also demonstrate the correlation between spectral indices with chlorophyll and carotenoid content in *Passiflora edulis*. In addition, we found that the MSI, WPI and PRI indices were able to measure the physiological data of water potential, leaf water loss and photosynthesis, respectively. In soybean plants remote hyperspectral analysis made it possible to estimate leaf level parameters such as *g*s, *E* and A_N in response to drought (Sobejano-Paz et al., 2020). Here, we show in plants exposed to a[CO_2]D reduced PRI and WBI and increased MSI compared to their well-watered control. In other words, drought in plants in a[CO_2] induced reduction in photosynthetic efficiency (PRI) and in water content (WBI), promoting increased stress (MSI). The same was not observed in plants under e[CO_2]D. Therefore, we can infer that the hyperspectral data allowed to detect the mitigating effect of e[CO_2] in *P. glomerata* under drought.

Effect of e[CO_2] on drought stress remediation can be seen by the reduction in *g*s, which culminated in greater water savings, indirectly suggested by the less negative water potential. The *gs* is sensitive to soil characteristics and plant hydraulic properties, as well as root length and density (Tuzet et al., 2003). Although the positive effects of reduced *g*s on water loss under drought stress, its reduction negatively impacts A_N and consequently on plant growth (Flexas et al., 2006). Here, drought alone led to significant reductions in growth parameters, reflecting the severe stress condition of the plants by total water restriction. We

found in plants exposed to a[CO_2]D an increase in the root/shoot ratio. Increased water uptake through increased root size and depth and changes in root morphology is one of the most expected drought tolerance mechanisms in plants (Blum, 2005; Farooq et al., 2009; Karcher et al., 2008). This possibly explains the increase in the number of vessel elements (xylem), and consequently, greater lignification in plants under drought, as we observed in this study. Interestingly, in the plants in e[CO_2]D there was no increase in the root/shoot ratio, instead they invested more biomass towards the stem. Therefore, our data show different morphophysiological strategies of [CO_2] dependent drought tolerance.

Another strategy of *P. glomerata* under e[CO_2] to alleviate water deficit data is the investment in osmoregulatory metabolites. We observed a strong increase in the content of soluble sugars, such as glucose (78-95%), fructose (73-93%), sucrose (24-50%) and myo-inositol (32%), as well as an increase in malate (30%) and free amino acid (37-86%) content in plants exposed to e[CO_2]D. Similarly, Rodrigues et al. (2021) reported an attenuated sugar and amino acid response in the combined drought and e[CO_2] stress condition in coffee plants. Osmoregulatory molecules play an important role in maintaining plant cell turgor, favoring the ability to withstand tissue dehydration and protecting cell functions under low water potentials (Turner and Jones, 1980). In contrast, in plants under a[CO_2], drought promoted a reduction in soluble sugars, but increased the content of free amino acids and malate content.

Furthermore, we observed in plants exposed to e[CO_2]D increased glutamate, valine and serine content. Studies have reported an increase in the concentration of these amino acids under drought conditions, contributing to osmotic adjustment (Ashrafi et al., 2018; Bowne et al., 2012; Qiu et al., 2020). Glutamate is the precursor of arginine, GABA and proline, important osmoregulatory molecules (Forde and Lea, 2007). Unexpectedly, no increase in proline content was found in plants under drought. Here we report down-accumulation of the proline--tRNA ligase, chloroplastic/mitochondrial protein (cds.comp65181_c0_seq1) in plants under drought compared to their well-watered controls (Table S1). Hara et al. (2003) demonstrate that proline accumulation during water stress can be regulated by the *ProRS* gene, which belongs to the proline--tRNA synthetase. Serine is a precursor to glycine that can be methylated into the osmoprotective compound glycine-betaine (Chen and Murata, 2011). But the increase in serine concentration in response to drought in plants on e[CO2] did not translate into an increase in glycine content. We identified the proteins glycine dehydrogenase (cds.comp66714_c0_seq1) and betaine aldehyde dehydrogenase (cds.comp66510_c0_seq4;

cds.comp66510_c0_seq3) (Table S1), but both remained unchanged between treatments. Therefore, possibly the increase in serine could not have contributed to the improvement of water stress tolerance through glycine-betaine synthesis. However, serine is also one of the intermediates of photorespiration (Timm et al., 2013). Studies show that photorespiration is generally increased during drought stress, due to lower *g*s, and consequently higher Ribulose-1,5-biphosphate (RuBisCo) oxygenase activity (Lawlor, 2002; Wingler et al., 2000; 1999).

On the other hand, we demonstrated that drought reduced total protein content, especially in plants under e[CO_2], and reduced alanine and aspartate content. It is well reported elsewhere that N plays a central role in protein synthesis and that e[CO_2] has a dilutive effect on N (Ebi et al., 2021; Keutgen et al., 1997; Lee et al., 2020; Novoa and Loomis, 1981; Singh et al., 2015; Taub et al., 2008). It is believed that this dilution effect is due to the increased carbohydrate production rate, which increases the C/N ratio (Reich et al. 2006; Shi et al. 2016). Maize plants exposed to drought and e[CO_2] also reported decreases in the amino acids alanine and aspartate, the authors correlated with N (Sicher and Barnaby, 2012). In addition, proteome analyses showed that e[CO_2] delayed or even eliminated many of the drought response proteins observed in plants grown under a[CO_2], such as plasma membrane associated cation binding protein 1 (cds.comp26143_c0_seq1), glutathione S-transferase U17-like (cds.comp69177_c0_seq1), thioredoxin-like protein CDSP32 (cds.comp62233_c0_seq1), and various heat shock (cds.comp68654_c2_seq1; cds.comp27325_c0_seq1; cds.comp17310_c0_seq1; cds.comp65506_c0_seq1; and cds.comp25021_c0_seq1) proteins (Table S1). Not only that, we report in almost all identified pathways (except amino sugar and nucleotide sugar metabolism) more DAPs in plants under drought in a[CO_2] than in e[CO_2]. Taken together, these facts can be taken as circumstantial evidence that the metabolic responses to drought in plants under e[CO_2] are modulated by the carbon and nitrogen balance.

Beyond to the distinct physiological and metabolic responses between plants grown on a[CO_2] and e[CO_2] under drought condition, we also observed differences in antioxidant mechanisms. The enzymatic (e.g. APX, CAT, POD, SOD and glutathione reductase) and non-enzymatic antioxidant systems, such as ascorbic acid (AsA), tocopherol (vitamin E), glutathione (GSH), carotenoids and anthocyanins, together combat oxidative damage caused by reactive oxygen species (ROS) in plants when subjected to environmental stresses (Ahmad et al., 2009; Irato and Santovito, 2021; Panda, 2012; Saed-Moucheshi et al., 2014). At the proteomic level, we identified in plants under drought DAPs common metabolic pathways of

ascorbate and glutathione metabolism, mainly at a[CO_2], that may have played a key role in stress tolerance responses. *P. glomerata* grown on a[CO_2]D showed accumulation of proteins regulating ascorbate and aldarate metabolism, such as polyamine oxidase-like (cds.comp25420_c0_seq1; cds.comp69345_c0_seq1); peroxisomal acyl-coenzyme A oxidase 1-like (cds.comp62191_c0_seq1); and aldehyde dehydrogenase family 7 member B4 (cds.comp18151_c0_seq1) in comparison with its well-watered control (Tables S1 and S2). Whereas plants in e[CO_2]D showed no significant difference in the accumulation of these proteins, but positively regulated protein bifunctional phosphatase IMPL2, chloroplastic (cds.comp66052_c0_seq1) in relation to its well-watered control (Tables S1 and S2). Similarly, we observed more proteins (8 specifically) up-accumulated from glutathione metabolism in plants under drought in a[CO_2] than in e[CO_2] relative to their well-watered controls. Nevertheless, two proteins, glutathione S-transferase DHAR3, chloroplastic (cds.comp19058_c0_seq1) and glutathione S-transferase-like (cds.comp54558_c0_seq2) were positively regulated in both [CO_2] and drought (Tables S1 and S2). Plant glutathione-S transferases are key phase II detoxification enzymes that work downstream of Cytochrome P450 (Cyt P450) in cellular metabolism (Vaish et al., 2020). In addition, we also observed reduced anthocyanin and carotenoid content in *P. glomerata* grown in e[CO_2]D compared to e[CO_2]WW. Interestingly, we found accumulation of the protein carotenoid cleavage dioxygenase 1 (cds.comp18706_c0_seq1) (Table S1), responsible for cleaving the carotenoids into various apocarotenoids (e.g. ABA and strigolactones) (Floss and Walter, 2009). On the other hand, plants exposed to a[CO_2]D showed increased accumulation of anthocyanins, as also observed in *P. glomerata* grown under oxidative stress from UV-B radiation (Felipe et al., 2019a).

Regarding the enzymatic antioxidant mechanisms, we observed in both [CO_2] that drought promoted an increase in CAT and SOD activity. The activity of these enzymes are usually stimulated by limited water availability in many plant species (Abid et al., 2017; Jabeen et al., 2021; Sarker and Oba, 2018; Yan, 2015). SOD helps in the detoxification of the superoxide radical (O_2^-), forming hydrogen peroxide (H_2O_2), which can be eliminated by CAT (Krishnamurthy and Wadhwani, 2012). Whereas, we found an increase in APX activity in plants under e[CO_2]D, compared to the a[CO_2]D and e[CO_2]WW treatments. The enzyme APX has a higher affinity for H_2O_2 and reduces H_2O in chloroplasts, cytosol, mitochondria, and peroxisomes, as well as in the apoplastic space, using ascorbate as a specific electron donor (Sofo et al., 2015). An indirect method to quantify lipid peroxidation caused by ROS is

by the production of malondialdehyde (MDA), its content can reflect the degree of cell membrane damage (Khan and Panda, 2007). Drought generally increases MDA content, but in the present study, MDA production increased only in plants exposed to e[CO_2]. In concordance with previous results, our data suggest that e[CO_2] could not recover membrane damage caused by drought (Li et al., 2013; Wu et al., 2022). Overall, the effects of e[CO_2] combined with drought on plants is not a simple superposition of drought breakdown and/or compensation effects, but rather complex responses that need to be better understood.

In fact, ROS cause cellular damage, but it is known that they can also act in signaling for the production of secondary metabolites in plants (Berni et al., 2019). Here, we report that drought induced an increase in 20E content independent of [CO_2]. However, only in e[CO_2]D did promote increased 20E production per plant, overcoming the biomass limitation caused by water deficit. We believe that lower antioxidant protection due to lower concentration of carotenoids, anthocyanins, ascorbate metabolism proteins and glutathione may have led to higher oxidative stress in plants under e[CO_2]D in response to increased ROS (indirectly suggested by increased MDA production), may have influenced the increased production of 20E. Corroborating with our data, studies show that 20E in *P. glomerata* is modulated o positively by changes in abiotic conditions. Bernardy et al. (2020) showed that the 20E content in *P. glomerata* increased as the zinc concentration increased, the authors hypothesize that these plants may use 20E as a ROS sequestering compound. Other studies have shown that UV-B radiation and moderate salt stress in *P. glomerata* promote an increase in 20E content and up-regulate *Spook* and *Phantom* genes of the Cyt P450 gene family (Felipe et al., 2019a,b).

The CYPS P450 are the largest group belonging to a class of oxidoreductases, they play critical roles in maintaining redox homeostasis and in protecting against ROS (Pandian et al., 2020). *De novo* assembly of the *P. glomerata* transcriptome revealed several genes from the CYPS P450 family related to secondary metabolism and stresses (Batista et al., 2019). These genes, *Phantom* (CYP76C) was directly correlated with 20E content, suggesting participation in the 20E biosynthesis pathway (Batista et al., 2019). Here, we report for the first time, the positive regulation of cytochrome P450 CYP72A219-like (cds.comp18142_c0_seq1) protein in *P. glomerata* grown on e[CO_2] and drought (Table S1). Arisha et al. (2018) reported 4 genes of the CYPs P450 family present in sweet potato plants, including CYP72A219, highly upregulated in leaf tissues under drought stress. In *Capsicum annuum*, the combination of UV-B radiation and cold promoted stress response genes, such as

those related to hormone biosynthesis (CYP72A219 and CYP736A12) and ROS oxidation (CAT and POD) (Morales-Merida, 2021). Study reports that CYPs P450 genes can up- or down-regulate antioxidant enzymes (CAT and POD) under abiotic stress conditions (Zhang et al., 2018). Given the above, considering the participation of the CYP72A219-like protein in the production of both antioxidant compounds and 20E, we believe in a possible signaling by ROS in the production of 20E during drought stress response.

CONCLUSION

Our results show that *P. glomerata* seems to mitigate the physiological responses of drought stress, mainly by reducing *g*s, which culminated in improved WUE and promoted less negative water potentials. Hyperspectral data corroborate these findings and are an excellent non-destructive tool for analyzing the effects of drought on plants. Comparative proteomic analysis revealed 405 common DAPs involved in 19 metabolic pathways, most of them related porphyrin metabolism, carbon metabolism, biosynthesis of amino acids, and biosynthesis of cofactors.

Here, for the first time, we report the up-accumulation of the CYP P450 CYP72A219-like protein in plants under e[CO_2]D. Therefore, we hypothesize a role of this protein in 20E biosynthesis and possible ROS signaling (indirectly by increased CAT and SOD) in 20E production under abiotic stress conditions.

REFERENCES

Abid, G., M'hamdi, M., Mingeot, D., Aouida, M., Aroua, I., Muhovski, Y., Sassi, K., Souissi, F., Mannai, K., Jebara, M. (2017). Effect of drought stress on chlorophyll fluorescence, antioxidant enzyme activities and gene expression patterns in faba bean (*Vicia faba* L.). *Archives of Agronomy and Soil Science*, *63*(4), 536–552. https://doi.org/10.1080/03650340.2016.1224857

Ahmad, P., Jaleel, C. A., Azooz, M. M., Nabi, G. (2009). Generation of ROS and non-enzymatic antioxidants during abiotic stress in plants. *Botany Research International*, *2*(1), 11–20.

Ainsworth, E. A., Long, S. P. (2005). What have we learned from 15 years of free-air CO_2 enrichment (FACE)? A meta-analytic review of the responses of photosynthesis, canopy properties and plant production to rising CO_2. *New Phytologist*, *165*(2), 351–372. https://doi.org/10.1111/j.1469-8137.2004.01224.x

Al Jaouni, S., Saleh, A. M., Wadaan, M. A. M., Hozzein, W. N., Selim, S., AbdElgawad, H. (2018). Elevated CO_2 induces a global metabolic change in basil (*Ocimum basilicum* L.) and peppermint (*Mentha piperita* L.) and improves their biological activity. *Journal of Plant Physiology*, *224–225*, 121–131. https://doi.org/10.1016/j.jplph.2018.03.016

Almeida, I. V., Düsman, E., Mattge, G. I., Toledo, F., Reusing, A. F., Vicentini, V. E. P. (2017). In vivo antimutagenic activity of the medicinal plants *Pfaffia glomerata* (Brazilian ginseng) and *Ginkgo biloba*. *Genetics and Molecular Research*, *16*(3), 16039785. https://doi.org/10.4238/gmr16039785

Almuhayawi, M. S., Hassan, A. H. A., Al Jaouni, S. K., Alkhalifah, D. H. M., Hozzein, W. N., Selim, S., AbdElgawad, H., Khamis, G. (2021). Influence of elevated CO_2 on nutritive value and health-promoting prospective of three genotypes of *Alfalfa sprouts* (Medicago Sativa). *Food Chemistry*, *340,* 128147. https://doi.org/10.1016/j.foodchem.2020.128147

Amaral, C. H., Almeida, T. I. R., Souza Filho, C. R., Roberts, D., Fraser, S., Alves, M., Botelho, M. (2018). Characterization of indicator tree species in neotropical environments and implications for geological mapping. *Remote Sens. Environ*, *216*, 385–400. https://doi.org/10.1016/j.rse.2018.07.009

Araújo, W. L., Nunes-Nesi, A., Osorio, S., Usadel, B., Fuentes, D., Nagy, R., Balbo, I.,

Lehmann, M., Studart-Witkowski, C., Tohge, T., Martinoia, E., Jordana, X., DaMatta, F. M., Fernie, A. R. (2011). Antisense inhibition of the iron-sulphur subunit of succinate dehydrogenase enhances photosynthesis and growth in tomato via an organic acid-mediated effect on stomatal aperture. *Plant Cell*, *23*(2), 600–627. https://doi.org/10.1105/tpc.110.081224

Arisha, M. H., Fathi, T., Taha, T. F., Elakkad, H. A. (2018). Expression profile of redox active secondary metabolites related genes obtained by transcriptome sequencing under salt and drought stress in sweet potato sweet potato breeding view project tomato breeding view project expression profile of redox active se. *Journal of Biology*, *2*(1), 1–10. https://doi.org/10.37229/fsa.fjb.2018.04.15

Aroca, R., Ferrante, A., Vernieri, P., Chrispeels, M. J. (2006). Drought, abscisic acid and transpiration rate effects on the regulation of pip aquaporin gene expression and abundance in *Phaseolus vulgaris* Plants. *Annals of Botany*, *98*(6), 1301–1310. https://doi.org/10.1093/aob/mcl219

Ashrafi, M., Azimi-Moqadam, M.R., Moradi, P., MohseniFard, E., Shekari, F., Kompany-Zareh, M. (2018). Effect of drought stress on metabolite adjustments in drought tolerant and sensitive thyme. *Plant Physiology and Biochemistry*, *132*, 391–399. https://doi.org/10.1016/j.plaphy.2018.09.009

Avila, R. T., Cardoso, A. A., de Almeida, W. L., Costa, L. C., Machado, K. L. G., Barbosa, M. L., de Souza, R. P. B., Oliveira, L. A., Batista, D. S., Martins, S. C. V., Ramalho, J. D. C., DaMatta, F. M. (2020). Coffee plants respond to drought and elevated [CO_2] through changes in stomatal function, plant hydraulic conductance, and aquaporin expression. *Environmental and Experimental Botany*, *177,* 104148. https://doi.org/10.1016/j.envexpbot.2020.104148

Avila, R. T., de Almeida, W. L., Costa, L. C., Machado, K. L. G., Barbosa, M. L., de Souza, R. P. B., Martino, P. B., Juárez, M. A. T., Marçal, D. M. S., Martins, S. C. V., Ramalho, J. D. C., DaMatta, F. M. (2020). Elevated air [CO_2] improves photosynthetic performance and alters biomass accumulation and partitioning in drought-stressed coffee plants. *Environmental and Experimental Botany*, *177,* 104137. https://doi.org/10.1016/j.envexpbot.2020.104137

Bakrim, A., Maria, A., Sayah, F., Lafont, R., Takvorian, N. (2008). Ecdysteroids in spinach (*Spinacia oleracea* L.): Biosynthesis, transport and regulation of levels. *Plant Physiology and Biochemistry*, *46*(10), 844–854. https://doi.org/10.1016/j.plaphy.2008.06.002

Bates, L. S., Waldren, R. P., Teare, I. D. (1973). Rapid determination of free proline for water-stress studies. *Plant and Soil*, *39*(1), 205–207. https://doi.org/10.1007/BF00018060

Batista, D. S., Dias, L. L. C., Rêgo, M. M. do, Saldanha, C. W., Otoni, W. C. (2017). Flask sealing on in vitro seed germination and morphogenesis of two types of ornamental pepper explants. *Ciência Rural*, *47*(3). https://doi.org/10.1590/0103-8478cr20150245

Batista, D. S., Koehler, A. D., Romanel, E., de Souza, V. C., Silva, T. D., Almeida, M. C., Maciel, T. E. F., Ferreira, P. R. B., Felipe, S. H. S., Saldanha, C. W., Maldaner, J., Dias, L. L. C., Festucci-Buselli, R. A., Otoni, W. C. (2019). *De novo* assembly and transcriptome of *Pfaffia glomerata* uncovers the role of photoautotrophy and the P450 family genes in 20-hydroxyecdysone production. *Protoplasma*, *256*(3), 601–614. https://doi.org/10.1007/s00709-018-1322-1

Bernardy, K., Farias, J. G., Pereira, A. S., Dorneles, A. O. S., Bernardy, D., Tabaldi, L. A., Neves, V. M., Dressler, V. L., Nicoloso, F. T. (2020). Plants' genetic variation approach applied to zinc contamination: secondary metabolites and enzymes of the antioxidant system in *Pfaffia glomerata* accessions. *Chemosphere*, *253*, 126692. https://doi.org/10.1016/j.chemosphere.2020.126692

Berni, R., Luyckx, M., Xu, X., Legay, S., Sergeant, K., Hausman, J.-F., Lutts, S., Cai, G., Guerriero, G. (2019). Reactive oxygen species and heavy metal stress in plants: Impact on the cell wall and secondary metabolism. *Environmental and Experimental Botany*, *161*, 98–106. https://doi.org/10.1016/j.envexpbot.2018.10.017

Birami, B., Nägele, T., Gattmann, M., Preisler, Y., Gast, A., Arneth, A., Ruehr, N. K. (2020). Hot drought reduces the effects of elevated CO_2 on tree water-use efficiency and carbon metabolism. *New Phytologist*, *226*(6), 1607–1621. https://doi.org/10.1111/nph.16471

Birami, B., Thomas, N., Gattmann, M., Preisler, Y., Gast, A., Arneth, A., Ruehr, N. K. (2020). Hot drought reduces the effects of elevated CO_2 on tree water- use efficiency and carbon metabolism. *New Phytologist*, *226*, 1607–1621. https://doi.org/10.1111/nph.16471

Blum, A. (2005). Drought resistance, water-use efficiency, and yield potential—are they compatible, dissonant, or mutually exclusive? *Australian Journal of Agricultural Research*, *56*(11), 1159. https://doi.org/10.1071/AR05069

Bodner, G., Nakhforoosh, A., Kaul, H.P. (2015). Management of crop water under drought: A review. *Agronomy for Sustainable Development*, *35*(2), 401–442.

https://doi.org/10.1007/s13593-015-0283-4

Bowes, G. (1991). Growth at elevated CO_2: photosynthetic responses mediated through Rubisco. *Plant, Cell and Environment*, *14*(8), 795–806. https://doi.org/10.1111/j.1365-3040.1991.tb01443.x

Bowne, J. B., Erwin, T. A., Juttner, J., Schnurbusch, T., Langridge, P., Bacic, A., Roessner, U. (2012). Drought responses of leaf tissues from wheat cultivars of differing drought tolerance at the metabolite level. *Molecular Plant*, *5*(2), 418–429. https://doi.org/10.1093/mp/ssr114

Bradford, M. (1976). A rapid and sensitive method for the quantitation of microgram quantities of protein utilizing the principle of protein-dye binding. *Anal Biochem*, *72*, 248–254. https://doi.org/10.1016/0003-2697(76)90527-3

Buniam, J., Chukijrungroat, N., Rattanavichit, Y., Surapongchai, J., Weerachayaphorn, J., Bupha-Intr, T., Saengsirisuwan, V. (2020). 20-hydroxyecdysone ameliorates metabolic and cardiovascular dysfunction in high-fathigh-fructose-fed ovariectomized rats. *BMC Complementary Medicine and Therapies*, *20*(1), 1–12. https://doi.org/10.1186/s12906-020-02936-1

Buschmann, C., Nagel, E. (1993). In vivo spectroscopy and internal optics of leaves as basis for remote sensing of vegetation. *International Journal of Remote Sensing*, *14*(4), 711–722. https://doi.org/10.1080/01431169308904370

Chance, B., Maehly, A. (1955). Assay of catalases and peroxidases. *Methods Enzymol*, *2*, 764–775. https://doi.org/10.1016/S0076-6879(55)02300-8

Chaubey, M. K. (2018). Role of phytoecdysteroids in insect pest management: a review. *Journal of Agronomy*, *17*, 1–10.

Chen, T. H. H., Murata, N. (2011). Glycinebetaine protects plants against abiotic stress: Mechanisms and biotechnological applications. *Plant, Cell & Environment*, *34*(1), 1–20. https://doi.org/10.1111/j.1365-3040.2010.02232.x

Corrêa, J. P. O., Vital, C. E., Pinheiro, M. V. M., Batista, D. S., Azevedo, J. F. L., Saldanha, C. W., da Cruz, A. C. F., DaMatta, F. M., Otoni, W. C. (2015). In vitro photoautotrophic potential and ex vitro photosynthetic competence of *Pfaffia glomerata* (Spreng.) Pedersen accessions. *Plant Cell, Tissue and Organ Culture*, *121*(2), 289–300. https://doi.org/10.1007/s11240-014-0700-4

Cruz, C. D. (2016). Genes Software – extended and integrated with the R, Matlab and Selegen. *Acta Scientiarum. Agronomy*, *38*(4), 547.

https://doi.org/10.4025/actasciagron.v38i3.32629

Damerval, C., De Vienne, D., Zivy, M., Thiellement, H. (1986). Technical improvements in two-dimensional electrophoresis increase the level of genetic variation detected in wheat-seedling proteins. *Electrophoresis*, *7*(1), 52–54. https://doi.org/10.1002/elps.1150070108

Danner, M., Locherer, M., Hank, T., Richter, K. (2015). *Spectral Sampling with the ASD FieldSpec 4 – Theory, Measurement, Problems, Interpretation*. https://doi.org/10.2312/enmap.2015.008

De la Mata, L., Cabello, P., De la Haba, P., Agüera, E. (2012). Growth under elevated atmospheric CO_2 concentration accelerates leaf senescence in sunflower (*Helianthus annuus* L.) plants. *Journal of Plant Physiology*, *169*(14), 1392–1400. https://doi.org/10.1016/j.jplph.2012.05.024

De Souza, A. P., Gaspar, M., Da Silva, E. A., Ulian, E. C., Waclawovsky, A. J., Nishiyama, M. Y., Dos Santos, R. V., Teixeira, M. M., Souza, G. M., Buckeridge, M. S. (2008). Elevated CO_2 increases photosynthesis, biomass and productivity, and modifies gene expression in sugarcane. *Plant, Cell and Environment*, *31*(8), 1116–1127. https://doi.org/10.1111/j.1365-3040.2008.01822.x

Deutsch, E. W., Bandeira, N., Sharma, V., Perez-Riverol, Y., Carver, J. J., Kundu, D. J., García-Seisdedos, D., Jarnuczak, A. F., Hewapathirana, S., Pullman, B. S., Wertz, J., Sun, Z., Kawano, S., Okuda, S., Watanabe, Y., Hermjakob, H., MacLean, B., MacCoss, M. J., Zhu, Y., Ishihama, Y., Vizcaíno, J. A. (2020). The ProteomeXchange consortium in 2020: enabling 'big data'approaches in proteomics. *Nucleic acids research*, *48*(D1), D1145-D1152. https://doi.org/10.1093/nar/gkz984

Dhami, N., Tissue, D. T., Cazzonelli, C. I. (2018). Leaf-age dependent response of carotenoid accumulation to elevated CO_2 in *Arabidopsis*. *Archives of Biochemistry and Biophysics*, *647*(March), 67–75. https://doi.org/10.1016/j.abb.2018.03.034

Dinan, L. (2001). Phytoecdysteroids: biological aspects. *Phytochemistry*, *57*, 325–339. https://doi.org/10.1016/S0031-9422(01)00078-4

Dinan, L., Balducci, C., Guibout, L., Foucault, A. S., Bakrim, A., Kumpun, S., Girault, J. P., Tourette, C., Dioh, W., Dilda, P. J., Veillet, S., Lafont, R. (2021). Ecdysteroid metabolism in mammals: The fate of ingested 20-hydroxyecdysone in mice and rats. *Journal of Steroid Biochemistry and Molecular Biology*, *212*, 105896. https://doi.org/10.1016/j.jsbmb.2021.105896

Dinan, L., Lafont, R. (2006). Effects and applications of arthropod steroid hormones (ecdysteroids) in mammals. *Journal Of Endocrinology*, *191*, 1–8. https://doi.org/10.1677/joe.1.06900

Dinan, L., Mamadalieva, N. Z., Lafont, R. (2020). Dietary phytoecdysteroids. *Handbook of Dietary Phytochemicals*, 1–54. Springer Singapore. https://doi.org/10.1007/978-981-13-1745-3_35-1

Distler, U., Kuharev, J., Navarro, P., Levin, Y., Schild, H., Tenzer, S. (2014). Drift time-specific collision energies enable deep-coverage data-independent acquisition proteomics. *Nature Methods*, *11*(2), 167–170. https://doi.org/10.1038/nmeth.2767

Dong, J., Gruda, N., Lam, S. K., Li, X., Duan, Z. (2018). Effects of elevated CO_2 on nutritional quality of vegetables: A review. *Frontiers in Plant Science*, *9*, 924. https://doi.org/10.3389/fpls.2018.00924

Dong, Y., Zhang, X., Liu, X., Ai, X., Li, Q. (2015). Responses of non-structural carbohydrate metabolism of cucumber seedlings to drought stress and doubled CO_2 concentration. *Chinese J. Appl. Ecol*, *26*(1), 53–60.

Dusenge, M. E., Duarte, A. G., Way, D. A. (2019). Plant carbon metabolism and climate change: elevated CO_2 and temperature impacts on photosynthesis, photorespiration and respiration. *New Phytologist*, *221*(1), 32–49. Blackwell Publishing Ltd. https://doi.org/10.1111/nph.15283

Earl, H. J. (2002). Stomatal and non-stomatal restrictions to carbon assimilation in soybean (*Glycine max*) lines differing in water use efficiency. *Environmental and Experimental Botany*, *48*(3), 237–246. https://doi.org/10.1016/S0098-8472(02)00041-2

Ebi, K. L., Anderson, C. L., Hess, J. J., Kim, S. H., Loladze, I., Neumann, R. B., Singh, D., Ziska, L., Wood, R. (2021). Nutritional quality of crops in a high CO_2 world: An agenda for research and technology development. *Environmental Research Letters*, *16*(6), 064045. https://doi.org/10.1088/1748-9326/abfcfa

Farooq, M., Wahid, A., Kobayashi, N., Fujita, D., Basra, S. M. A. (2009). Plant drought stress: effects, mechanisms and management. *Agronomy for Sustainable Development*, *29*(1), 185–212. https://doi.org/10.1051/agro:2008021

Fathi, A., Tari, D. B. (2016). Effect of drought stress and its mechanism in plants. *International Journal of Life Sciences*, *10*(1), 1–6. https://doi.org/10.3126/ijls.v10i1.14509

Felipe, S. H. S., Batista, D. S., Chagas, K., Correia, L. N. F., Silva, T. D., Fortini, E. A., Silva,

P. O., Otoni, W. C. (2019a). Accessions of Brazilian ginseng (*Pfaffia glomerata*) with contrasting anthocyanin content behave differently in growth, antioxidative defense, and 20-hydroxyecdysone levels under UV-B radiation. *Protoplasma*, *256*(6), 1557–1571. https://doi.org/10.1007/s00709-019-01400-3

Felipe, S. H. S., Batista, D. S., Vital, C. E., Chagas, K., Silva, P. O., Silva, T. D., Fortini, E. A., Correia, L. N. de F., Avila, R. T., Maldaner, J., Festucci-Buselli, R. A., DaMatta, F. M., Otoni, W. C. (2019b). Salinity-induced modifications on growth, physiology and 20-hydroxyecdysone levels in Brazilian-ginseng [*Pfaffia glomerata* (Spreng.) Pedersen]. *Plant Physiology and Biochemistry*, *140*(4), 43–54. https://doi.org/10.1016/j.plaphy.2019.05.002

Fernandes, A. M., Fortini, E. A., Müller, L. A. de C., Batista, D. S., Vieira, L. M., Silva, P. O., Amaral, C. H., Poethig, R. S., Otoni, W. C. (2020). Leaf development stages and ontogenetic changes in passionfruit (*Passiflora edulis* Sims.) are detected by narrowband spectral signal. *Journal of Photochemistry and Photobiology B: Biology*, *209*, 111931. https://doi.org/10.1016/j.jphotobiol.2020.111931

Ferreira, P. R. B., da Cruz, A. C. F., Batista, D. S., Nery, L. A., Andrade, I. G., Rocha, D. I., Felipe, S. H. S., Koehler, A. D., Nunes-Nesi, A., Otoni, W. C. (2019). CO_2 enrichment and supporting material impact the primary metabolism and 20-hydroxyecdysone levels in Brazilian ginseng grown under photoautotrophy. *Plant Cell, Tissue and Organ Culture*, *139*(1), 77–89. https://doi.org/10.1007/s11240-019-01664-w

Festucci-Buselli, R. A., Contim, L. A. S., Barbosa, L. C. A., Stuart, J., Otoni, W. C. (2008). Biosynthesis and potential functions of the ecdysteroid 20-hydroxyecdysone - A review. *Botany*, *86*(9), 978–987. https://doi.org/10.1139/B08-049

Flexas, J., Bota, J., Galmés, J., Medrano, H., Ribas-Carbó, M. (2006). Keeping a positive carbon balance under adverse conditions: responses of photosynthesis and respiration to water stress. *Physiologia Plantarum*, *127*(3), 343–352. https://doi.org/10.1111/j.1399-3054.2006.00621.x

Floss, D. S., Walter, M. H. (2009). Role of carotenoid cleavage dioxygenase 1 (CCD1) in apocarotenoid biogenesis revisited. *Plant Signaling & Behavior*, *4*(3), 172–175. https://doi.org/10.4161/psb.4.3.7840

Forde, B. G., Lea, P. J. (2007). Glutamate in plants: metabolism, regulation, and signalling. *Journal of Experimental Botany*, *58*(9), 2339–2358. https://doi.org/10.1093/jxb/erm121

Fortini, E. A., Batista, D. S., de Castro, K. M., Silva, T. D., Felipe, S. H. S., Correia, L. N. F.,

Chagas, K., Farias, L. M., Leite, J. P. V., Otoni, W. C. (2020). Photoperiod modulates growth and pigments and 20-hydroxyecdysone accumulation in Brazilian ginseng [*Pfaffia glomerata* (Spreng.) Pedersen] grown in vitro. *Plant Cell, Tissue and Organ Culture*, *142*(3), 595–611. https://doi.org/10.1007/s11240-020-01886-3

Franco, R. R., de Almeida Takata, L., Chagas, K., Justino, A. B., Saraiva, A. L., Goulart, L. R., de Melo Rodrigues Ávila, V., Otoni, W. C., Espindola, F. S., da Silva, C. R. (2021). A 20-hydroxyecdysone-enriched fraction from *Pfaffia glomerata* (Spreng.) Pedersen roots alleviates stress, anxiety, and depression in mice. *Journal of Ethnopharmacology*, *267*, 113599. https://doi.org/10.1016/j.jep.2020.113599

Gamon, J., Serrano, L., Surfus, J.S. (1997). The photochemical reflectance index: an optical indicator of photosynthetic radiation use efficiency across species, functional types, and nutrient levels. *Oecologia*, *112*, 492–501. https://doi.org/10.1007/s004420050337

Giannopolitis, C. N., Ries, S. K. (1977). Superoxide dismutases: I. occurrence in higher plants. *Plant Physiology*, *59*(2), 309–314. https://doi.org/10.1104/pp.59.2.309

Gitelson, A.A., Merzlyak, M.N., Chivkunova, O.B. (2001). Optical properties and non-destructive estimation of anthocyanin content in plant leaves. *Photochemistry and Photobiology*, *74*(1), 38–45. https://doi.org/10.1562/0031-8655(2001)0740038OPANEO2.0.CO2

Gitelson A.A., Kaufman Y.J., Stark R., Rundquist D. (2002). Novel algorithms for remote estimation of vegetation fraction. *Remote Sensing of Environment*, *80*, 76–87. https://doi.org/10.1016/S0034-4257(01)00289-9

Guo, S., Tian, Z., Wu, Q. W., King-Jones, K., Liu, W., Zhu, F., Wang, X. P. (2021). Steroid hormone ecdysone deficiency stimulates preparation for photoperiodic reproductive diapause. *PLoS Genetics*, *17*(2), e1009352. https://doi.org/10.1371/JOURNAL.PGEN.1009352

Hara, M., Sugano, Y., Kuboi, T. (2003). Drought-regulated expression of prolyl-tRNA synthetase genes in radish (*Raphanus sativus*) seedlings. *Plant Science*, *165*(1), 129–137. https://doi.org/10.1016/S0168-9452(03)00151-1

Hatfield, J. L., Dold, C. (2019). Water-use efficiency: Advances and challenges in a changing climate. *Frontiers in Plant Science*, *10*, 103. https://doi.org/10.3389/fpls.2019.00103

Havaux, M., Tardy, F. (1999). Loss of chlorophyll with limited reduction of photosynthesis as an adaptive response of Syrian barley landraces to high-light and heat stress. *Australian Journal of Plant Physiology*, *26*, 569–578. https://doi.org/10.1071/PP99046

Havir, E. A., McHale, N. A. (1987). Biochemical and developmental characterization of multiple forms of catalase in tobacco leaves. *Plant Physiology*, *84*(2), 450–455. https://doi.org/10.1104/pp.84.2.450

Heath, R. L., Packer, L. (1968). Photoperoxidation in isolated chloroplasts: I. Kinetics and stoichiometry of fatty acid peroxidation. *Archives of Biochemistry and Biophysics*, *125*, 189–198. https://doi.org/10.1016/0003-9861(68)90654-1

Hossain, M. A., Wani, S. H., Bhattacharjee, S., Burritl, D. J., Tran, L. S. P. (2016). Drought stress tolerance in plants. *Drought Stress Tolerance in Plants: Physiology and Biochemistry*, 1. Springer International Publishing. https://doi.org/10.1007/978-3-319-28899-4

Houshmandfar, A., Fitzgerald, G. J., Tausz, M. (2015). Elevated CO_2 decreases both transpiration flow and concentrations of Ca and Mg in the xylem sap of wheat. *Journal of Plant Physiology*, *174*, 157–160. https://doi.org/10.1016/j.jplph.2014.10.008

Hozzein, W. N., Saleh, A. M., Habeeb, T. H., Wadaan, M. A. M., AbdElgawad, H. (2020). CO_2 treatment improves the hypocholesterolemic and antioxidant properties of fenugreek seeds. *Food Chemistry*, *308,* 125661. https://doi.org/10.1016/j.foodchem.2019.125661

Hsu, P.-K., Takahashi, Y., Munemasa, S., Merilo, E., Laanemets, K., Waadt, R., Pater, D., Kollist, H., Schroeder, J. I. (2018). Abscisic acid-independent stomatal CO_2 signal transduction pathway and convergence of CO_2 and ABA signaling downstream of OST1 kinase. *Proceedings of the National Academy of Sciences of the United States of America*, *115*(42), E9971–E9980. https://doi.org/10.1073/pnas.1809204115

Hu, G., Yalpani, N., Briggs, S. P., Johal, G. S. (1998). A Porphyrin pathway impairment is responsible for the phenotype of a dominant disease lesion mimic mutant of maize. *The Plant Cell*, *10*(7), 1095–1105. https://doi.org/10.1105/tpc.10.7.1095

Hunt, R., Rock, B.N (1989). Detection of changes in leaf water content using near-and middle infrared reflectances. *Remote Sensing of Environment*, *30*(1), 43–54. https://doi.org/10.1016/0034-4257(89)90046-1

Iarema, L., da Cruz, A. C. F., Saldanha, C. W., Dias, L. L. C., Vieira, R. F., de Oliveira, E. J., Otoni, W. C. (2012). Photoautotrophic propagation of Brazilian ginseng [*Pfaffia glomerata* (Spreng.) Pedersen]. *Plant Cell, Tissue and Organ Culture*, *110*(2), 227–238. https://doi.org/10.1007/s11240-012-0145-6

IPCC (2022). Global Warming of 1.5 °C. An IPCC Special Report on the impacts of global warming of 1.5°C above pre-industrial levels and related global greenhouse gas emission

pathways, in the context of strengthening the global response to the threat of climate change. Cambridge University Press. https://doi.org/10.1017/9781009157940

Irato, P., Santovito, G. (2021). Enzymatic and non-enzymatic molecules with antioxidant function. *Antioxidants*, *10*(4), 579. https://doi.org/10.3390/antiox10040579

Jabeen, M., Akram, N. A., Ashraf, M., Alyemeni, M. N., Ahmad, P. (2021). Thiamin stimulates growth and secondary metabolites in turnip (*Brassica rapa* L.) leaf and root under drought stress. *Physiologia Plantarum*, *172*(2), 1399–1411. https://doi.org/10.1111/ppl.13215

Janeczko, A., Oklestkova, J., Tarkowská, D., Drygaś, B. (2021). Naturally occurring ecdysteroids in *Triticum aestivum* L. and evaluation of fenarimol as a potential inhibitor of their biosynthesis in plants. *International Journal of Molecular Sciences*, *22*(6), 1–13. https://doi.org/10.3390/ijms22062855

Jindra, M., Palli, S. R., Riddiford, L. M. (2013). The juvenile hormone signaling pathway in insect development. *Annual Review of Entomology*, *58*, 181–204). https://doi.org/10.1146/annurev-ento-120811-153700

Karcher, D. E., Richardson, M. D., Hignight, K., Rush, D. (2008). Drought tolerance of tall fescue populations selected for high root/shoot ratios and summer survival. *Crop Science*, *48*(2), 771–777. https://doi.org/10.2135/cropsci2007.05.0272

Karnovsky, M. J. (1965). A Formaldehyde-glutaraldehyde fixative of high osmolality for use in electron microscopy. *The Journal of Cell Biology*, *27*(2), 1A-149A.

Keutgen, N., Chen, K., Lenz, F. (1997). Responses of strawberry leaf photosynthesis, chlorophyll fluorescence and macronutrient contents to elevated CO_2. *Journal of Plant Physiology*, *150*(4), 395–400. https://doi.org/10.1016/S0176-1617(97)80088-0

Kim, M. S. (1994). The use of narrow spectral bands for improving remote sensing estimation of fractionally absorbed photosynthetically active radiation (fAPAR). Master Thesis. Department of Geography, University of Maryland, College Park, MD.

Khan, M. H., Panda, S. K. (2007). Alterations in root lipid peroxidation and antioxidative responses in two rice cultivars under NaCl-salinity stress. *Acta Physiologiae Plantarum*, *30*(1), 81–89. https://doi.org/10.1007/s11738-007-0093-7

Krishnamurthy, P., Wadhwani, A. (2012). Antioxidant Enzymes and Human Health. *Antioxidant Enzyme*, *1*, 3–18. https://doi.org/10.5772/48109

Kumari, S., Agrawal, M., Singh, A. (2015). Effects of ambient and elevated CO_2 and ozone on physiological characteristics, antioxidative defense system and metabolites of potato

in relation to ozone flux. *Environmental and Experimental Botany*, *109*, 276–287. https://doi.org/10.1016/j.envexpbot.2014.06.015

Lafont, R. (1997). Ecdysteroids and related molecules in animals and plants. *Archives of Insect Biochemistry and Physiology*, *35*(1–2), 3–20. https://doi.org/10.1002/(SICI)1520-6327(1997)35:1/2<3:AID-ARCH2>3.0.CO;2-X

Lawlor, D. W. (2002). Limitation to photosynthesis in water-stressed leaves: stomata vs. metabolism and the role of ATP. *Annals of Botany*, *89*(7), 871–885. https://doi.org/10.1093/aob/mcf110

Lawson, T., Blatt, M. R. (2014). Stomatal size, speed, and responsiveness impact on photosynthesis and water use efficiency. *Plant Physiology*, *164*(4), 1556–1570. https://doi.org/10.1104/pp.114.237107

Le Gall, H., Philippe, F., Domon, J. M., Gillet, F., Pelloux, J., Rayon, C. (2015). Cell wall metabolism in response to abiotic stress. *Plants*, *4*(1) 112–166. https://doi.org/10.3390/plants4010112

Lee, Y. H., Sang, W. G., Baek, J. K., Kim, J. H., Shin, P., Seo, M. C., Cho, J. Il. (2020). The effect of concurrent elevation in CO_2 and temperature on the growth, photosynthesis, and yield of potato crops. *PLoS ONE*, *15*(10), e0189308. https://doi.org/10.1371/journal.pone.0241081

Lei, X. Y., Xia, J., Wang, J. W., Zheng, L. P. (2018). Comparative transcriptome analysis identifies genes putatively involved in 20-hydroxyecdysone biosynthesis in *Cyanotis arachnoidea*. *International Journal of Molecular Sciences*, *19*(7), 1885. https://doi.org/10.3390/ijms19071885

Lemonnier, P., Ainsworth, E. A. (2018). Crop responses to rising atmospheric [CO_2] and global climate change. *Food security and climate change*, 51-69.

Li, D., Liu, H., Qiao, Y., Wang, Y., Dong, B., Cai, Z., Shi, C., Liu, Y., Li, X., Liu, M. (2013). Physiological regulation of soybean (*Glycine max* L. Merr.) growth in response to drought under elevated CO_2. *Journal of Food, Agriculture and Environment*, *11*(2), 649–654.

Li, D., Zhang, X., Li, L., Aghdam, M. S., Wei, X., Liu, J., Xu, Y., Luo, Z. (2019). Elevated CO_2 delayed the chlorophyll degradation and anthocyanin accumulation in postharvest strawberry fruit. *Food Chemistry*, *285*, 163–170. https://doi.org/10.1016/j.foodchem.2019.01.150

Li, P., Li, H., Zong, Y., Li, F. Y., Han, Y., Hao, X. (2017). Photosynthesis and metabolite

responses of *Isatis indigotica* Fortune to elevated [CO_2]. *The Crop Journal*, *5*(4), 345–353. http://dx.doi.org/10.1016/j.cj.2017.03.007

Li, S., Li, X., Wei, Z., Liu, F. (2020). ABA-mediated modulation of elevated CO_2 on stomatal response to drought. *Current Opinion in Plant Biology*, *56*, 174–180. https://doi.org/10.1016/j.pbi.2019.12.002

Lin, X., Smagghe, G. (2019). Roles of the insulin signaling pathway in insect development and organ growth. *Peptides*, *122*. https://doi.org/10.1016/j.peptides.2018.02.001

Lisec, J., Schauer, N., Kopka, J., Willmitzer, L., Fernie, A. R. (2006). Gas chromatography mass spectrometry–based metabolite profiling in plants. *Nature Protocols*, *1*(1), 387–396. https://doi.org/10.1038/nprot.2006.59

Liu, X., Zhang, H., Wang, J., Wu, X., Ma, S., Xu, Z., Zhou, T., Xu, N., Tang, X., An, B. (2019). Increased CO_2 concentrations increasing water use efficiency and improvement PSII function of mulberry seedling leaves under drought stress. *Journal of Plant Interactions*, *14*(1), 213–223. https://doi.org/10.1080/17429145.2019.1603405

Louback, E., Batista, D. S., Pereira, T. A. R., Mamedes-Rodrigues, T. C., Silva, T. D., Felipe, S. H. S., Rocha, D. I., Steinmacher, D. A., Otoni, W. C. (2021). CO_2 enrichment leads to altered cell wall composition in plants of *Pfaffia glomerata* (Spreng.) Pedersen (Amaranthaceae). *Plant Cell, Tissue and Organ Culture*, *145*(3), 603–613. https://doi.org/10.1007/s11240-021-02031-4

Luo, T., Fan, T., Liu, Y., Rothbart, M., Yu, J., Zhou, S., Grimm, B., Luo, M. (2012). Thioredoxin redox regulates ATPase activity of magnesium chelatase CHLI subunit and modulates redox-mediated signaling in tetrapyrrole biosynthesis and homeostasis of reactive oxygen species in pea plants. *Plant Physiology*, *159*(1), 118–130. https://doi.org/10.1104/pp.112.195446

Marchioretto, M. S., Miotto, S. T. S., Siqueira, C. De. (2010). O gênero *Pfaffia* Mart. (Amaranthaceae) no Brasil Maria. *Hoehnea*, *37*(3), 461–511.

Meerdink, S. K., Roberts, D. A., King, J. Y., Roth, K. L., Dennison, P. E., Amaral, C. H., Hook, S. J. (2016). Linking seasonal foliar traits to VSWIR-TIR spectroscopy across California ecosystems. *Remote Sens. Environ*, *186*, 322–338. https://doi.org/10.1016/j.rse.2016.08.003

Mehmood, I., Bari, A., Irshad, S., Khalid, F., Liaqat, S., Anjum, H., Fahad, S. (2020). Climate change forecasting and modeling for the year of 2050. *Environment, Climate, Plant and Vegetation Growth* (pp. 109–122). Springer International Publishing.

https://doi.org/10.1007/978-3-030-49732-3_5

Morales-Merida, B. E. (2021). Transcriptomic Analysis in response to combined stress by UV-B radiation and cold in belle pepper (*Capsicum annuum*). *International Journal of Agriculture and Biology*, *25*(05), 969–980. https://doi.org/10.17957/IJAB/15.1753

Morison, J. I. L., Gifford, R. M. (1983). Stomatal Sensitivity to carbon dioxide and humidity. *Plant Physiology*, *71*(4), 789–796. https://doi.org/10.1104/pp.71.4.789

Murashige, T., Skoog, F. (1962). A revised medium for rapid growth and bio assays with tobacco tissue cultures. *Physiologia Plantarum*, *15*(3), 473–497. https://doi.org/10.1111/j.1399-3054.1962.tb08052.x

Nackley, L. L., Jeong, J. H., Oki, L. R., Kim, S. H. (2016). Photosynthetic acclimation, biomass allocation, and water use efficiency of garlic in response to carbon dioxide enrichment and nitrogen fertilization. *Journal of the American Society for Horticultural Science, 141*(4). https://doi.org/10.21273/JASHS.141.4.373

Nakagawa, Y., Henrich, V. C. (2009). Arthropod nuclear receptors and their role in molting. *The FEBS Journal*, *276*, 6128–6157. https://doi.org/10.1111/j.1742-4658.2009.07347.x

Nakano, Y., Asada, K. (1981). Hydrogen peroxide is scavenged by ascorbate-specific peroxidase in spinach chloroplasts. *Plant and Cell Physiology*, *22*(5), 867–880. https://doi.org/10.1093/oxfordjournals.pcp.a076232

Neff, M. M., Chory, J. (1998). Genetic interactions between phytochrome A, phytochrome B, and cryptochrome 1 during *Arabidopsis* development 1. *Plant Physiology*, *118*(1), 27-35. https://doi.org/10.1104/pp.118.1.27

Neto, A. G., Costa, J. M. L. C., Belati, C. C., Vinhólis, A. H. C., Possebom, L. S., Da Silva Filho, A. A., Cunha, W. R., Carvalho, J. C. T., Bastos, J. K., E Silva, M. L. A. (2005). Analgesic and anti-inflammatory activity of a crude root extract of *Pfaffia glomerata* (Spreng) Pedersen. *Journal of Ethnopharmacology*, *96*(1–2), 87–91. https://doi.org/10.1016/j.jep.2004.08.035

Neves, C. S., Gomes, S. S. L., Santos, T. R. do., de Almeida, M. M., de Souza, Y. O., Garcia, R. M. G., Otoni, W. C., Chedier, L. M., Raposo, N. R. B., Viccini, L. F., de Campos, J. M. S. (2016). “Brazilian ginseng” (*Pfaffia glomerata* Spreng. Pedersen, Amaranthaceae) methanolic extract: Cytogenotoxicity in animal and plant assays. *South African Journal of Botany*, *106*, 174–180. https://doi.org/10.1016/j.sajb.2016.07.003

Novoa, R., Loomis, R. S. (1981). Nitrogen and plant production. *Plant and Soil*, *58*(1–3), 177–204. https://doi.org/10.1007/BF02180053

Nunes-Nesi, A., Carrari, F., Gibon, Y., Sulpice, R., Lytovchenko, A., Fisahn, J., Graham, J., Ratcliffe, R. G., Sweetlove, L. J., Fernie, A. R. (2007). Deficiency of mitochondrial fumarase activity in tomato plants impairs photosynthesis via an effect on stomatal function. *Plant Journal*, *50*(6), 1093–1106. https://doi.org/10.1111/j.1365-313X.2007.03115.x

O'Brien, T., McCully, M. (1981). *T*he study of plant structure principles and selected methods. *Termarcarphi*, *4*, 581.

Panda, S. K. (2012). *A*ssay guided comparison for enzymatic and non-enzymatic antioxidant activities with special reference to medicinal plants. *Antioxidant enzyme*, *14*, 382-400.

Pandian, B. A., Sathishraj, R., Djanaguiraman, M., Prasad, P. V. V., Jugulam, M. (2020). Role of cytochrome P450 enzymes in plant stress response. *Antioxidants*, *9*(5), 454. https://doi.org/10.3390/antiox9050454

Park, H., Park, G., Jeon, W., Ahn, J., Yang, Y.H., Choi, K.Y. (2020). Whole-cell biocatalysis using cytochrome P450 monooxygenases for biotransformation of sustainable bioresources (fatty acids, fatty alkanes, and aromatic amino acids). *Biotechnology Advances*, *40*(12), 107504. https://doi.org/10.1016/j.biotechadv.2020.107504

Passamani, L. Z., Reis, R. S., Vale, E. M., Sousa, K. R., Aragão, V. P. M., Santa-Catarina, C., Silveira, V. (2020). Long-term culture with 2,4-dichlorophenoxyacetic acid affects embryogenic competence in sugarcane callus via changes in starch, polyamine and protein profiles. *Plant Cell, Tissue and Organ Culture*, *140*(2), 415–429. https://doi.org/10.1007/s11240-019-01737-w

Pazzagli, P. T., Weiner, J., Liu, F. (2016). Effects of CO_2 elevation and irrigation regimes on leaf gas exchange, plant water relations, and water use efficiency of two tomato cultivars. *Agricultural Water Management*, *169*, 26–33. https://doi.org/10.1016/j.agwat.2016.02.015

Peñuelas, J., Filella, I., Gamon, J.A., Field, C. (1997). Assessing photosynthetic radiation-use efficiency of emergent aquatic vegetation from spectral reflectance. *Aquatic Botany*, *58*(3-4), 307–315. https://doi.org/10.1016/S0304-3770(97)00042-9

Peñuelas, J., Baret, F., Filella, I. (1995). Semi-empirical indices to assess carotenoids/chlorophyll a ratio from leaf spectral reflectance. *Photosynthetica, 3011*(2), 221–230.

Perez-Riverol, Y., Csordas, A., Bai, J., Bernal-Llinares, M., Hewapathirana, S., Kundu, D. J., Inuganti, A., Griss, J., Mayer, G., Eisenacher, M., Pérez, E., Uszkoreit, J., Pfeuffer, J.,

Sachsenberg, T., Yılmaz, S., Tiwary, S., Cox, J., Audain, E., Walzer, M., Jarnuczak, A. F., Ternent, T. T., Brazma, A., Vizcaíno, J. A. (2019). The PRIDE database and related tools and resources in 2019: improving support for quantification data. *Nucleic Acids Research*, *47*(D1), D442-D450. https://doi.org/10.1093/nar/gky1106

Pontius, J., Martin, M., Plourde, L., Hallett, R. (2008). Ash decline assessment in emerald ash borer-infested regions: A test of tree-level, hyperspectral technologies, *Remote Sensing of Environment, 112*(5), 2665–2676. https://doi.org/10.1016/j.rse.2007.12.011

Porra, R. J., Thompson, W., Kriedemann, P. (1989). Determination of accurate extinction coefficients and simultaneous equations for assaying chlorophylls a and b extracted with four different solvents: verification of the concentration of chlorophyll standards by atomic absorption spectroscopy. *Biochimica et Biophysica Acta*, *975*, 384–394. https://doi.org/10.1016/S0005-2728(89)80347-0

Prasad, D. D. K., Prasad, A. R. K. (1987). Altered δ-aminolevulinic acid metabolism by lead and mercury in germinating seedlings of Bajra (*Pennisetum typhoideum*). *Journal of Plant Physiology*, *127*(3–4), 241–249. https://doi.org/10.1016/S0176-1617(87)80143-8

Prasad, P. V. V., Vu, J. C. V., Boote, K. J., Allen, L. H. (2009). Enhancement in leaf photosynthesis and upregulation of Rubisco in the C4 sorghum plant at elevated growth carbon dioxide and temperature occur at early stages of leaf ontogeny. *Functional Plant Biology*, *36*(9), 761. https://doi.org/10.1071/FP09043

Prasch, C. M., Sonnewald, U. (2013). Simultaneous application of heat, drought, and virus to *Arabidopsis* plants reveals significant shifts in signaling networks. *Plant Physiology*, *162*(4), 1849–1866. https://doi.org/10.1104/pp.113.221044

Qiao, Y., Zhang, H., Dong, B., Shi, C., Li, Y., Zhai, H., Liu, M. (2010). Effects of elevated CO_2 concentration on growth and water use efficiency of winter wheat under two soil water regimes. *Agricultural Water Management*, *97*(11), 1742–1748. https://doi.org/10.1016/j.agwat.2010.06.007

Qiu, X.M., Sun, Y.Y., Ye, X.Y., Li, Z.G. (2020). Signaling role of glutamate in plants. *Frontiers in Plant Science*, *10*(1), 1–11. https://doi.org/10.3389/fpls.2019.01743

Ramakrishna, A., Ravishankar, G. A. (2013). Role of plant metabolites in abiotic stress tolerance under changing climatic conditions with special reference to secondary compounds. *Climate Change and Plant Abiotic Stress Tolerance*, 705–726. https://doi.org/10.1002/9783527675265.ch26

Reis R.S., Vale E.M., Sousa K.R., Santa-Catarina C., Silveira, V. (2021) Pretreatment free of

2,4-dichlorophenoxyacetic acid improves the diferentiation of sugarcane somatic embryos by afecting the hormonal balance and the accumulation of reserves. *Plant Cell, Tissue and Organ Culture,145*, 101–115. https://doi.org/10.1007/ s11240-020-01995-z

Rharrabe, K., 1Δ, S., Lafont, R. (2010). Dietary effects of four phytoecdysteroids on growth and development of the Indian meal moth, *Plodia interpunctella*. *Journal of Insect Science*, *10*(13). https://academic.oup.com/jinsectscience/article/10/1/13/825747

Riddiford, L. M., Hiruma, K., Zhou, X., Nelson, C. A. (2003). Insights into the molecular basis of the hormonal control of molting and metamorphosis from *Manduca sexta* and *Drosophila melanogaster*. *Insect Biochemistry and Molecular Biology*, *33*(12), 1327–1338. Elsevier Ltd. https://doi.org/10.1016/j.ibmb.2003.06.001

Rodrigues, A. M., Jorge, T., Osorio, S., Pott, D. M., Lidon, F. C., DaMatta, F. M., Marques, I., Ribeiro-Barros, A. I., Ramalho, J. C., António, C. (2021). Primary Metabolite Profile Changes in *Coffea* spp. Promoted by single and combined exposure to drought and elevated CO_2 concentration. *Metabolites*, *11*(7), 427. https://doi.org/10.3390/metabo11070427

Roy, S., Mathur, P. (2021). Delineating the mechanisms of elevated CO_2 mediated growth, stress tolerance and phytohormonal regulation in plants. *Plant Cell Reports*, *40*(8), 1345–1365. https://doi.org/10.1007/s00299-021-02738-w

Saed-Moucheshi, A., Shekoofa, A., Pessarakli, M. (2014). Reactive oxygen species (ROS) generation and detoxifying in plants. *Journal of Plant Nutrition*, *37*(10), 1573–1585. https://doi.org/10.1080/01904167.2013.868483

Saldanha, C. W., Otoni, C. G., Notini, M. M., Kuki, K. N., da Cruz, A. C. F., Neto, A. R., Dias, L. L. C., Otoni, W. C. (2013). A CO_2-enriched atmosphere improves in vitro growth of Brazilian ginseng [*Pfaffia glomerata* (Spreng.) Pedersen]. *In Vitro Cellular & Developmental Biology - Plant*, *49*(4), 433–444. https://doi.org/10.1007/s11627-013-9529-5

Saldanha, C. W., Otoni, C. G., Rocha, D. I., Cavatte, P. C., Detmann, K. da S. C., Tanaka, F. A. O., Dias, L. L. C., DaMatta, F. M., Otoni, W. C. (2014). CO_2-enriched atmosphere and supporting material impact the growth, morphophysiology and ultrastructure of in vitro Brazilian-ginseng [*Pfaffia glomerata* (Spreng.) Pedersen] plantlets. *Plant Cell, Tissue and Organ Culture*, *118*(1), 87–99. https://doi.org/10.1007/s11240-014-0464-x

Sarker, U., Oba, S. (2018). Catalase, superoxide dismutase and ascorbate-glutathione cycle enzymes confer drought tolerance of *Amaranthus tricolor*. *Scientific Reports*, *8*(1),

16496. https://doi.org/10.1038/s41598-018-34944-0

Schneider, C., Rasband, W., Eliceiri, K. (2012). NIH Image to ImageJ: 25 years of image analysis. *Nat Methods*, *9*(7), 671–675. https://doi.org/10.1038/nmeth .2089

Scholander, P. F., Hammel, H. T., Hemmingsen, E. A., Bradstreet, E. D. (1964). Hydrostatic pressure and osmotic potential in leaves of mangroves and some other plants. *Proceedings of the National Academy of Sciences*, *52*(1), 119–125. https://doi.org/10.1073/pnas.52.1.119

Sicher, R. C., Barnaby, J. Y. (2012). Impact of carbon dioxide enrichment on the responses of maize leaf transcripts and metabolites to water stress. *Physiologia Plantarum*, *144*(3), 238–253. https://doi.org/10.1111/j.1399-3054.2011.01555.x

Silva, T. D., Batista, D. S., Castro, K. M., Fortini, E. A., Felipe, S. H. S., Fernandes, A. M., Sousa, R. M. J., Chagas, K., da Silva, J. V. S., Correia, L. N. F., Torres-Silva, G., Farias, L. M., Otoni, W. C. (2021). Irradiance-driven 20-hydroxyecdysone production and morphophysiological changes in *Pfaffia glomerata* plants grown in vitro. *Protoplasma*, *258*(1), 151-167. https://doi.org/10.1007/s00709-020-01558-1

Silva, T. D., Batista, D. S., Fortini, E. A., Castro, K. M., Felipe, S. H. S., Fernandes, A. M., Sousa, R. M. J., Chagas, K., Silva, J. V. S., Correia, L. N. F., Farias, L. M., Leite, J. P. V., Rocha, D. I., Otoni, W. C. (2020). Blue and red light affects morphogenesis and 20-hydroxyecdisone content of in vitro *Pfaffia glomerata* accessions. *Journal of Photochemistry and Photobiology B: Biology*, *203*(10), 111761. https://doi.org/10.1016/j.jphotobiol.2019.111761

Silva, T. D., Chagas, K., Batista, D. S., Felipe, S. H. S., Louback, E., Machado, L. T., Fernandes, A. M., Buttrós, V. H. T., Koehler, A. D., Farias, L. M., Santos, A. F., Silva, P. O., Otoni, W. C. (2019). Morphophysiological in vitro performance of Brazilian ginseng (*Pfaffia glomerata* (Spreng.) Pedersen) based on culture medium formulations. *In Vitro Cellular & Developmental Biology - Plant*, *55*(4), 454–467. https://doi.org/10.1007/s11627-019-10003-9

Singh, A., Pandey, B., Kumari, S., Agrawal, M. (2015). Nitrogen availability modulates CO_2-induced responses of *Catharanthus roseus*: Biomass allocation, carbohydrates and alkaloids profile. *Journal of Applied Research on Medicinal and Aromatic Plants*, *2*(4), 160–167. https://doi.org/10.1016/j.jarmap.2015.07.002

Soares, J. C., Santos, C. S., Carvalho, S. M. P., Pintado, M. M., Vasconcelos, M. W. (2019). Preserving the nutritional quality of crop plants under a changing climate: importance

and strategies. *Plant and Soil*, *443*(1–2). https://doi.org/10.1007/s11104-019-04229-0

Sobejano-Paz, V., Mikkelsen, T. N., Baum, A., Mo, X., Liu, S., Köppl, C. J., Johnson, M. S., Gulyas, L., García, M. (2020). Hyperspectral and Thermal sensing of stomatal conductance, transpiration, and photosynthesis for soybean and maize under drought. *Remote Sensing*, *12*(19), 3182. https://doi.org/10.3390/rs12193182

Sofo, A., Scopa, A., Nuzzaci, M., Vitti, A. (2015). Ascorbate peroxidase and catalase activities and their genetic regulation in plants subjected to drought and salinity stresses. *International Journal of Molecular Sciences*, *16*(12), 13561–13578. https://doi.org/10.3390/ijms160613561

Song, H., Li, Y., Xu, X., Zhang, J., Zheng, S., Hou, L., Xing, G., Li, M. (2020). Analysis of genes related to chlorophyll metabolism under elevated CO_2 in cucumber (*Cucumis sativu*s L.). *Scientia Horticulturae*, *261*(10), 108988. https://doi.org/10.1016/j.scienta.2019.108988

Sun, P., Mantri, N., Lou, H., Hu, Y., Sun, D., Zhu, Y., Dong, T., Lu, H. (2012). Effects of elevated CO_2 and temperature on yield and fruit quality of strawberry (*Fragaria* × *ananassa* Duch.) at two levels of nitrogen application. *PLoS ONE*, *7*(7), e41000. https://doi.org/10.1371/journal.pone.0041000

Taub, D. R., Miller, B., Allen, H. (2008). Effects of elevated CO_2 on the protein concentration of food crops: A meta-analysis. *Global Change Biology*, *14*(3), 565–575. https://doi.org/10.1111/j.1365-2486.2007.01511.x

Timm, S., Florian, A., Wittmiß, M., Jahnke, K., Hagemann, M., Fernie, A. R., Bauwe, H. (2013). Serine Acts as a metabolic signal for the transcriptional control of photorespiration-related genes in *Arabidopsis*. *Plant Physiology*, *162*(1), 379–389. https://doi.org/10.1104/pp.113.215970

Tsukagoshi, Y., Ohyama, K., Seki, H., Akashi, T., Muranaka, T., Suzuki, H., Fujimoto, Y. (2016). Functional characterization of CYP71D443, a cytochrome P450 catalyzing C-22 hydroxylation in the 20-hydroxyecdysone biosynthesis of *Ajuga hairy* roots. *Phytochemistry*, *127*, 23–28. https://doi.org/10.1016/j.phytochem.2016.03.010

Turner, N. C., Jones, H. G. (1980). Turgor maintenance by osmotic adjustment: a review and evaluation. *Adaptation* of plants to water and high temperature stress, p. 87-103.

Tuzet, A., Perrier, A., Leuning, R. (2003). A coupled model of stomatal conductance, photosynthesis and transpiration. *Plant, Cell & Environment*, *26*(7), 1097–1116. https://doi.org/10.1046/j.1365-3040.2003.01035.x

Vaish, S., Gupta, D., Mehrotra, R., Mehrotra, S., Basantani, M. K. (2020). Glutathione S-transferase: a versatile protein family. *3 Biotech*, *10*(7), 321. https://doi.org/10.1007/s13205-020-02312-3

Varga, B., Vida, G., Varga-László, E., Hoffmann, B., Veisz, O. (2017). Combined effect of drought stress and elevated atmospheric CO_2 concentration on the yield parameters and water use properties of winter wheat (*Triticum aestivum* L.) genotypes. *Journal of Agronomy and Crop Science*, *203*(3), 192–205. https://doi.org/10.1111/jac.12176

Vivin, P., Guehl, J., Clément, A., Aussenac, G. (1996). The effects of elevated CO_2 and water stress on whole plant CO_2 exchange, carbon allocation and osmoregulation in oak seedlings. *Annales Des Sciences Forestières*, *53*(2–3), 447–459. https://doi.org/10.1051/forest:19960226

Wang, Y., Yang, Y., Chi, D. (2018). Transcriptome analysis of abscisic acid induced 20E regulation in suspension *Ajuga lobata* cells. *3 Biotech*, *8*(8), 320. https://doi.org/10.1007/s13205-018-1352-6

Wingler, A., Lea, P. J., Quick, W. P., Leegood, R. C. (2000). Photorespiration: metabolic pathways and their role in stress protection. *Philosophical Transactions of the Royal Society of London. Series B: Biological Sciences*, *355*(1402), 1517–1529. https://doi.org/10.1098/rstb.2000.0712

Wingler, A., Quick, W. P., Bungard, R. A., Bailey, K. J., Lea, P. J., Leegood, R. C. (1999). The role of photorespiration during drought stress: an analysis utilizing barley mutants with reduced activities of photorespiratory enzymes. *Plant, Cell and Environment*, *22*(4), 361–373. https://doi.org/10.1046/j.1365-3040.1999.00410.x

Wu, Y., Zhong, H., Li, J., Xing, J., Xu, N., Zou, H. (2022). Water use efficiency and photosynthesis of *Calamagrostis angustifolia* leaves under drought stress through CO_2 concentration increase. *Journal of Plant Interactions*, *17*(1), 60–74. https://doi.org/10.1080/17429145.2021.2011444

Xavier Do Nascimento, E., Hortêncio Mota, J., Do, M., Vieira, C., Antonio, N., Zárate, H. (2007). *Pfaffia glomerata* (Spreng.) Pedersen and *Plantago major L.* biomass production in single culture and intercropped. *Ciência e Agrotecnologia*, *31*, 724-730. https://doi.org/10.1590/S1413-70542007000300019

Xu, Z., Jiang, Y., Jia, B., Zhou, G. (2016). Elevated-CO_2 response of stomata and its dependence on environmental factors. *Frontiers in Plant Science*, *7*(5). https://doi.org/10.3389/fpls.2016.00657

Yan, M. (2015). Seed priming stimulate germination and early seedling growth of Chinese cabbage under drought stress. *South African Journal of Botany*, *99*, 88–92. https://doi.org/10.1016/j.sajb.2015.03.195

Zhang, H., Li, J., Yoo, J.H., Yoo, S.C., Cho, S.H., Koh, H.J., Seo, H. S., Paek, N.C. (2006). Rice Chlorina-1 and Chlorina-9 encode ChlD and ChlI subunits of Mg-chelatase, a key enzyme for chlorophyll synthesis and chloroplast development. *Plant Molecular Biology*, *62*(3), 325–337. https://doi.org/10.1007/s11103-006-9024-z

Zhang, L., Takahashi, Y., Hsu, P.-K., Kollist, H., Merilo, E., Krysan, P. J., Schroeder, J. I. (2020). FRET kinase sensor development reveals SnRK2/OST1 activation by ABA but not by MeJA and high CO_2 during stomatal closure. *ELife*, *9*, 1–74. https://doi.org/10.7554/eLife.56351

Zhang, W., Chen, W., Li, Z., Ma, L., Yu, J., Wang, H., Liu, Z., Xu, B. (2018). Identification and characterization of three new cytochrome P450 genes and the use of RNA interference to evaluate their roles in antioxidant defense in *Apis cerana cerana* Fabricius. *Frontiers in Physiology*, *9*(11), 1–16. https://doi.org/10.3389/fphys.2018.01608

Zhang, X., Wang, X., Zhuang, L., Gao, Y., Huang, B. (2019). Abscisic acid mediation of drought priming-enhanced heat tolerance in tall fescue (*Festuca arundinacea*) and *Arabidopsis*. *Physiologia Plantarum*, *167*(4), 488–501. https://doi.org/10.1111/ppl.12975

Zinta, G., AbdElgawad, H., Domagalska, M. A., Vergauwen, L., Knapen, D., Nijs, I., Janssens, I. A., Beemster, G. T. S., Asard, H. (2014). Physiological, biochemical, and genome-wide transcriptional analysis reveals that elevated CO_2 mitigates the impact of combined heat wave and drought stress in *Arabidopsis thaliana* at multiple organizational levels. *Global Change Biology*, *20*(12), 3670–3685. https://doi.org/10.1111/gcb.1262

FIGURES

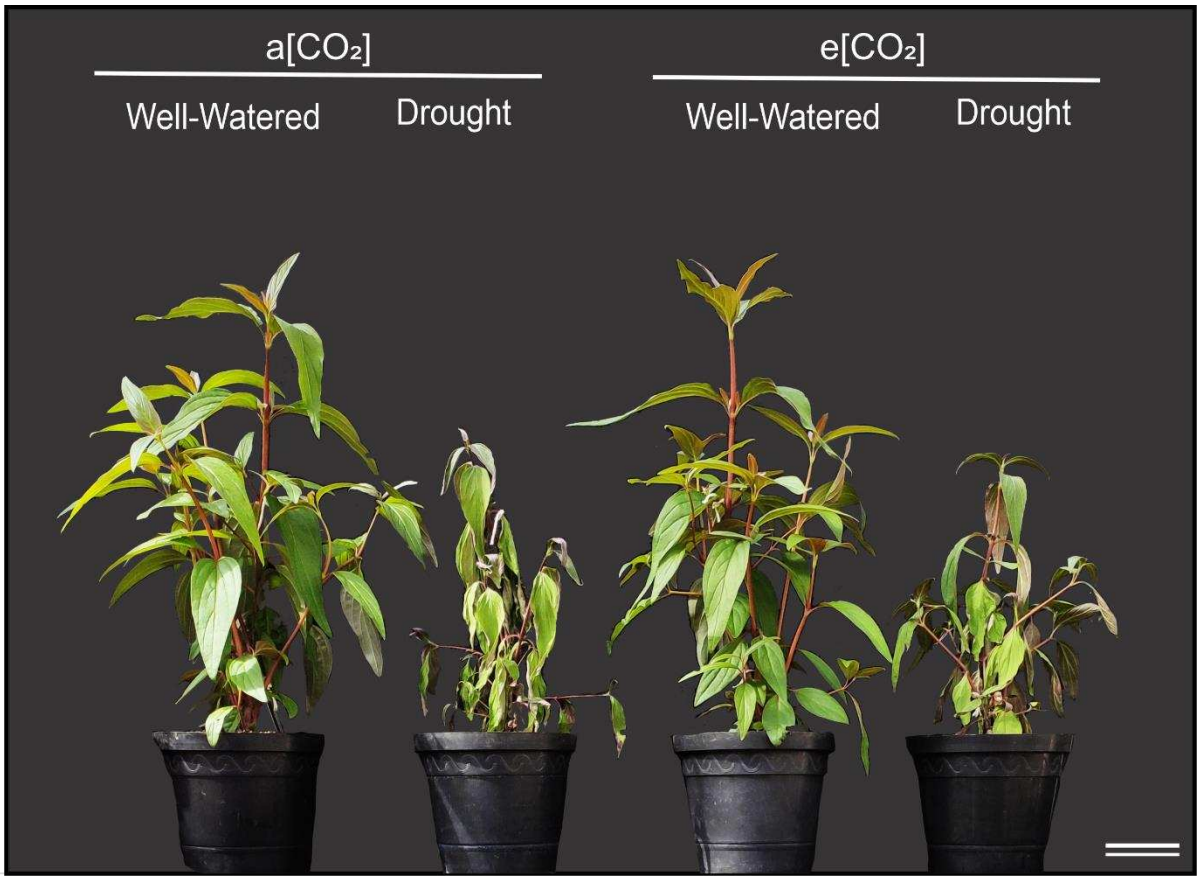

Fig. 1. Visual aspect of well-watered and drought-stressed *P. glomerata* plants (accession 22) under ambient (a[CO_2]) and elevated (e[CO_2]) CO_2 concentration. Bar = 10 cm.

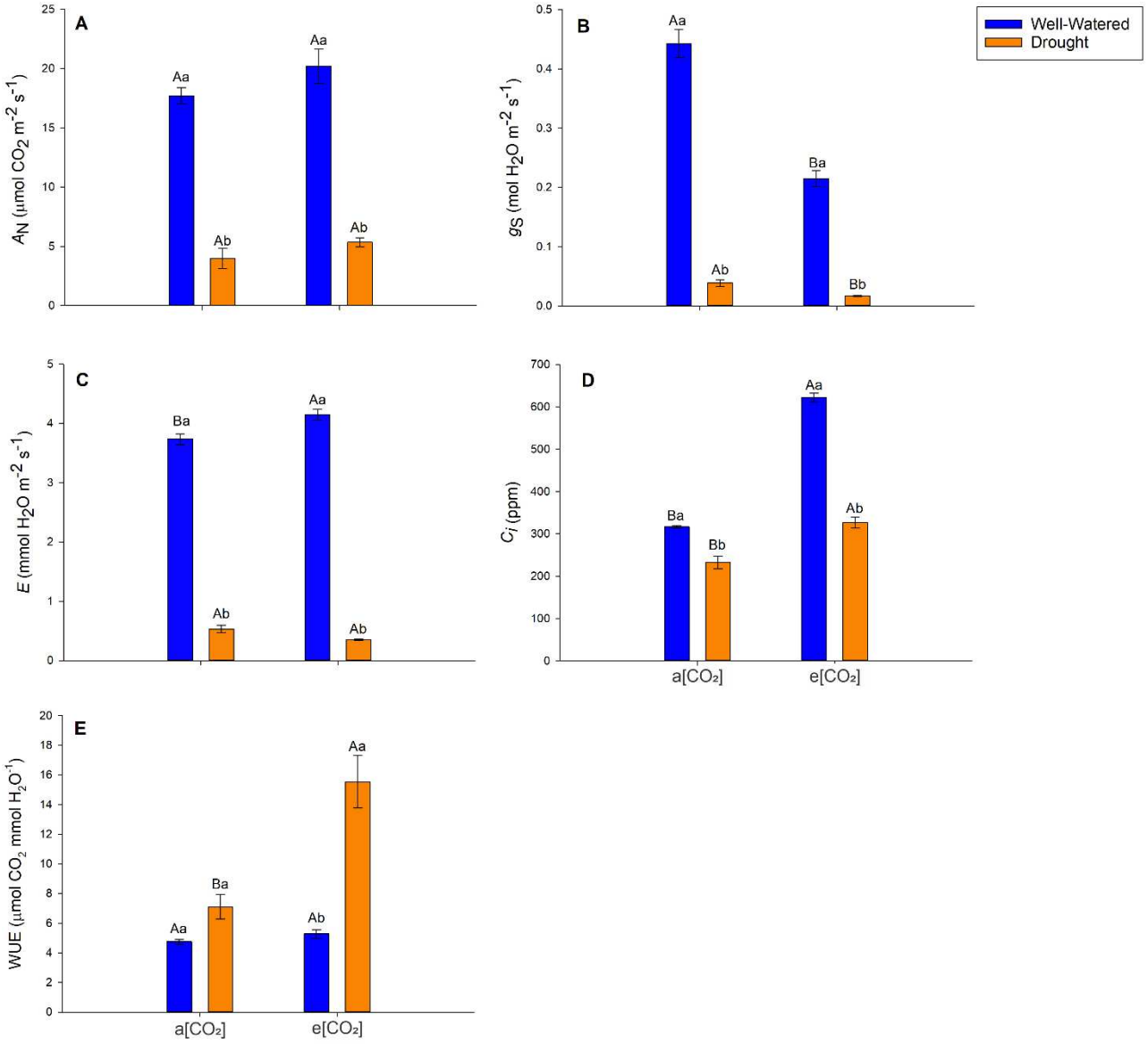

Fig 2. The effect of watering (well-watered or drought-stressed plants) and CO_2 supply ambient (a[CO_2]) or elevated (e[CO_2]) on the gas exchange parameter in *P. glomerata*. (**A**) Net CO_2 net assimilation rate (A_N); (**B**) Stomatal conductance (g_S); (**C**) Transpiration rate (E); (**D**) internal CO_2 concentration (C_i); and (**E**) instantaneous water use efficiency (WUE). Uppercase letters indicate differences between CO_2 treatments within the same watering regime; lowercase letters indicate differences between watering regimes within the same CO_2 supply (Tukey's test; $P \leq 0.05$), values represent means (n=6) ± standard error.

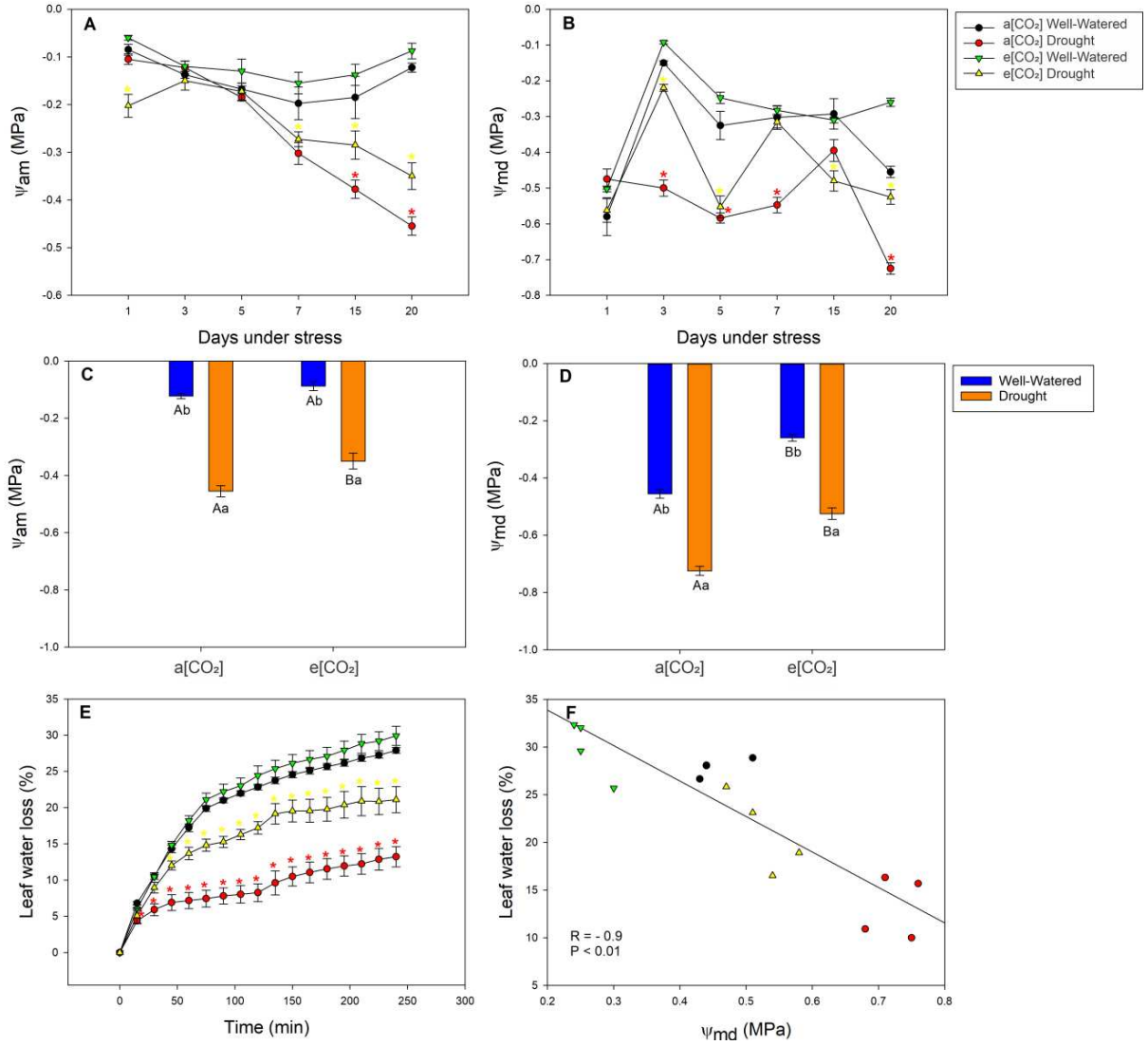

Fig 3. The effect of watering (well-watered or drought-stressed plants) and CO_2 supply ambient (a[CO_2]) or elevated (e[CO_2]) on the water potential in *P. glomerata*. (**A**) Water potential measured at anti-morning (Ψam) and (**B**) midday (Ψmd) during the period of stress; (**C**) water potential at anti-morning and (**D**) midday at 20 days of stress; (**E**) leaf water loss; and (**F**) linear correlation between Ψmd vs. leaf water loss. Asterisks of figures A, B and E indicate significant difference (*t*-Student; $P \leq 0.05$) among different watering regimes compared to the same CO_2 treatments. In figure C and D, uppercase letters indicate differences between CO_2 treatments within the same watering regime; lowercase letters indicate differences between watering regimes within the same CO_2 supply (Tukey's test; $P \leq 0.05$). In figure F, points represent the average of replicas and coefficient of correlation (R) and the p-value (*p*) is shown in the figure. The values represent means (n=4) ± standard error.

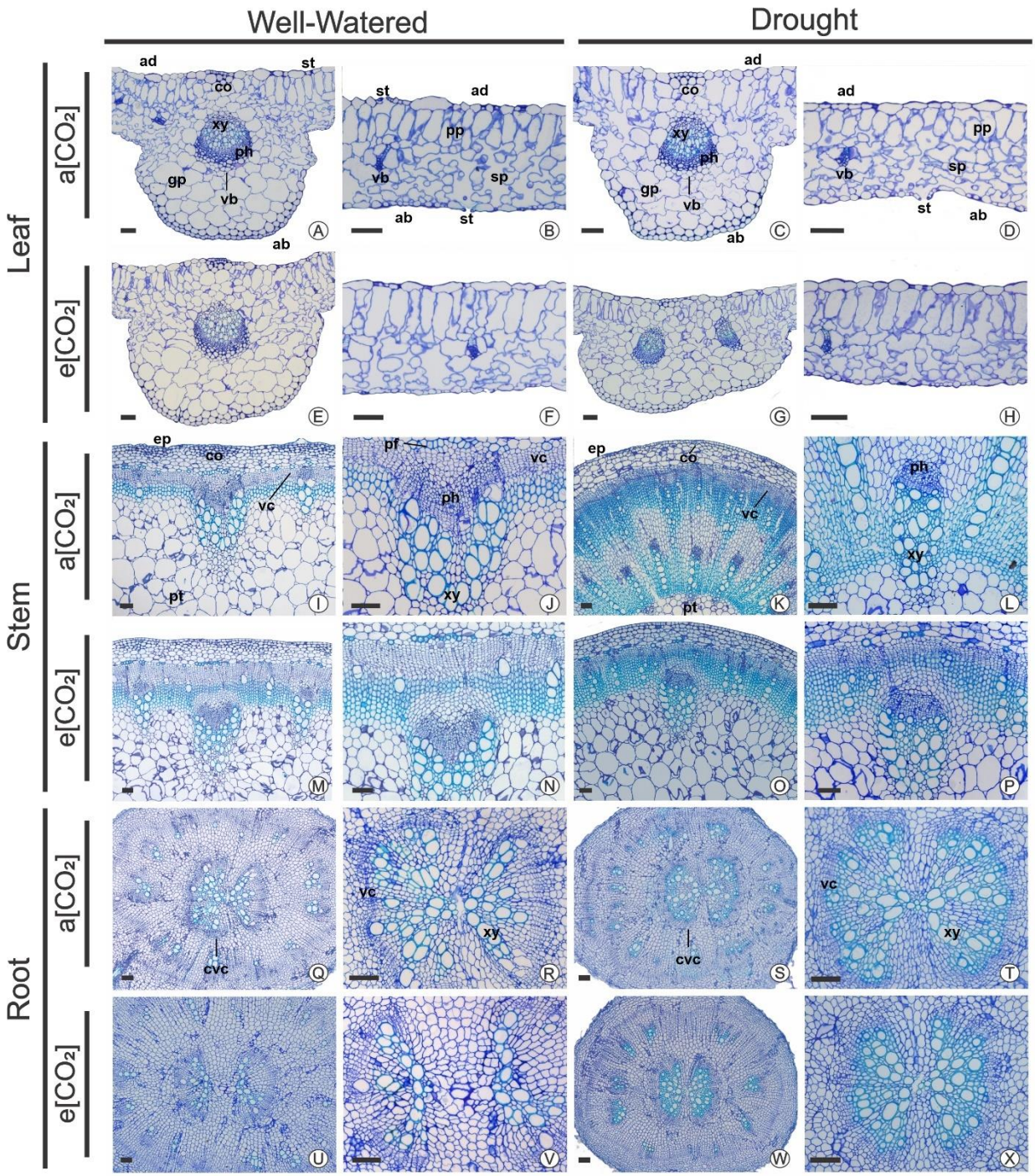

Fig 4. The effect of watering (well-watered or drought-stressed plants) and CO_2 supply ambient (a[CO_2]) or elevated (e[CO_2]) on leaf, stem, and root midrib cross-sections in *P. glomerata*. (**A-H**) Leaf section; (**I-P**) stem section; and (**Q-X**) root section. *Abbreviations:* ab, abaxial epidermis; ad, adaxial epidermis; co, collenchyma; cvc, vascular cambium central; ep, epidermis; gp, ground parenchyma; pf, perivascular fibers; ph, phloem; pp, palisade parenchyma; pt, pith; sp, spongy parenchyma; st, stomata; xy, xylem; vb, vascular bundle; vascular cambium. Bar = 200 μm.

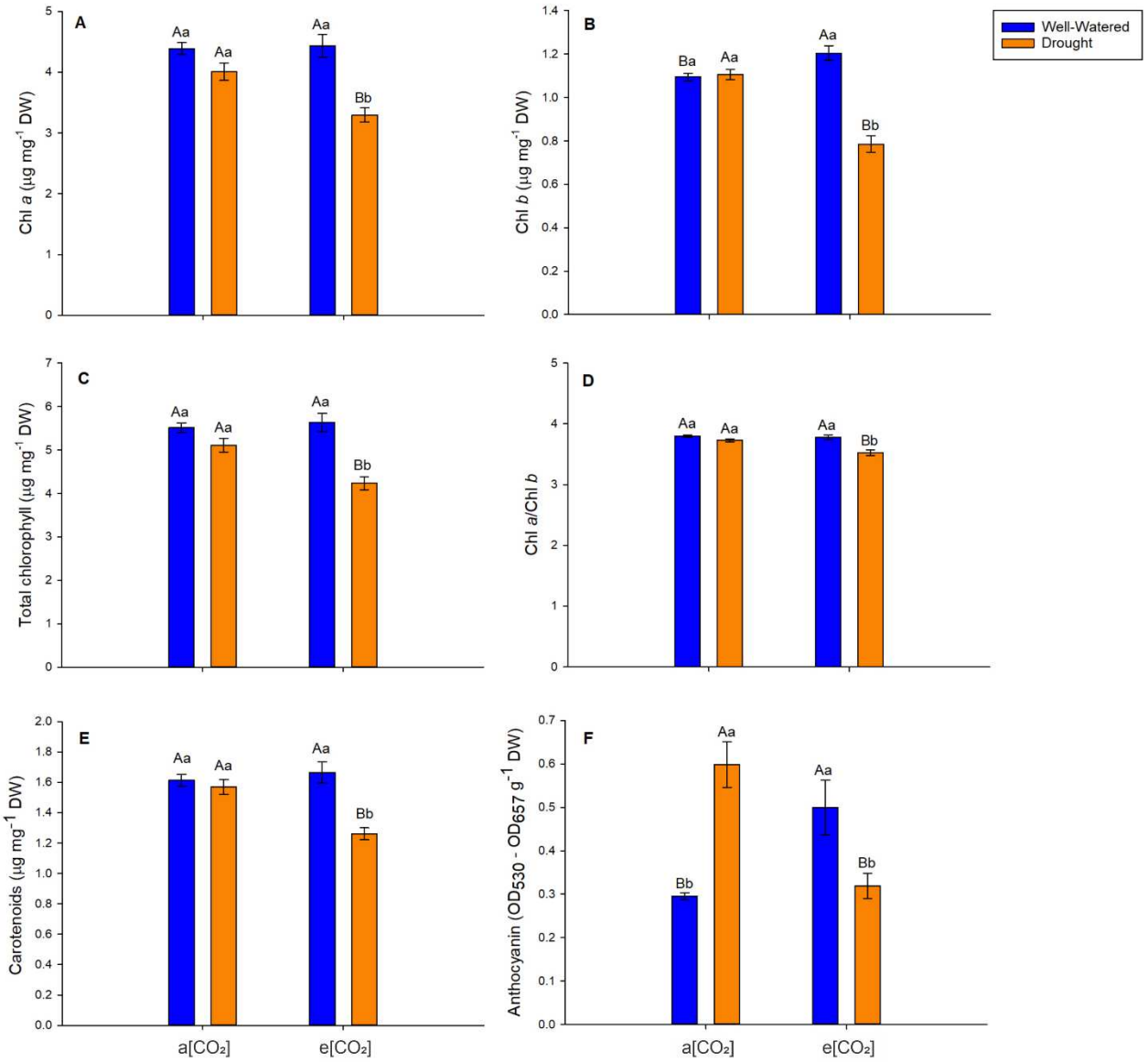

Fig. 5. The effect of watering (well-watered or drought-stressed plants) and CO_2 supply ambient (a[CO_2]) or elevated (e[CO_2]) on the pigment content in *P. glomerata*. (**A**) Chlorophyll a (Chl a); (**B**) chlorophyll b (Chl b); (**C**) total chlorophyll; (**D**) chlorophyll a and chlorophyll b ratio (Chl a/Chl b); (**E**) carotenoids; and (**F**) anthocyanin. Uppercase letters indicate differences between CO_2 treatments within the same watering regime; lowercase letters indicate differences between watering regimes within the same CO_2 supply (Tukey's test; $P \leq 0.05$), values represent means (n=6) ± standard error.

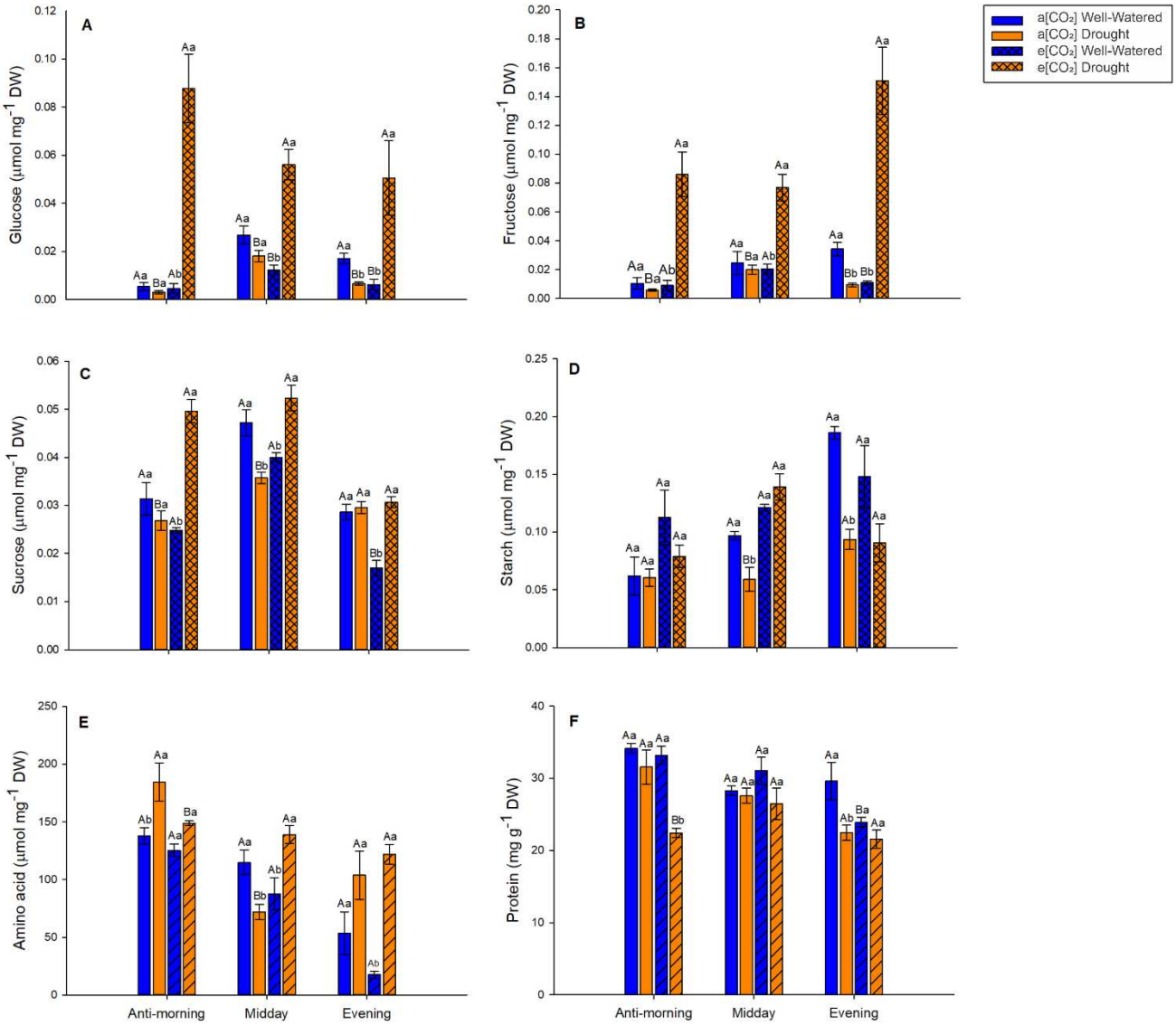

Fig. 6. The effect of watering (well-watered or drought-stressed plants) and CO_2 supply ambient (a[CO_2]) or elevated (e[CO_2]) on the metabolite contents involved in carbon metabolism in *P. glomerata*. (**A**) Glucose; (**B**) fructose; (**C**) sucrose; (**D**) starch; (**E**) amino acid and; and (**F**) protein. Uppercase letters indicate differences between CO_2 treatments within the same watering regime; lowercase letters indicate differences between watering regimes within the same CO_2 supply (Tukey's test; $P \leq 0.05$), values represent means (n=6) ± standard error.

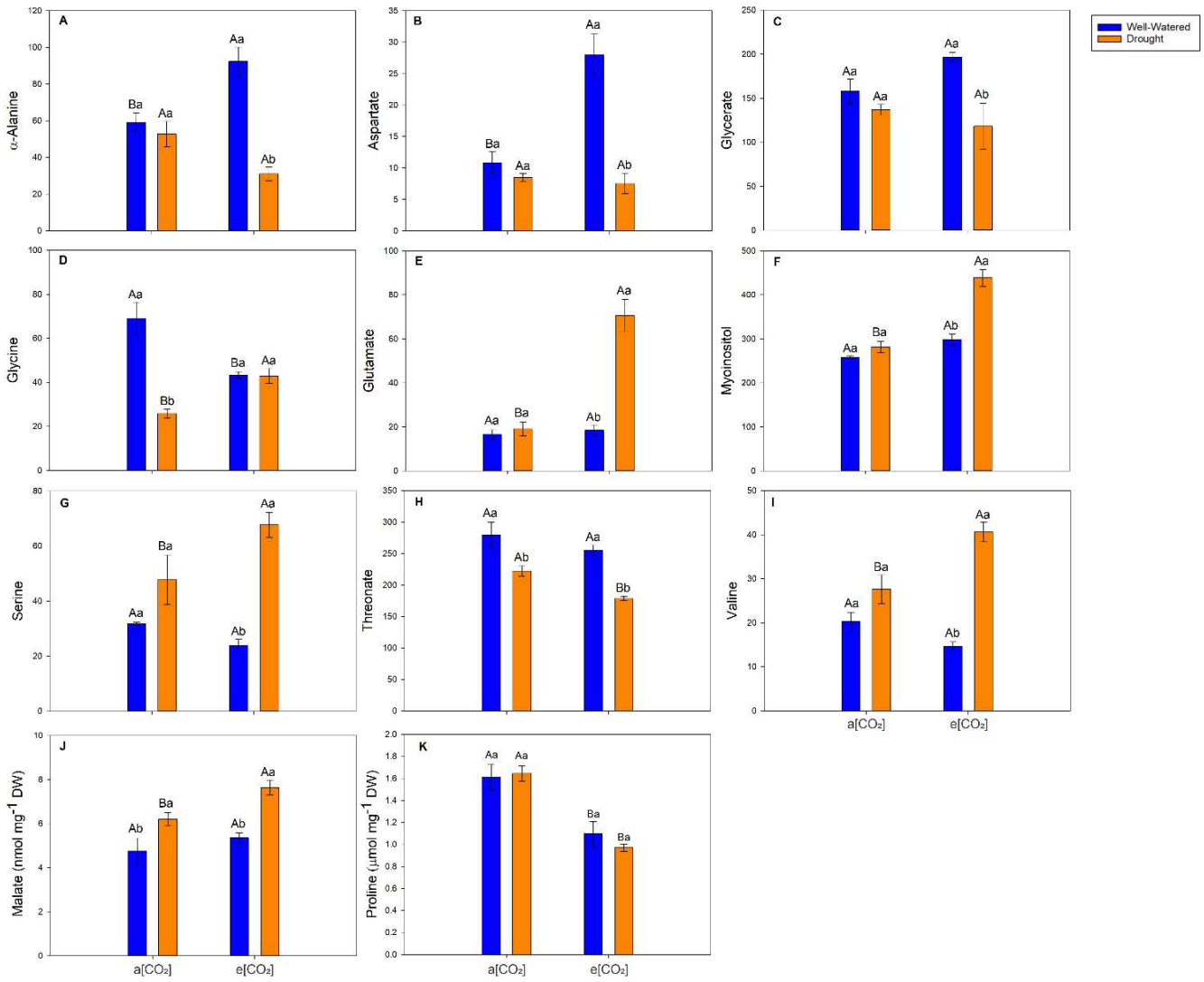

Fig. 7. The effect of watering (well-watered or drought-stressed plants) and CO_2 supply ambient (a[CO_2]) or elevated (e[CO_2]) on relative metabolite content from GC-MS (figures A-I) and malate and proline content in *P. glomerata* leaves. (**A**) α-Alanine; (**B**) aspartate; (**C**) glycerate; (**D**) glycine; (**E**) glutamate; (**F**) myoinositol; (**G**) serine; (**H**) threonate; (**I**) valine; (**J**) malate; and (**K**) proline. GC MS data were normalized to the corresponding dry weight and peak area of the internal standard (ribitol). Uppercase letters indicate differences between CO_2 treatments within the same watering regime; lowercase letters indicate differences between watering regimes within the same CO_2 supply (Tukey's test; $P \leq 0.05$), values represent means (n=6) ± standard error.

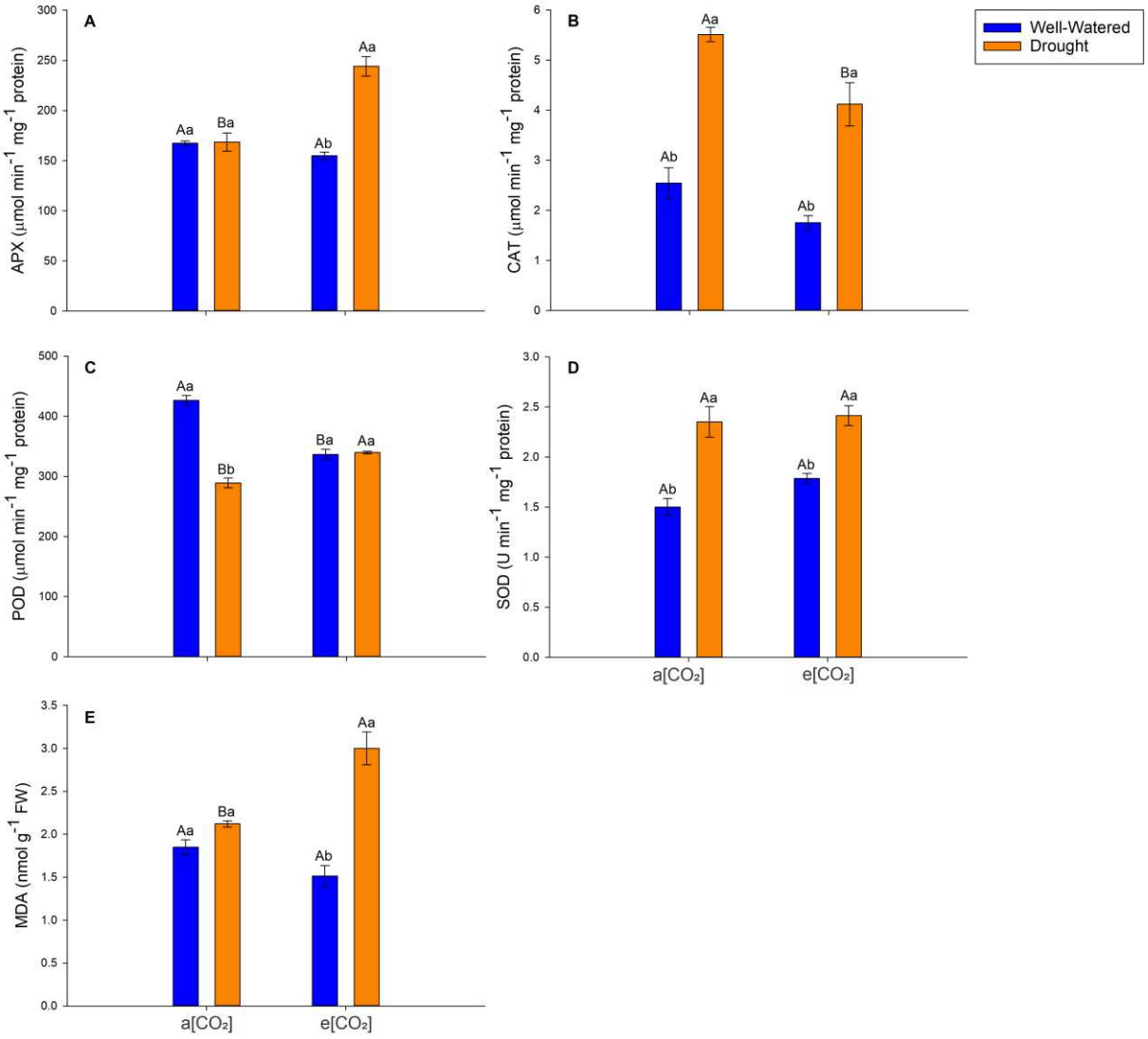

Fig. 8. The effect of watering (well-watered or drought-stressed plants) and CO_2 supply ambient (a[CO_2]) or elevated (e[CO_2]) on the antioxidant enzymatic activity and lipid peroxidation (MDA content) in *P. glomerata*. (**A**) ascorbate peroxidase (APX); (**B**) Catalase (CAT); (**C**) peroxidases (POD); (**D**) superoxide dismutase (SOD) and; (**E**) malonaldehyde (MDA). Uppercase letters indicate differences between CO_2 treatments within the same watering regime; lowercase letters indicate differences between watering regimes within the same CO_2 supply (Tukey's test; $P \leq 0.05$), values represent means (n=6) ± standard error.

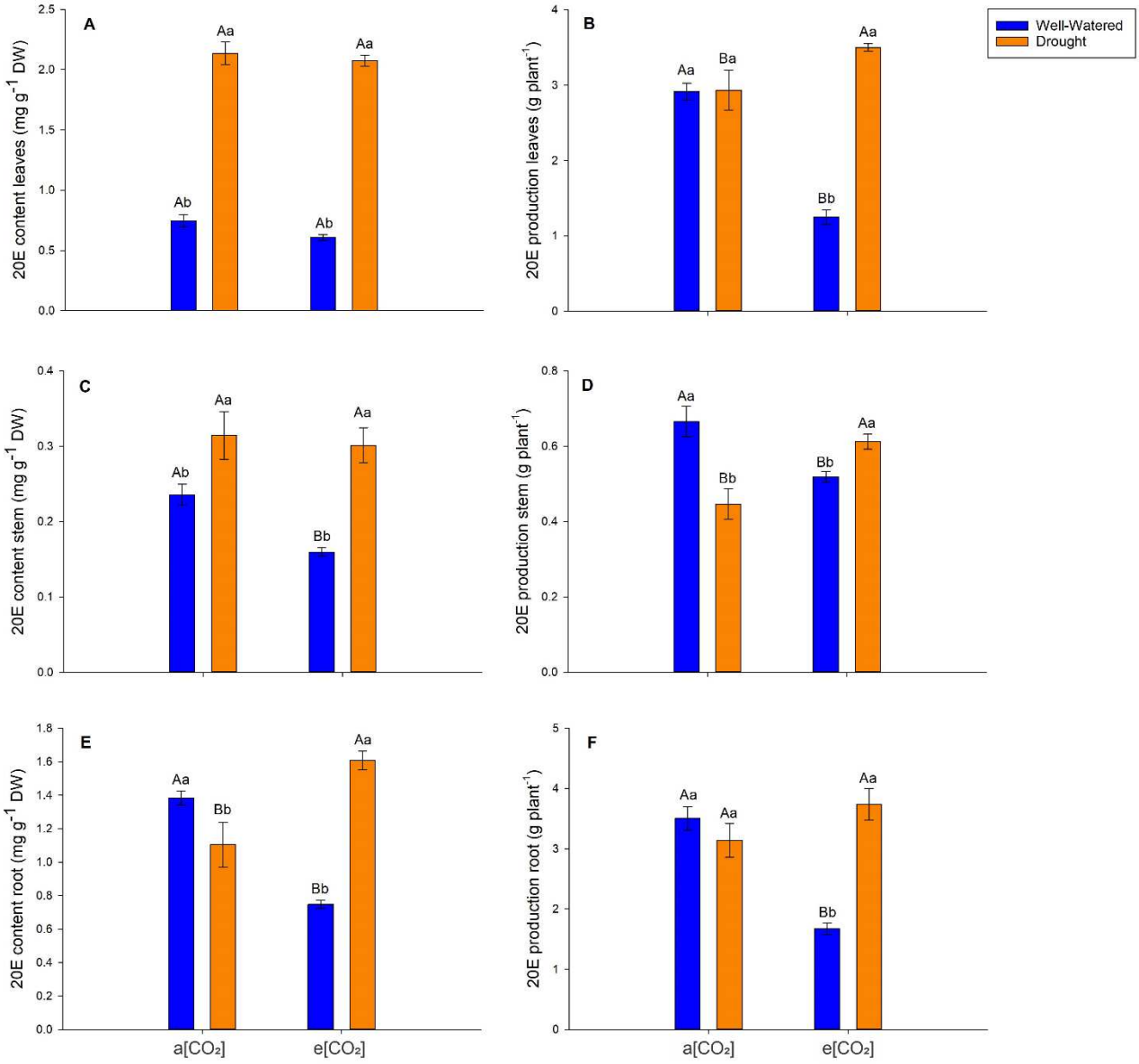

Fig. 9. The effect of watering (well-watered or drought-stressed plants) and CO_2 supply ambient (a[CO_2]) or elevated (e[CO_2]) on the 20-hydroxyecdysone (20E) content in *P. glomerata*. 20E content (mg g^{-1} DW) in (**A**) leaves, (**C**) stem and (**E**) root; and 20E production (g) in (**B**) leaves, (**D**) stem and (**F**) root. Uppercase letters indicate differences between CO_2 treatments within the same watering regime; lowercase letters indicate differences between watering regimes within the same CO_2 supply (Tukey's test; $P \leq 0.05$), values represent means (n=6) ± standard error.

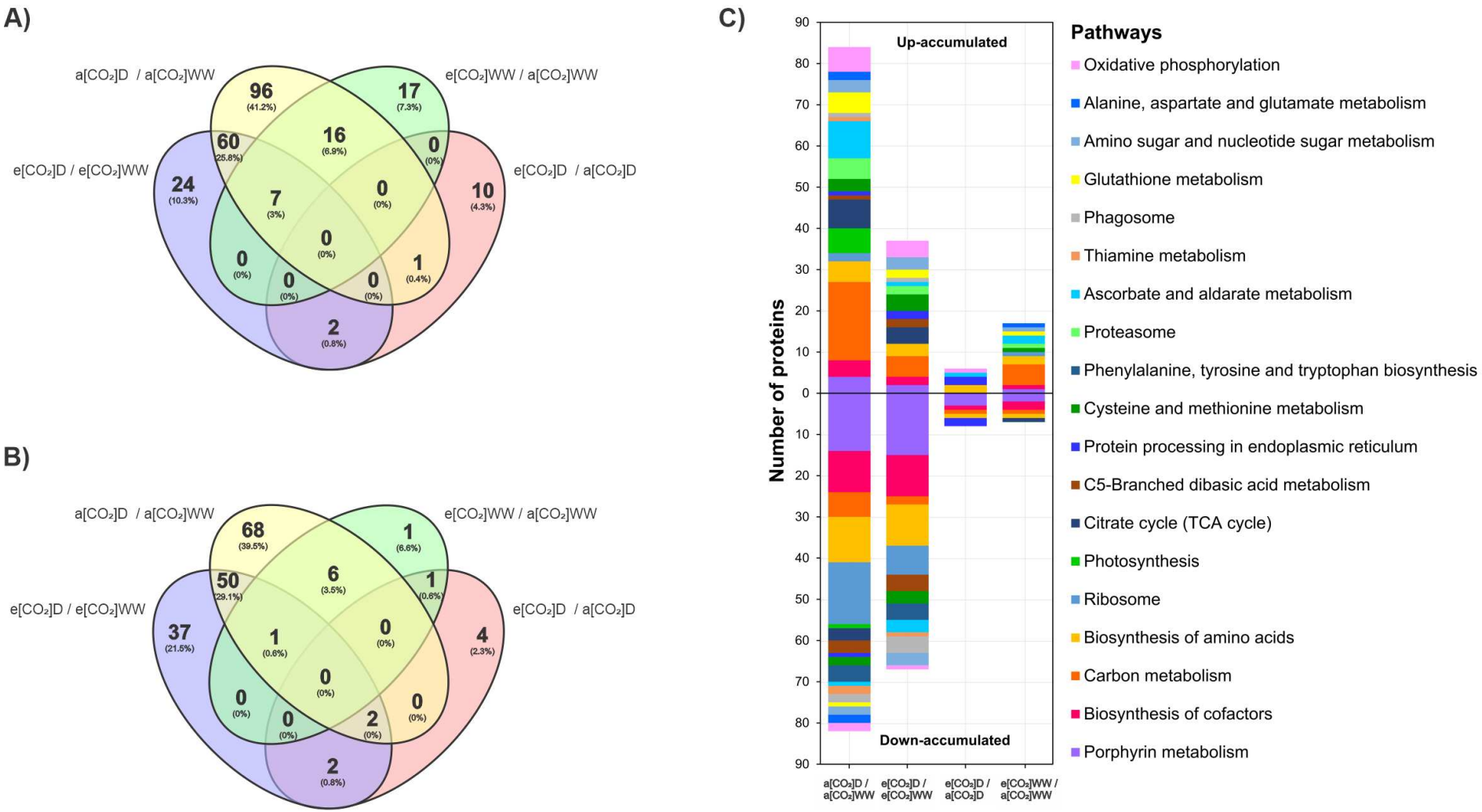

Fig. 10. Analysis of differentially accumulated proteins (DAPs) of well-watered (WW) and drought-stressed (D) in *P. glomerata* plants under ambient (a[CO_2]) and elevated (e[CO_2]) CO_2 concentration. Venn diagram showing common DAPs proteins (**A**) up- and (**B**) down-accumulated and; (**C**) pathway enrichment analysis revealed by KEGG analyzes (Kyoto Encyclopedia of Genes and Genomes).

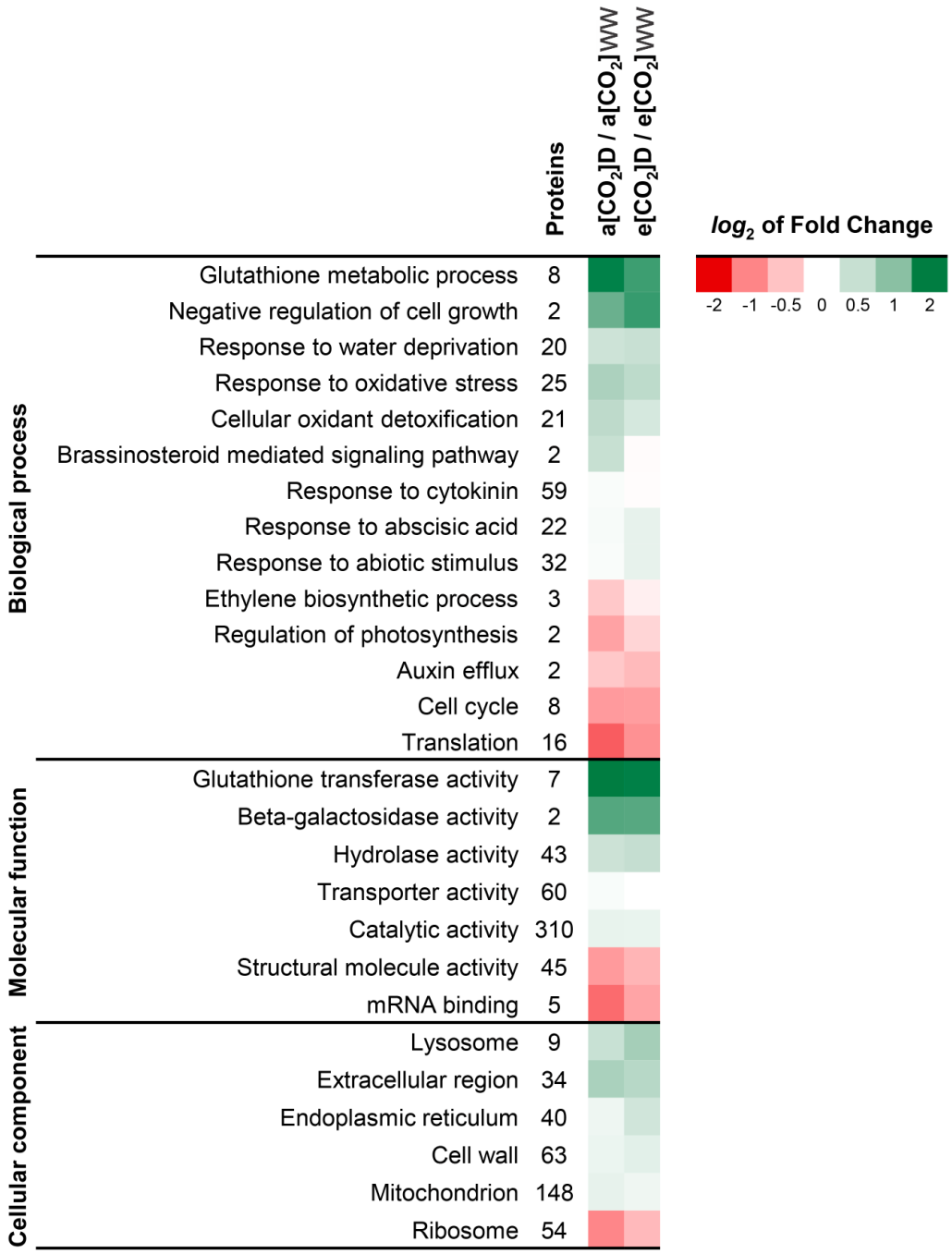

Fig. 11. Heatmap of differential accumulated proteins (DAPs) of well-watered (WW) and drought-stressed (D) *P. glomerata* plants under ambient (a[CO_2]) and elevated (e[CO_2]) CO_2 concentration. For the construction of the heatmap, the Log_2 Fold change (FC) criterion was used to calculate the DAPs, being considered up-accumulated when Log_2 FC > 0.6 and down-accumulated when Log_2 FC < -0.6. Functional annotation related to DAPs based on the gene ontology (GO). Red, down-accumulated and Green, up-accumulated.

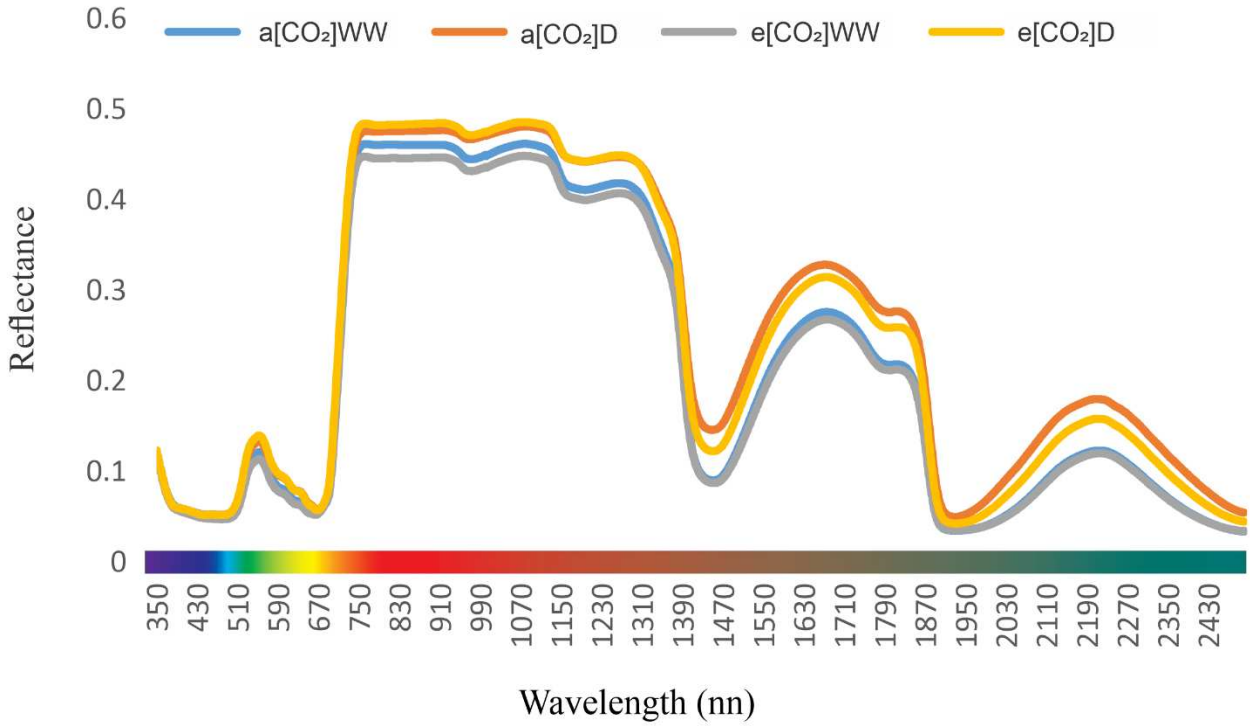

Fig. 12. Median reflectance spectra of fresh leaves of well-watered (WW) and drought-stressed (D) *P. glomerata* plants under ambient (a[CO_2]) and elevated (e[CO_2]) CO_2 concentration. The lines represent the average of each treatment.

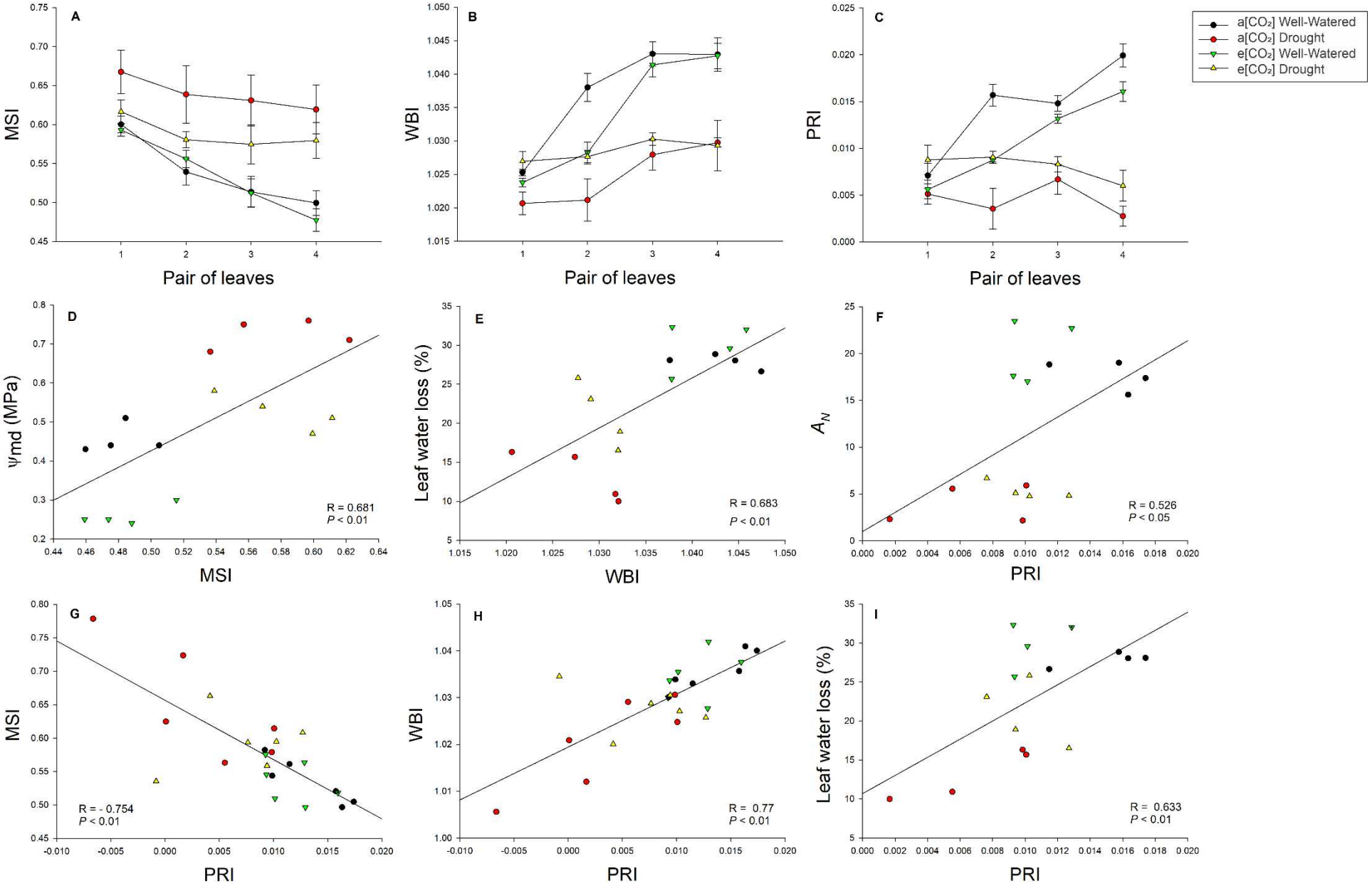
A
MSI
Pair of leaves
B
WBI
Pair of leaves
C
PRI
Pair of leaves
a[CO2] Well-Watered
a[CO2] Drought
e[CO2] Well-Watered
e[CO2] Drought
D
Ψmd (MPa)
MSI
R = 0.681
P < 0.01
E
Leaf water loss (%)
WBI
R = 0.683
P < 0.01
F
AN
PRI
R = 0.526
P < 0.05
G
MSI
PRI
R = - 0.754
P < 0.01
H
WBI
PRI
R = 0.77
P < 0.01
I
Leaf water loss (%)
PRI
R = 0.633
P < 0.01

Fig. 13. The effect of watering (well-watered or drought-stressed plants) and CO_2 supply ambient (a[CO_2]) or elevated (e[CO_2]) on narrowband vegetation indexes and linear correlation between indexes and physiological analysis in *P. glomerata*. Variation among leaf pairs of the vegetation indexes (**A**) Moisture Stress Index (MSI); (**B**) Water Band Index (WBI); and (**C**) Photochemical Reflectance Index (PRI). Linear correlation between (**D**) MSI vs. water potential at midday (Ψmd); (**E**) WBI vs. leaf water loss; (**F**) PRI vs. net CO_2 net assimilation rate (A_N); (**G**) PRI vs. MSI; (**H**) PRI vs. WBI; and (**I**) PRI vs. leaf water loss. In figures A-C, points represent the means (n=4) ± standard error. The points represent the means (n=4) in figures D-I and coefficient of correlation (R) and the p-value (p) is shown in the figure.

TABLES

Table 1. Narrowband vegetation indexes calculated from leaf spectral reflectance of leaves of *P. glomerata.*

Index	Equation	Reference
ARI1 = Anthocyanin Reflectance Index 1	(1/ρ550)-(1/ρ700)	Gitelson et al. (2001)
Achl = Absorption of Chlorophyll Index	(ρ550/ρ500)	Pontius et al. (2008)
BNb = Index for Chlorophyll Content	(ρ800/ρ550)	Pontius et al. (2008); Buschmann (1993)
CARI = Chlorophyll Absorption in Reflectance Index	(ρ700-ρ670)-0.2*(ρ700-ρ550)	Kim (1994)
CRI1 = Carotenoid Reflectance Index 1	(1/ρ510)-(1/ρ550)	Gitelson et al. (2002)
CRI2 = Carotenoid Reflectance Index 2	(1/ρ510)-(1/ρ700)	Gitelson et al. (2002)
PSRI = Plant Senescence Reflectance Index	(ρ680-ρ500)/ρ750)	Penuelas et al. (1995)
PRI = Photochemical Reflectance Index	(ρ530-ρ570)/(ρ530+ρ570)	Gamon et al. (1997)
SIPI = Structurally Insensitive Pigment Index	(ρ800-ρ445)/(ρ800-ρ680)	Penuelas et al. (1995)
MSI = Moisture Stress Index	ρ1600/ρ820	Hunt and Rock (1989)
WBI = Water Band Index	ρ900/ρ970	Penuelas et al. (1997)

* ρ=wavelength

Table 2. The effect of watering (well-watered or drought-stressed plants) and CO_2 supply ambient (a[CO_2]) or elevated (e[CO_2]) on the biometric parameters in *P. glomerata*. Uppercase letters indicate differences between CO_2 treatments within the same watering regime; lowercase letters indicate differences between watering regimes within the same CO_2 supply (Tukey's test; $P \leq 0.05$), values represent means (n=6) ± standard error.

Variables	**[CO_2]**	**Well-Watered**	**Drought**
Leaf área (cm^2 plant)	a[CO_2]	1487.4 Aa	427.5 Ab
	e[CO_2]	1442.9 Aa	492.2 Ab
Number of leaves	a[CO_2]	98 Aa	72 Ab
	e[CO_2]	104 Aa	67 Ab
Stem length (cm)	a[CO_2]	46.9 Aa	32.9 Ab
	e[CO_2]	46.0 Aa	32.2 Ab
Largest root length (cm)	a[CO_2]	49.8 Aa	35.2 Bb
	e[CO_2]	52.6 Aa	45.1 Ab
Total dry weight (g)	a[CO_2]	6.44 Ba	5.48 Bb
	e[CO_2]	8.84 Aa	6.44 Ab
Leaves biomass partitioning (%)	a[CO_2]	32.77 Aa	25.68 Ab
	e[CO_2]	30.53 Aa	25.04 Ab
Stem biomass partitioning (%)	a[CO_2]	39.31 Aa	26.92 Bb
	e[CO_2]	35.52 Aa	35.75 Aa
Root biomass partitioning (%)	a[CO_2]	27.92 Bb	47.40 Aa
	e[CO_2]	33.95 Aa	39.21 Ba
Root/Shoot	a[CO_2]	0.39 Bb	0.90 Aa
	e[CO_2]	0.52 Aa	0.65 Ba

Table 3. The effect of watering (well-watered or drought-stressed plants) and CO_2 supply ambient (a[CO_2]) or elevated (e[CO_2]) on the narrowband indexes vegetation applied to spectral data of leaves of *P. glomerata*. Uppercase letters indicate differences between CO_2 treatments within the same watering regime; lowercase letters indicate differences between watering regimes within the same CO_2 supply (Tukey's test; $P \leq 0.05$), values represent means (n=6) ± standard error.

Variables	[CO_2]	Well-Watered	Drought
ARI1	a[CO_2]	0.7020 Ba	0.8717 Aa
	e[CO_2]	1.1686 Aa	0.7259 Ab
Achl	a[CO_2]	2.2508 Aa	2.3060 Ba
	e[CO_2]	2.2636 Ab	2.4274 Aa
BNb	a[CO_2]	3.8157 Aa	3.3379 Aa
	e[CO_2]	3.9481 Aa	3.5445 Ab
CARI	a[CO_2]	0.0749 Ab	0.0886 Aa
	e[CO_2]	0.0735 Ab	0.0932 Aa
CRI1	a[CO_2]	7.8936 Aa	7.0270 Aa
	e[CO_2]	8.4831 Aa	7.3473 Ab
CRI2	a[CO_2]	8.5956 Aa	7.8987 Aa
	e[CO_2]	9.6517 Aa	8.0732 Ab
PSRI	a[CO_2]	0.0162 Ba	0.0145 Aa
	e[CO_2]	0.0255 Aa	0.0164 Ab
PRI	a[CO_2]	0.0133 Aa	0.0034 Ab
	e[CO_2]	0.0118 Aa	0.0072 Aa
SIPI	a[CO_2]	1.0233 Bb	1.0297 Aa
	e[CO_2]	1.0342 Aa	1.0315 Aa
MSI	a[CO_2]	0.5349 Ab	0.6473 Aa
	e[CO_2]	0.5347 Aa	0.5923 Aa
WBI	a[CO_2]	1.0356 Aa	1.0205 Ab
	e[CO_2]	1.0344 Aa	1.0278 Aa

SUPPLEMENTARY MATERIAL

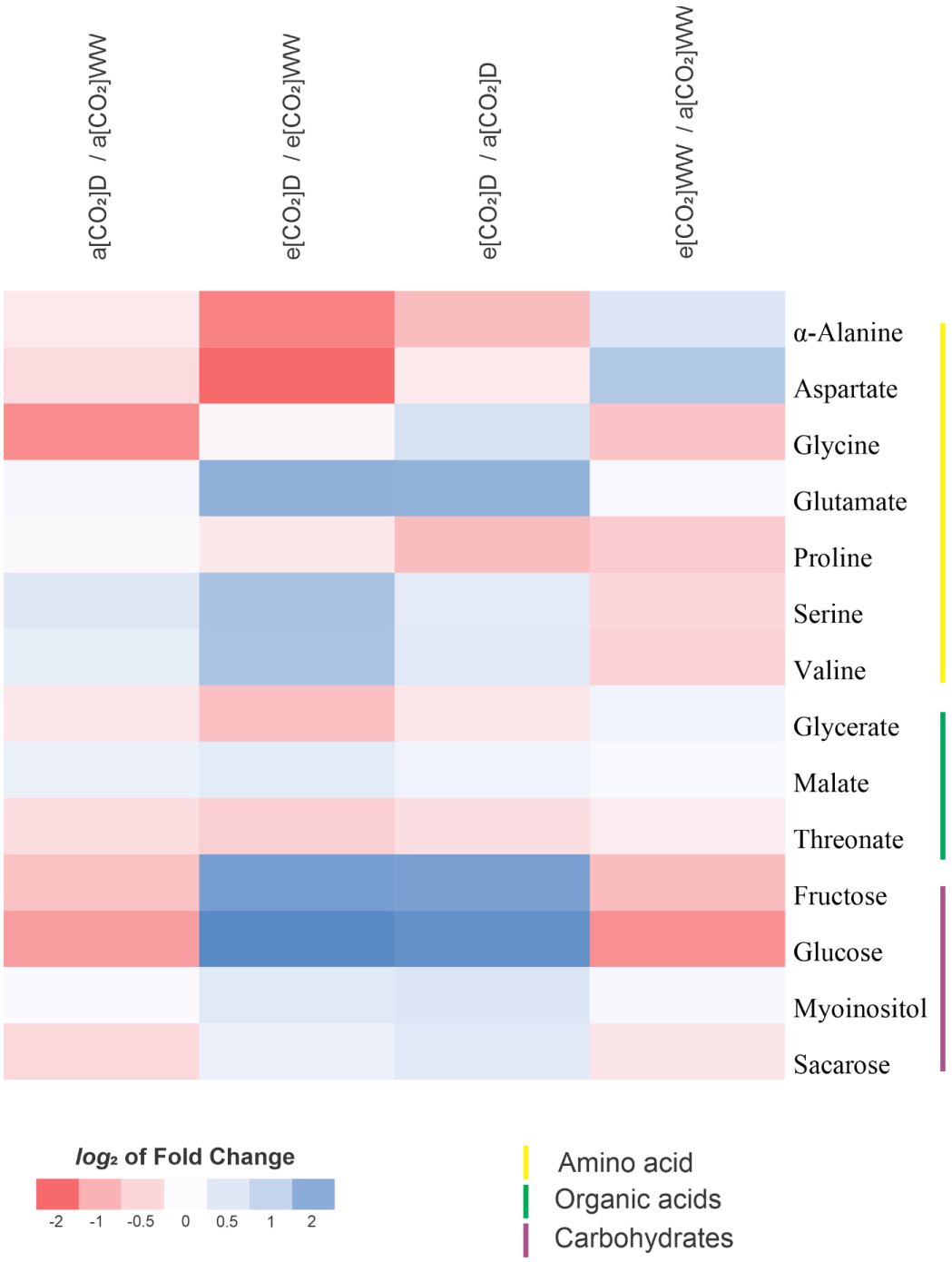

Fig. S1. Heatmap of representing the changes in relative metabolite content of well-watered (WW) and drought-stressed (D) in *P. glomerata* leaves under ambient (a[CO_2]) and elevated (e[CO_2]) CO_2 concentration. For the construction of the heatmap, the Log_2 Fold change (FC) criterion was used to compare the relative metabolite content, being considered up-accumulated when Log_2 FC > 0.6 and down-accumulated when Log_2 FC < -0.6. Red, down-accumulated and Blue, up-accumulated.

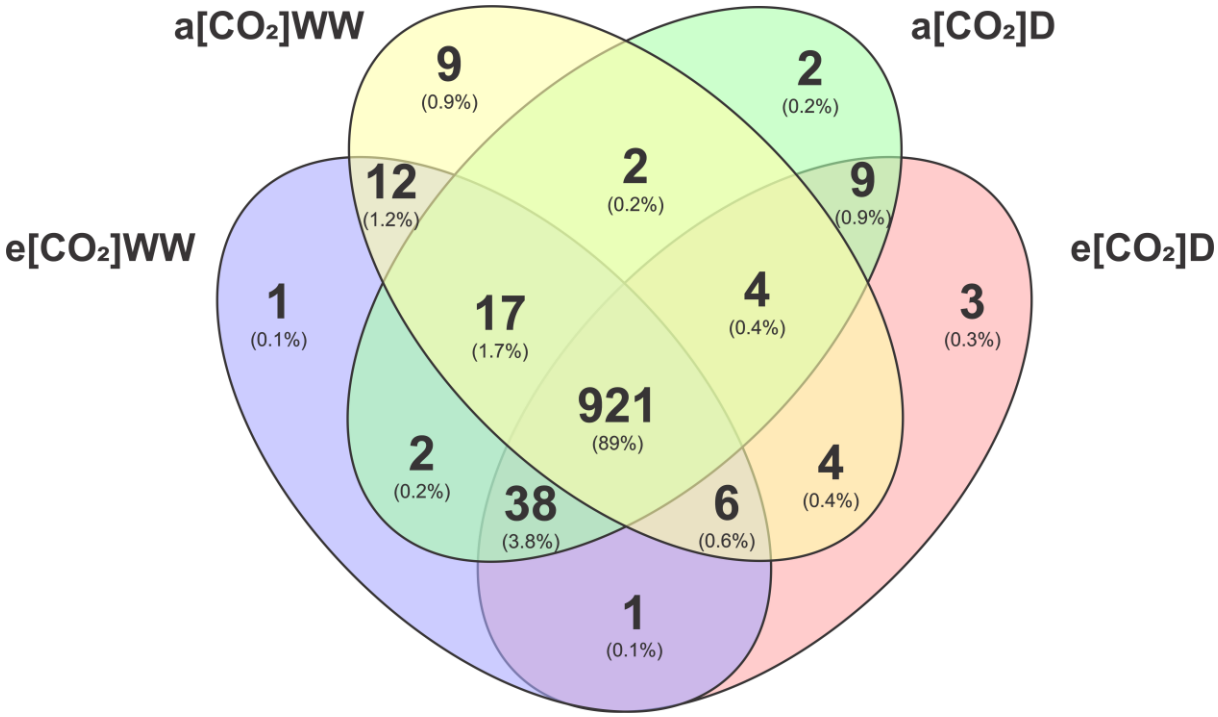

Fig. S1. Venn diagram illustrating the numbers of proteins identified in well-watered (WW) and drought-stressed (D) *P. glomerata* plants under a[CO_2] and e[CO_2]. The diagram shows common and unique proteins at each treatment.

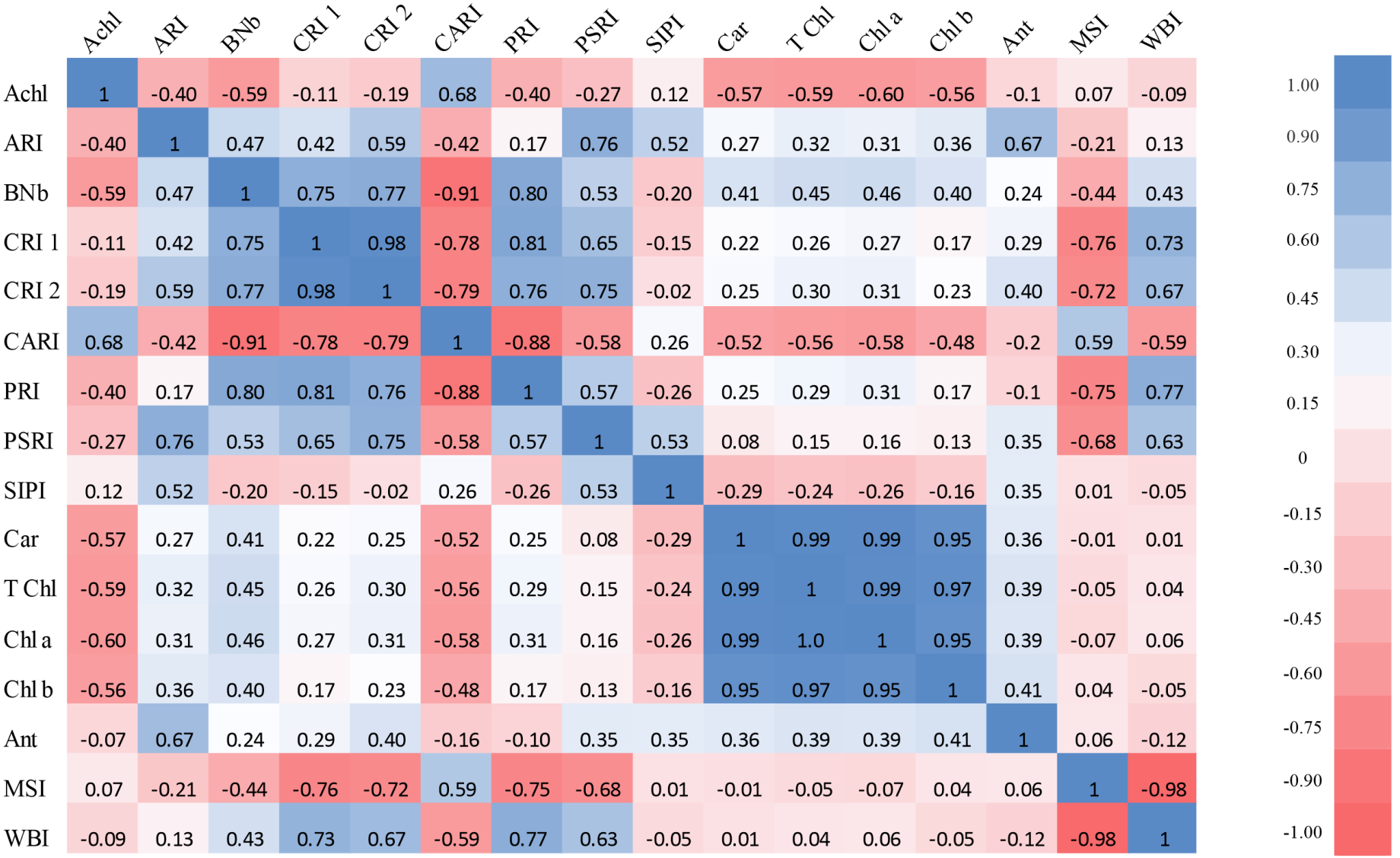
Achl ARI BNb CRI 1 CRI 2 CARI PRI PSRI SIPI Car T Chl Chl a Chl b Ant MSI WBI
Achl 1 -0.40 -0.59 -0.11 -0.19 0.68 -0.40 -0.27 0.12 -0.57 -0.59 -0.60 -0.56 -0.1 0.07 -0.09
ARI -0.40 1 0.47 0.42 0.59 -0.42 0.17 0.76 0.52 0.27 0.32 0.31 0.36 0.67 -0.21 0.13
BNb -0.59 0.47 1 0.75 0.77 -0.91 0.80 0.53 -0.20 0.41 0.45 0.46 0.40 0.24 -0.44 0.43
CRI 1 -0.11 0.42 0.75 1 0.98 -0.78 0.81 0.65 -0.15 0.22 0.26 0.27 0.17 0.29 -0.76 0.73
CRI 2 -0.19 0.59 0.77 0.98 1 -0.79 0.76 0.75 -0.02 0.25 0.30 0.31 0.23 0.40 -0.72 0.67
CARI 0.68 -0.42 -0.91 -0.78 -0.79 1 -0.88 -0.58 0.26 -0.52 -0.56 -0.58 -0.48 -0.2 0.59 -0.59
PRI -0.40 0.17 0.80 0.81 0.76 -0.88 1 0.57 -0.26 0.25 0.29 0.31 0.17 -0.1 -0.75 0.77
PSRI -0.27 0.76 0.53 0.65 0.75 -0.58 0.57 1 0.53 0.08 0.15 0.16 0.13 0.35 -0.68 0.63
SIPI 0.12 0.52 -0.20 -0.15 -0.02 0.26 -0.26 0.53 1 -0.29 -0.24 -0.26 -0.16 0.35 0.01 -0.05
Car -0.57 0.27 0.41 0.22 0.25 -0.52 0.25 0.08 -0.29 1 0.99 0.99 0.95 0.36 -0.01 0.01
T Chl -0.59 0.32 0.45 0.26 0.30 -0.56 0.29 0.15 -0.24 0.99 1 0.99 0.97 0.39 -0.05 0.04
Chl a -0.60 0.31 0.46 0.27 0.31 -0.58 0.31 0.16 -0.26 0.99 1.0 1 0.95 0.39 -0.07 0.06
Chl b -0.56 0.36 0.40 0.17 0.23 -0.48 0.17 0.13 -0.16 0.95 0.97 0.95 1 0.41 0.04 -0.05
Ant -0.07 0.67 0.24 0.29 0.40 -0.16 -0.10 0.35 0.35 0.36 0.39 0.39 0.41 1 0.06 -0.12
MSI 0.07 -0.21 -0.44 -0.76 -0.72 0.59 -0.75 -0.68 0.01 -0.01 -0.05 -0.07 0.04 0.06 1 -0.98
WBI -0.09 0.13 0.43 0.73 0.67 -0.59 0.77 0.63 -0.05 0.01 0.04 0.06 -0.05 -0.12 -0.98 1
1.00
0.90
0.75
0.60
0.45
0.30
0.15
0
-0.15
-0.30
-0.45
-0.60
-0.75
-0.90
-1.00

Fig. S3. Pearson correlation coefficients between narrowband vegetation indexes and biochemical measures of pigments in fresh leaves of *P. glomerata* under ambient (a[CO_2]) and elevated (e[CO_2]) CO_2 concentration and of well-watered (WW) and drought-stressed (D) conditions. Apreviations: **Achl**, Absorption of Chlorophyll Index; **Ant**, anthocyanin content; **ARI**, Anthocyanin Reflectance Index 1; **BNb**, Index for Chlorophyll Content; **Car**, carotenoid content; **Chl *a***, chlorophyll *a* content; **Chl *b***, chlorophyll *b* content; **CRI 1**, Carotenoid Reflectance Index 1; **CRI 2**, Carotenoid Reflectance Index 2; **CARI**, Chlorophyll Absorption in Reflectance Index; **MSI**, Moisture Stress Index; **PRI**, Photochemical Reflectance Index; **PSRI**, Plant Senescence Reflectance Index; **SIPI**, Structurally Insensitive Pigment Index; **T Chl**, total chlorophyll content; **WBI,** Water Band Index.

Table S1. Complete list of identified proteins, functional protein annotations, and configuration parameters.

https://ufvcv-my.sharepoint.com/:x:/g/personal/tatiane_dulcineia_ufv_br/EVFJ26EoZZFCpWCdUfCE6ogBRePdn_BBqmY7VYrdCOcY0w?e=43PiOG

Table S2. List of metabolic pathways identified in the KEGG (Kyoto Encyclopedia of Genes and Genomes), created from the analysis of differential accumulated proteins

https://ufvcv-my.sharepoint.com/:x:/g/personal/tatiane_dulcineia_ufv_br/ETyLPWihDqBMpzgUnCMOKxUBkNtLEsTQOy8z1S6enMSZKw?e=ZXKSHk

Table S3. List of proteins accession classified in biological process, molecular function and cellular component based on gene ontology (GO).

https://ufvcv-my.sharepoint.com/:x:/g/personal/tatiane_dulcineia_ufv_br/EVagUwk0RL9Nq3hGzAP9V0wBmGGJHFJ4G2kkzEYDbsRneg?e=EyHyVE